

THE UNIVERSITY OF CALGARY

PHYSICALLY-BASED STATISTICAL CHARACTERISTICS OF
SIMULATED RANDOM PEAK FLOWS

BY

ANIL KUMAR BEERSING

A THESIS

SUBMITTED TO THE FACULTY OF GRADUATE STUDIES
IN PARTIAL FULFILLMENT OF THE REQUIREMENTS FOR THE
DEGREE OF DOCTOR OF PHILOSOPHY

DEPARTMENT OF CIVIL ENGINEERING

CALGARY, ALBERTA

NOVEMBER, 1988

© ANIL KUMAR BEERSING 1988

Permission has been granted to the National Library of Canada to microfilm this thesis and to lend or sell copies of the film.

The author (copyright owner) has reserved other publication rights, and neither the thesis nor extensive extracts from it may be printed or otherwise reproduced without his/her written permission.

L'autorisation a été accordée à la Bibliothèque nationale du Canada de microfilmer cette thèse et de prêter ou de vendre des exemplaires du film.

L'auteur (titulaire du droit d'auteur) se réserve les autres droits de publication; ni la thèse ni de longs extraits de celle-ci ne doivent être imprimés ou autrement reproduits sans son autorisation écrite.

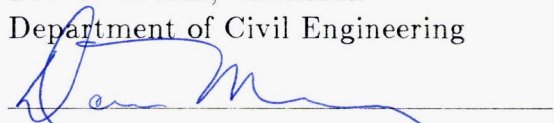
ISBN 0-315-50286-X

THE UNIVERSITY OF CALGARY
FACULTY OF GRADUATE STUDIES

The undersigned certify that they have read, and recommend to the Faculty of Graduate Studies for acceptance, a thesis entitled, "Physically-based Statistical Characteristics of Simulated Random Peak Flows," submitted by Anil Kumar Beersing in partial fulfillment of the requirements for the degree of Doctor of Philosophy.



Dr. I. Muzik, Chairman
Department of Civil Engineering




Dr. D. H. Manz
Department of Civil Engineering



Dr. J. F. Morrall
Department of Civil Engineering



Dr. R. D. Rowe
Department of Mechanical Engineering



Dr. B. C. Yen, External Examiner
Department of Civil Engineering
University of Virginia

Date November 4th, 1988

Abstract

A composite deterministic-statistical approach is used to study the relationships between the coefficients of variation and skewness of simulated random peak flows and the characteristics of watershed and rainfall. Random rainfall events are generated from their assumed probability distributions using the Monte Carlo technique. Each random rainfall event is simulated over a watershed of known characteristics. A finite difference explicit scheme is used to numerically solve the equations of flow for the peak flow. The watersheds range from single runoff planes to networks of stream-plane combinations. The runoff planes may be pervious and the rainfall events may have correlated intensities and durations. The resulting series of random peak flows are analysed for their statistical characteristics.

The results indicate that the coefficients of variation and skewness of the random peak flows lie within mathematically definable regions on a coefficient of variation-coefficient of skewness plot for given probability distributions of rainfall intensity. The coefficients of variation and skewness are at their maximum values for watersheds which have a relatively high degree of flow attenuation. Such watersheds include those with large drainage areas as well as the smaller watersheds under low intensity, short duration rainfall events. Stream-plane networks with relatively lower basin orders, smaller stream-length ratios, and longer flow paths generate random peak flows having their coefficients of variation and skewness close to the theoretical maximums. The coefficients of variation and skewness from watersheds with relatively lower attenuation rates are more sensitive to the temporal and spatial distribution of the rainfall intensities. Compared to temporally

uniform rainfall intensity, non-uniform temporal distribution of rainfall intensities tend to shift the coefficients towards their maximums. For "large" watersheds, the duration of the rainfall events is more critical than the spatial and temporal distribution of the rainfall intensity. When the rainfall durations and intensities are related according to an inverse power function, the coefficients of variation and skewness become independent of the characteristics of the watershed and depend only on the exponent in the power function. This result holds both for single runoff planes and stream-planes networks. For correlated rainfall inputs the coordinates of the coefficients of variation and skewness lie on a line joining the theoretical maximums to those of the rainfall intensity probability distribution. This line forms the outer limit of the region within which the coefficients of variation and skewness lie. For constant duration rainfalls, inclusion of infiltration increases the coefficients of variation and skewness of the random peak flows. The regions within which they lie can still be determined by using the probability distributions of the effective rainfall intensity. For correlated rainfall events, the behaviour of the coefficients of variation and skewness of random peak flows generated from pervious watersheds become very complex and no definite pattern is immediately apparent.

Acknowledgements

The author thanks Dr. I. Muzik for supervising the progress of this work.

The financial support from the University of Calgary is gratefully acknowledged.

Contents

Abstract	iii
Acknowledgements	v
1 INTRODUCTION	1
1.1 General	1
1.2 Deterministic and Statistical Approaches to Flood Prediction	1
1.3 Composite Deterministic-Statistical Approach	3
1.4 Objective and Scope of Study	4
2 LITERATURE REVIEW	6
2.1 Physically-based Stochastic Hydrology	6
2.2 Hydrodynamical Approach	7
2.2.1 Stochastic Kinematic Wave Model	7
2.2.2 Comments on the Hydrodynamical Approach	15
2.3 Geomorphoclimatic IUH Approach	17
2.3.1 Geomorphologic IUH	17
2.3.2 Geomorphoclimatic IUH	22
2.3.3 Stochastic GcIUH	23
2.3.4 Probabilities of Peak Flows using the GcIUH	25
2.3.5 Comments on the GcIUH Approach	26
2.4 Summary	27
3 STATISTICAL CHARACTERISTICS OF RANDOM PEAK FLOWS FROM SINGLE PLANES	29
3.1 Introduction	29
3.2 The Rainfall-Runoff Process on a Single Plane	31
3.2.1 Characterization of Rainfall, Infiltration, and Runoff Plane	31
3.2.2 Modelling of Surface Flow over a Single Plane	35
3.3 Intrinsic Nature of a Probabilistic Rainfall-Peak Flow Process for a Single Plane	45
3.3.1 Random Rainfall Rates of Constant Duration on an Impervious Plane	47
3.3.2 Random Uniform Rainfall with Correlated Intensities and Durations on an Impervious Plane	68
3.3.3 Random Rainfall Events on a Pervious Plane	78
3.4 Effects of Non-uniform Random Inputs on Peak Flow Probabilities	87

3.4.1	Triangular Distribution of Rainfall Intensity on an Impervious Plane	91
3.4.2	Triangular Distribution of Rainfall Intensity on a Pervious Plane	97
3.4.3	Correlated Non-Uniform Rainfall Inputs on a Pervious Plane	100
3.5	Summary	100
4	STATISTICAL CHARACTERISTICS OF RANDOM FLOOD EVENTS ALONG A STREAM	105
4.1	Introduction	105
4.2	Random Flood Events along a Stream with Upstream Point Inflow .	107
4.2.1	Characterization of Upstream Flood Hydrograph	108
4.2.2	Rate of Flood Level Subsidence with Distance	110
4.2.3	Rate of Flood Peak Subsidence with Distance	114
4.2.4	Effects of Flood and Stream Parameters on the Statistical Characteristics of Random Peak Depths	116
4.2.5	Statistical Characteristics of Random Peak Flows	123
4.3	Random Flood Events along a Stream with Lateral Inflow	125
4.3.1	Numerical Simulation of Flow in a Stream-Plane Configuration	127
4.3.2	Method for obtaining Statistical Parameters of Random Peak Flows	127
4.3.3	Uniform Rainfall Intensity on an Impervious Plane	128
4.3.4	Uniform Rainfall Intensities on Planes with Non-uniform Characteristics	137
4.3.5	Spatially Non-uniform Rainfall Intensity	141
4.3.6	Temporally Non-uniform Rainfall Intensity	143
4.3.7	Non-uniform Rainfall Intensities, Non-uniform Plane Characteristics, and Constant Infiltration Rate	145
4.4	Summary	150
5	STATISTICAL CHARACTERISTICS OF RANDOM PEAK FLOWS FROM A NETWORK OF STREAMS	153
5.1	Introduction	153
5.2	Numerical Simulation of Peak Flows from Stream Networks	155
5.2.1	Numerical Simulation	155
5.2.2	Evaluation of the Numerical Procedure	157
5.3	Statistical Characteristics of Random Peak Flows from Constant Duration Rainfalls	162
5.3.1	Topological Description of a Network of Streams	163

5.3.2	Effect of Basin Order	164
5.3.3	Influence of Stream Length Ratio on Statistical Characteristics of Peak Flows	170
5.3.4	Spatially Non-uniform Runoff Contributing Areas	173
5.3.5	Triangular Temporal Distribution of Rainfall Intensity	177
5.3.6	Spatially Non-uniform Distribution of Rainfall Intensity	179
5.3.7	Spatially and Temporally Non-uniform Rainfall Intensity on Spatially Non-uniform Runoff Contributing Areas	179
5.4	Statistical Characteristics of Peak Flows from Correlated Rainfall Inputs	181
5.4.1	Spatially and Temporally Uniform Rainfall Intensity	183
5.4.2	Non-uniform Runoff Contributing Areas	187
5.4.3	Temporally Non-uniform Rainfall Intensity	189
5.4.4	Spatially Non-uniform Rainfall Intensity	192
5.4.5	Combined Effect of Spatially and Temporally Non-uniform Rainfall Intensity	192
5.4.6	Uniform Rainfall Intensity and Constant Infiltration Rate	195
5.4.7	Non-uniform Rainfall and Runoff Area Parameters and Constant Infiltration Rate	198
5.5	Discussion of Results From Single Planes, Single Streams, and Networks of Streams	199
6	CONCLUSIONS AND RECOMMENDATIONS	206
6.1	Scope of Study	206
6.2	Conclusions	207
6.3	Recommendations	211
	Bibliography	213
A	STATISTICAL CHARACTERISTICS OF POWER FUNCTIONS OF A GAMMA VARIABLE	217

List of Figures

2.1	Schematic of a first-order watershed (Eagleson, 1971)	9
2.2	A third-order basin and its trapping state (Rodriguez-Iturbe and Valdes, 1979)	18
3.1	Typical plot of rainfall hyetograph and infiltration curve. . .	34
3.2	Definition sketch of flow over a sloping plane.	36
3.3	Representation of overland flow by a series of reaches with uniform depths of flow (Muzik, 1974).	40
3.4	Dimensionless curves for the Kinematic and Diffusion models.	42
3.5	Cs-Cv relationships for the Normal, Gamma, and Log-normal distributions.	48
3.6	Probability distribution curves of peak flows for mean rainfall intensities equal to 50 and 200 mm/hr.	50
3.7	Probability distribution curves of peak flows for rainfall durations equal to 600 and 1300 seconds.	51
3.8	Probability distribution curves of peak flows for slopes of planes equal to 0.01 and 0.08.	52
3.9	Probability distribution curves of peak flows for roughness of planes equal to 0.02 and 0.007.	53
3.10	Probability distribution curves of peak flows for lengths of planes equal to 500 and 175 metres.	54
3.11	$Cs(q_p) - Cv(q_p)$ relationships for a plane with $f(i)$: Normal.	56
3.12	Rainfall intensity-peak flow curve for given plane and rainfall characteristics.	58
3.13	Geometrical transformation of a Normal $f(i)$ into $g(q_p)$ for 3 $i - q_p$ shapes.	59
3.14	$Cs(q_p) - Cv(q_p)$ relationships for a plane with $f(i)$: Gamma.	60
3.15	Effect of model used to obtain peak runoff on the relationship between the statistical parameters of the peak runoff series.	62
3.16	Comparing exact probability distribution curve of peak runoff with Pearson Type III fit when $f(i)$ is Normal.	69
3.17	Comparing exact probability distribution curve of peak runoff with Pearson Type III fit when $f(i)$ is Gamma.	70
3.18	Peak flow and Intensity-Duration-Frequency curves.	73

3.19	Comparing $C_s - C_v$ relations of peak flows from constant duration rainfall inputs with those from correlated rainfall inputs when $f(i)$ is Gamma.	79
3.20	$C_s - C_v$ relationships of peak flows from pervious planes with $f(i)$: Normal and $h(f)$: Uniform.	81
3.21	$C_s - C_v$ relationships of peak flows from pervious planes with $f(i)$: Gamma and $h(f)$: Uniform.	83
3.22	$C_s - C_v$ relationships for maximum peak flows and for the corresponding effective rainfall intensities when rainfall inputs are correlated and include infiltration.	85
3.23	Return periods of peak flows and corresponding rainfall intensities from pervious planes under correlated rainfall inputs.	86
3.24	Effect of constant infiltration rate on the return periods of peak flows from correlated and spatially uniform rainfall.	88
3.25	Non-uniform rainfall and infiltration rates.	90
3.26	$C - C_v$ relationships of peak runoff from triangular temporal distributions of rainfall intensity when $f(i)$ is Normal.	92
3.27	$C_s - C_v$ relationships of peak runoff from triangular temporal distributions of rainfall intensity when $f(i)$ is Gamma.	93
3.28	Rainfall intensity-peak flow curves for temporally non-uniform rainfall intensity.	95
3.29	Infiltration curves for 3 soil types.	98
3.30	$C_s - C_v$ relationships of peak flows from non-uniform temporal distribution of rainfall intensities and infiltration rates for $f(i)$: Gamma.	99
3.31	Effect of non-uniform temporal distribution of rainfall intensity and constant infiltration rate on the return periods of maximum peak flows and the corresponding rainfall intensities when the rainfall inputs are correlated.	101
4.1	Gamma-type input flood hydrographs.	109
4.2	Crest profile of a flood wave (Henderson, 1966).	111
4.3	Stage-discharge curves for two shapes of flood hydrographs.	117
4.4	$C_s - C_v$ relationships of peak depth along the length of a stream for three types of time-to-peak-depth to peak-depth relationships.	119
4.5	Relationships between upstream and downstream peak flow depths along a stream for two types of time to peak depth-peak depth relationships.	121

4.6	$C_s - C_v$ curves of peak flows along a stream for two types of time to peak-peak depth relationships.	124
4.7	Schematic of a stream-plane configuration.	126
4.8	Change in C_s and C_v of peak flow pdf along the length of a stream for $f(i)$: Normal.	130
4.9	Change in C_s and C_v of peak flow pdf along the length of a stream for $f(i)$: Gamma.	131
4.10	$C_s - C_v$ curves of peak flows at three sections along a stream for a range of mean spatially uniform rainfall intensities with $f(i)$: Gamma.	135
4.11	Limiting region within which the coefficients of skewness and variation of the peak flow pdf can be expected to be found when $f(i)$ is Gamma with $C_v(i) = 0.3$	138
4.12	$C_s - C_v$ curves of peak flow pdfs from planes with non-uniform widths, slopes, and roughnesses when $f(i)$: Gamma.	140
4.13	$C_s - C_v$ curves of peak flow pdfs for spatially non-uniform rainfall intensity when $f(i)$: Gamma and $C_v(i) = 0.3$	142
4.14	$C_s - C_v$ curves of peak flow pdfs for temporally non-uniform rainfall intensity when $f(i)$: Gamma.	144
4.15	$C_s - C_v$ curves of peak flow pdfs along a stream for non-uniform rainfall and plane characteristics.	148
5.1	Schematic of flow at a confluence of streams.	156
5.2	Schematic of river system used in testing the explicit numerical scheme against the 1-D hydrodynamic model.	160
5.3	Comparison of hyrographs from the explicit numerical scheme with that from the 1-D hydrodynamic model.	161
5.4	Synthetic networks of order 2, 3, and 4 with each having a stream length ratio ≈ 1.5	166
5.5	$C_s - C_v$ relationships of peak runoff from synthetic networks of order 2, 3, and 4.	168
5.6	$C_s - C_v$ relationships of peak flows from networks of different stream-length ratios.	172
5.7	$C_s - C_v$ relationships of peak flows from two networks with non-uniform runoff contributing areas.	176
5.8	$C_s - C_v$ relationships of peak flows from networks under temporally non-uniform rainfall intensity.	178
5.9	$C_s - C_v$ relationships of peak flows from two networks under spatially non-uniform rainfall intensity.	180

5.10	$C_s - C_v$ relationships of peak flows from networks with non-uniform distribution of runoff-contributing areas and non-uniform distribution of rainfall intensities.	182
5.11	Return periods of maximum peak flows and corresponding rainfall intensities from two networks under uniform and correlated rainfall intensities.	185
5.12	Return periods of maximum peak flows and corresponding rainfall intensities from two networks with non-uniform distribution of runoff areas and under uniform correlated rainfall intensities.	188
5.13	Return periods of maximum peak flows and corresponding rainfall intensities from two networks under temporally non-uniform and correlated rainfall intensities with $p = 3/10$	190
5.14	Return periods of maximum peak flows and corresponding rainfall intensities from two networks under temporally non-uniform and correlated rainfall intensities with $p = 7/10$	191
5.15	Return periods of maximum peak flows and corresponding rainfall intensities from two networks under spatially non-uniform and correlated rainfall intensities.	193
5.16	Return periods of maximum peak flows and corresponding rainfall intensities from two networks under spatially and temporally non-uniform and correlated rainfall intensities. .	194
5.17	Return periods of maximum peak flows and corresponding rainfall intensities from network (1) under uniform and correlated rainfall intensities and constant infiltration rate.	196
5.18	Return periods of maximum peak flows and corresponding rainfall intensities from network (2) under uniform and correlated rainfall intensities and constant infiltration rate.	197
5.19	Return periods of maximum peak flows and corresponding rainfall intensities from network (1) under non-uniform distribution of runoff areas and non-uniform distribution of correlated rainfall intensities.	200
5.20	Return periods of maximum peak flows and corresponding rainfall intensities from network (2) under non-uniform distribution of runoff areas and non-uniform distribution of correlated rainfall intensities.	201

List of Tables

4.1	Characteristics of stream-plane configuration	139
4.2	Non-uniform rainfall and plane characteristics along length of stream	146
5.1	Characteristics of networks illustrated in Figure 5.4.	167
5.2	Characteristics of 6 synthetic networks with different stream length ratios	171
5.3	$C_s - C_v$ values for the nine networks listed in Tables 5.1 and 5.2 under mean rainfall intensities of 50 and 80 mm/hr.	174

Chapter 1

INTRODUCTION

1.1 General

During the past decades there has been a consistent increase in the use of areas close to rivers for agricultural, industrial, and recreational purposes. It is expected that this trend will continue, together with an expected increase in aggravation caused by floodings. Because of their engineering, economic, and social implications, it is important that these floods be made predictable both for short and long terms.

1.2 Deterministic and Statistical Approaches to Flood Prediction

A physically-based deterministic approach to the problem of flood prediction is based to some extent on Newtonian mechanics, that, given the initial state of a system and the forces acting on it, the state of the system for any future period can be accurately determined. The transformation of climatic and physiographic data into a discharge record at the desired location in a watershed can in principle be derived from the solution of the equations of motion, continuity, energy balance, etc. , with the appropriate boundary conditions. For simple boundary conditions the solution is already a matter of difficulty, while the solution for complex heterogeneous watersheds is not yet in sight. Furthermore, it is impossible to forecast

the hydrometeorological factors acting on a watershed for a long time ahead, for instance for the service life of hydraulic structures (say, 50 to 100 years). A purely deterministic approach, therefore, has a limited forecast range. Its advantage lies in the possibility of assessing the consequences of various input parameters and flood mitigating structures during the planning and design stages of a project.

A watershed has very many variables whose exact states along the time axis cannot be precisely determined, only their most probable states and possible fluctuations about the latter can be postulated. This alternative viewpoint forms the basis of the statistical approach to the analysis of floods. There are two steps to this method:

1. Estimation of the statistical parameters of the random peak flow series.
2. Selection of a probability distribution curve.

The main problem in this approach is associated with the special importance of low-frequency floods in engineering design. It is in this zone that the commonly used distributions such as the Normal, Gamma, Extreme-value, and Pearson III distributions exhibit large divergencies from one another. The selection of a distribution is sensitive to the amount of data available. When the peak flow records are short, as very often is the case, errors in the estimation of the statistical parameters and in the choice of the "proper" distribution can lead to serious under- or over-estimation of design floods.

1.3 Composite Deterministic-Statistical Approach

The deterministic and statistical approaches to flood prediction appear to be contradictory, but the difference is only conceptual. The presence of an element of uncertainty, as is the case in the statistical approach, does not deny the existence of cause-effect relationships in the physical processes generating the floods. A random effect is just as causally determined as a certain event, but differs from it in the character of its causes (Lebedev, 1958). It is the hypothesis of this dissertation that the prediction of floods (or any other hydrological variable) must involve both deterministic and statistical methods. Yevjevich (1972) states that

Future progress of hydrology may depend to a large extent on how these two approaches are combined for discovering, understanding, and generalizing hydrologic regularities of nature.

An approach based on the genetic relationships between runoff and its causative factors and on the probable combination and occurrence of these factors can significantly increase the amount of information on the nature of floods. The essence of this composite technique is to seek the statistical properties of the peak flows from the statistical properties of the inputs and the deterministic transformation of inputs into peak runoffs.

The relative degree of importance of the two approaches in the composite technique is determined by the forecast range required (Kalinin, 1971). For forecasts confined to some initial period of time during which the influence of the initial conditions is adequately strong and the meteorological factors are predictable with the required degree of accuracy, the deterministic part of the composite technique plays the major role. The statistical part takes account of observational errors and

evaluates the deviations from predicted values. The forecast range in this instance rarely exceeds a year. A fundamental principle in hydrology is the attenuating effects of time on the importance of initial conditions, i. e. , the longer the time from the start, the smaller is the effect of the initial state. The attenuation rate is relatively more rapid for the "smaller" watersheds. For forecasts for a period of time during which the initial conditions have lost their influence and meteorological factors are no longer predictable, statistical methods play the leading role. The role of the deterministic methods is

1. to provide a physical basis for the probability distribution curves of the random peak flow series.
2. to incorporate the effects of changes (man-made or otherwise) on the watershed.

The forecast range in this instance is practically unlimited but usually lies between 2 and 200 years. This thesis will deal solely with the latter type of forecast.

1.4 Objective and Scope of Study

The objective of this study is to determine the effects of climatic and physiographic characteristics of a watershed on the statistical parameters, especially the coefficients of variation and skewness, of the probability distribution of the peak flows from the watershed. These two coefficients are very important in the estimation of low-frequency peak flows. The study is limited to conceptual watersheds. A watershed is conceptualised as a network of streams, every stream having a runoff plane on each side. The streams are assumed to have rectangular cross-sections and to be prismatic. The runoff planes can be either impervious or pervious. In-

filtration rates may be constant for all rainfall events or be random variables. The climate is characterised by the intensity and duration of the rainfall. The probability distribution of the rainfall intensity is assumed known. The duration of the rainfall may be constant for all events or may be correlated with rainfall intensity. Monte Carlo technique is used to generate random series of rainfall intensity and infiltration values. The flow through the network is simulated for each event by a numerical solution of the equations of continuity and momentum at each time step. The numerical method employs an explicit finite difference scheme. The corresponding random series of peak flows are then obtained and analysed for their statistical parameters.

Two current methods of establishing a physical theory for the stochastic properties of peak flows are reviewed in Chapter 2. In Chapter 3, a composite deterministic-statistical approach is used to investigate the statistical properties of random peak flows from single runoff planes. The runoff plane is, in a hydraulic sense, the most basic component of a watershed. The objective in Chapter 4 is to determine the change that a combination of a single stream with one runoff plane on each side makes to the statistical parameters of the peak flows. In Chapter 5, the watershed in its most general form, i.e., a network of streams and planes, is considered. The overall objective is to determine if statistical patterns detected at the single plane level persist when the more complex watersheds are considered. The analysis should also provide some information on the extent of the effect of non-uniform rainfall and watershed characteristics. The conclusions reached are of course pertinent to conceptual watersheds and their extrapolations to natural watersheds are discussed.

Chapter 2

LITERATURE REVIEW

2.1 Physically-based Stochastic Hydrology

Yevjevich (1972) states that

... a simultaneous use of both deterministic and stochastic (statistical) methods of analysis and description of hydrologic processes in nature is necessary for producing the best scientific and practical information for hydrology ...

Klemes (1978) puts this idea into focus by defining a physically based stochastic theory of the hydrological cycle as one which seeks to deduce the stochastic properties of a hydrologic phenomenon from their physical causes rather than only to describe them and manipulate their characteristics. The simplicity and rationale of this concept, however, hide the difficulty of its application to the rainfall-runoff process. The difficulty stems mainly from the complexities of the two primary processes, precipitation and its transformation into runoff. A review of the literature reveals two conceptually different approaches to the formulation of a physical theory for the stochastic properties of peak flows from watersheds. They are the hydrodynamical and the geomorphoclimatic instantaneous unit hydrograph (GcIUH) approaches. In the hydrodynamical method, proposed by Eagleson (1971,1972), the flow in the watershed is described explicitly in terms of an approximate form of the fundamental equations of water flow, i.e., the equations of continuity and momentum. The rainfall and watershed are characterized by the probability distri-

butions of their respective parameters. After some assumptions and simplifications, Eagleson obtains an analytical solution for the probability density function (pdf) of peak flows. In the GcIUH method, advocated by Rodriguez-Iturbe and Valdes (1979), the instantaneous unit hydrograph (IUH) is interpreted as the pdf of the travel time that a drop of water, landing anywhere in the watershed, takes to reach the outlet, assuming that the time of travel in streams of a given order obeys the exponential distribution. The resulting GcIUH, characterized by its peak value and the time to the peak value, is a function of the velocity of flow at peak discharge from a 1st order watershed and some parameters of the watershed. The effective rainfall is treated as a stochastic variable and convoluted with the GcIUH to obtain an analytical solution for the pdf of peak flows. The difference between the hydrodynamical and GcIUH methods lies in the characterization of the transformation mechanism of rainfall into runoff. There is a direct link between rainfall and runoff in the hydrodynamical method, while, in the GcIUH approach the rainfall is related to the runoff through a probabilistic form of a response function. Once the transformation mechanism is formulated, finding the pdf of peak flows follows the same procedure in each case. In the next sections, these two methods are described in more detail and their outcomes discussed.

2.2 Hydrodynamical Approach

2.2.1 Stochastic Kinematic Wave Model

Eagleson (1971,1972) used an approximate form of the equations of continuity and momentum, the Kinematic Wave equations, on a conceptual watershed consisting

of one runoff plane on each side of a stream to study the effects of random variations in rainfall and watershed parameters on the pdf of peak flows. A schematic of the watershed is shown in Figure 2.1. The rainfall, watershed, and runoff were characterized as follows.

Rainfall Characteristics

The rainfall events were described in terms of their depths, durations and correlation between the two parameters. Stochasticity was introduced by describing the rainfall parameters in terms of their probability distributions. Eagleson expressed the marginal pdf of point rainfall duration, t_r , as

$$f(t_r) = \lambda \exp(-\lambda t_r), \quad t_r \geq 0 \quad (2.1)$$

The marginal pdf of the point rainfall depth, d , was expressed as

$$f(d) = \frac{k}{d^{1.5}} \quad (2.2)$$

The conditional pdf of point rainfall depth given the storm duration was written as

$$f(d | t_r) = \frac{\beta}{t_r} \exp(-\frac{\beta d}{t_r}), \quad t_r \geq 0, \quad d \geq 0 \quad (2.3)$$

For 546 storms (hourly rainfall) at Boston, Massachusetts, Eagleson found that the above distributions gave good fits. The parameters λ , k , and β were computed to be 0.13, 0.10, and 30 respectively, for t_r in hours and d in inches. The pdf of the time average point rainfall intensity, i_o , was defined as

$$f(i_o) = \frac{\delta F(i_o)}{\delta i_o} \quad (2.4)$$

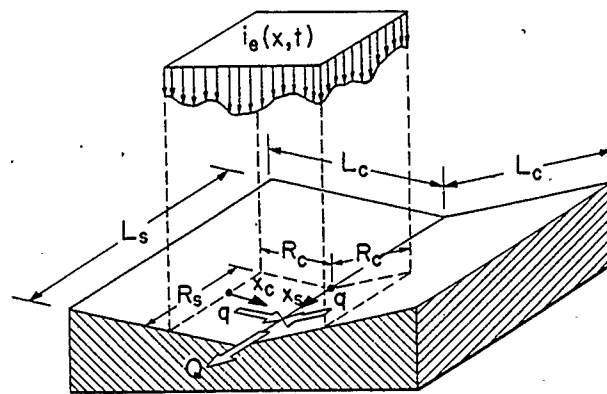


Figure 2.1: Schematic of a first-order watershed (Eagleson, 1971).

where

$$F(i_o) = \int_0^\infty dt_r \int_0^{i_o t_r} f(d, t_r) dd \quad (2.5)$$

and

$$f(\bar{d}, t_r) = f(d | t_r) \cdot f(t_r) \quad (2.6)$$

The point rainfall intensity was converted to an areal intensity by using the following correction factor :

$$\frac{d_A}{d} = 1 - \exp(-1.1t_r^{0.25}) + \exp(-1.1t_r^{0.25} - 0.01A) \quad (2.7)$$

where A is area in square miles and d_A is the areal average rainfall depth.

Assuming that d_A and t_r are independent of each other and approximating t_r by its average value, $\frac{1}{\lambda}$, Eagleson arrived at the following equation for the areal average intensity, \bar{i}_o ,

$$f(\bar{i}_o) = \frac{\beta}{k} \exp(-\frac{\beta \bar{i}_o}{k}), \quad \bar{i}_o \geq 0 \quad (2.8)$$

where

$$k = 1 - \exp(-\lambda^{-0.25}) + \exp(-\lambda^{-0.25} - 0.01A_c) \quad (2.9)$$

and A_c is the area of the catchment in square miles. For a given catchment it was assumed that infiltration, interception, and evaporation could be lumped into a single constant "loss" rate, ϕ . The areal average rainfall excess, \bar{i}_e , was then given by

$$\bar{i}_e = \bar{i}_o - \phi, \quad \phi < \bar{i}_o \quad (2.10)$$

For ϕ equal to a constant value, the pdf of \bar{i}_e was

$$f(\bar{i}_e) = \frac{\beta}{k} \exp(-\frac{\beta \bar{i}_e}{k}), \quad \bar{i}_e \geq 0 \quad (2.11)$$

The areal and temporal variability in the rainfall intensity was taken into account by defining a rainfall excess, i_e , as

$$i_e = \bar{i}_e + I(x_c, t) \quad (2.12)$$

where $I(x_c, t)$ is the fluctuating term in i_e representing the random temporal and areal variability and x_c is a coordinate of distance in the direction of overland flow. The fluctuating term $I(x_c, t)$ has a zero mean.

Watershed Characteristics

The only watershed characteristic considered by Eagleson was the area producing direct runoff. A probabilistic description of the direct runoff area, A_r , should be jointly expressed in terms of the geomorphological characteristics of the watershed, storm size, and antecedent moisture conditions accompanying a given storm. The form of such an equation is not known and Eagleson assumed a marginal triangular distribution for A_r which reflected a bias towards small fractions of the catchment area, A_c (Betson, 1964) :

$$f(A_r) = \frac{2}{A_c} \left(1 - \frac{A_r}{A_c}\right), \quad 0 \leq A_r \leq A_c \quad (2.13)$$

Rainfall-Runoff Transformation

The maximum discharge, Q_m , from the watershed was the only runoff parameters investigated. Eagleson identified two flow regimes for which Q_m had to be evaluated separately. Those were

1. Q_m when $t_{re} \geq t_*$
2. Q_m when $t_{re} < t_*$

where t_{re} is the duration of the areally averaged rainfall excess and t_* is the time of concentration of the combined overland-stream direct runoff area. To find the desired composite cumulative pdf of Q_m , $F(Q_m)$, Eagleson weighted the cumulative pdf of each flow regime with its cumulative pdf of occurrence.

$$F(Q_m) = F_1(Q_m)F(t_{re} \geq t_*) + F_2(Q_m)F(t_{re} < t_*) \quad (2.14)$$

The time of concentration of the combined overland-stream area t_* can be expressed as

$$t_* = t_c + t_s \quad (2.15)$$

or,

$$\frac{t_*}{t_c} = 1 + \frac{t_s}{t_c} \quad (2.16)$$

where, t_c is the time of concentration of overland direct runoff and t_s is the time of concentration of the stream segment within the direct runoff area. Eagleson approximated $\frac{t_*}{t_c}$ to 1 quoting Wooding (1966) who reported $\frac{t_s}{t_c}$ to be less than 0.5 for catchments of areas between 0.84 and 3383 sq. miles. Eagleson further assumed t_c to be smaller than t_{re} so that

$$F(t_{re} < t_*) = 0 \quad (2.17)$$

Hence

$$F(t_{re} \geq t_*) = 1 \quad (2.18)$$

and equation 2.14 becomes

$$F(Q_m) = F_1(Q_m) \quad (2.19)$$

Therefore Q_m for $t_{re} \geq t_*$ only need to be calculated. The derivation was as follows.

Eagleson used the Kinematic Wave equations to derive the relationship between peak flow and rainfall parameters, however, the condition $t_{re} \geq t_*$ requires that the overland peak flow is equal to the rainfall intensity to satisfy the equation of continuity. Therefore the maximum overland flow per unit width was

$$q_m = R_c \left(1 + \frac{\bar{I}(t_c)}{\bar{i}_e}\right) \bar{i}_e, \quad t_{re} \geq t_c \quad (2.20)$$

where R_c is a dimension (perpendicular to the stream) of the area producing direct runoff and $\bar{I}(t_c)$ is the fluctuating term, $I(x_c, t)$, averaged over t_c , assuming the temporal fluctuations to be independent of location.

Denoting R_s as a dimension (along the stream) of the area producing runoff and assuming the watershed to be symmetrical about the stream, Q_m was expressed as

$$Q_m = 2 \int_0^{R_s} q_m dx_s, \quad t_{re} \geq t_* \quad (2.21)$$

Assuming that $\frac{\bar{I}(t_c)}{\bar{i}_e} \ll 1$, Eagleson obtained the following equation

$$Q_m = 2R_s R_c \bar{i}_e, \quad t_{re} \geq t_* \quad (2.22)$$

or,

$$Q_m = A_r \bar{i}_e, \quad t_{re} \geq t_* \quad (2.23)$$

where A_r is the area producing direct runoff. When \bar{i}_e is in inches per hour and A_r in square miles, Q_m is given by

$$Q_m = 645 A_r \bar{i}_e, \quad t_{re} \geq t_* \quad (2.24)$$

Eagleson assumed the variability of A_r to be independent of time and dependent primarily on geomorphology. He then averaged Q_m over the population of runoff areas for a given catchment size :

$$\bar{Q}_m = \int^{A_r} Q_m f(A_r) dA_r \quad (2.25)$$

Hence,

$$\bar{Q}_m = 645 \bar{A}_r \bar{r}_e, \quad t_{re} \geq t_* \quad (2.26)$$

where, $\bar{A}_r = \frac{A_c}{3}$ from equation 2.13.

Probability Distribution of Peak Flows

Combining equations 2.11 and 2.26, Eagleson obtained the following equation for $F(\bar{Q}_m)$:

$$F(\bar{Q}_m) = \exp\left(-\frac{\beta \bar{Q}_m}{645k\bar{A}_r}\right) \quad (2.27)$$

Eagleson then converted equation 2.27 to include base flow and the resulting equation was expressed in terms of the return period of the peak flow.

$$\bar{Q}_p = \frac{215kA_c}{\beta} \ln(\phi_1 \phi_2 \theta T_E) + 0.074(1 - \phi_2) \phi_1 P A_c \quad (2.28)$$

where,

1. \bar{Q}_p = peak flow from watershed
2. A_c = watershed area (square miles)
3. ϕ_1 = fraction of rainfall occurring as runoff
4. ϕ_2 = fraction of runoff occurring as direct runoff
5. k = fraction of point rainfall occurring as areal rainfall
6. P = average annual rainfall (inches)

7. β = parameter of conditional distribution of rainstorm depth given duration (hours/inch)
8. θ = average annual number of independent rainfall events
9. T_E = recurrence interval of \bar{Q}_p

The equation given by equation 2.28 was then tested on two Connecticut catchments. The fit was best for T_E in the range $1 \leq T_E \leq 10$. At higher T_E s, equation 2.28 underestimated the peak flows by a considerable amount.

2.2.2 Comments on the Hydrodynamical Approach

The analysis as described above shows both the possibility of deriving the pdf of a hydrologic variable from the pdfs of its causative factors and also the difficulties involved in trying to obtain an analytical solution. It illustrates the fact that when one starts from such a fundamental level, then, a lot of assumptions and approximations are necessary to maintain mathematical tractability. In particular, Eagleson assumed statistical independence among variables which are known to be strongly interdependent, he approximated several random quantities by their averages and some distribution models were chosen on the basis of their easy integrability. He attributed the inaccuracy of the model at high return periods to the assumed distribution of A_r . He pointed out that the Kinematic Wave equations may not be appropriate in all cases. Klemes (1978) went even further by arguing that the relationship derived was prohibitively complex and superfluous in view of the uncertainties inherent in the parameters included in the analysis. He pointed out that a reduction in the average value of A_r from $1/2$ to $1/3$ of the catchment area resulted in an increase of the return period of a given peak flow from 10 years

to about 100 years. Wood (1976) replaced the constant "loss" rate ϕ with a random "loss" rate having a Uniform, Gamma, or Exponential distribution and reported that in a typical case, such a change affected the return period significantly.

While all the criticisms of Eagleson's approach may have some validity, they are levelled against the approximations made rather than the concept. And the approximations are necessary for an analytical solution. The necessity for analytical pdf transformations can be removed by working with the moments of the pdfs rather than their functional forms. Although a random variable is fully characterized by its pdf, the first few (e.g. three) moments of the pdf can in many cases provide just as much information on the random variable. The calculation of the moments can proceed through a Monte Carlo simulation of all the random variables involved. The only constraint is the computational time required for generating a sufficient number of the random variables and obtaining the peak flow for each input. With the high-speed computers available today (1988), the problem is not insurmountable. Furthermore, this approach allows the detailed study of the effects of each variable. This composite deterministic-statistical approach is adopted for the purposes of this dissertation because the physics of the hydrological process is explicitly included in the analysis and the numerical (Monte Carlo) procedure provides the flexibility to study the rainfall-runoff phenomenon from very simple runoff planes to complex river systems.

2.3 Geomorphoclimatic IUH Approach

Rodriguez-Iturbe and Valdes (1979) and Rodriguez-Iturbe and Gonzalez-Sanabrio (1982) have used the concept of the instantaneous unit hydrograph (IUH) to link the hydrologic response of a basin with its geomorphological parameters. The IUH which is equivalent to the unit impulse response function of the basin has been re-interpreted as the frequency distribution of the times of arrival at the outlet of the basin of water particles, given an instantaneous application of unit volume of rainfall excess uniformly spread over the basin at zero time. The influence of climatic factors is incorporated in the geomorphologic IUH (GIUH) by including the rainfall intensity i_r and the rainfall duration t_r . The peak and time to peak, q_p and t_p respectively, of a now geomorphoclimatic IUH (GcIUH) become random variables whose distributions depend on the geomorphology of the basin and climate specified through the pdfs of i_r and t_r . The GcIUH is convoluted with random rainfall parameters to obtain the pdf of peak discharges. Cordova and Rodriguez-Iturbe (1983) have used with some success this GcIUH concept for the estimation of extreme flow probabilities on some basins in Venezuela.

2.3.1 Geomorphologic IUH

Figure 2.2 illustrates a 3rd order basin (Strahler's ordering system) and its trapping state which is an imaginary 4th order stream represented by a bucket collecting the output from the basin. The imaginary stream must be distinct from the highest stream order and therefore has an order one unit higher than that of the basin. Assume that a unit volume of rainfall excess uniformly distributed over the basin

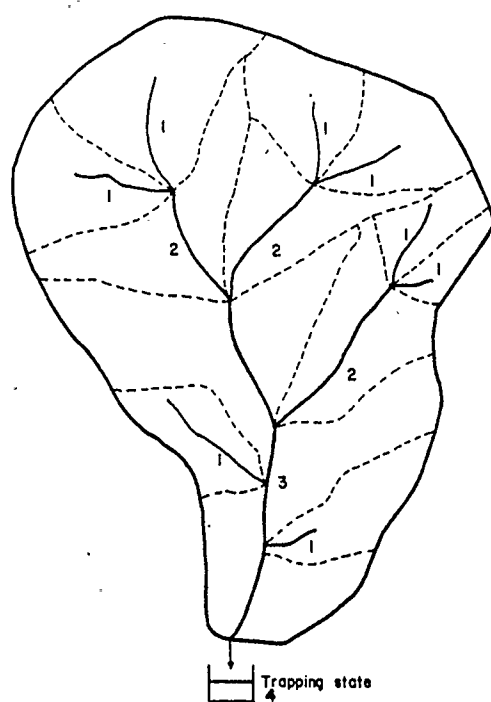


Figure 2.2: A third-order basin and its trapping state (Rodriguez-Iturbe and Valdes, 1979).

is instantaneously imposed upon it. The IUH at the outlet is the time derivative of the observed cumulative volume of water in the bucket. A probabilistic approach to the same system looks for the probability that a rainfall drop chosen at random from the input has reached the bucket at time t . For the 3rd order basin shown in Figure 2.2, this probability is given by

$$\theta_4(t) = \theta_1(0) \cdot \phi_{14}(t) + \theta_2(0) \cdot \phi_{24}(t) + \theta_3(0) \cdot \phi_{34}(t) \quad (2.29)$$

The terms in the equation 2.29 are defined as follows :

1. $\theta_i(t)$ = probability that the drop is in a stream of order i at time t (the bucket is of order 4)
2. $\theta_i(0)$ = probability that the drop is in a stream of order i at time $t = 0$ ($\theta_4(0) = 0$)
3. $\phi_{ij}(t)$ = probability that the drop goes from a stream of order i to one of order j in a time interval t

The geomorphological structure of the basin plays an explicit role in the evaluation of these probabilities.

For a uniformly distributed rainfall over the whole basin area,

$$\theta_i(0) = \frac{A_i^*}{A_T} \quad (2.30)$$

where A_i^* ($i = 1, 2, 3$) represents the total area of order i draining directly in a stream of order i and A_T is the total area of the basin. From Horton's laws of stream numbers, stream lengths, and stream area the following expressions are derived :

$$\theta_1(0) = \frac{A_1^*}{A_T} = \frac{R_B^2}{R_A^2} \quad (2.31)$$

$$\theta_2(0) = \frac{A_2^*}{A_T} = \frac{R_B}{R_A} - \frac{R_B^3 + 2R_B^2 - 2R_B}{R_A^2(2R_B - 1)} \quad (2.32)$$

$$\theta_3(0) = \frac{A_3^*}{A_T} = 1 - \frac{R_B}{R_A} - \frac{1}{R_A^2} \left(\frac{R_B[R_B^2 - 3R_B + 2]}{2R_B - 1} \right) \quad (2.33)$$

where R_B is the stream bifurcation ratio and R_A is the area ratio. These parameters are defined and explained in section 5.3.1.

The probability $\phi_{ij}(t)$ depends on (1) $\frac{1}{\lambda_i}$, the mean waiting time in a stream of order i and (2) p_{ij} , the probability that the drop makes a transition from a stream of order i to one of order j . The random holding time τ_i that a drop spends in state i is assumed to be independent of its next destination and to be exponentially distributed. The waiting time density is then given by

$$\omega_i(\tau) = \lambda_i \exp(-\lambda_i \tau) \quad (2.34)$$

By defining an average streamflow velocity for the whole basin as ν , λ_1 can be evaluated from

$$\lambda_1 = \frac{\nu}{\bar{L}_1} \quad (2.35)$$

where \bar{L}_1 is the mean length of streams of order 1. Similarly, for streams of order i ($i > 1$),

$$\lambda_i = \frac{\lambda_1}{R_L^{(i-1)}}, \quad i > 1 \quad (2.36)$$

where R_L is the stream length ratio. ν introduces a dynamic parameter in the formulation of the IUH. The reciprocal values of λ can be collected in a matrix Λ .

p_{1i} , the probability that a drop moves from state 1 to state i , is defined in terms of the structure of the drainage network as

$$p_{1i} = \frac{\text{no. of streams of order 1 draining into streams of order } i}{\text{total no. of streams of order } i} \quad (2.37)$$

The probabilities p_{12} and p_{13} can be written in terms of Horton's geomorphological parameters as

$$p_{12} = \frac{R_B^2 + 2R_B - 2}{2R_B^2 - R_B} \quad (2.38)$$

$$p_{13} = \frac{R_B^2 - 3R_B + 2}{2R_B^2 - R_B} \quad (2.39)$$

The p_{ij} values can be collected in a transition probability matrix P .

By defining a transition rate matrix as

$$A = \Lambda(P - I) \quad (2.40)$$

where I is the identity matrix, the interval transition probability matrix becomes

$$\Phi(t) = \exp(At) \quad (2.41)$$

Since the IUH is the time derivative of the volume of water in the bucket, therefore, the IUH for the 3rd order basin depicted in Figure 2.2 is

$$IUH(t) = \frac{d\theta_4(t)}{dt} = \theta_1(0) \cdot \frac{d\phi_{14}(t)}{dt} + \theta_2(0) \cdot \frac{d\phi_{24}(t)}{dt} + \theta_3(0) \cdot \frac{d\phi_{34}(t)}{dt} \quad (2.42)$$

The solution of equation 2.42 gives IUH(t), the pdf of the time of arrival of a randomly chosen raindrop to the trapping state, in terms of the geomorphological characteristics of the basin shown in Figure 2.2. The main characteristics of the GIUH are its peak and the time to peak. Using regression analysis on the outcomes from simulating a range of basin parameters, Rodriguez-Iturbe and Valdes (1979) generalize their results to

$$q_p = \frac{1.31}{L_\Omega} R_L^{0.43} \nu \quad (2.43)$$

$$t_p = \frac{0.44 L_\Omega}{\nu} \left(\frac{R_B}{R_A} \right)^{0.55} \frac{1}{R_L^{0.38}} \quad (2.44)$$

where Ω is the order of the basin and ν is an assumed average stream velocity for the whole basin. The GIUH as defined by equations 2.43 and 2.44 was tested against IUH obtained from direct rainfall-runoff simulations and were found to be reasonably accurate.

2.3.2 Geomorphoclimatic IUH

Introduction of the rainfall parameters through the velocity parameter ν transforms the GIUH into the Geomorphoclimatic IUH (GcIUH). The velocity parameter ν at a given time during a spatially uniform storm over a basin has been found to be reasonably constant (Pilgrim, 1977). ν can then be expressed analytically as a function of i_r , the intensity of the effective rainfall, t_r , the duration of the rainfall, and the geomorphological characteristics of the first order basin. Rodriguez-Iturbe and Valdes (1979) then assumed that the duration of the rainfall t_r exceeds the time of concentration t_c of the first order basin. This means that ν is now the peak velocity from a first order basin and is calculated as follows :

$$\nu = ki_r^\xi \quad (2.45)$$

where

$$k = \alpha_1^{1/m_s} A_1^{(m_s - 1)/m_s} \quad (2.46)$$

$$\alpha_1 = \frac{\sqrt{S_1}}{n} \quad (2.47)$$

$$m_s = \frac{5}{3} \quad (2.48)$$

$$\xi = (m_s - 1)/m_s \quad (2.49)$$

The subscript 1 refers to the first order basin, S is the slope of the corresponding stream and n its roughness coefficient.

The parameters of the first order basin are related to those of the highest order (Ω) basin according to the following :

$$\alpha_1 = \alpha_\Omega (R_A^\Omega - 1)^{m_s - 1} \quad (2.50)$$

$$\bar{A}_1 = A_\Omega R_A^{1 - \Omega} \quad (2.51)$$

After approximating $\frac{R_B}{R_A}$ to 0.80 and some algebraic manipulations Rodriguez-Iturbe and Valdes (1979) expressed the characteristics of the GcIUH as

$$q_p = \frac{0.871}{\Pi_i^{0.4}} \quad (2.52)$$

$$t_p = 0.585 \Pi_i^{0.4} \quad (2.53)$$

where q_p and t_p are in 1/hr. and hours. Π_i is defined as

$$\Pi_i = \frac{L_\Omega^{2.5}}{i_e A_\Omega R_L \alpha_\Omega^{1.5}} \quad (2.54)$$

where L_Ω is the length of the stream of the highest order (km), A_Ω is the area of order Ω in km^2 , i_e is the effective rainfall intensity ($cm\ hr.^{-1}$), R_L is the stream length ratio, and α_Ω is the kinematic wave parameter for the stream of highest order defined by

$$\alpha_\Omega = \frac{\sqrt{S_\Omega}}{n_\Omega b_\Omega^{2/3}} \quad (2.55)$$

b is the width of the stream.

2.3.3 Stochastic GcIUH

When i_r and t_r are, as in nature, random variables whose pdfs represent the influence of climate, the GcIUH then becomes the stochastic unit impulse response

function of the basin. The pdfs of q_p and t_p , each defined by equations 2.43 and 2.44 respectively, were obtained as follows. The intensity and duration of effective rainfall were assumed to be independent random variables with an exponential distribution, a description which has been found to be satisfactory by Eagleson (1970, 1982). The distribution of the depth of rainfall, $h(i_r.t_r)$, is given by Eagleson (1982) as

$$f(h) = 4\beta\delta K_0\sqrt{\beta\delta h} \quad (2.56)$$

where K_0 is a modified Bessel function. For the case $t_r > t_c$ the pdf of the flow velocity ν is

$$f(\nu) = \frac{1}{k\xi} \left(\frac{\nu}{k}\right)^{(1-\xi)/\xi} f_{i_r} \left[\left(\frac{\nu}{k}\right)^{1/\xi}\right] \quad (2.57)$$

After some algebraic manipulations and simplifications the following pdfs for q_p and t_p were obtained :

$$f(q_p) = 3.534\Pi q_p^{1.5} \exp(-1.412\Pi q_p^{2.5}) \quad (2.58)$$

$$f(t_p) = \frac{0.656\Pi}{t_p^{3.5}} \exp\left(\frac{-0.262\Pi}{t_p^{2.5}}\right) \quad (2.59)$$

where

$$\Pi = L_\Omega^{2.5} / (i_r A_\Omega R_L \alpha_s^{1.5}) \quad (2.60)$$

The only parameter controlling both distributions is Π which is a function of both the climate and the geomorphology of the basin. The statistical characteristics of $f(q_p)$ and $f(t_p)$ are

$$E(q_p) = 0.774/\Pi^{0.4} \quad (2.61)$$

$$\sigma(q_p) = 0.327/\Pi^{0.4} \quad (2.62)$$

$$Cv(q_p) = 0.423 \quad (2.63)$$

$$E(t_p) = 0.858\Pi^{0.4} \quad (2.64)$$

$$\sigma(t_p) = 0.915\Pi^{0.4} \quad (2.65)$$

$$Cv(t_p) = 1.066 \quad (2.66)$$

It is noticed that the coefficient of variation (Cv) is a constant in both distributions, independent of climate and geomorphology.

2.3.4 Probabilities of Peak Flows using the GcIUH

The GcIUH allows the estimation of the unit impulse response function for a given particular input of effective rainfall. Rodriguez-Iturbe et al. (1982) assumed the GcIUH to be of a triangular shape with height q_p and time base t_p . Convoluting the triangular GcIUH with an effective rainfall intensity i_e and duration t_e , the following equation for peak discharge was obtained :

$$Q_p = 2.42 \left(\frac{i_e A_s t_e}{\Pi_i^{0.4}} \right) \left(1 - \frac{0.218 t_e}{\Pi_i^{0.4}} \right) \quad (2.67)$$

where t_e is in *hours*, Q_p in $m^3 s^{-1}$, and A_s is the site area in km^2 . Π_i has been defined in equation 2.54. Equation 2.67 is valid for t_e less than or equal to the time of concentration of the whole basin given by

$$t_c = \frac{2}{q_p} = 2.3\Pi_i^{0.4} \quad (2.68)$$

Through a combination of the Π_i , soil, and rainfall parameters, equation 2.67 was used by Cordova and Rodriguez-Iturbe (1983) to estimate the return periods of peak flows from a basin in Venezuela. The results from a GcIUH approach

was compared with historical records (26 years of data) and found to be reasonable as long as the "correct" CN (U.S. Soil Conservation Service Curve Number), (U.S.B.R. , 1965) value for the soil characteristics was used.

2.3.5 Comments on the GcIUH Approach

The GcIUH approach has been explored by other investigators such as Gupta et al. (1980), Wang and Gupta (1981), Kirshen and Bras (1983), and Diaz-Grandos et al. (1984). The basic approach by all of them is not very different from the GcIUH, the essence of which is to develop a rainfall-runoff response function and convolute the latter with stochastic rainfall parameters to analytically obtain the pdfs for peak flows. The analyses indicate that this approach gives reasonable results when compared to historical records of peak flows. However, the "goodness of fit" depends very much on the selection of the proper values for such parameters as the Curve Number, average values for slopes and roughness coefficients, topological characteristics of river network, etc.. This is not unexpected because these parameters determine the most important characteristics of a pdf, i.e. its mean value. The determination of the mean peak runoff cannot be expected to be accurate if it is determined by a lumped approach, which is the case with a probabilistic IUH. The assumption of a constant velocity throughout the basin for a given discharge may be valid on an "average" basis but is certainly not correct for every form and shape of a watershed. Furthermore, there is no physical basis for the choice of an exponential pdf for the probability distribution of the velocity. These deficiencies make the approach difficult to use to investigate the detailed effects of non-uniform rainfall parameters, the changes in the pdfs along the river

network, and the effects of artificial changes to the streams.

As pointed out in section 2.2.2, the necessity for an analytical solution of the peak flow pdf is not very important. Very slight changes to the shape of a pdf can drastically change the equation form of the pdf. The moments of a pdf are more robust descriptors of the random variations in a variable. Changes in the magnitudes of the moments are more easy to interpret than changes in the equations of pdfs. This is especially important when investigating the changes in flood probabilities along a river system.

2.4 Summary

Two methods of establishing a physical basis for the stochastic properties of peak flows have been reviewed. The hydrodynamic approach, proposed by Eagleson (1971,1972) uses the Kinematic Wave equations to deterministically relate rainfall intensity to peak flow from an impervious stream-plane catchment. Then, assuming an exponential pdf for both rainfall depth and rainfall duration, Eagleson derives an equation for the pdf of peak flow. The resulting equation performs well only for return periods less than 10 years when tested on two Connecticut, USA catchments. The "lack of fit" is attributed to the assumptions and simplifications in the search for an analytical solution.

The second method, proposed by Rodrigues-Iturbe and Valdes (1979), is less direct than the hydrodynamic approach. A geomorphoclimatic IUH is derived based on a probabilistic interpretation of the motion of water "particles" through the network of streams of a river system. The GcIUH is then convoluted with

random effective rainfall intensities and rainfall durations to determine the return period of peak flows. The accuracy of this method depends on a "correct" selection of the CN value for the soil characteristics.

The main advantage of the hydrodynamic approach lies in the possibility of assessing the effects of individual parameters involved in the rainfall-runoff process. However, mathematical difficulties prevent an expansion of the method in its present form to more complicated watersheds. The GcIUH approach is better suited to deal with real-scale watersheds, but the generalisation necessary to derive a probabilistic IUH limits its use in the study of the effects of individual parameters in the rainfall-runoff process.

Chapter 3

STATISTICAL CHARACTERISTICS OF RANDOM PEAK FLOWS FROM SINGLE PLANES

3.1 Introduction

A necessary step in the design of regulatory and service structures across streams is the identification and description of statistical patterns in random peak flow series. When "sufficient" data on peak flows are available at the desired location, standard frequency analysis may be adequate. This situation is more the exception than the rule. As yet, sufficiently rigorous methods for a theoretical determination of the probability density function (pdf) of the peak runoffs are not available. It is the hypothesis of this dissertation that a composite deterministic-statistical approach to the rainfall-runoff transformation process can suggest the presence of certain regularities in the statistical characteristics of peak flows and hence become an important source of supplementary information on peak runoff frequencies. This approach is based on the genetic relationships between runoff and the probable combination of its causative factors. The rainfall-runoff transformation process is governed by the deterministic equations of flow and the external hydrometeorological factors are formulated in terms of their pdfs. The physiographic structure of the watershed is explicitly incorporated within the transformation process. Under

some simplifying assumptions an analytical solution of the peak flow pdf is possible. In the majority of cases Monte Carlo simulation of the hydrometeorological factors and numerical solution of the governing equations of flow are used to obtain random peak runoff series. The latter can then be analysed for inherent patterns using standard statistical techniques.

In general, the pdf of peak runoffs can take an infinite variety of forms depending upon the physical and probabilistic structures of each and every component in the rainfall-runoff process. A study of the statistical nature of random peak runoff series at an elemental level is then necessary to evaluate the intrinsic form of the peak runoff probability curve. In a hydraulic sense, the sloping terrain along the sides of a stream forms the basic unit in the physiographic description of a watershed. These units are interconnected in a tree-like pattern to form a river system. The runoff from any one basic unit is dependent only upon the terrain and rainfall characteristics and is not affected by the other units and streams. The sloping terrain is then a convenient starting place to study the statistical characteristics of random peak flow series. It is conceptualized as a single rectangular plane of constant slope and roughness. The flow on the plane is assumed to be "sheet" flow and is analysed using the equations of continuity and momentum. In this chapter, the effects of storm, infiltration, and plane characteristics on the statistical parameters of random peak runoff series are investigated. The effects of streams and the connectivity patterns are described in the next chapters.

3.2 The Rainfall-Runoff Process on a Single Plane

A comprehensive study of the climatic and physiographic effects on the statistical relationships between rainfall and peak runoff would have to consider a physical system comprising the entire watershed, all its inputs and outputs, and all the laws governing their interactions. The mathematical difficulties involved in the solution of such a system are enormous. It therefore becomes necessary to use simplified mathematical formulations and to include only those components of the system which are essential to the specific objectives of the study. At the elemental level, the characteristics of the rainfall and plane are important factors in the formation of runoff. The specific output of interest is the instantaneous peak discharge at the end of the plane. Surface runoff is assumed to be the primary mode of water transport to the edge of the plane.

3.2.1 Characterization of Rainfall, Infiltration, and Runoff Plane

The key hydrometeorological variables in the genesis of peak flows are the rainfall intensity, rainfall duration, and infiltration rate. Each has to be described in terms of both its intrinsic physical and probabilistic structures. The latter is necessary because of present day impossibility of forecasting rainfall and antecedent soil moisture conditions for long periods into the future.

Recent research (Amorocho and Wu, 1977 and Lloyd et al., 1979) into the physical structure of rainstorms reveals complex precipitation fields generated by random and deterministic processes interacting in very intricate ways. For practical purposes, however, the degree of representational faithfulness of such a structure

need not be high because of the natural dampening effects of real watersheds. Thus, for some "large" watersheds, the banded structures of cyclonic rainstorms may be grossly equivalent in the production of runoff to areally uniform rains with the same mean intensities. On "smaller" watersheds, as on a single plane, similar rainstorms would be perceived as sequences of spatially and temporally non-uniform rainfalls. For the purposes of this study, the shape of the rainfall hyetograph will be either rectangular (temporally uniform intensity) or triangular (temporally non-uniform intensity). For triangular hyetographs, the peak intensity can occur at specified times along the duration axis. Although the peak intensities occur at random times for natural rainstorms, they will be assumed to be constant and known for every series of simulated rainstorms. Spatially non-uniform rainfall is simulated by assigning different mean intensities to various locations in the precipitation field.

Infiltration is defined as the movement of water through the soil surface into the ground. The rate of infiltration is very difficult to evaluate because it depends on many factors and varies both temporally and spatially. General observations on infiltration rates indicate that they are highest at the beginning of the rainfall. The rate decreases rapidly at first because of changes in the surface soil structure and increases in the surface soil moisture content, and then gradually approaches a somewhat stable minimum. Overland flow is generated during the periods that the rainfall rate is higher than the infiltration rate. The extreme complexity of the infiltration process has hindered exact solutions. Of the semi-empirical equations, Horton's equation is one of the simpler and better known. It is given by

$$f = f_c + (f_o - f_c)e^{-f_k t} \quad (3.1)$$

where f is the infiltration rate (mm/hr) at time t (s), f_0 is its value at $t = 0$, f_c is the infiltration capacity at infinite t , and f_k is a decay constant. f_0 depends on the initial soil moisture conditions and f_c and f_k are dependent on the soil types and to a smaller extent on the rainfall rate. Figure 3.1 shows a typical plot of the infiltration rate superimposed on the rainfall hyetograph. It is assumed that at t less than t_{of} all the rainfall is lost to infiltration and overland flow begins at t_{of} . In Figure 3.1 the value of f_0 is taken as that of f at $t = t_{of}$. The volume of the surface runoff is given by the shaded area. A simple way of representing infiltration curve would be to assume a constant rate (f_c) over the duration of the rainfall.

The probabilistic structures of the rainfall and infiltration parameters can take many forms reflecting the great diversity in meteorological and soil conditions. Physically-based probability distributions for these parameters are still lacking. Uncertainty about their probabilistic structures necessitates some empirical assumptions about their pdfs. As far as rainfall parameters are concerned, their distribution curves can be empirically obtained from a frequency analysis of their respective records, since such records are usually more plentiful and more accurate than runoff records. Also, since they have not been affected by the more complex processes operating on a watershed, they may be assumed to have simpler probabilistic structures than those of peak runoffs. In this study, the pdf of the rainfall intensity will be either the Normal, Gamma or Gumbel distributions. Since a random variable with a Normal distribution can be negative, therefore the coefficient of variation of a Normal pdf of rainfall intensity is chosen such that the probability of a negative rainfall intensity is negligible. The upper limit of the coefficient of variation for this case is 0.3. A special case of the Gamma distribution,

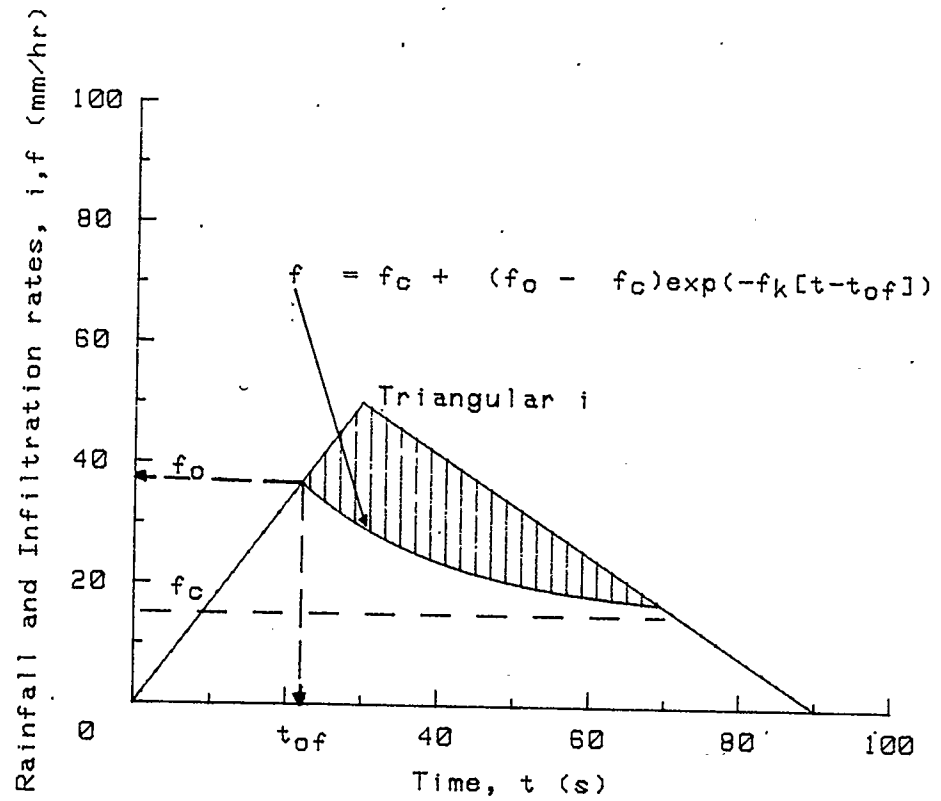


Figure 3.1: Typical plot of rainfall hyetograph and infiltration curve.

the Exponential distribution, has been extensively used by several investigators for describing the pdf of rainfall intensity. The pdfs of the infiltration parameters (f_o, f_c) are arbitrarily assumed to be independent of the rainfall pdfs and to have the Uniform distributions. The decay parameter f_k is assumed to be a known constant for a given soil type. In some instances, it is assumed that the infiltration rate is a constant for all rainfall events.

The transformation mechanism in the genesis of peak flows from rainfall is a direct function of the physical characteristics of the watershed. For a plane these characteristics are its runoff length, slope, and roughness. The slope and roughness will be assumed to be constant during all simulated rainfall events.

3.2.2 Modelling of Surface Flow over a Single Plane

In its simplest form, the basic watershed is represented by a single impervious sloping plane and the surface runoff is then a thin sheet of flow called overland flow. A schematic of the system is shown in Figure 3.2. After neglecting minor contributions such as the momentum of the raindrops and the effect of the vertical distribution of the flow velocity at a section, and approximating the surface slope $S_o \approx \sin\theta \approx \tan\theta$, (Raudkivi, 1979), the x -component of the equation of motion becomes

$$\frac{1}{g} \frac{\delta u}{\delta t} + \frac{u}{g} \frac{\delta u}{\delta x} + \frac{\delta y}{\delta x} + \frac{i}{gy} = S_o - S_f \quad (3.2)$$

and the continuity equation becomes

$$\frac{\delta y}{\delta t} + \frac{\delta q}{\delta x} = i \quad (3.3)$$

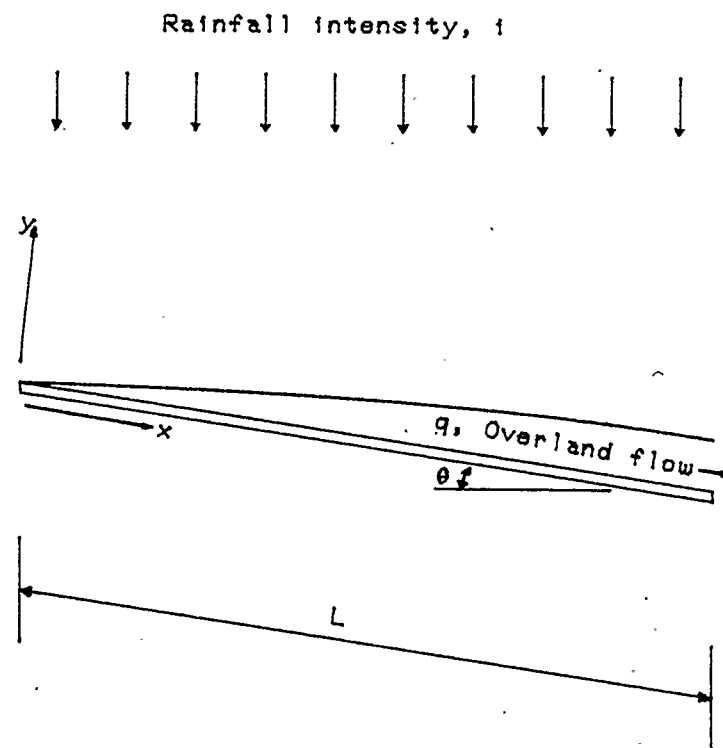


Figure 3.2: Definition sketch of flow over a sloping plane.

where i is the rainfall intensity, y is the flow depth normal to the plane, q ($= uy$) is the outflow per unit width of the plane, u is the average flow velocity in the x -direction, S_o is the slope of the plane, and S_f is the friction slope. The St. Venant equations as equations 3.2 and 3.3 are commonly known as, can only be solved numerically for a general case.

Kinematic Wave Model

Experience with the St. Venant equations has shown that for certain situations some terms in equation 3.2 can become insignificant relative to the others. For example, Overton (1970) has shown that for planes with long runoff lengths, steep slopes, and high rainfall intensities all the terms on the left hand side of equation 3.2 are negligible compared to the terms on the right hand side such that

$$S_o = S_f \quad (3.4)$$

Equation 3.4 implies that the discharge is now a function of flow depth only and in general is given by

$$q = \alpha y^m \quad (3.5)$$

For laminar flow,

$$q = \frac{gS_o}{3\nu} y^3 \quad (3.6)$$

in which ν is the kinematic viscosity. For turbulent flow,

$$q = \frac{\sqrt{S_o}}{n} y^{5/3} \quad (3.7)$$

in which n is the Manning's coefficient of roughness. Equations 3.3 and 3.5 are the so-called Kinematic Wave equations of flow and have been treated by Lighthill and

Whitham (1955). For flow over a single plane due to a constant rainfall intensity the solution of the Kinematic Wave equations gives the peak flow per unit width q_p as

$$q_p = \alpha(i t_o)^m, \quad t_o < t_s \quad (3.8)$$

and

$$q_p = Li, \quad t_o \geq t_s \quad (3.9)$$

where t_o is the duration of the rainfall, L is the length of the runoff plane in the direction of flow, and t_s is the time taken to reach steady state of flow. t_s is given by

$$t_s = \left(\frac{L}{\alpha i^{(m-1)}} \right)^{1/m} \quad (3.10)$$

Equations 3.8 and 3.9 give a deterministic relationship between rainfall intensity i and peak flow q_p when the Kinematic Wave model is assumed to represent the surface runoff process.

Diffusion Wave Model

For the Kinematic Wave model, all the terms on the left hand side of equation 3.2 are neglected. According to Henderson (1966), the next most significant term is the water surface slope $\frac{\delta y}{\delta x}$. Inclusion of this term gives the Diffusion Wave model of flow, and the momentum equation becomes

$$S_f = S_o - \frac{\delta y}{\delta x} \quad (3.11)$$

Together with equation 3.3 representing conservation of mass, equation 3.11 describes the surface flow. In this system of equations, in contrast to the Kinematic Wave equations, the flow is dependent upon the backwater effects and hence takes

account of the past history of the flow build-up. Such a model has been used by Muzik (1974, 1976) to model the flow over a sloping impervious plane. The Diffusion Wave equations were solved numerically and the results were found to closely approximate experimental data.

The numerical procedure is an explicit finite difference scheme and is as follows. The unsteady spatially varied flow due to rain falling on a sloping impervious plane is computed by dividing the plane into a number of reaches as shown in Figure 3.3. The flow in each reach is assumed to be of uniform depth so that the water surface in each reach is always parallel to the plane's surface. The friction slope S_f serves as a bond of interaction between reaches. Assuming slowly varying flow and a sufficiently short distance increment Δx , the friction slope at the beginning of each time step may be approximated by

$$S_{f,j} = S_o + \frac{y_j - 1 - y_j + 1}{2\Delta x} \quad (3.12)$$

The flow from one reach into another is expressed for laminar flow as

$$q_j = \frac{g}{3\nu} S_{f,j} y_j^3 \quad (3.13)$$

and for turbulent flow as

$$q_j = \frac{\sqrt{S_{f,j}}}{n} y_j^{5/3} \quad (3.14)$$

The roughness coefficient n is assumed to be constant both spatially and temporally. The continuity equation for the j^{th} reach written in finite difference form is

$$\Delta y_j = (i_j + \frac{q_j - 1 - q_j}{\Delta x}) \Delta t \quad (3.15)$$

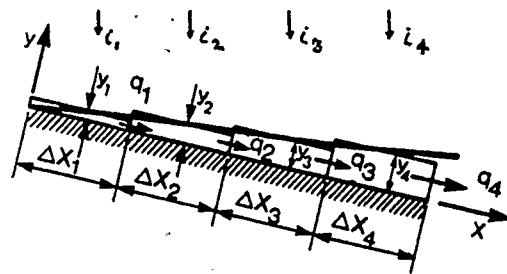


Figure 3.3: Representation of overland flow by a series of reaches with uniform depths of flow (Muzik, 1974).

in which Δy is the change in the flow depth during the time interval Δt , i_j is the rainfall intensity on the j^{th} reach, q_{j-1} and q_j are the inflow and outflow per unit width of the reach respectively, and Δx is the length of the reach. The downstream boundary condition is specified through Manning's uniform flow equation (equation 3.7). Given the initial and boundary conditions of the system, the outflow from the last reach can be calculated for every time increment and hence the peak flow for any rainfall of given intensity and duration can be obtained. The Courant condition for stability of the scheme is given by

$$\frac{\Delta t}{\Delta x} \leq \frac{1}{u + \sqrt{gy}} \quad (3.16)$$

Semi-empirical Solution to the Diffusion Wave Equations

In the general case, the Diffusion Wave equations can only be solved numerically and a complete simulation over the duration of the runoff is necessary to obtain the peak runoff. For the special case of a system with uniform rainfall intensity (spatially and temporally) of a constant duration over an impervious rectangular plane of constant slope and roughness a semi-empirical equation relating peak flow to the system characteristics has been obtained. For planes of various lengths (L), slopes (S_o), roughnesses (n), and rainfall of various intensities (i), and durations (t_o), the resulting peak flows (q_p) were obtained by numerically solving the Diffusion Wave equations assuming turbulent flow conditions. When $\frac{q_p}{i}$ is plotted against $i^{0.4} t_o (\frac{\sqrt{S_o}}{nL})^{0.6}$ a dimensionless curve, relatively unchangeable over a wide range of plane and rainfall characteristics, is obtained and is shown in Figure 3.4. The curve corresponding to a semi-empirical equation approximating the numerical solution is also shown in Figure 3.4, together with the analytical solution to

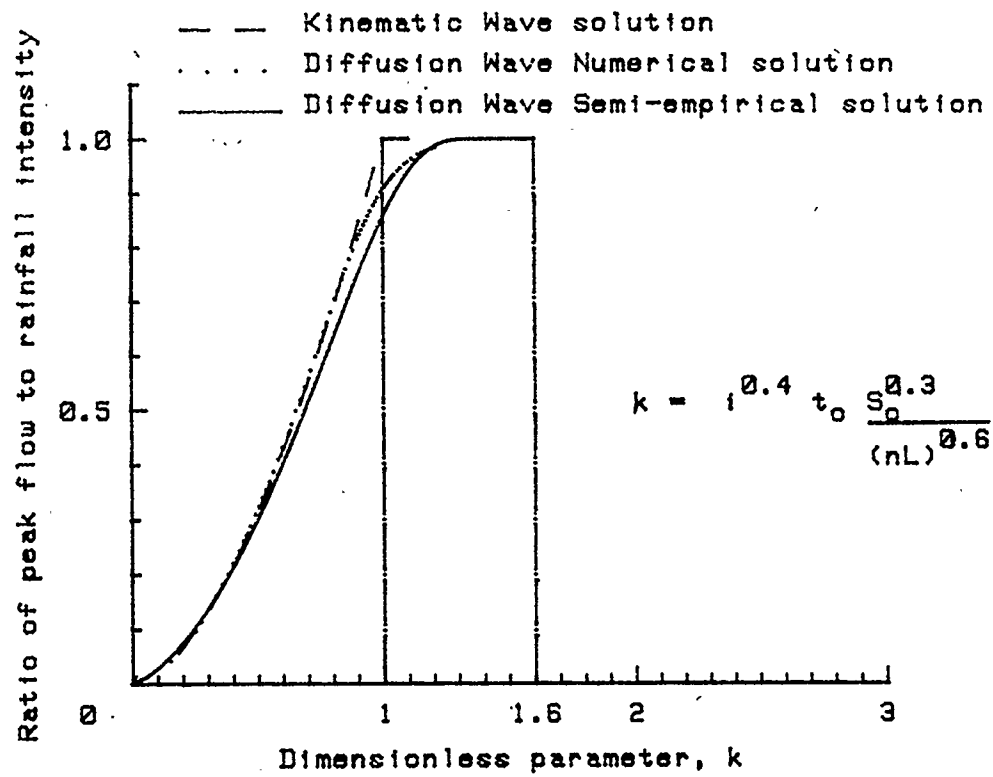


Figure 3.4: Dimensionless curves for the Kinematic and Diffusion models.

the Kinematic Wave equations. The semi-empirical equation is deduced from a consideration of the time to steady state, i.e., the time taken for a "particle" of water to travel the length of the runoff plane.

For the Kinematic model, the time to steady state assuming turbulent flow is given by

$$t_s = \left(\frac{Ln}{\sqrt{S_o}} \right)^{3/5} \frac{1}{i^{2/5}} \quad (3.17)$$

An approximate time to equilibrium for the Diffusion model is obtained as follows.

At steady state the flow at a distance x from upstream is

$$q(x) = ix \quad (3.18)$$

Manning's formula for normal flow at a distance x from upstream is

$$q(x) = \frac{\sqrt{S_o}}{n} y(x)^{5/3} \quad (3.19)$$

where $y(x)$ is the depth at x . Upon eliminating $q(x)$ from equations 3.18 and 3.19, the depth profile at steady state is

$$y(x) = \left(\frac{n}{\sqrt{S_o}} \right)^{3/5} i^{3/5} x^{3/5} \quad (3.20)$$

The velocity of flow at x is

$$v(x) = \frac{\sqrt{S_o}}{n} y(x)^{2/3} \quad (3.21)$$

Substituting $y(x)$ from equation 3.20 into equation 3.21 gives the velocity of flow at x as

$$v(x) = \left(\frac{\sqrt{S_o}}{n} \right)^{3/5} i^{2/5} x^{2/5} \quad (3.22)$$

The time t_e taken by a "particle" to reach $(x = L)$ from $(x = 0)$ is

$$\begin{aligned}
\int_0^{t_e} \delta t &= \int_0^L \frac{\delta x}{v(x)} \\
t_e &= \int_0^L \left(\frac{n}{\sqrt{S_o}} \right)^{3/5} \frac{1}{i^{2/5}} x^{-2/5} \delta x \\
t_e &= \left(\frac{n}{\sqrt{S_o}} \right)^{3/5} \frac{1}{i^{2/5}} \frac{5}{3} L^{3/5} \\
t_e &= \frac{5}{3} \left(\frac{nL}{\sqrt{S_o}} \right)^{3/5} \frac{1}{i^{2/5}}
\end{aligned} \tag{3.23}$$

Comparing equations 3.17 and 3.23 the following expression between t_e and t_s is obtained

$$t_e = 1.667 t_s \tag{3.24}$$

Figure 3.4 indicates that $\frac{t_e}{t_s}$ is approximately equal to 1.6.

The semi-empirical equation fitting the Diffusion model curve is

$$\frac{qp}{i} = 1 - \exp\left[-\left(\frac{k}{1.6 - k}\right)^{1.3}\right], \quad k < 1.6 \tag{3.25}$$

where

$$k = i^{0.4} t_o \left(\frac{\sqrt{S_o}}{nL} \right)^{3/5} \tag{3.26}$$

For $k \geq 1.6$,

$$\frac{qp}{i} = 1 \tag{3.27}$$

The numbers 1.6 and 1.3 are the only empirically fitted parameters. The number 1.6 has been shown to be close to an approximate analytical solution (1.667). It will be shown in the next section that the number 1.3 is also close to an approximate analytical solution. For the Kinematic model, the corresponding analytical equations for the curve are

$$\frac{qp}{i} = k^{5/3}, \quad k < 1 \tag{3.28}$$

and

$$\frac{qp}{i} = 1, \quad k \geq 1 \quad (3.29)$$

Figure 3.4 shows that while the Kinematic curve has a continuously increasing gradient until steady state is reached, each of the Diffusion curves (numerical and semi-empirical) possesses a point of inflexion and reaches steady state values gradually. The latter properties are characteristics of "real" flow conditions. The curves coincide with one another at low values of $i^{0.4} t_o (\frac{\sqrt{S_o}}{nL})^{0.6}$, i.e., for cases with low rainfall intensities, short rainfall durations, shallow slopes, long runoff lengths and low values for surface roughness. The curves, however, show some divergencies close to steady state conditions. The Diffusion models predict longer times to steady state than the Kinematic model does. The accuracy of the semi-empirical diffusion equations and the Kinematic Wave equations relative to the numerical solution of the Diffusion Wave equations as far as the statistical parameters of peak flows are concerned are discussed in section 3.3.1.

For a simple system consisting of uniform rainfall intensity over a plane with constant length, slope, and roughness equations 3.25, 3.26, and 3.27 can be used to obtain the peak flow directly without a numerical solution of the Diffusion Wave equations.

3.3 Intrinsic Nature of a Probabilistic Rainfall-Peak Flow Process for a Single Plane

For a real watershed the statistical relationships between rainfall and peak flow can take an infinite variety of forms depending upon the physical and probabilistic

structures of each contributing factor. To evaluate the intrinsic nature of that relationship it is necessary to reduce the number of contributing factors to a minimum while still retaining the essential character of a rainfall-runoff process. Uniform rainfall intensities (spatially and temporally) of a constant duration with or without uniform infiltration rates on a rectangular plane of constant slope and roughness is an example of a hydrologic system with a minimum number of variables. This deterministic system is made probabilistic by assuming that the magnitude of each rainfall intensity (and infiltration rate) is a random variable. If the pdf of the rainfall intensity i is $f(i)$ and there is a one to one and deterministic relationship between i and peak flow q_p then the pdf of the peak runoff $g(q_p)$ is given by (Sveshnikov, 1968)

$$g(q_p) = f(i) \frac{di}{dq_p} \quad (3.30)$$

When an analytical solution of the peak flow pdf is not feasible the random rainfall intensities are generated using the Monte Carlo simulation method. These intensities are then converted to peak flows by a numerical simulation of the Diffusion Wave equations. The random series of peak flows so generated can then be analysed for their statistical characteristics. A useful way of investigating the relationships between the statistical characteristics of the rainfall intensity and those of the peak runoff is through a plot of the coefficients of variation (Cv) and skewness (Cs) of the two variables (Frind, 1969). For certain theoretical distributions the $Cs - Cv$ relationships are known, e.g., for a Normal distribution,

$$Cs = 0 \quad (3.31)$$

for a two-parameter Gamma distribution,

$$Cs = 2Cv \quad (3.32)$$

and for a Log-normal distribution,

$$Cs = 3Cv + Cv^3 \quad (3.33)$$

When these curves are plotted, (see Figure 3.5), they represent the loci of all co-ordinates (Cs, Cv) corresponding to the respective distributions.

Using equation 3.30 or the $Cs-Cv$ approach, the intrinsic nature of a probabilistic rainfall-runoff process on a single plane is examined under various assumptions in the next sections.

3.3.1 Random Rainfall Rates of Constant Duration on an Impervious Plane

For a system with uniform rainfall rates on an impervious plane, the relation between rainfall intensity and peak flow, assuming the Diffusion model of flow, is given by the semi-empirical equations 3.34 and 3.35 (equations 3.25 and 3.27 rearranged).

$$qp = i(1 - \exp[-(\frac{k}{1.6 - k})^{1.3}]), \quad k < 1.6 \quad (3.34)$$

$$qp = i, \quad k \geq 1.6 \quad (3.35)$$

where

$$k = i^{0.4} t_o (\frac{\sqrt{S_o}}{nL})^{0.6} \quad (3.36)$$

An element of randomness is introduced in these equations by assuming that the magnitude of the rainfall intensity i is a random variable from a given probability

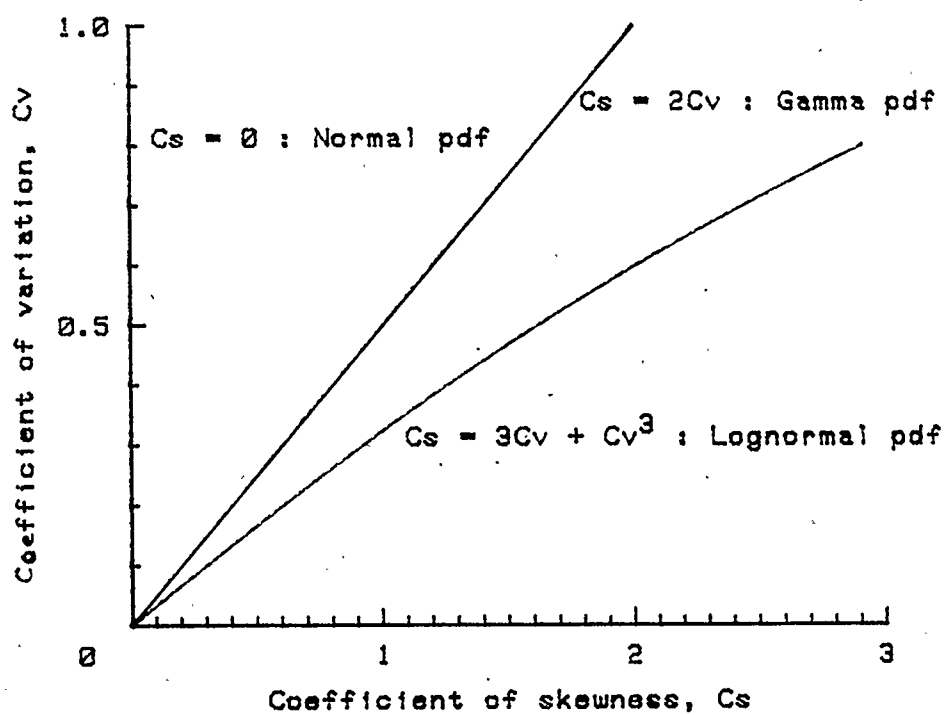


Figure 3.5: Cs-Cv relationships for the Normal, Gamma, and Log-normal distributions.

distribution $f(i)$ with known parameters. It is of interest to determine the characteristics of the resulting probability distribution $g(q_p)$ of the peak runoff. Using equation 3.30, $g(q_p)$ is given by

$$g(q_p) = \frac{f(i)}{k1}, \quad k < 1.6 \quad (3.37)$$

where

$$k1 = 1 - \exp\left(-\left(\frac{1.6 - k}{k}\right)^{1.3}\right)\left(1 - \frac{0.832}{k}\left(\frac{1.6 - k}{k}\right)^{-2.3}\right) \quad (3.38)$$

and

$$g(q_p) = f(i), \quad k \geq 1.6 \quad (3.39)$$

For a specified $f(i)$, $g(q_p)$ can be analysed for changes in every parameter in equations 3.37 and 3.39.

$f(i)$: Normal

Assume that $f(i)$ is the Normal distribution (equation 3.40) with mean i_m and standard deviation i_s . The Normal distribution is symmetrical about the mean, has a coefficient of skewness equal to zero, and is given by the equation

$$f(i) = \frac{1}{\sqrt{2\pi}i_s^2} \exp\left(-0.5\left(\frac{i - i_m}{i_s}\right)^2\right) \quad (3.40)$$

Figures 3.6 to 3.10 illustrate the transformation of $f(i)$ to $g(q_p)$ for various specified values of i_m , t_o , L , S_o , and n . The mean of $g(q_p)$ is always less than or equal to the mean of $f(i)$ by virtue of the fact that peak flow is always less than or equal to the corresponding rainfall rate. The shape of $g(q_p)$ can be either positively skewed, negatively skewed, or symmetrical. Figures 3.6 to 3.10 indicate that relatively smaller i_m , t_o , and S_o and relatively higher n and L produce $g(q_p)$ with a relatively

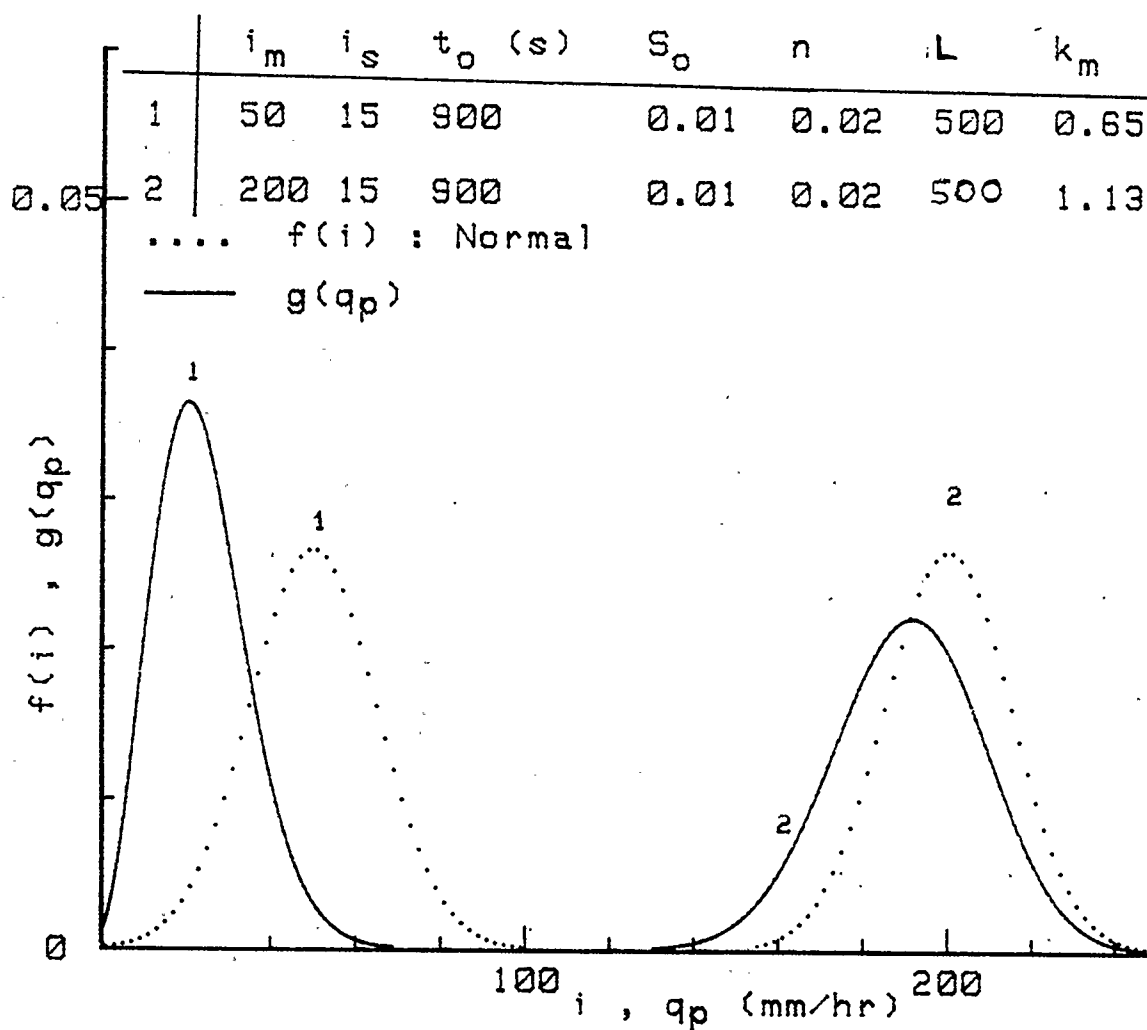


Figure 3.6: Probability distribution curves of peak flows for mean rainfall intensities equal to 50 and 200 mm/hr.

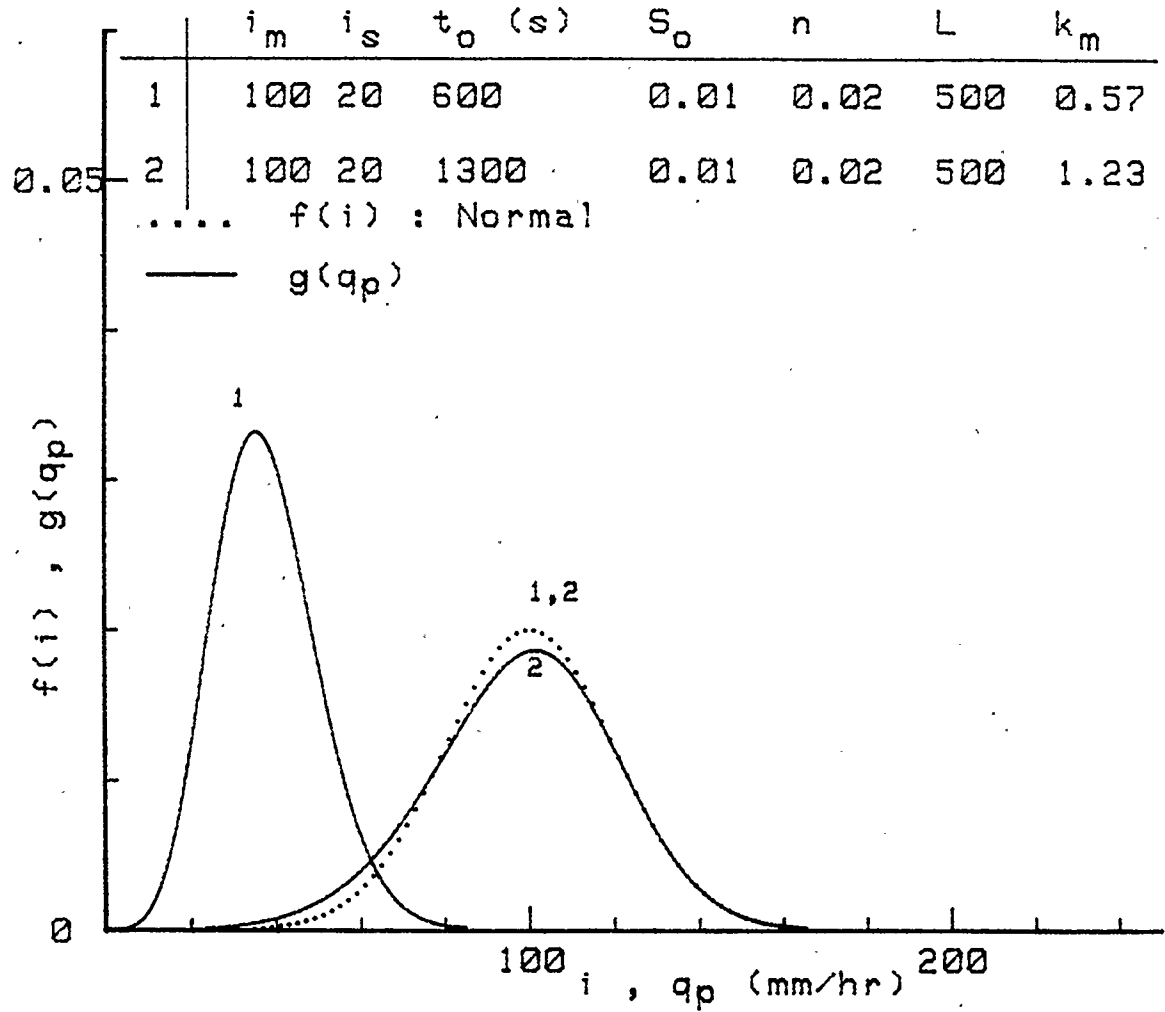


Figure 3.7: Probability distribution curves of peak flows for rainfall durations equal to 600 and 1300 seconds.

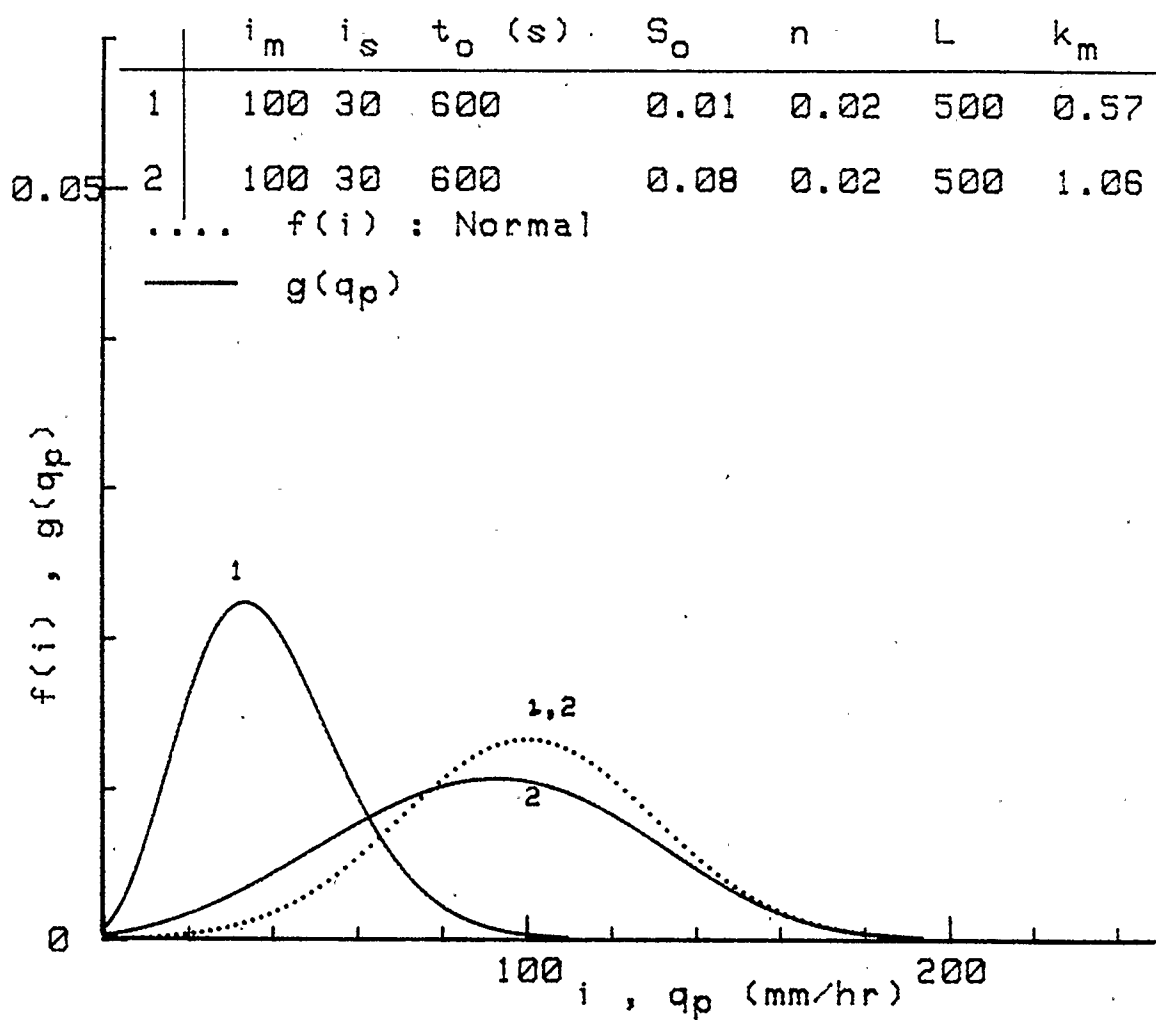


Figure 3.8: Probability distribution curves of peak flows for slopes of planes equal to 0.01 and 0.08.

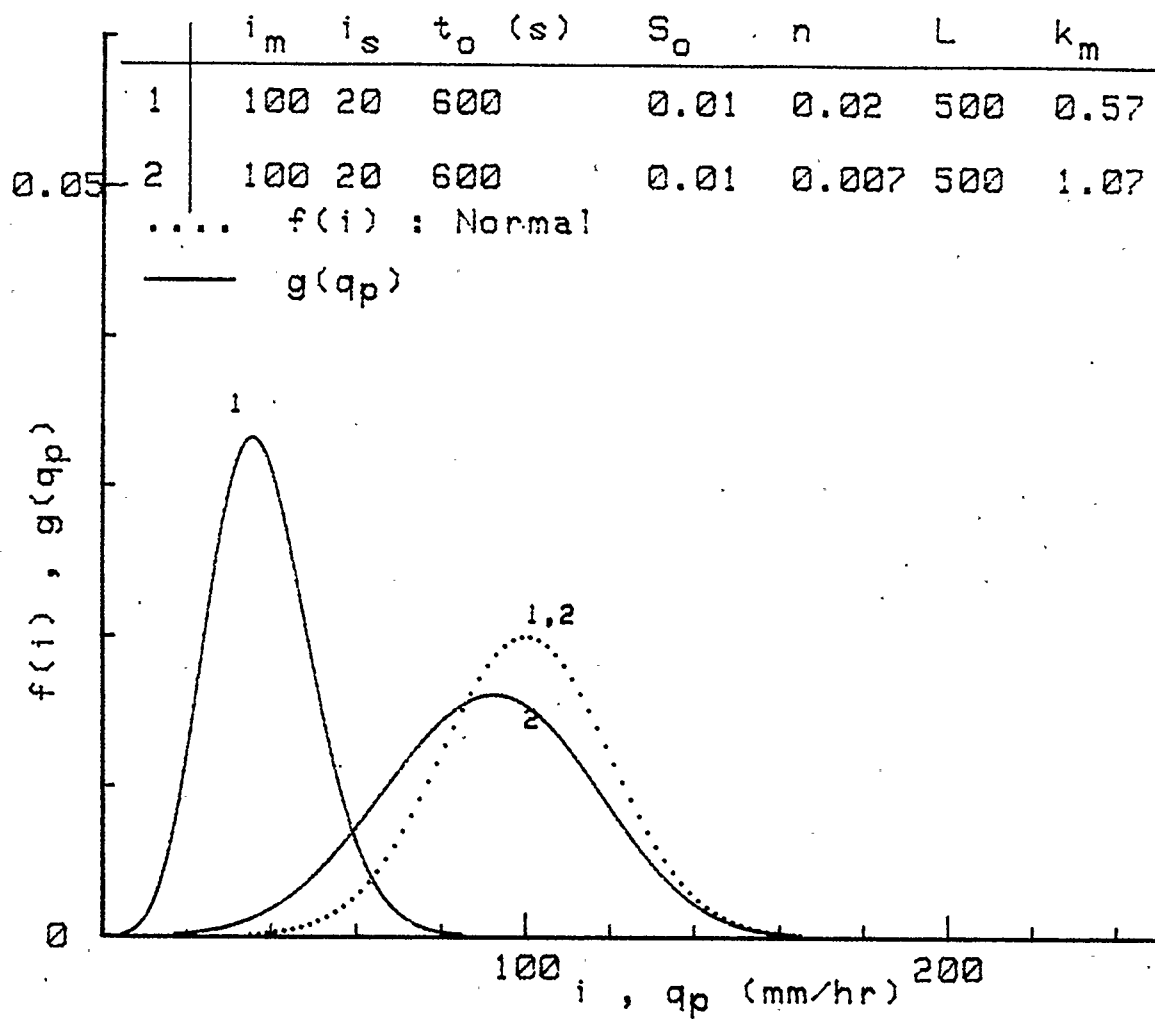


Figure 3.9: Probability distribution curves of peak flows for roughness of planes equal to 0.02 and 0.007.

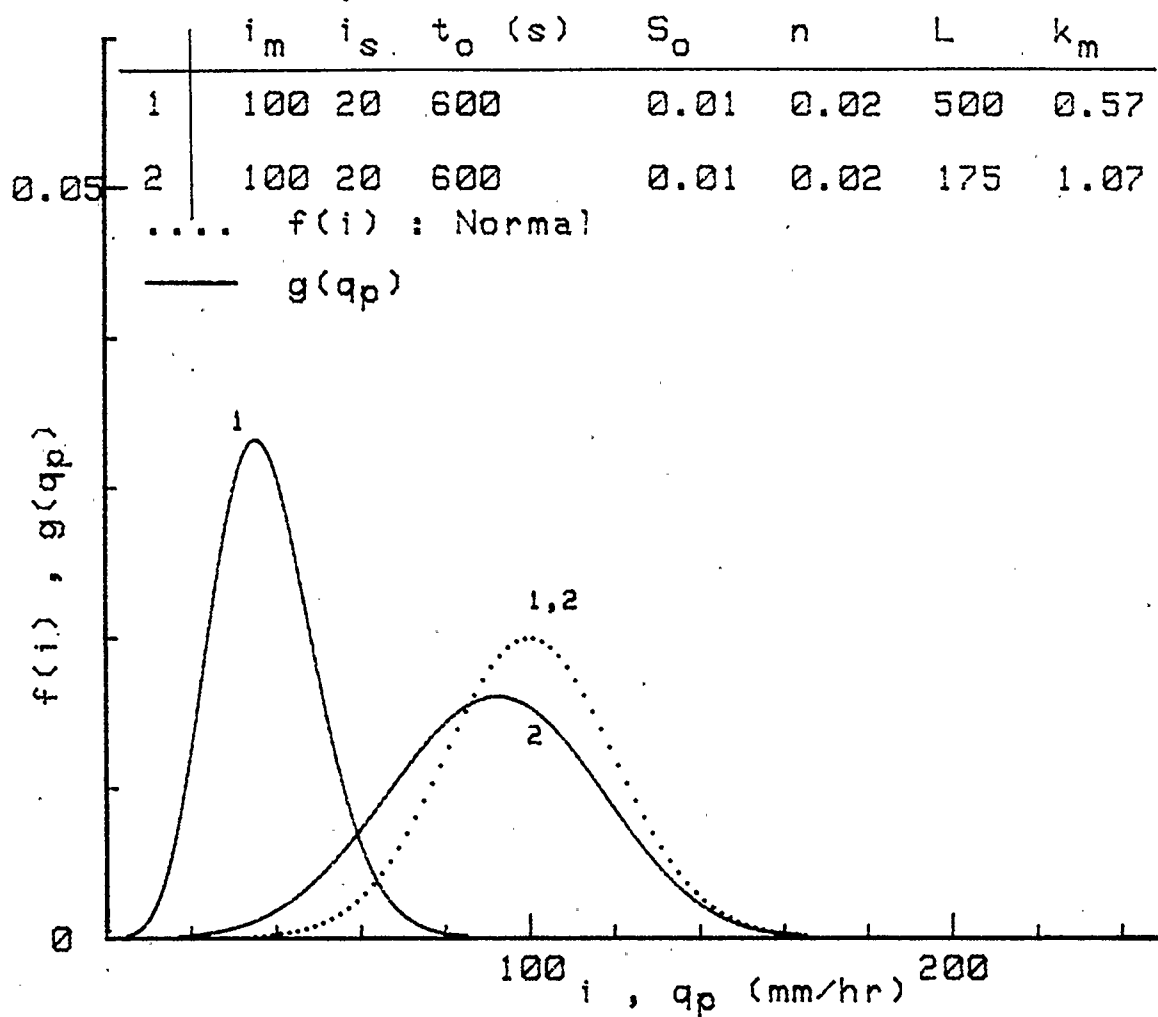


Figure 3.10: Probability distribution curves of peak flows for lengths of planes equal to 500 and 175 metres.

higher skewness. Conversely, higher i_m , t_o , and S_o and smaller n and L produce $g(q_p)$ with a skewness equal to or less than that of $f(i)$. In fact, if a parameter k_m is defined as

$$k_m = i_m^{0.4} t_o \left(\frac{\sqrt{S_o}}{nL} \right)^{0.6} \quad (3.41)$$

then, it can be generally stated that when comparing different basic hydrologic systems a relatively lower k_m would indicate a more skewed $g(q_p)$ and a relatively higher k_m a lesser skewed $g(q_p)$. A study of the relationship between the statistical parameters of $f(i)$ and $g(q_p)$ and k_m is therefore necessary.

Statistical Relationships between $f(i)$ and $g(q_p)$

The coefficients of variation (Cv) and skewness (Cs) of $f(i)$ and $g(q_p)$ were determined using the Monte Carlo simulation method. 6000 random values of i were generated from $f(i)$. These values were then converted into corresponding peak flow values using equations 3.34 and 3.35 and their statistical parameters determined. Figure 3.11 shows the $Cs - Cv$ relationships between $f(i)$ and $g(q_p)$ for $Cv(i)$ equal to 0.1, 0.2, and 0.3. Also, loci of all $(Cs(q_p), Cv(q_p))$ corresponding to certain constant values of k_m have been drawn. For a particular $Cv(i)$, $(Cs(q_p), Cv(q_p))$ starts at a maximum, decreases with increasing k_m until $Cs(q_p)$ reaches a minimum (negative values for the cases shown), and then tends towards $(Cv(i), 0)$. This behaviour can be explained by examining the $i - q_p$ transformation process characterized by equations 3.34 and 3.35. Any variable other than i could have been chosen because $(Cs(q_p), Cv(q_p))$ depends on k_m rather than the individual variables on their own. The $i - q_p$ relationship is however intuitively more understandable. Figure 3.12 shows the variation of q_p with i for $t_o = 1000$

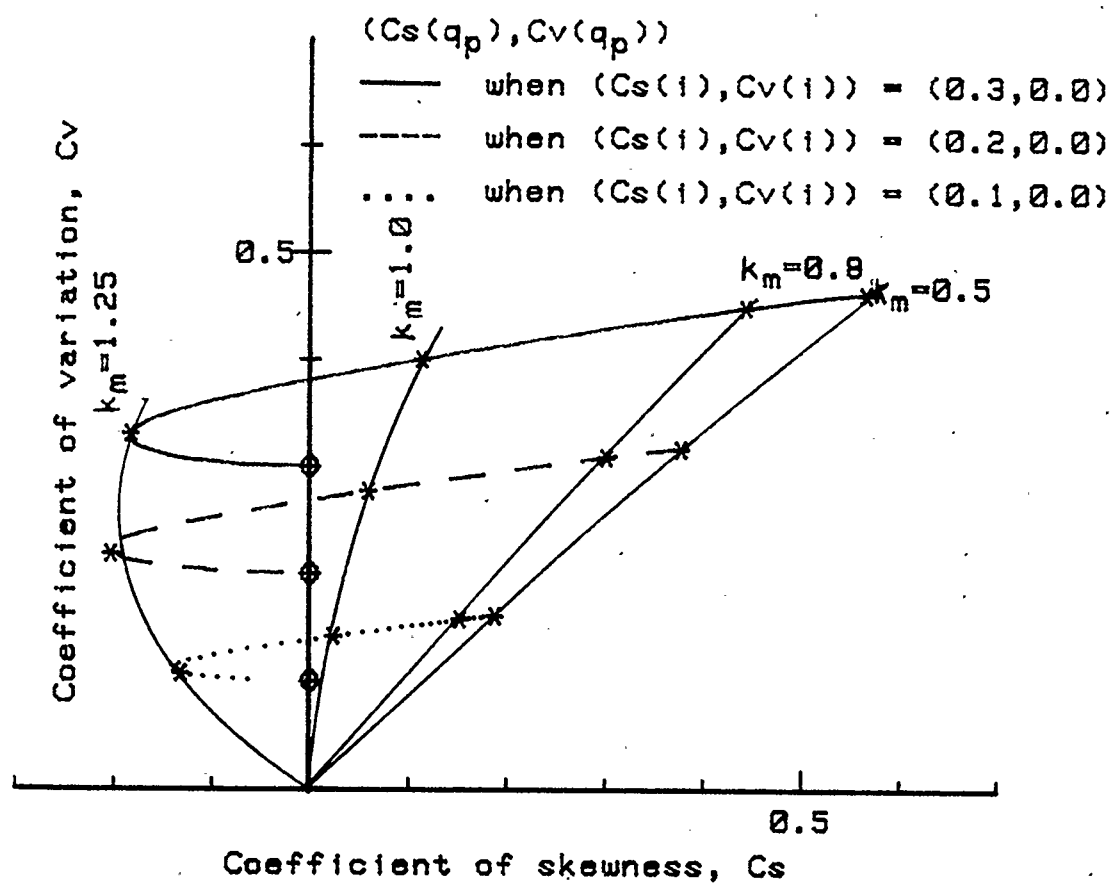


Figure 3.11: $Cs(q_p) - Cv(q_p)$ relationships for a plane with $f(i)$: Normal.

s, $S_o = 0.01$, $n = 0.02$, and $L = 500$ m. The $i - q_p$ relationship is typical of a "real" $i - q_p$ curve with a concave rising part, an inflexion point, and a convex part gradually tending towards the steady state line. On the same curve, the ranges of i within two standard deviations of i_m producing positively skewed, symmetrical, and negatively skewed $g(q_p)$ are shown. It is apparent that the shape of $i - q_p$ has an important influence on the skewness of the peak runoff pdf. Figure 3.13 gives a geometrical interpretation of how the three shape components of the $i - q_p$ curve transforms $f(i)$ into $g(q_p)$. The effects of the shape of the $i - q_p$ curve can be generalised by stating that when $\frac{d^2i}{dq_p^2}$ is greater than, less than, or equal to zero, then the skewness of $g(q_p)$ is greater than, less than, or equal to the skewness of $f(i)$ (assuming that most random i are contained within one shape).

$f(i)$: Gamma

Figure 3.14 shows the $Cs - Cv$ relationships between $f(i)$ and $g(q_p)$ when $f(i)$ is the Gamma distribution with parameters λ and η :

$$f(i) = \frac{\lambda^\eta}{\Gamma(\eta)} i^{\eta-1} \exp(-\lambda i), \quad i, \lambda, \eta > 0 \quad (3.42)$$

The mean, variance, coefficient of variation, and coefficient of skewness of $f(i)$ respectively are

$$i_m = \frac{\eta}{\lambda} \quad (3.43)$$

$$V(i) = \frac{\eta}{\lambda^2} \quad (3.44)$$

$$Cv(i) = \frac{1}{\sqrt{\eta}} \quad (3.45)$$

$$Cs(i) = \frac{2}{\sqrt{\eta}} \quad (3.46)$$

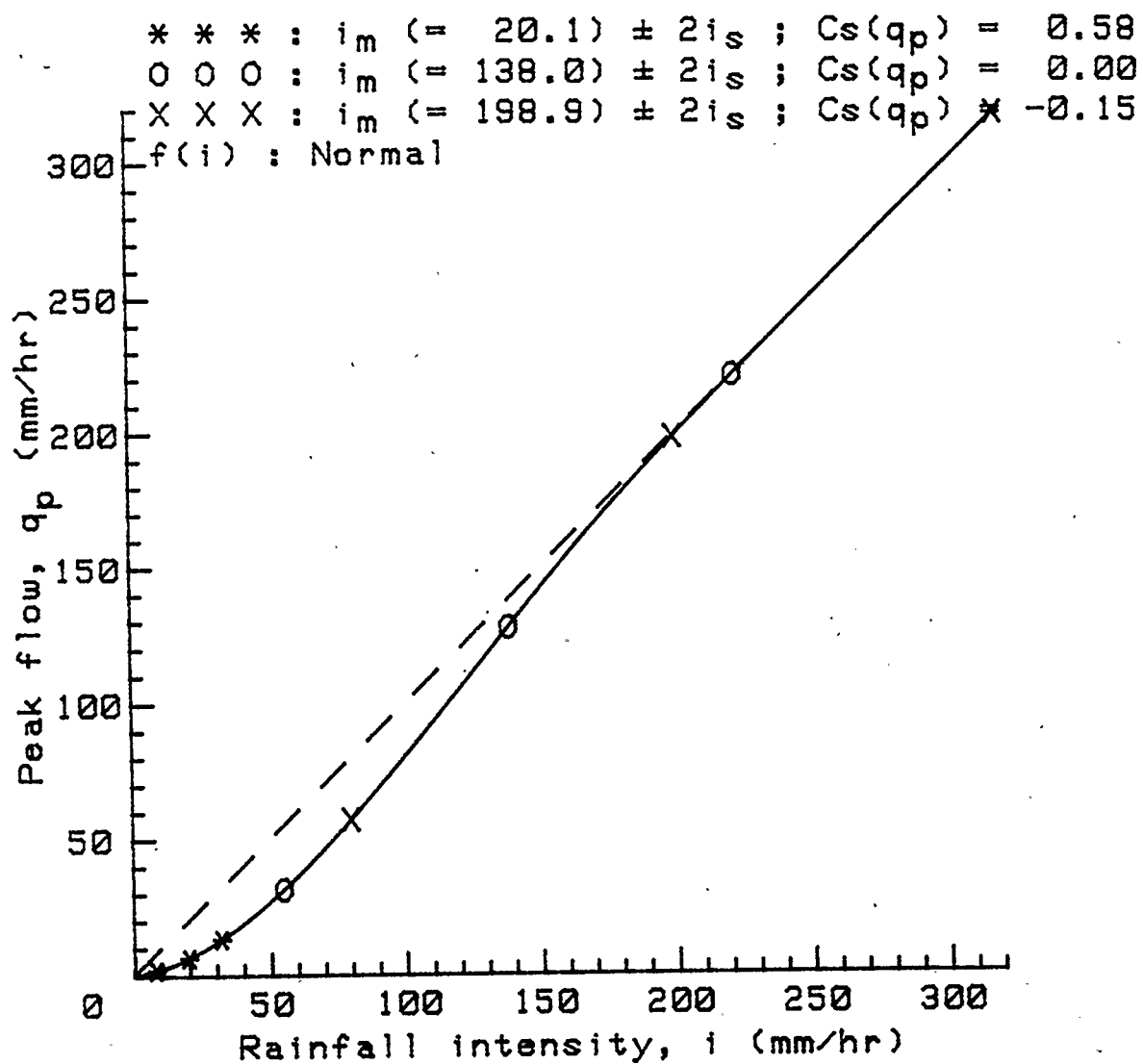


Figure 3.12: Rainfall intensity-peak flow curve for given plane and rainfall characteristics.

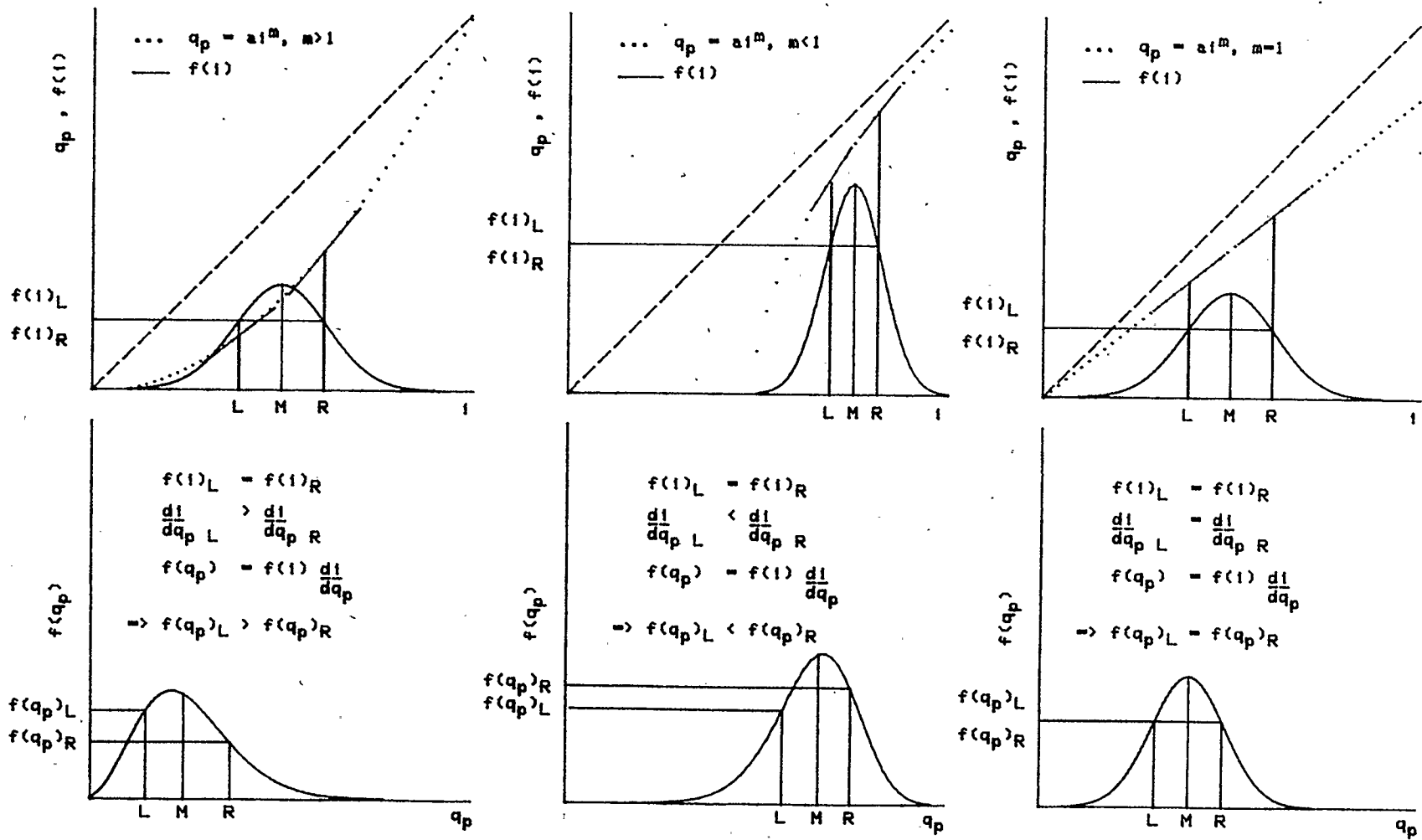


Figure 3.13: Geometrical transformation of a Normal $f(i)$ into $g(q_p)$ for 3 $i - q_p$ shapes.

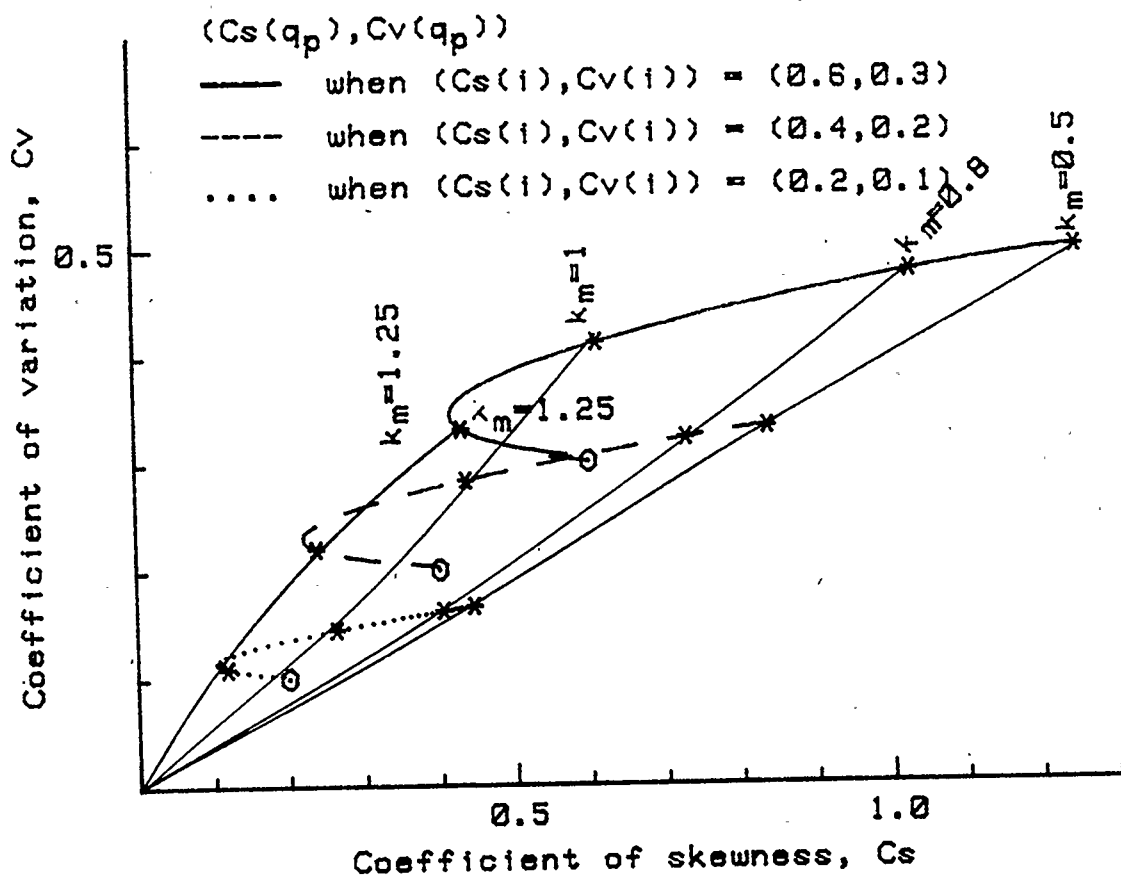


Figure 3.14: $Cs(q_p) - Cv(q_p)$ relationships for a plane with $f(i) : \text{Gamma}$.

The Gamma distribution is positively skewed. The shape of the $Cs - Cv$ curves for peak flows are similar to those obtained for Normal $f(i)$. $(Cs(q_p), Cv(q_p))$ starts from a maximum, decreases to a minimum $Cs(q_p)$, and then tends towards $(Cs(i), Cv(i))$.

Comparison of Statistical Results from the Kinematic, Diffusion, and Semi-empirical Diffusion Models

In the previous section it was assumed that the peak runoffs can be obtained from the semi-empirical equations 3.34, 3.35 and 3.36 which approximate the numerical solutions of the Diffusion Wave equations 3.3 and 3.11. The equations relating peak runoff to rainfall intensity when the Kinematic Wave Model is used are equations 3.26, 3.28, and 3.29. The effect of these methods of obtaining peak runoffs on the $Cs(q_p) - Cv(q_p)$ curve for $Cv(i) = 0.3$ and $f(i)$ Normal is shown in Figure 3.15. The $Cs(q_p) - Cv(q_p)$ curve corresponding to the Kinematic Wave model is obtained by the method outlined for the semi-empirical diffusion equations in the previous section. The $Cs(q_p) - Cv(q_p)$ curve corresponding to a numerical solution of the Diffusion Wave equations is obtained as follows. The peak flows (q_p) were obtained for rainfall intensities (i) ranging from 1 to 200 mm/hr in steps of 1 mm/hr. The rainfall duration and the plane's characteristics were kept at constant values. 6000 random values of i were then generated from $f(i)$. The corresponding 6000 random values of q_p were obtained by interpolation of the numerically obtained peak flows. Standard statistical methods were then used to determine their statistical parameters.

Figure 3.15 shows that the three curves have their maximum $(Cs(q_p), Cv(q_p))$

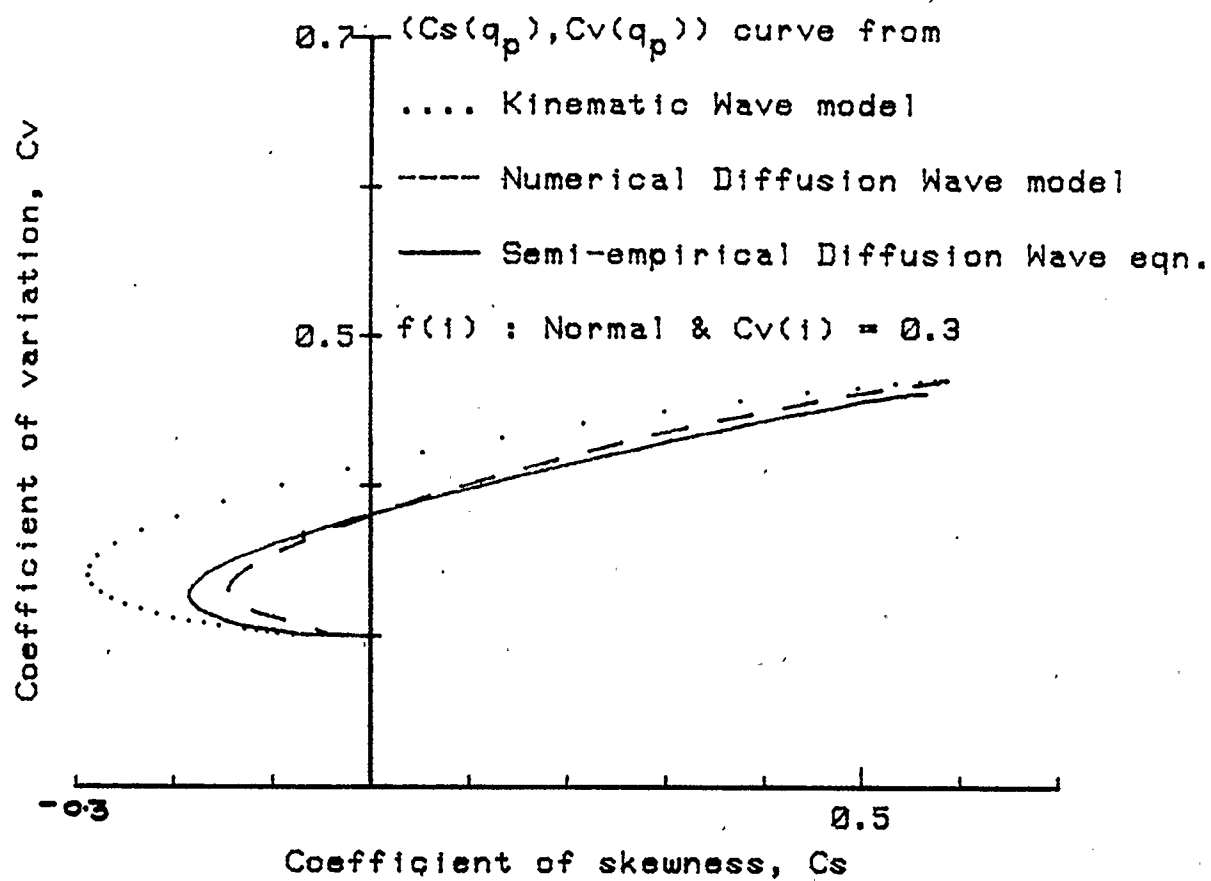


Figure 3.15: Effect of model used to obtain peak runoff on the relationship between the statistical parameters of the peak runoff series.

close to one another. The greatest discrepancy between the curves occur at the point of minimum skewness. These observations can be explained with reference to Figure 3.4. The latter indicates that all three methods of obtaining the peak runoffs are indistinguishable for low k_m values and diverge from one another when flows conditions are close to steady state. The discrepancies are reflected in the $Cs(q_p) - Cv(q_p)$ curves since the lower concave parts of the curves in Figure 3.4 produce concave-shaped $i - q_p$ curves and therefore give rise to the highest coefficient of skewness, while, the upper convex parts produce convex and linear-shaped $i - q_p$ curves and therefore give rise to minimum skewness (see Figure 3.13). Figure 3.15 indicates that the semi-empirical diffusion equations closely approximate the numerical solutions as far as the statistical parameters of the random peak flow series are concerned. Hence, the results of the previous section which were based on the semi-empirical equations are close to what would have been obtained had the Diffusion Wave equations been solved numerically to obtain the statistical parameters.

Further Remarks on the $Cs - Cv$ Relationship of $g(q_p)$

Figures 3.11 and 3.14 show that when k_m (equation 3.41) is less than a certain value (depending on the specification of $f(i)$) ($Cs(q_p), Cv(q_p)$) remains at a constant maximum value for a given $Cv(i)$. And the maximums from different $Cv(i)$'s seem to fall on the same curve. For example, when $f(i)$ is Normal (see Figure 3.12)

$$Cs(q_p) \approx 1.21Cv(q_p) \quad (3.47)$$

This relationship is empirical. Under some assumptions, a similar relationship between $Cs(q_p)$ and $Cv(q_p)$ when $f(i)$ is Gamma is analytically possible. Such

a relationship is useful because it gives the limiting values of the coefficients of skewness and variation. Equation 3.34 stating the relationship between peak flow and rainfall intensity is reproduced below :

$$q_p = i(1 - \exp(-(\frac{k}{1.6 - k})^{1.3})), \quad k < 1.6 \quad (3.48)$$

k is defined by equation 3.36. When $(Cs(q_p), Cv(q_p))$ is a maximum, k_m is much smaller than 1.6. So, for each individual i , equation 3.48 can be approximated by

$$q_p \approx i(1 - \exp(-(\frac{k}{1.6})^{1.3})) \quad (3.49)$$

Equation 3.49 can be written in expanded form as

$$q_p \approx i(1 - \frac{1}{1 + (k/1.6)^{1.3} + 0.5(k/1.6)^{2.6} + \dots}) \quad (3.50)$$

For small k 's, equation 3.50 is approximated by taking only the first two terms of the expansion in the denominator :

$$q_p \approx i(\frac{1 + (k/1.6)^{1.3} - 1}{1 + (k/1.6)^{1.3}}) \quad (3.51)$$

$$q_p \approx \frac{i(k/1.6)^{1.3}}{1 + (k/1.6)^{1.3}} \quad (3.52)$$

Assuming that for small k 's, $(k/1.6)^{1.3} \ll 1$, then

$$q_p \approx i(\frac{k}{1.6})^{1.3} \quad (3.53)$$

Equation 3.53 can be written as

$$q_p = i(\frac{i^{0.4}}{1.6} t_o \frac{\sqrt{S_o}}{nL})^{1.3} \quad (3.54)$$

or,

$$q_p = (\frac{t_o \sqrt{S_o}}{1.6 nL})^{1.3} i^{1.52} \quad (3.55)$$

or,

$$q_p = ai^{1.52} \quad (3.56)$$

where a is a constant for given rainfall duration and plane characteristics. It is interesting to note that the exponent on i (1.52) is less than but close to 1.667, the exponent on i for the Kinematic Wave model, i.e., for small k values the Diffusion and Kinematic models give almost the same results. The value of 1.3 used in the semi-empirical equations for the Diffusion model of flow is therefore not totally a fitting parameter. Using equation 3.30 and assuming that equation 3.56 relates q_p to i and that $f(i)$ is Gamma, the pdf of $g(q_p)$ is given by

$$g(q_p) = f\left(\left(\frac{1}{a}\right)^{1/1.52} q_p^{1/1.52}\right) \frac{1}{1.52} \left(\frac{1}{a}\right)^{1/1.52} - 1 \quad (3.57)$$

or,

$$g(q_p) = \frac{\lambda^\eta}{\Gamma(\eta)} \frac{1}{1.52} \left(\frac{1}{a}\right)^{\eta/1.52} q_p^{(\eta-1.52)/1.52} \exp\left(-\lambda \left(\frac{1}{a}\right)^{1/1.52} q_p^{1/1.52}\right) \quad (3.58)$$

The mean, variance, coefficient of variation, and coefficient of skewness of $g(q_p)$ are derived in Appendix A. The equations for $Cv(q_p)$ and $Cs(q_p)$ are

$$Cv(q_p) = \frac{(\Gamma(\eta)\Gamma(3.04 + \eta) - \Gamma^2(1.52 + \eta))^{1/2}}{\Gamma(1.52 + \eta)} \quad (3.59)$$

$$Cs(q_p) = \frac{\Gamma^2(\eta)\Gamma(4.56 + \eta) - 3\Gamma(\eta)\Gamma(3.04 + \eta)\Gamma(1.52 + \eta) + \Gamma^3(1.52 + \eta)}{(\Gamma(\eta)\Gamma(3.04 + \eta) - \Gamma^2(1.52 + \eta))^3} \quad (3.60)$$

The relationship between $Cs(q_p)$ and $Cv(q_p)$ is given by

$$Cs(q_p)Cv^3(q_p) = \frac{\Gamma^2(\eta)\Gamma(4.56 + \eta) - 3\Gamma(\eta)\Gamma(3.04 + \eta)\Gamma(1.52 + \eta) + 2\Gamma^2(1.52 + \eta)}{\Gamma^3(1.52 + \eta)} \quad (3.61)$$

where $\eta = \frac{1}{Cv^2(i)}$ from equation 3.45. Equations 3.59 and 3.60 indicate that for small k 's, $Cv(qp)$ and $Cs(qp)$ are independent of the plane characteristics and rainfall duration and are only functions of the coefficient of variation $Cv(i)$ of $f(i)$. For an Exponential $f(i)$, a distribution which has often been used to fit rainfall intensities,

$$Cv(i) = 1 \quad (3.62)$$

and therefore

$$Cv(qp) = 1.57 \quad (3.63)$$

and

$$Cs(qp) = 3.89 \quad (3.64)$$

These values are the theoretical maximums for an Exponential $f(i)$. Figure 3.14 shows a plot of equation 3.61 and it can be observed that this curve is valid only for k_m less than or equal to 0.5.

For increasing k_m , $(Cs(qp), Cv(qp))$ curves indicate a very flexible relationship between $Cs(qp)$ and $Cv(qp)$. Since $g(qp)$ may not be theoretically derivable for all $f(i)$, an attempt was made to find a distribution which may only approximate the exact $g(qp)$, yet reflects the main features of the latter, the most important of which is that it must exhibit a variable relationship between its Cv and Cs .

The Pearson Type III Distribution as an Approximation to $g(qp)$

The Pearson Type III distribution is essentially a three-parameter Gamma distribution. It is expressed as

$$f(X : m, a, b) = \frac{1}{a\Gamma(b+1)} \left(\frac{X-m}{a}\right)^b \exp(-(X-m)/a) \quad (3.65)$$

m is a location parameter. The mean, coefficient of variation, and coefficient of skewness of the Pearson III distribution are respectively

$$\mu = m + a(b + 1) \quad (3.66)$$

$$Cv = \frac{a\sqrt{b+1}}{m + a(b+1)} \quad (3.67)$$

$$Cs = \frac{2}{\sqrt{b+1}} \quad (3.68)$$

The log form of the Pearson III distribution is recommended by the Water Resources Council (1967) as the distribution to use to fit flood peaks. The Pearson III distribution has a flexible relationship between its coefficient of variation and coefficient of skewness, the latter can be positive or negative, and under special conditions it can degenerate into the Normal and Gamma distributions. The magnitude of peak flows for various return periods given that the theoretical underlying distribution is the Pearson III is determined by using Chow's frequency factors method (Chow, 1964). If $q_{p,T}$ is the peak flow having a return period T , then

$$q_{p,T} = q_p, m(1 + Cv(q_p)K_T) \quad (3.69)$$

where K_T is a frequency factor. K_T is a function of the skewness of the distribution and the return period. It has been tabulated by the Water Resources Council (1967) for $Cs(q_p)$ ranging from -3.0 to $+3.0$ and for various T 's ranging from 1.0101 to 200 years. If annual peaks are being analysed, then T is expressed in years. If all peaks above a certain level are being analysed, then T is the inverse of the "percent of time" a particular value of q_p has been exceeded. For T greater than 10 years or equivalently for "exceedance less than 10% of the time" the two systems become indistinguishable.

To test the adequacy of the Pearson III distribution as an approximate but close representation of $g(q_p)$ as given by equations 3.37 and 3.39, the latter equations were numerically integrated. The values of q_p corresponding to various return periods T (or equivalently "probability of exceedance") were plotted on probability paper. The statistical parameters of $g(q_p)$ were determined by Monte Carlo simulation. Knowing the mean q_p (q_p, m), $Cv(q_p)$, and $Cs(q_p)$ and using equation 3.69, $q_{p,T}$ was determined for various T 's assuming that the underlying distribution is the Pearson III. These values were plotted on the same graph as the theoretically determined co-ordinates. The procedure was done for k_m equal to 0.5 and 1.0. Figure 3.16 and 3.17 show the results when $f(i)$ is assumed to be Normal and Gamma respectively. It is observed that for a single plane under uniform rainfall intensity of constant duration, the Pearson Type III distribution is a good approximation to the theoretical $g(q_p)$ for $k_m = 0.5$. For $k_m > 1$ the fit is not good, especially when $T > 100$ years. The Pearson Type III distribution may therefore approximate the actual pdf of the peak flows for conditions where flows close to the steady state are unlikely to occur.

3.3.2 Random Uniform Rainfall with Correlated Intensities and Durations on an Impervious Plane

The previous section dealt only with rainfall of random intensities and constant durations. Rainfall records indicate that there is a physical correlation between rainfall intensity and duration, i.e., rainfall of high intensities tend to be of short durations, typical of thunderstorms, and rainfall of low intensities tend to be of long durations, typical of convective storms. The probabilistic structure of such

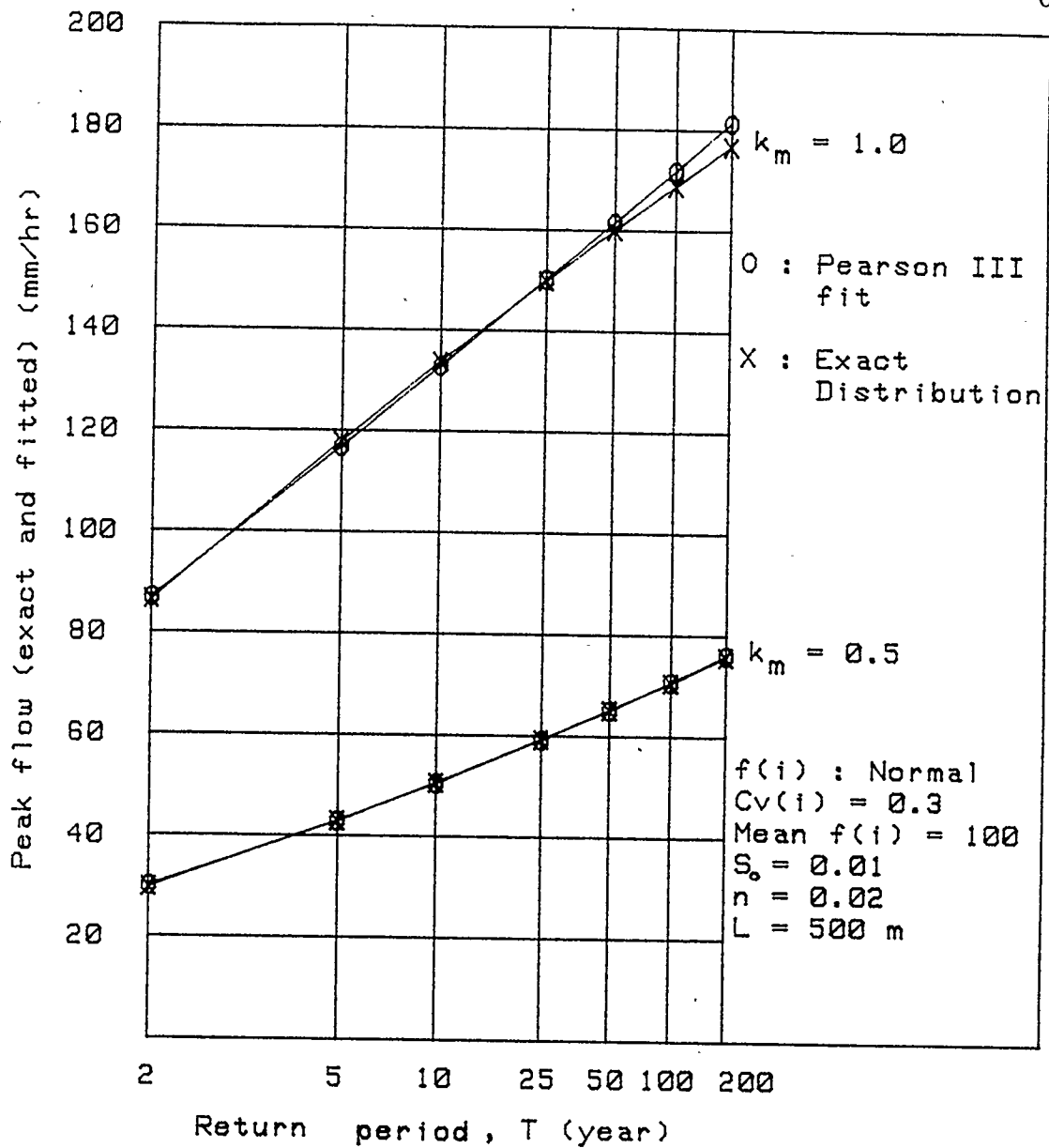


Figure 3.16: Comparing exact probability distribution curve of peak runoff with Pearson Type III fit when $f(i)$ is Normal.

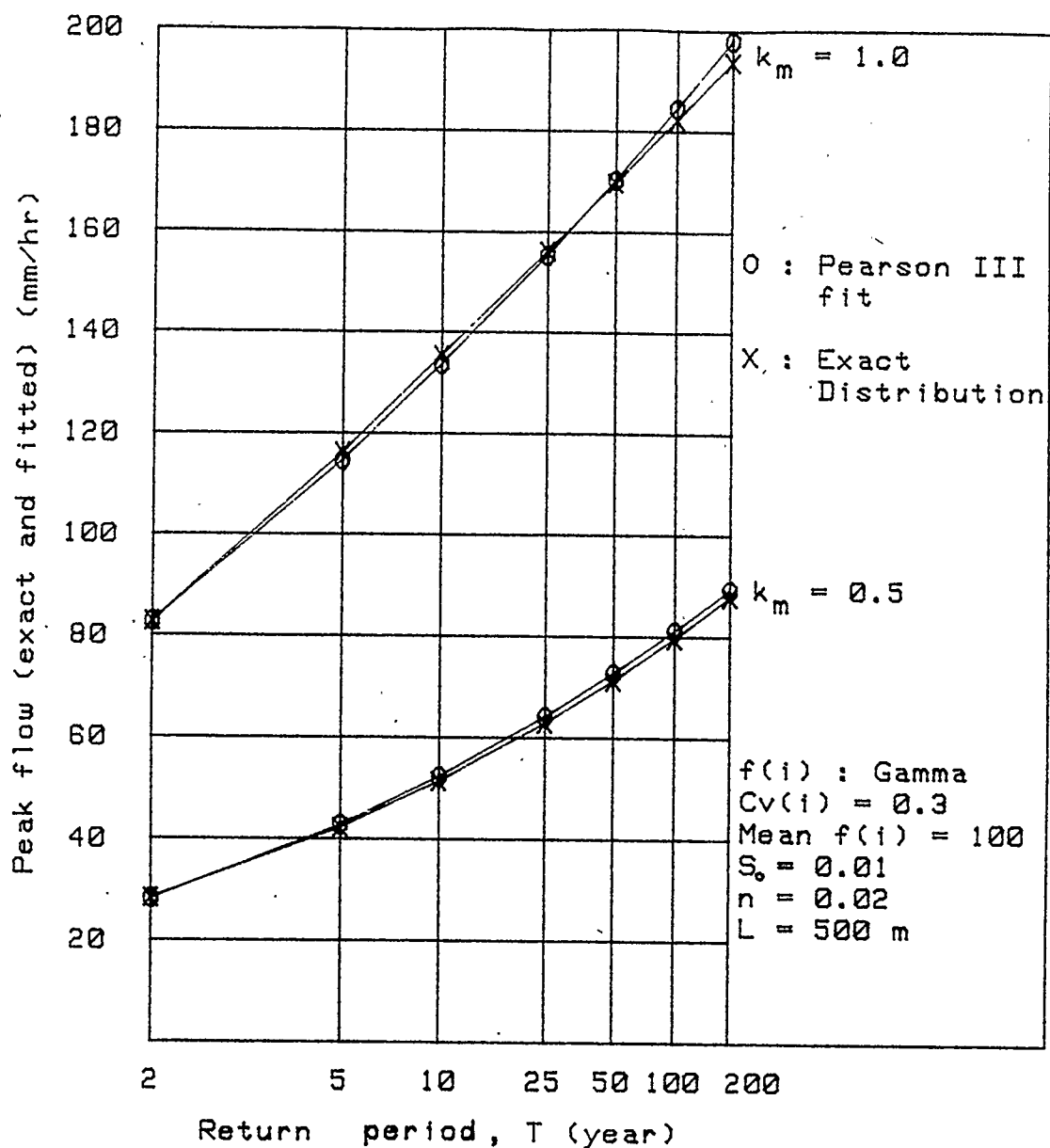


Figure 3.17: Comparing exact probability distribution curve of peak runoff with Pearson Type III fit when $f(i)$ is Gamma.

rainfall events is, in practice, expressed as Intensity-Duration-Frequency (IDF) curves. Such curves are shown as solid lines in Figure 3.18. For example, the rainfall event with intensity I_2 and duration t_2 has an exceedance probability of 0.02 (\equiv a return period of 50 years). These curves are synthetic curves constructed from rainfall records. For given t_0 , the rainfall intensities are in practice fitted by the Gumbel distribution, an Extreme Value distribution. In the discussion that follows it will be assumed that the pdf of i for given t_0 is Gamma. It will also be assumed that $Cv(i)$ is constant for all t_0 's. The relationship between the mean of $f(i)$, i_m , and t_0 is taken to be of the form

$$i_m = \frac{a}{t_0^b}, \quad a, b, t_0 > 0 \quad (3.70)$$

where a and b are regionally determined constants. Equation 3.70 is a generalised form of one proposed by Steel (1960). Since t_0 can theoretically range between 0 and infinity, therefore a probability distribution for peak flows where all durations are considered is not very useful. And different ranges of t_0 will result in different $g(q_p)$'s. For a given return period of i , the different combinations of rainfall intensities and durations will result in a range of q_s . For design purposes, only the extreme of these values of q_p and its corresponding return periods are of importance. Figure 3.18 shows the IDF curves and the corresponding peak flow curves (dotted lines) for t_0 between 30 and 1800 seconds. The semi-empirical diffusion equations of flow were used to determine the peak flows. The rainfall intensity was uniformly distributed over the runoff plane. The characteristics of the plane were $S_o = 0.01$, $n = 0.02$, and $L = 500$ m. $f(i)$ was Gamma with $Cv(i) = 0.3$. a and b in equation 3.70 were 456.2 and 0.62 respectively with i_m in mm/hr and t_0 in

minutes. These values of a and b were obtained by correlating mean rainfall intensities of various return periods with their corresponding durations. The rainfall data were extracted from the Hydrological Atlas of Canada (1978). The peak flow for a given return period first increases with increasing rainfall duration until a maximum is reached. Further increase in the rainfall duration decreases the peak flow. The duration of rainfall that gives the maximum peak flow varies with the return period under consideration.

The maximum peak flows are joined by a dashed line AB. When for each T , the maximum peak flow is divided by the corresponding rainfall intensity of the same return period (shown as a solid line with crosses : A'B'), a constant coefficient C is obtained, i.e.,

$$q_p(M), T = C i_T \quad (3.71)$$

where $q_p(M), T$ denotes the extreme of the peak flows of a return period T . Equation 3.71 is analogous to the Rational formula used for design purposes. The Rational formula assumes that the time of concentration is always equal to the duration of the rainfall and consequently $C = 1$ for an impervious plane. However, C in equation 3.71 varies with coefficient b in equation 3.70. C is independent of a in equation 3.70. For b between 0.52 and 0.72, C varies between 0.95 and 0.89 with $C = 0.93$ at $b = 0.62$. This is the case because in the Diffusion model steady state is reached asymptotically and hence peak flows in Figure 3.18 depend on the rate at which i_T is decreasing, i.e. on b .

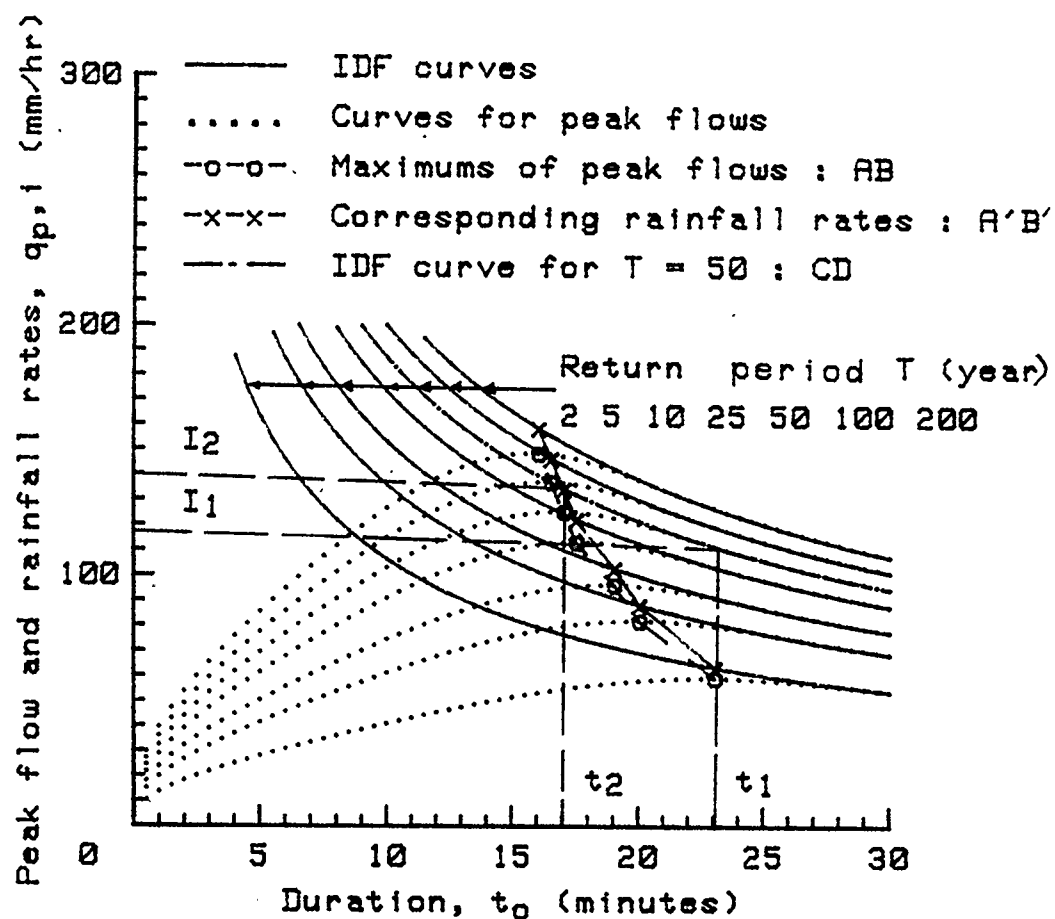


Figure 3.18: Peak flow and Intensity-Duration-Frequency curves.

Analytical Proof that C is a Constant for a Given b

The peak flow q_p from a uniformly distributed rainfall of intensity i and duration t_o on an impervious plane of slope S_o , runoff length L , and roughness n is given by the semi-empirical equation 3.25 in expanded form :

$$q_p = i \left(1 - \exp \left[- \left(\frac{i^{0.4} t_o \left(\frac{\sqrt{S_o}}{nL} \right)^{0.6}}{1.6 - i^{0.4} t_o \left(\frac{\sqrt{S_o}}{nL} \right)^{0.6}} \right)^{1.3} \right] \right) \quad (3.72)$$

For correlated inputs, the rainfall intensity i is related to the rainfall duration t_o by synthetic IDF curves. For a given and constant t_o , i is assumed to have a probability distribution $f(i)$. It is further assumed that the mean rainfall intensity i_m of $f(i)$ for all t_o is related to t_o by the empirical equation

$$i_m = \frac{a}{t_o^b} \quad (3.73)$$

where a and b are regionally determined constants. For a given t_o , the rainfall intensity of any return period T can be determined by the use of frequency factors K_T if they are available for $f(i)$. i_T is given by

$$i_T = i_m (1 + Cv(i) K_T) \quad (3.74)$$

where $Cv(i)$ is the coefficient of variation of $f(i)$ and is assumed to be constant for all durations t_o . The equation for any IDF curve is then

$$i_T = \frac{a}{t_o^b} (1 + Cv(i) K_T) \quad (3.75)$$

or,

$$i_T = \frac{a_T}{t_o^b} \quad (3.76)$$

where a_T is a constant for a particular return period T . For a particular rainfall event of duration t and return period T the rainfall intensity is therefore given by

$$i_{T,t} = \frac{a_T}{t^b} \quad (3.77)$$

The peak flow corresponding to $i_{T,t}$ is then

$$q_{p,T,t} = i_{T,t} \left(1 - \exp \left[- \left(\frac{s i_{T,t}^{0.4} t}{1.6 - s i_{T,t}^{0.4} t} \right)^{1.3} \right] \right) \quad (3.78)$$

where $s = (\frac{\sqrt{S_o}}{nL})^{0.6}$. $q_{p,T,t}$ will vary with t for a given return period of i .

The maximum $q_{p,T,t}$, $q_{M,p,T,t}$, is obtained by determining t which will make $\frac{dq_{p,T,t}}{dt}$ equal to 0. Let t_m be the duration for which maximum peak flow occurs.

After differentiating $q_{p,T,t}$ and some algebraic manipulation, at t_m the following relation holds :

$$1 = \exp \left[\left(\frac{k}{1.6 - k} \right)^{1.3} \right] \left(1 + \frac{1.3}{b} \left[\frac{k}{1.6 - k} \right]^{0.3} \left[\frac{(1 - 0.4b)k}{1.6 - k} + \frac{(1 - 0.4b)k^2}{(1.6 - k)^2} \right] \right) \quad (3.79)$$

where $k = i_{T,t}^{0.4} t_m (\frac{\sqrt{S_o}}{nL})^{0.6}$. The left hand-side of the equation is a constant, therefore, if b is a regional constant for the IDF curves, then k must be a constant for all T s. If k is a constant, equation 3.78 implies that the ratios $\frac{q_{M,p,T,t_m}}{i_{T,t_m}}$ and C are constants. This proves that the maximum peak flow from correlated uniform inputs on an impervious plane is linearly related to the rainfall intensity of the same return period.

Relation between the Maximum Peak Flows and Rainfall Intensities of a Constant Duration

Comparing equations 3.71 and 3.34, for C constant, $i^{0.4}t_o(\frac{\sqrt{S_o}}{nL})^{0.6}$ is a constant for all maximum peak flows. Along the crossed line A'B' in Figure 3.18 then

$$k = i^{0.4}t_o(\frac{\sqrt{S_o}}{nL})^{0.6} \quad (3.80)$$

where i and t_o are the rainfall intensity and duration corresponding to the maximum peak flows for all return periods. Since C is a constant, it suffices to find the probability distribution of i , $h(i)$, along the crossed line A'B' to determine $g(q_p(M))$. The latter will be a linear transformation of $h(i)$.

Assume that for a rainfall duration, $t_o = t_1$, the rainfall pdf is $f(i)$. Let $i = I_1$ for a given return period T_1 and duration t_1 . Refer to Figure 3.18. For T_1 , the corresponding rainfall intensity generating the maximum peak flow with return period T_1 is I_2 with duration t_2 . Along curve CD in Figure 3.18 for any I and t

$$I = \frac{a_1}{t^b} \quad (3.81)$$

where a_1 is the coefficient for $T = T_1$. Using equation 3.81, I_1 and I_2 are related as

$$\frac{I_2}{I_1} = (\frac{t_1}{t_2})^b \quad (3.82)$$

Along A'B' equation 3.80 requires that

$$I_2^{0.4}t_2 = k(\frac{nL}{\sqrt{S_o}})^{0.6} \quad (3.83)$$

Eliminating t_2 from equations 3.82 and 3.83 results in

$$I_2 = [\frac{1}{k}(\frac{\sqrt{S_o}}{nL})^{0.6}]^{b/(1-0.4b)} t_1^{b/(1-0.4b)} I_1^{1/(1-0.4b)} \quad (3.84)$$

where k is obtained from the solution of equation 3.79. Equation 3.71 states that the maximum peak flow is related to I_2 by

$$q_p(M), T = C I_{2,T} \quad (3.85)$$

Therefore, in general, the maximum peak flows of any return period are related to rainfall intensities i with a constant duration t_1 as

$$q_p(M) = W_1 i^{1/(1-0.4b)} \quad (3.86)$$

where W_1 is a constant corresponding to a constant duration t_1 . If the pdf of i ($f(i)$) is known, then the pdf $g(q_p(M))$ can be obtained from equation 3.86 and 3.30, i.e.,

$$g(q_p(M)) = f(i) \frac{di}{dq_p(M)} \quad (3.87)$$

$g(q_p(M))$ when $f(i)$ is Gamma

Equation 3.86 is a power function similar to equation 3.56. It was proven for equation 3.56 that if $f(i)$ is Gamma, then the coefficients of variation and skewness of $g(q_p)$ are independent of the constant, being dependent solely on $Cv(i)$ and the exponent in the power function. By analogy with equation 3.59 and 3.60

$$Cv(q_p(M)) = \frac{(\Gamma(\eta)\Gamma(2b' + \eta) - \Gamma^2(b' + \eta))^{1/2}}{\Gamma(2b' + \eta)} \quad (3.88)$$

$$Cs(q_p(M)) = \frac{\Gamma^2(\eta)\Gamma(3b' + \eta) - 3\Gamma(\eta)\Gamma(2b' + \eta)\Gamma(b' + \eta) + 2\Gamma^3(b' + \eta)}{(\Gamma(\eta)\Gamma(2b' + \eta) - \Gamma^2(b' + \eta))^{3/2}} \quad (3.89)$$

For both equations 3.88 and 3.89, $\eta = \frac{1}{Cv^2(i)}$ and $b' = \frac{1}{1-0.4b}$. Equations 3.88 and 3.89 demonstrate that for correlated rainfall inputs with b in equation 3.73 a constant, the coefficients of variation and skewness of the maximum peak flow

probability distribution are constants. Since by equation 3.71 maximum peak flows and the corresponding rainfall intensities are linearly related, then both $g(q_p(M))$ and $h(i)$ (the pdf of the rainfall intensities corresponding to the maximum peak flows) will have exactly the same Cv and Cs . This result is very different from that obtained for constant duration rainfall (i.e. uncorrelated inputs). Figure 3.19 shows the $Cs - Cv$ relationships for both constant duration rainfalls and correlated rainfall inputs. The two sets of curves have only their two extremities in common when b is variable and $Cv(i)$ is constant. For a constant b and variable $Cv(i)$, all $(Cs(q_p(M)), Cv(q_p(M)))$ lie on a single line. The equation of the pdf of the maximum peak flows given that $f(i)$ is Gamma, is by analogy with equation 3.58 given by

$$g(q_p(M)) = \frac{\lambda^\eta}{\Gamma(\eta)} \frac{1}{b'} \left(\frac{1}{W_1}\right)^{\eta/b'} \frac{(\eta - b')/b'}{q_p(M)} \exp\left[-\lambda \left(\frac{1}{W_1}\right)^{1/b'} \frac{1/b'}{q_p(M)}\right] \quad (3.90)$$

where W_1 is defined in equation 3.86, λ and η are parameters of $f(i)$ and $b' = \frac{1}{1 - 0.4b}$.

The foregoing analysis and results apply to the case where $f(i)$ is Gamma. For any other $f()$, equations 3.86 and 3.87 can still be used to find $g(q_p(M))$, although an analytical solution may not always be possible.

3.3.3 Random Rainfall Events on a Pervious Plane

In this subsection, the effects of infiltration are investigated. The system is kept simple by assuming that both the rainfall rates (i) and the infiltration rates (f) are uniformly distributed over time and space. The infiltration rate f can either be constant for all rainfall events or have a pdf $h(f)$ which will be the uniform

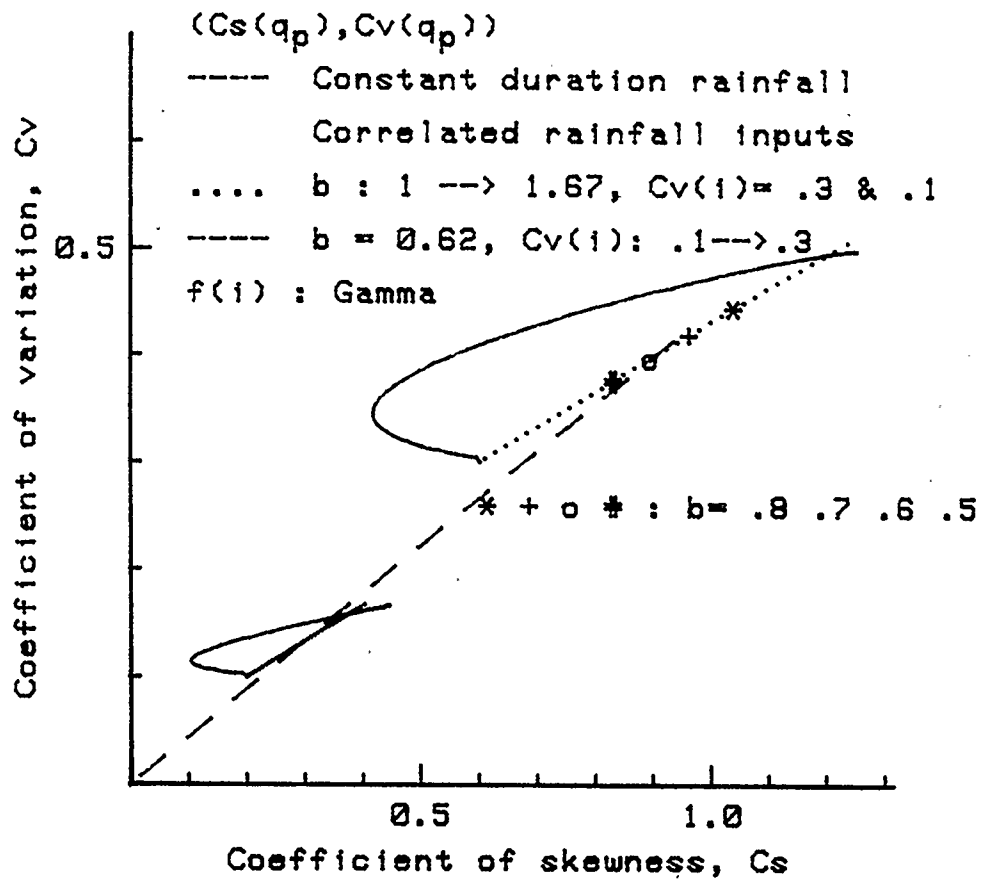


Figure 3.19: Comparing $Cs - Cv$ relations of peak flows from constant duration rainfall inputs with those from correlated rainfall inputs when $f(i)$ is Gamma.

distribution with a lower limit $fmin$ and an upper limit $fmax$. Monte Carlo simulation will be used to generate random rainfall and infiltration rates. Since i and f are uniform over time, the random effective rainfall intensity i_e is

$$i_e = i - f \quad (3.91)$$

The peak runoff for any random i_e is then

$$q_p = i_e \left(1 - \exp \left[- \left(\frac{k}{1.6 - k} \right)^{1.3} \right] \right), \quad k < 1.6 \quad (3.92)$$

$$q_p = i_e, \quad \geq 1.6 \quad (3.93)$$

where

$$k = i_e^{0.4} t_o \left(\frac{\sqrt{S_o}}{nL} \right)^{0.6} \quad (3.94)$$

Constant Duration Rainfall

For a Normal $f(i)$ with mean i_m and a Uniform $h(f)$ with mean $fmean = 0.5(fmin + fmax)$, the $Cs - Cv$ relationships for $g(q_p)$ are shown in Figure 3.20. The minimum infiltration rate, $fmin$, and i_m were set to 0 and 100 mm/hr respectively. Figure 3.20 indicates that the $Cs - Cv$ curves are displaced to the right and upwards for increasing $fmax$. As with the impervious plane, each curve starts from a maximum $(Cs(q_p), Cv(q_p))$, and then tends towards a limiting $Cv(q_p)$ approximately equal to $\frac{i_m - fmean}{i_s}$. i_s is the standard deviation of $f(i)$. The lowest $Cv(q_p)$ is approximately equal to the Cv of the effective rainfall instead of the total rainfall as was the case with the impervious plane. The shift in the $Cs - Cv$ curves means that the skewness of $g(q_p)$ has increased.

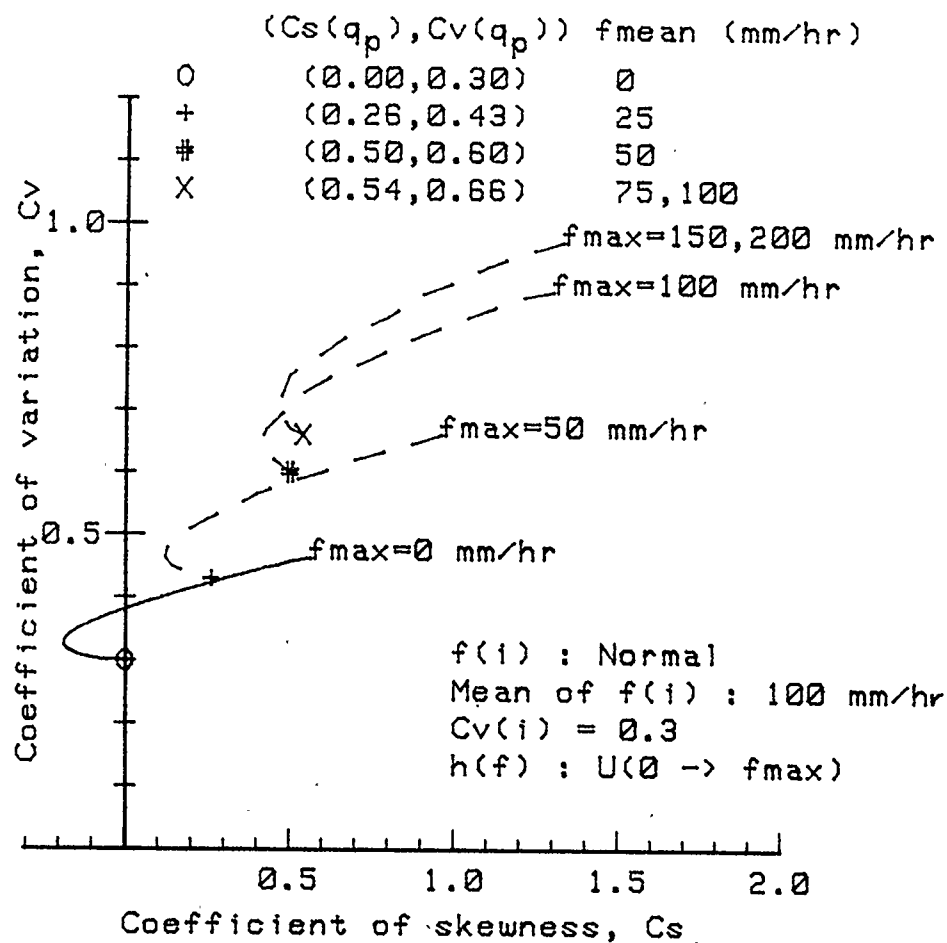


Figure 3.20: $Cs - Cv$ relationships of peak flows from pervious planes with $f(i) : \text{Normal}$ and $h(f) : \text{Uniform}$.

For a given $fmax$, $(Cv(qp), Cv(qp))$ is a constant for a constant kme . The latter is defined as

$$kme = (ie)^{0.4} t_o \left(\frac{\sqrt{S_o}}{nL} \right)^{0.6} \quad (3.95)$$

and

$$(ie)_m = im - fmean \quad (3.96)$$

For constant kme and $Cv(i)$, $Cv(qp)$ and $Cs(qp)$ increase with increasing $fmax$. However, after a certain $fmax$, the $Cv(qp) - Cs(qp)$ curve is not very sensitive to further increase in $fmax$. This limiting $fmax$ is approximately equal to $2im$, or $fmean \approx im$. The dashed line in Figure 3.20 shows the approximate location of the limiting $Cs - Cv$ curve when $f(i)$ is Normal. Figure 3.21 shows the corresponding results when $f(i)$ is Gamma.

Correlated Rainfall Inputs with Random Infiltration Rates

For correlated inputs, the mean rainfall intensity im is assumed to be related to the rainfall duration t_o by the equation which has been reproduced below :

$$im = \frac{a}{t_o^b} \quad (3.97)$$

As described for the case of an impervious plane, $Cv(qp)$ and $Cs(qp)$ are determined by the Monte Carlo simulation method. The characteristics of the plane are $S_o = 0.01$, $n = 0.02$, and $L = 500$ m. $f(i)$ and $h(f)$ are the Gamma and Uniform distributions respectively. a in equation 3.97 is 456.2 and b in the same equation will be allowed to take a constant value between 0.42 and 0.72 for a number of runs. The minimum infiltration rate is 0 mm/hr and the maximum infiltration rate is a random value between 0 and 70 mm/hr for each run. The maximum peak

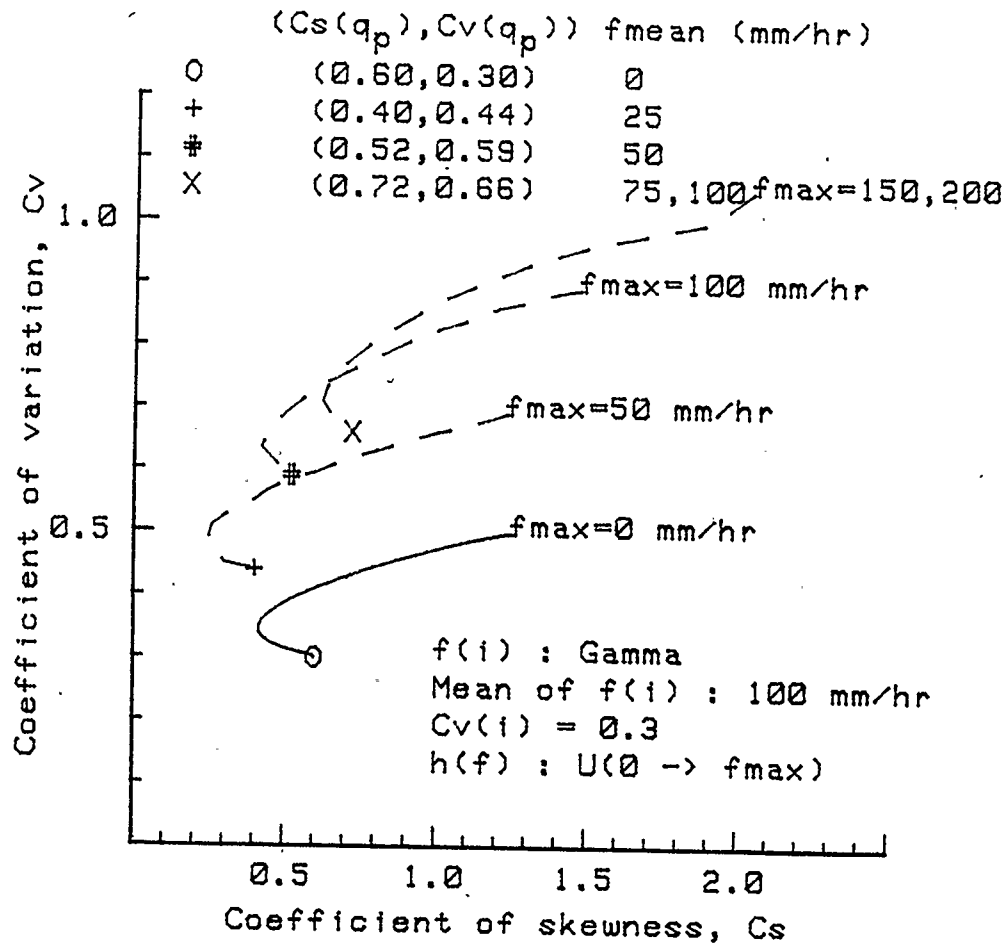


Figure 3.21: $Cs - Cv$ relationships of peak flows from pervious planes with $f(i) : \text{Gamma}$ and $h(f) : \text{Uniform}$.

flow is that peak flow which is greatest for increasing duration of rainfall, all other parameters held constant.

Figure 3.22 shows the $C_s - C_v$ relationships for the maximum peak flows and effective rainfall intensities. The coefficient of variation of $f(i)$, the total rainfall intensity pdf, is 0.3. Unlike the case of the impervious plane, $(C_s(q_p(M)), C_v(q_p(M)))$ is no longer coincident the (C_s, C_v) of the effective rainfall pdf and the difference increases with an increase in $fmax$ and a decrease in b (equation 3.93). This means that for correlated inputs with infiltration, the pdf's of the maximum peak flows and effective rainfall are no longer linearly related. This is further confirmed by Figure 3.23 which is a plot of the maximum peak flows and effective rainfall intensities against return period. If a ratio C_T is defined as

$$C_T = \frac{q_p(M), T}{i_{e, T}} \quad (3.98)$$

then, it is observed that C_T is smaller for smaller T 's and vice-versa. For a given b (equation 3.93) C_T increases with T until it is the same as C (equation 3.71) for an impervious plane. This implies that infiltration reduces the higher frequency peak flows more than the lower frequency peak flows. The latter are also very close to the maximum peak flows of the same frequency from impervious planes. For a given $fmax$ and T , a higher b decreases C_T . These results are at variance with the Rational method which assumes C to be only the fraction of rainfall lost and not to be dependent on the return period of the design peak flow required. The next section examines the effect of a constant infiltration rate for all rainfall intensities.

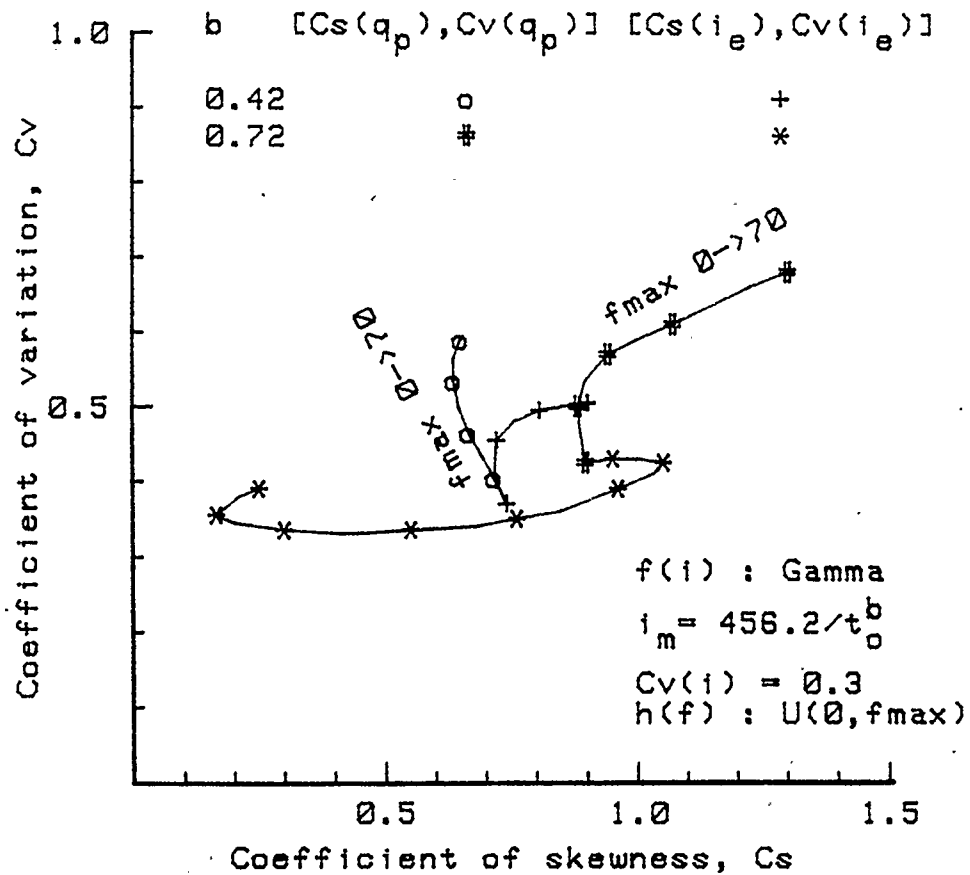


Figure 3.22: $Cs - Cv$ relationships for maximum peak flows and for the corresponding effective rainfall intensities when rainfall inputs are correlated and include infiltration.

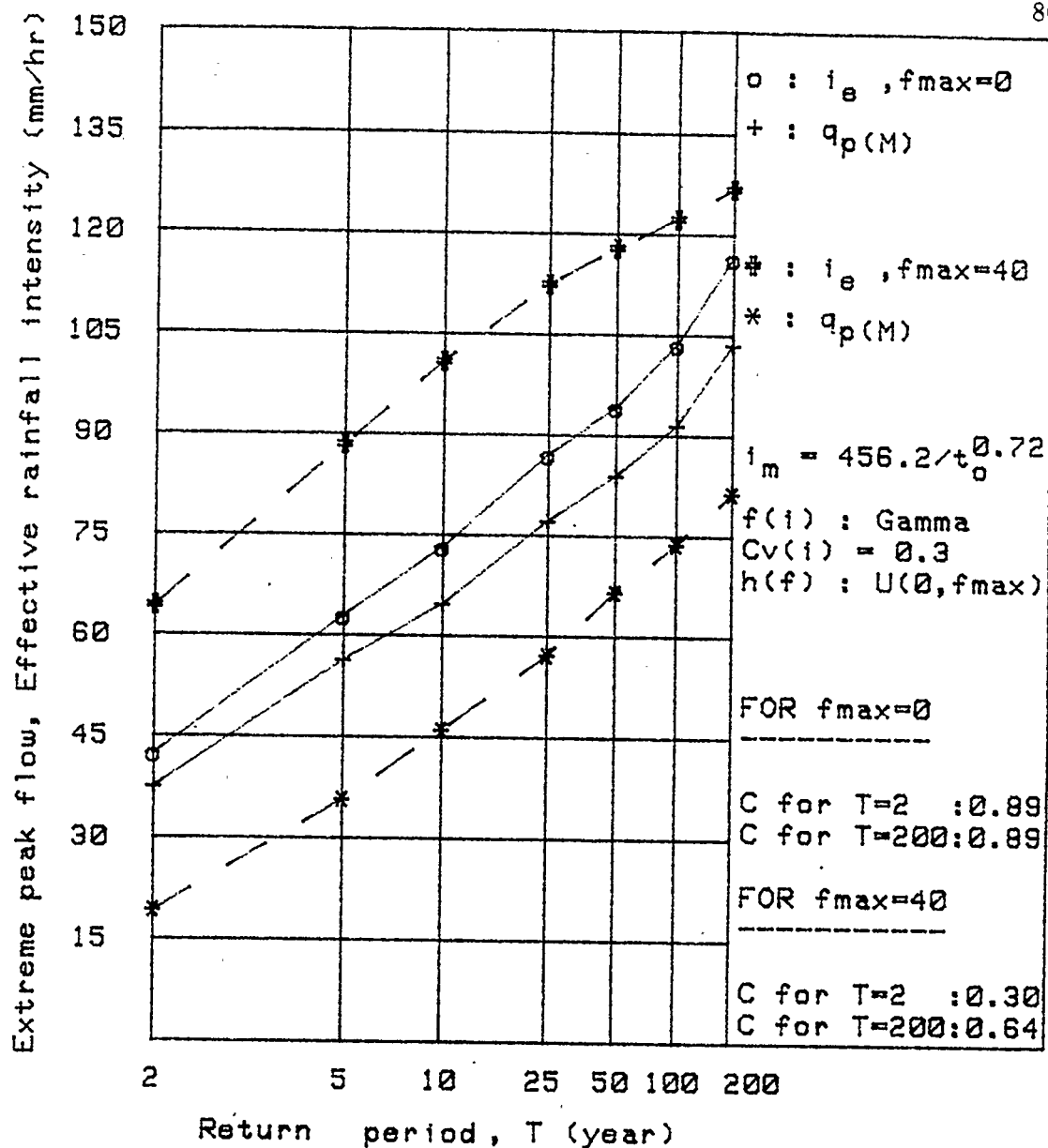


Figure 3.23: Return periods of peak flows and corresponding rainfall intensities from pervious planes under correlated rainfall inputs.

Correlated Rainfall Inputs With Constant Infiltration Rates

The behaviour of $q_p(M), T$ and i_T under constant infiltration rates are shown in Figure 3.24. The plane has the following characteristics : length = 1500 m, slope = 0.03, and roughness = 0.04. The regional constants for the correlated rainfall inputs are : $a = 338.7$ and $b = 0.70$. The rainfall intensity pdf $f(i)$ is the Gumbel distribution with $Cv(i) = 0.3$ and $Cs(i) = 1.14$. The coefficient of skewness of the Gumbel distribution is a constant at 1.14. For a particular return period T , i_T was simulated for various durations as determined by the IDF curves and the maximum peak runoff was obtained. The no-infiltration case shows that the flows with high return periods (i.e. rare events) are generated by shorter duration and higher intensity rainfalls. When infiltration is considered, however, the rare events tend to be those of lower intensities and longer durations than the more frequent events. Also, the ratio C of $q_p(M), t_m$ to i_T, t_m is no longer constant. And for an infiltration rate exceeding 20 mm/hr, it seems that the rainfall events yielding maximum peak runoffs have almost a constant rainfall intensity for T between 2 and 200, only the duration of each event changes.

3.4 Effects of Non-uniform Random Inputs on Peak Flow Probabilities

In the previous sections rainfall and infiltration rates were assumed to be uniform both areally and temporally. While uniform rates are characterized by single values, truly non-uniform rates have to be specified for each unit area at every time step. The infinite number of possible configurations precludes an all encompass-

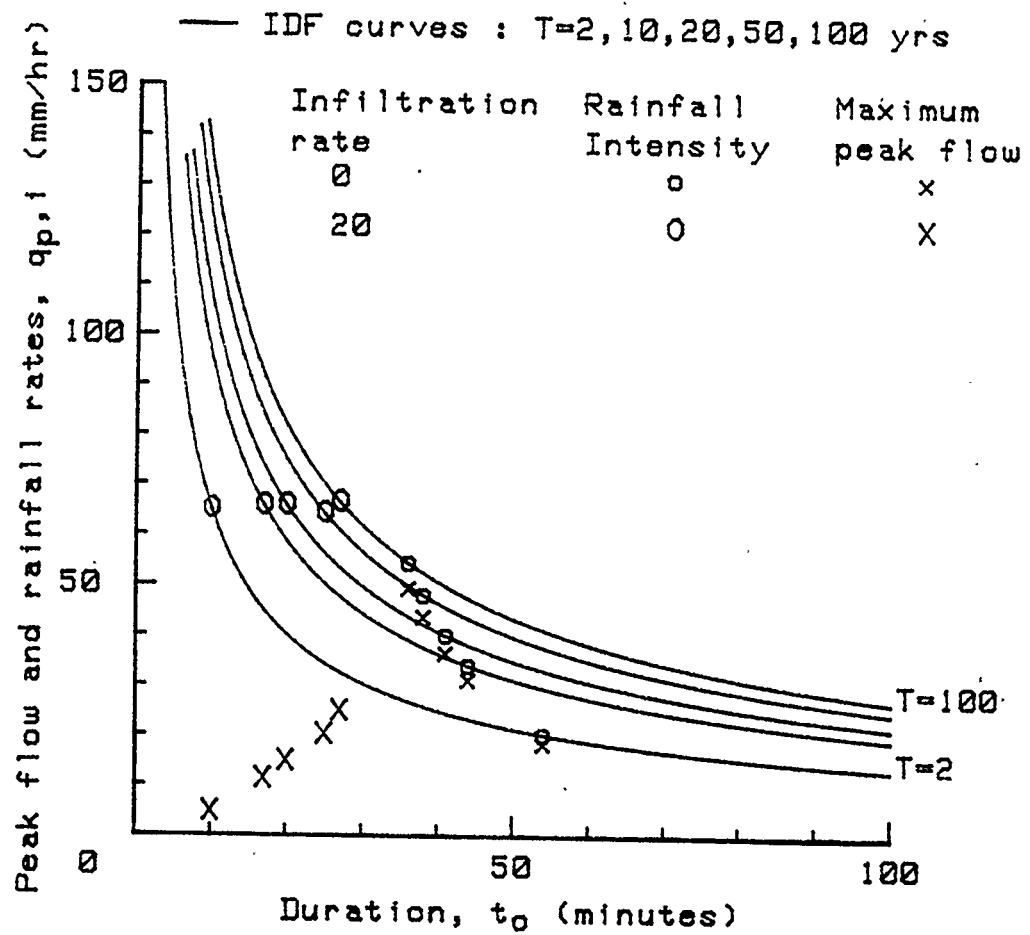


Figure 3.24: Effect of constant infiltration rate on the return periods of peak flows from correlated and spatially uniform rainfall.

ing solution to the rainfall-runoff process. An alternative approach is to adopt an easily describable form of the most usual distributional shape of the variable and determine the sensitivity of the statistical parameters of the peak runoff series to the characteristics of the shape. The critical shape will evidently be a function of plane and other input characteristics.

The time distribution of rainfall intensity i is assumed to be triangular in shape with the peak intensity i_p occurring at time t_p which is usually in the first or second quartile of the total rainfall duration t_o . The ratio $\frac{t_p}{t_o}$ can vary between 0 and 1. The corresponding uniform hyetograph with an equal volume of rainfall over t_o has a constant intensity of $\frac{i_p}{2}$. These variables are illustrated in Figure 3.25. The time distribution of infiltration rate f is of a decreasing exponential type. The infiltration rate f at any time $t \geq t_{of}$ is given by an equation similar in form to equation 3.1 :

$$f = f_c + (f_o - f_c)\exp(-f_k(t - t_{of})) \quad (3.99)$$

f_k is a decay constant dependent on the soil type. The runoff is assumed to be produced by the rainfall excess depicted by the shaded area.

In the following subsections the effects of $\frac{t_p}{t_o}$, f_c , f_o , and f_k on the statistical characteristics of random peak flows series are examined. i , f_c , and f_o are assumed to random variables generated from known pdfs. For these complex cases there is no analytical or even semi-empirical equation relating i to q_p . Hence, for every random input the Diffusion equations have to be solved numerically over the duration of the runoff to obtain the peak runoff.

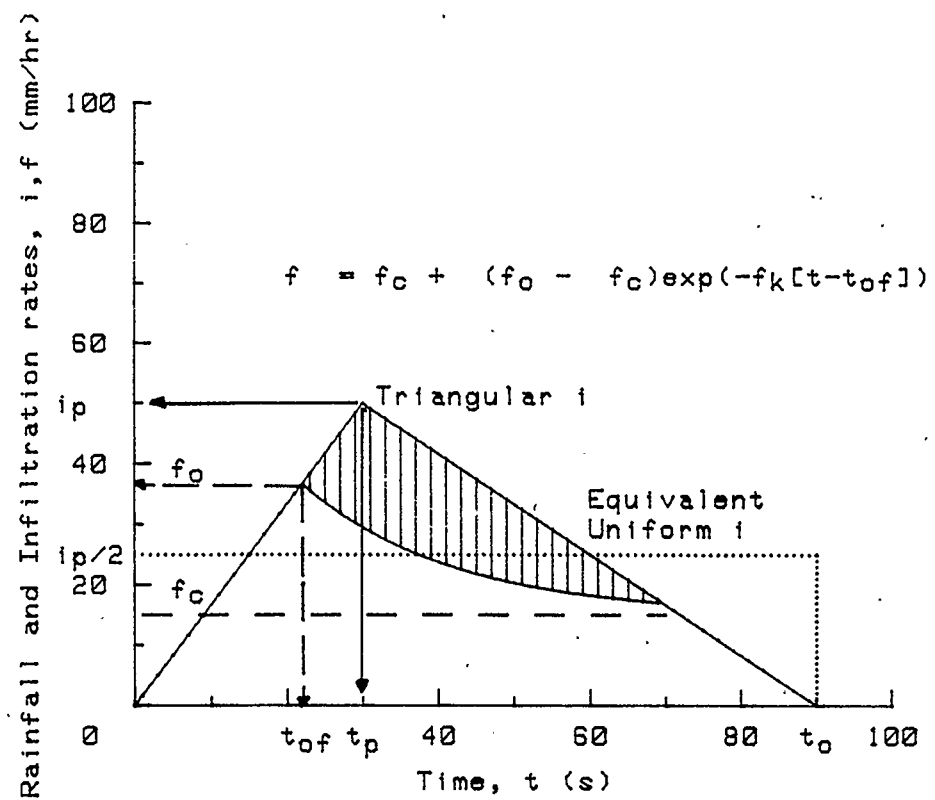


Figure 3.25: Non-uniform rainfall and infiltration rates.

3.4.1 Triangular Distribution of Rainfall Intensity on an Impervious Plane

In this subsection the rainfall intensity is assumed to be spatially uniform and to have a triangular distribution over its duration. For a given rainfall duration t_o , the volume of precipitation it_o is triangularly distributed over t_o such that the peak intensity i_p ($= 2i$) occurs at t_p where $0 \leq t_p \leq t_o$. The ratio, p , of t_p to t_o is kept constant for a particular random series of rainfall intensities. The runoff due to average (i.e. 1/2 of the peak intensity) rainfall intensity ranging between 1 mm/hr and 200 mm/hr in steps of 1 mm/hr are numerically simulated and the corresponding peak flows q_p determined. 6000 random average rainfall intensity values are generated from $f(i)$. The corresponding 6000 random values of peak flows q_p are obtained by interpolating between the numerically simulated values. The resulting random series of q_p are analysed for their statistical parameters. Figures 3.26 and 3.27 show the $Cs(q_p) - Cv(q_p)$ relationships for $f(i)$ Normal and Gamma respectively ($Cv(i) = 0.3$ for both cases). p varies between $\frac{1}{6}$ and $\frac{9}{10}$ where

$$p = \frac{t_p}{t_o} \quad (3.100)$$

The $Cs(q_p) - Cv(q_p)$ curve for spatially uniform rainfall intensity is shown on the respective figures when $f(i)$ is Normal and Gamma.

For all p 's, the $Cs(q_p) - Cv(q_p)$ curves including that of the uniformly distributed i , start from the same maximum $(Cs(q_p), Cv(q_p))$ and converge to the $Cv(i)$ of $f(i)$. This is an expected result because for low rainfall intensities of short durations over runoff planes with rough surfaces over shallow slopes the temporal

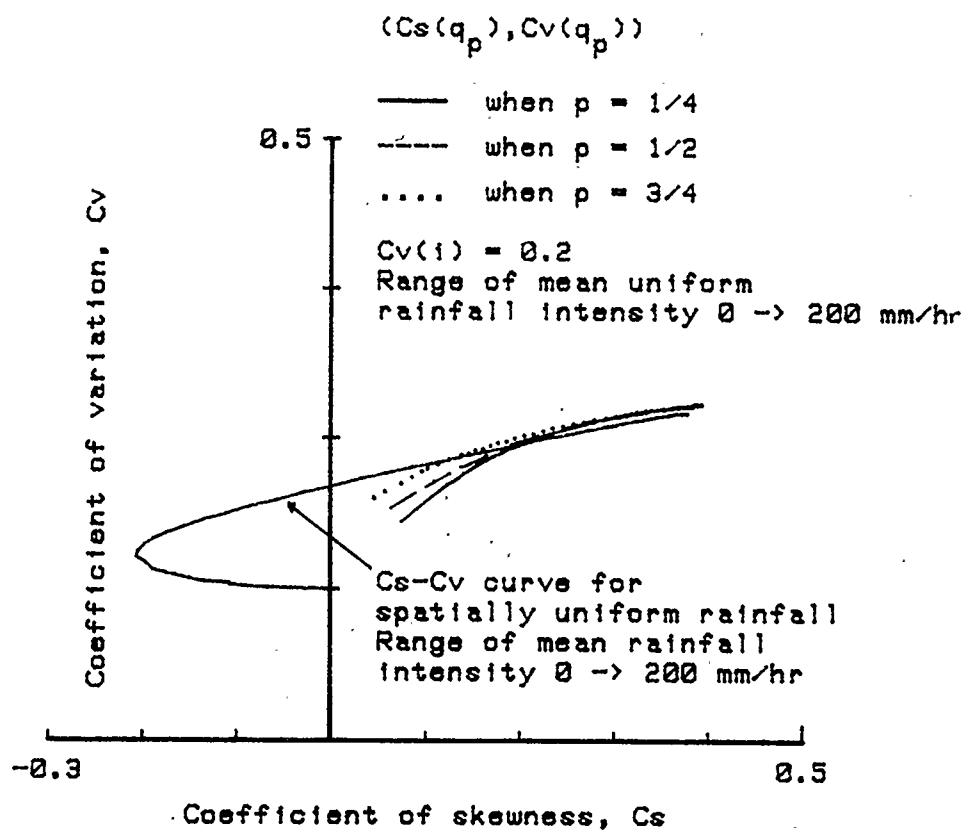


Figure 3.26: Cs - Cv relationships of peak runoff from triangular temporal distributions of rainfall intensity when $f(i)$ is Normal.

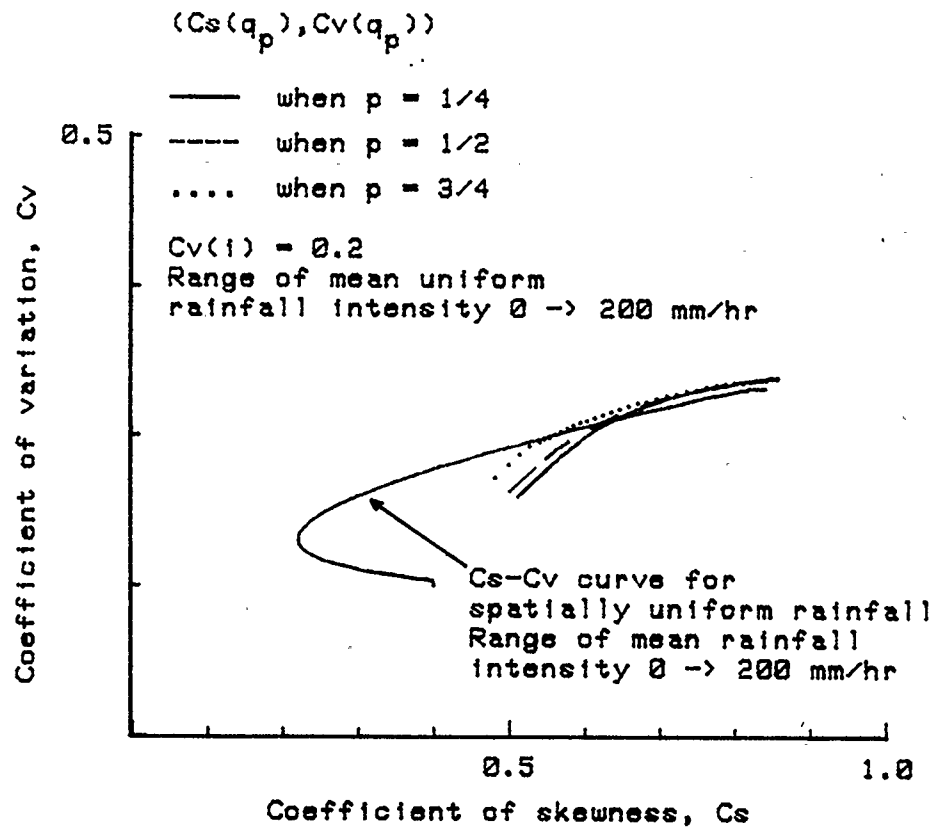


Figure 3.27: $Cs-Cv$ relationships of peak runoff from triangular temporal distributions of rainfall intensity when $f(i)$ is Gamma.

distribution of the rainfall intensity is not very significant. For the other extreme of the conditions mentioned, i.e, high rainfall intensities with long durations, etc., the temporal distribution of i is again not significant because the peak runoff is probably equal to the rainfall intensity. Between the two limiting co-ordinates, the curves from the triangularly distributed rainfall intensities separate from that of the uniformly distributed i . The separation between the curves for the triangularly distributed rainfall intensities increase for decreasing p until it becomes insignificant over most of the curve for $p < \frac{1}{6}$.

The behaviour of the $Cs(qp) - Cv(qp)$ curves for the triangularly distributed rainfall intensities can be explained by examining the $i - qp$ curves for different ps . The latter curves are shown in Figure 3.28 for $p = \frac{1}{4}, \frac{1}{2}$, and $\frac{3}{4}$. For these curves, qp is plotted against $\frac{ip}{2}$, the equivalent uniform rainfall intensity. It was demonstrated in Figure 3.13 that the coefficient of skewness of the peak runoff series was related to the curvature of the $i - qp$ curve. When the curve is concave and $f(i)$ is Normal, the coefficient of skewness of the peak flow series is positive, conversely, when the curve is convex the coefficient of skewness is negative. When the curve transits from a concave shape to a convex shape through an inflexion point, the coefficient of skewness will range between a maximum and a minimum. For the lower range of $\frac{ip}{2}$, the curves for triangular and uniform distributions of rainfall intensity are concave and coincident and therefore explains why the maximum $(Cs(qp), Cv(qp))$ from either distribution of rainfall is the same. For increasing i , the $i - qp$ curve for uniformly distributed rainfall intensity becomes convex after an inflexion point, however, the corresponding curves for triangularly distributed rainfall intensities continue on a concave path. So, while the $(Cs(qp), Cv(qp))$

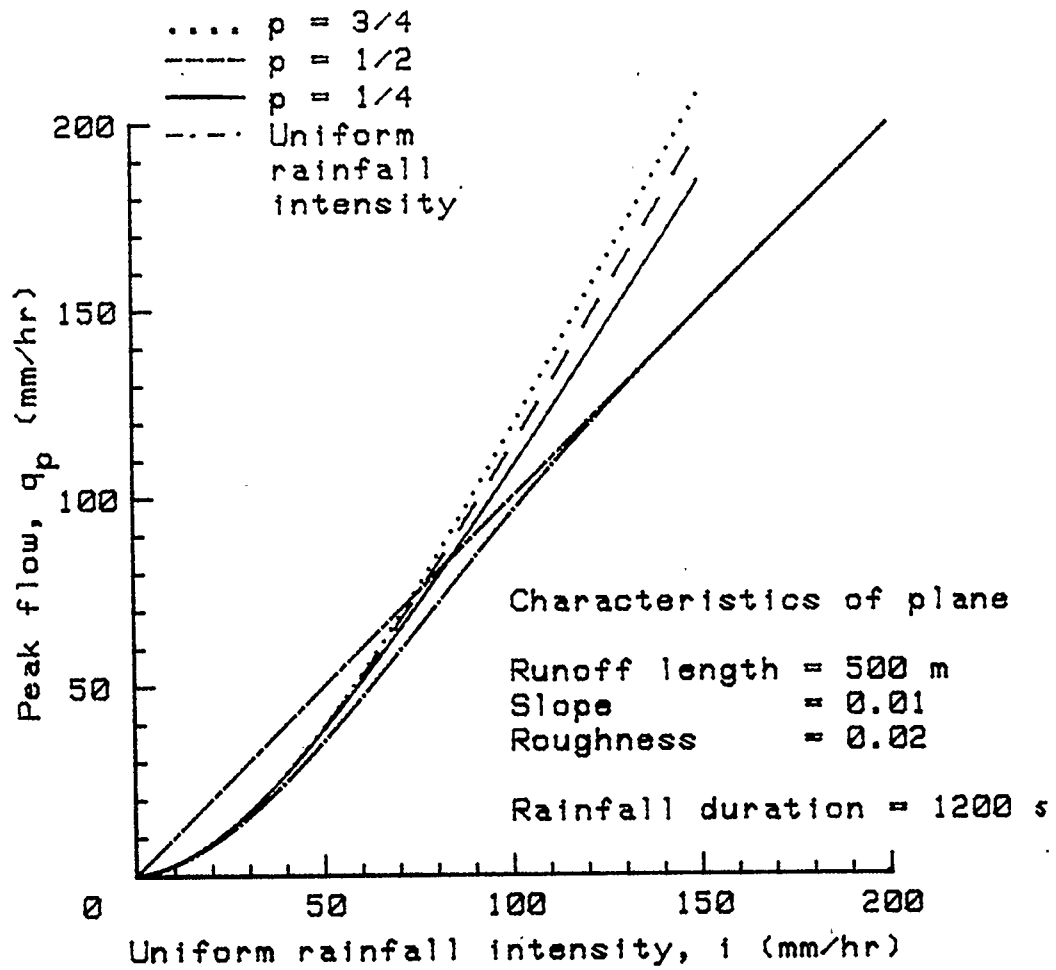


Figure 3.28: Rainfall intensity-peak flow curves for temporally non-uniform rainfall intensity.

coordinates of the uniformly distributed rainfall intensity decrease, those of the triangularly distributed rainfall intensity remain at the maximum for a longer range of i . The $i - q_p$ curves for the triangular distribution of rainfall intensity eventually reach an inflexion point, however the latter is not well defined. The consequence of this behaviour is that the relationship between i and q_p can be approximated by power function types of equations over a considerable range of i . It has been shown in section 3.3.2 (see Figure 3.19) that for a variable b in equation 3.56 and a constant $Cv(i)$, the relationship between the coefficients of variation and skewness of the peak flow series is almost a straight line between the point of maximum skewness and the skewness of the rainfall intensity distribution $f(i)$. Of the three curves for triangularly distributed rainfall intensity, the one for $p = \frac{1}{4}$ is better approximated by power functions (its point of inflexion occurs outside the range of rainfall intensities tested and is at a higher intensity than the other two curves) and its $Cs(q_p) - Cv(q_p)$ curve is almost a straight line between the maximum coefficient of skewness of q_p and $(Cs(i), Cv(i))$. The $i - q_p$ curves for the other two values of p have their inflexion points at lower rainfall intensities and their $Cs(q_p) - Cv(q_p)$ curves are in between that of the uniformly distributed rainfall intensity and that of $p = \frac{1}{4}$.

An interesting observation from Figure 3.28 is that for triangularly distributed rainfall intensities, the coefficients of skewness and variation of the peak runoff series are close to the maximum over a large range of mean rainfall intensities and are not too sensitive to the time of occurrence of the peak rainfall intensity. If this observation holds true for more complicated hydrological systems, then, detailed measurement of rainfall intensity distributions over time may not be very

important, at least as far as the coefficients of variation and skewness of the peak flows are concerned.

3.4.2 Triangular Distribution of Rainfall Intensity on a Pervious Plane

The case of non-uniform rainfall intensity on a pervious plane is very close to a natural situations. The number of variables has increased considerably compared to the basic system of uniform rainfall intensity over an impervious plane. The ratio is now 5 to 1. f_o , f_c , and f_k have to be specified for the infiltration curve and i and p for the rainfall hyetograph. f_o and f_c are Uniformly distributed random variables while i , the equivalent temporally uniform rainfall intensity, has a Gamma pdf. p is taken to be $\frac{1}{3}$ and f_k is assumed to be constant for a given soil type. The plane characteristics are $L = 500$ m, $S_o = 0.01$ and $n = 0.02$. f_o is $U(100,25)$ and f_c is $U(25,0)$. The infiltration curves for the cases of $f_o = 100$ mm/hr, $f_c = 25$ mm/hr, and $f_k = (0.005, 0.05, 0.02)$ are shown in Figure 3.29. The curve with $f_k = 0.05$ can nearly simulate the case of uniform loss rate. This case is dealt with in the next section for correlated rainfall inputs.

199 values of each random variable (f_c , f_o , and i) were generated by the Monte Carlo simulation technique. The peak runoffs were obtained by numerical simulation of the Diffusion Wave equations. The $C_s - C_v$ relationships of the random peak flows for i_m ranging between 10 and 150 mm/hr are shown in Figure 3.30. Compared to the impervious case, both $C_s(q_p)$ and $C_v(q_p)$ from a pervious plane have increased. The curves for the three f_k are very close to one another until i_m goes below 50 mm/hr. For very low mean rainfall intensities, the effect of the infiltration is very significant.

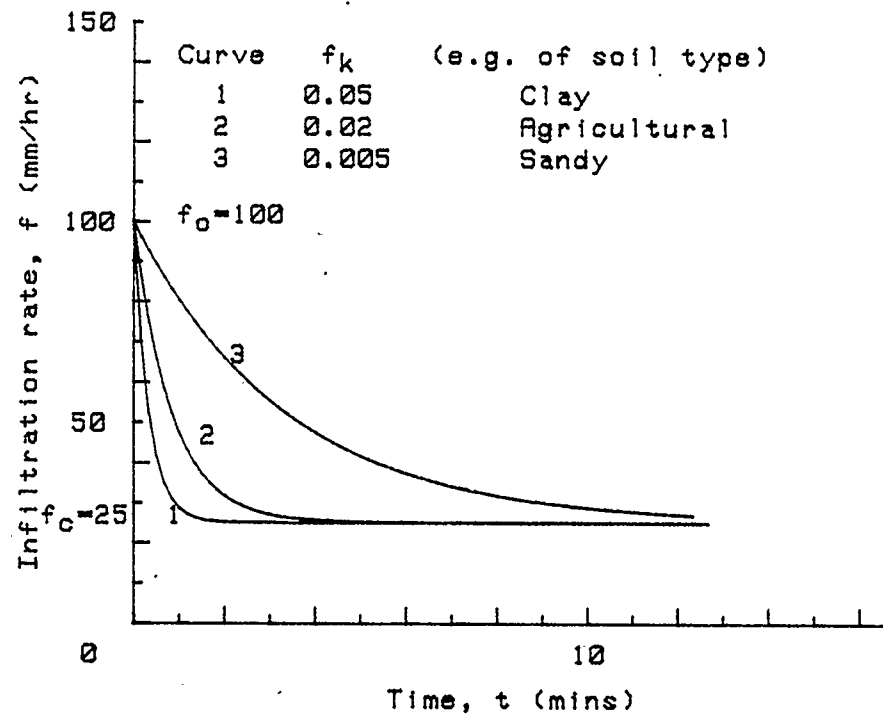


Figure 3.29: Infiltration curves for 3 soil types.

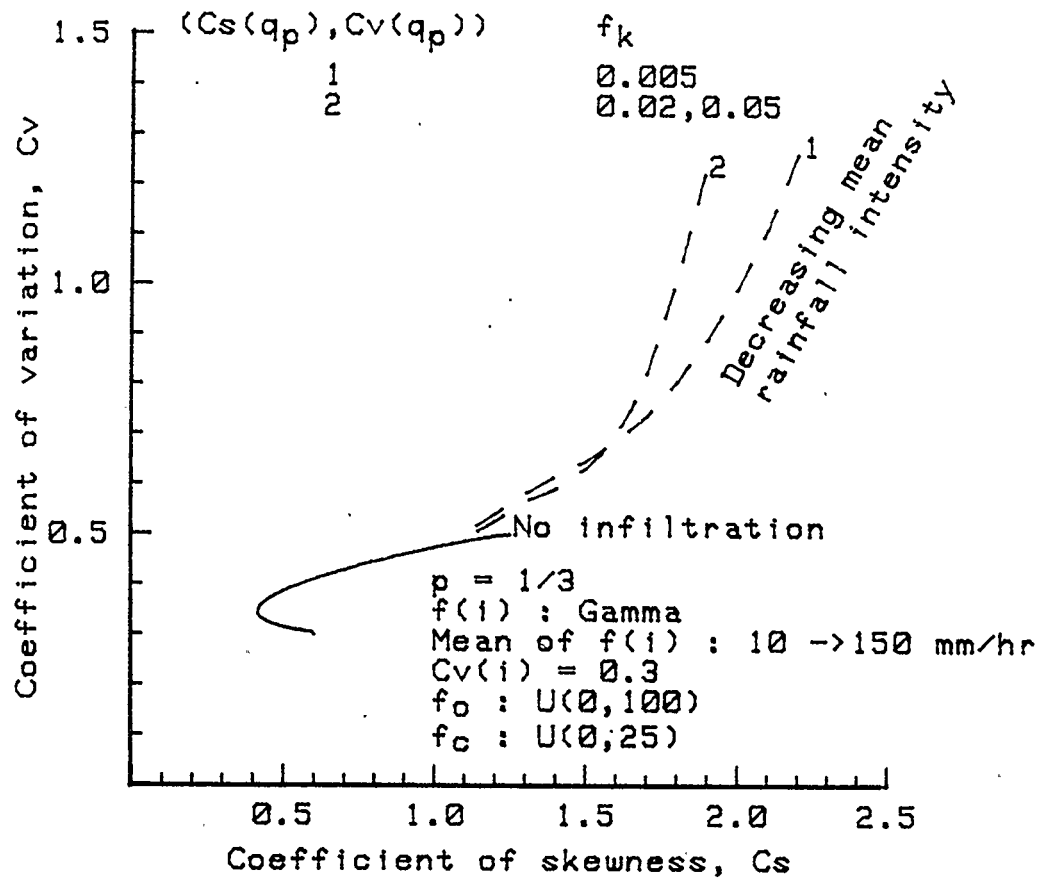


Figure 3.30: $Cs - Cv$ relationships of peak flows from non-uniform temporal distribution of rainfall intensities and infiltration rates for $f(i) : \text{Gamma}$.

3.4.3 Correlated Non-Uniform Rainfall Inputs on a Pervious Plane

The analysis performed for correlated rainfall inputs with constant infiltration rates and spatially uniform rainfall intensity in section 3.3.3 is repeated in this section for rainfall intensity having a triangular distribution in time. The ratio p of time to peak intensity to duration of rainfall is $\frac{2}{5}$. The same plane and rainfall characteristics are used. The results are shown in Figure 3.31. The behaviour of $q_p(M), t_m$ and I_{T, t_m} with t_m are similar to that observed for the uniform rainfall case in Figure 3.24. The ratios of $q_p(M), t_m$ to I_{T, t_m} are no longer constants with T . And, low frequency peak flow events tend to be from lower intensity and longer duration rainfall events than the high frequency peak flow events.

3.5 Summary

The relationships between the coefficients of variation and skewness of random peak flow series were studied for the most basic element of a conceptual watershed, the single sloping plane. Assuming that the flow could be approximately described by the numerical solutions to the Diffusion Wave equations, the results obtained for the different plane and rainfall parameters considered were as follows.

For uniform and constant duration rainfall events with no infiltration, the $(Cs(q_p), Cv(q_p))$ coordinates of the peak flow series start from a maximum location determined by the pdf of the rainfall intensity $f(i)$, its coefficient of variation $Cv(i)$, its coefficient of skewness $Cs(i)$, and a parameter $k (= i^{0.4} t_o (\frac{\sqrt{S_o}}{nL})^{0.6})$ taking a value less than 0.5. When k increases, the magnitudes of $Cs(q_p)$ and $Cv(q_p)$ decrease until $Cs(q_p)$ reaches a minimum which is less than $Cs(i)$, at this

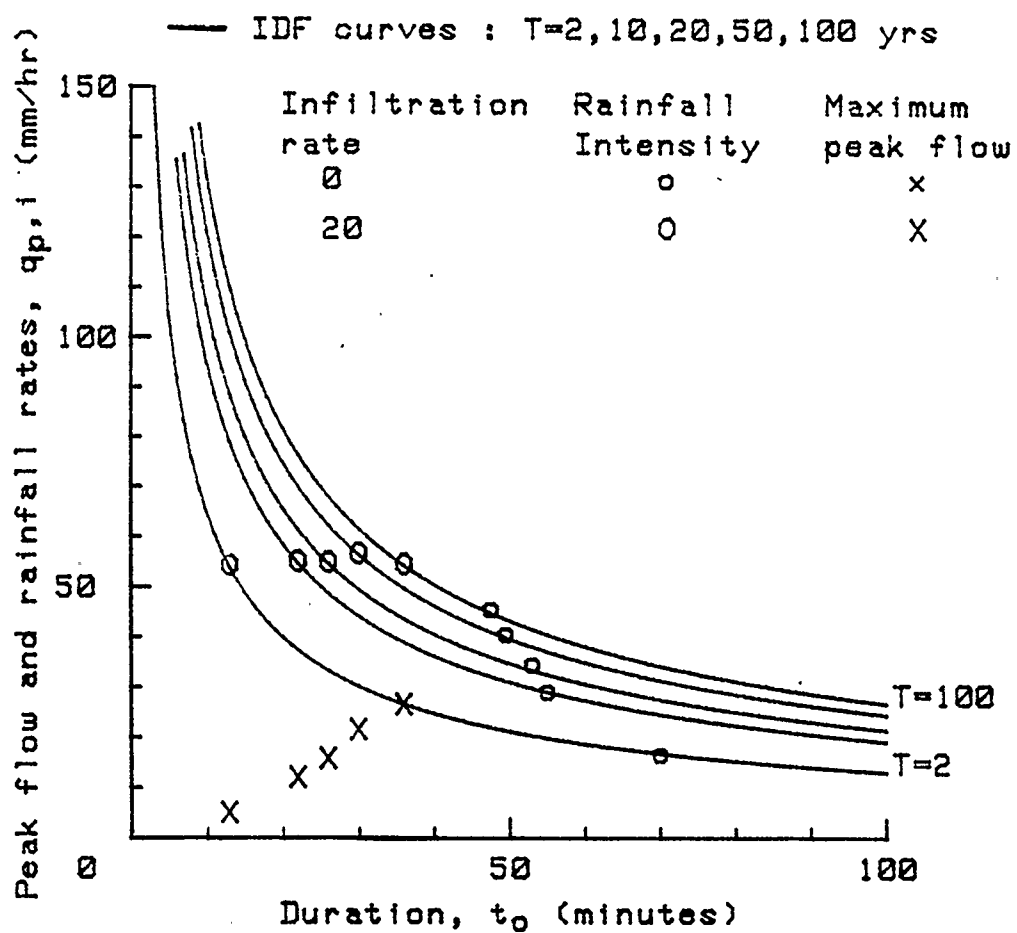


Figure 3.31: Effect of non-uniform temporal distribution of rainfall intensity and constant infiltration rate on the return periods of maximum peak flows and the corresponding rainfall intensities when the rainfall inputs are correlated.

minimum $Cv(q_p)$ is still greater than $Cv(i)$. On further increase of k , when some peak flows are the steady state values, the $Cs(q_p) - Cv(q_p)$ curve moves towards $(Cs(i), Cv(i))$. The behaviour of $(Cs(q_p), Cv(q_p))$ is related to the shape of the $i - q_p$ curve. When the latter is concave, at low k values, then $Cs(q_p)$ and $Cv(q_p)$ are greater than $Cs(i)$ and $Cv(i)$ respectively. Conversely, when the shape of the $i - q_p$ curve is convex, the coefficient of skewness of the random peak flow series is lower than the corresponding than that of the rainfall intensity. Since a "real" $i - q_p$ curve starts off as concave, goes through an inflexion point, becomes convex and finally becomes linear (at steady states), therefore the shape of the $Cs(q_p) - Cv(q_p)$ curve is as described above.

For a given $f(i)$, the maximum $(Cs(q_p), Cv(q_p))$ coordinates for varying values of $Cv(i)$ lie on a single curve. For a Normal $f(i)$, the curve is almost linear with the ratio of $Cs(q_p)$ to $Cv(q_p)$ approximately equal to 1.21.

When infiltration is taken into account, the $(Cs(q_p), Cv(q_p))$ coordinates increase relative to those from impervious planes. The increase occurs because infiltration changes the pdf $f(i)$ of the rainfall intensity and the coefficients of variation and skewness of the effective rainfall intensity increase. When $Cv(i)$ and $Cs(i)$ are increased to $Cv(i_e)$ and $Cs(i_e)$, the same conclusions as for impervious cases are reached.

The effect of a non-uniform temporal distribution (triangular) distribution of rainfall intensity on the coefficients of variation and skewness of the random peak flow series is important only when very high mean rainfall intensities are being considered. For low mean rainfall intensities the maximum $(Cs(q_p), Cv(q_p))$ coordinates are exactly the same as for uniformly distributed rainfall intensities,

independent of the shape of the rainfall hyetograph. When the mean rainfall intensities are increased the $Cs(q_p) - Cv(q_p)$ curves separate from that of uniformly distributed rainfall intensities, although their general shape are very similar for hyetographs where the peak rainfall intensity occurs close to the end of the storm. When the peak rainfall intensity occurs close to the start of the rainfall event, then the $Cs(q_p) - Cv(q_p)$ curve is almost a straight line joining the maximum $(Cs(q_p), Cv(q_p))$ coordinate to $(Cs(i), Cv(i))$.

For correlated rainfall inputs, characterised by IDF curves, the most important result obtained is that for a given meteorological region, $(Cs(q_p), Cv(q_p))$ of the maximum peak flows are constants for given $Cv(i)$ and independent of the characteristics of the plane. The ratio of maximum peak flow of given return period to the corresponding rainfall intensity of the same return period is a constant for all return periods. The ratio, however, varies with the rainfall characteristics (i.e. different regions) and is not equal to 1 as assumed in the Rational Method for impervious catchments. The ratio becomes variable when infiltration is taken into account. The statistical parameters of the peak flows then become sensitive to the characterisation of the infiltration rates. For impervious planes, the low frequency flood events are caused by longer duration and smaller intensity rainfall events than the high frequency floods events are. The addition of infiltration reverses the latter conclusion. The effect of non-uniform rainfall intensity on impervious planes is nil. The coefficients of skewness and variation of the peak flows are independent of the temporal distribution of the rainfall intensity and depend only on the characteristics of the IDF curves. The ratio of maximum peak flow of a given return period to the corresponding rainfall intensity of the same return period is still a

constant. As with the case of temporally uniform rainfall, inclusion of infiltration makes the ratios variable.

Chapter 4

STATISTICAL CHARACTERISTICS OF RANDOM FLOOD EVENTS ALONG A STREAM

4.1 Introduction

In hydrology, floods are extreme events of great importance. A flood may be characterized by its peak flow rate, level, volume, or duration depending upon which parameter is critical for design and planning purposes. Consequently, the definition of a flood has to take account of engineering and/or water management features. For example, peak flow rate is critical for the design of culverts, whereas peak flood level is very important in relation to human activities along a stream. In this chapter, peak flow rate and flood level are the two flood parameters under study.

Because of the extreme complexities of flow generating processes, an exact and continuous simulation of streamflow is not possible as yet. Records of peak flow rates and flood levels indicate that these quantities are functions of time and space, and appear to fluctuate in a random manner. For practical applications then, these variables must necessarily be expressed in terms of probabilities. When historic flood records for a sufficient number of years are available, a frequency analysis of the relevant flood parameter can give its sample probability distribution. This

distribution can then be used to predict the probable flood at the gaged location for return periods generally not exceeding twice the number of years of data. Such a probabilistic analysis assumes that the floods are time independent, which may not be totally true even when annual floods are being analysed. This assumption will, however, be taken for granted throughout this chapter. Two other problems associated with frequency analysis of floods are (1) the relative shortness of flow records, and (2) the transposition of the probability distribution of the floods from a well-gaged location to a section several kilometres upstream or downstream. These two problems can be circumvented by a composite physical-probabilistic approach to the determination of the statistical patterns in random flood events. As outlined in Chapters 1 and 3, this approach is based on a Monte Carlo simulation of the flood causative factors and a deterministic evaluation of the flood parameters (depth or peak flow).

In the next two sections, the effects of two modes of generating random flood series on the statistical characteristics of peak flows and flood levels at various locations along a stream are investigated. In the first mode, it is assumed that the flood wave enters the upstream end of the stream as a point input, and that there is no lateral inflow along the length of the stream. This situation can be representative of the lower reaches of a river system and is typified by a long stream with relatively mild slopes. The input flood hydrograph is assumed to have a gamma-type distribution over time with the peak level occurring at either predetermined or random times. The peak levels and consequently the peak flow rates are assumed to be randomly distributed with known statistical parameters. In the second mode it is assumed that the flood is generated by lateral inflow only. This

situation is conceptualized as a stream with two side planes. Rainfall on the planes generates overland flow and this input, distributed along the length of the stream, creates the flood. Such a mode of flood generation would be typical of the upstream region of a watershed. The rainfall intensities and infiltration rates are assumed to be random quantities with known probability distribution functions (pdf). In a natural watershed both modes of flood generation occur simultaneously and such cases are treated in Chapter 5.

4.2 Random Flood Events along a Stream with Upstream Point Inflow

An important step in the design of regulatory and service structures across natural streams is the identification and description of statistical patterns in seemingly random peak flows and depths at the desired locations. When "sufficient" data are available at the section of interest, the assignment of probability levels to various magnitudes of floods is not difficult. Very often, though, the location of interest is several kilometers upstream of the gaging station. It is common knowledge that as a flood wave moves downstream it attenuates. One immediate consequence of the subsidence of the flood wave is that the mean of the random peak flows and depths will be lower at sections downstream of the gaging station. The change in the other statistical parameters of the random series, such as its coefficients of variation and skewness, is however more complex. This section explores the change in the statistical parameters of the probability distribution of a flood along the length of the stream as a function of the stream and flood characteristics.

The streams under consideration in this section are assumed to have a wide and rectangular cross-section and are prismatic. The flood hydrograph at the upstream end of a particular stream is described in terms of rate of change of depth of flow with time and is assumed to have the shape of a gamma-type curve. The time to peak depth can either increase or decrease with increasing peak depth. The flow in the stream is assumed to be uniform before the flood wave arrives. The probability distribution of the peak depth is assumed to be known together with its statistical parameters. An approximate analytical solution of the flood level subsidence together with a Monte Carlo simulation of the peak depths is used to determine the change in the statistical parameters of the peak depths' probability distribution. Similar changes for the case of peak flows are determined.

4.2.1 Characterization of Upstream Flood Hydrograph

The change in depth of flow with time at a particular section is approximated by a two-parameter gamma distribution equation

$$y = y_p \left(\frac{t}{t_p}\right)^{\xi - 1} \exp\left[(1 - \xi)\left(\frac{t}{t_p} - 1\right)\right] + y_o \quad (4.1)$$

where y is the depth of flow at time t , y_o is the uniform depth existing at $t = 0$, y_p is the maximum rise in flow depth, t_p is the time to peak depth ($y_o + y_p$), and ξ is an empirical fitting parameter. A similar form of equation for fitting unit hydrographs is suggested by Gray (1968). Figure 4.1 illustrates the flood hydrograph for some values of y_p , t_p , and ξ . When all other parameters are constant, an increase in ξ causes an increase in the rate of rise of the depth of flow. Conversely, an increase in t_p decreases the rate of increase of y . Equation 4.1 can then be used to generate

$$y = y_p (t/t_p)^{\xi-1} \exp[(1-\xi)(t/t_p - 1)] + y_o$$

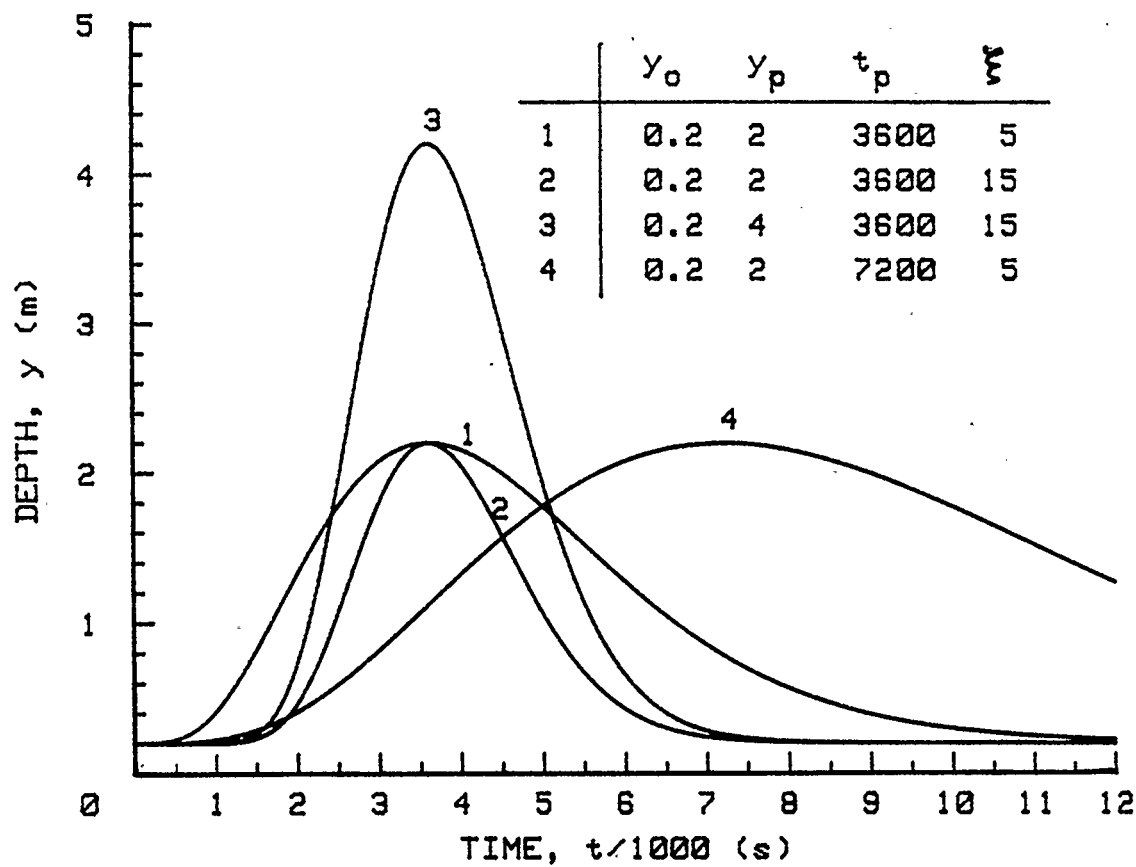


Figure 4.1: Gamma-type input flood hydrographs.

flood hydrographs of a wide range of shapes.

4.2.2 Rate of Flood Level Subsidence with Distance

Henderson (1963, 1966) has established an expression for the rate of subsidence of the maximum flood level at a section with distance. The theory applies to slow rising floods in wide rectangular prismatic streams. The essential steps in the derivation of the space rate of subsidence are given in this section. An approximate but explicit equation for the maximum depth of flow along the stream is then obtained as a function of the stream and flood characteristics.

Figure 4.2 shows the crest part of an instantaneous profile of the flood wave along the stream. A is the point where the depth of flow is a maximum at this particular moment. Therefore at A ,

$$\frac{\delta y_A}{\delta x} = 0 \quad (4.2)$$

The distance along the length of the stream is denoted by x . B is the point where the flow rate is a maximum at the same moment. Therefore at B ,

$$\frac{\delta Q}{\delta x} = 0 \quad (4.3)$$

Substituting equation 4.3 into the equation of continuity :

$$\frac{\delta Q}{\delta x} + b \frac{\delta y}{\delta t} = 0 \quad (4.4)$$

where b is the width of the stream, results in

$$\frac{\delta y_B}{\delta t} = 0 \quad (4.5)$$

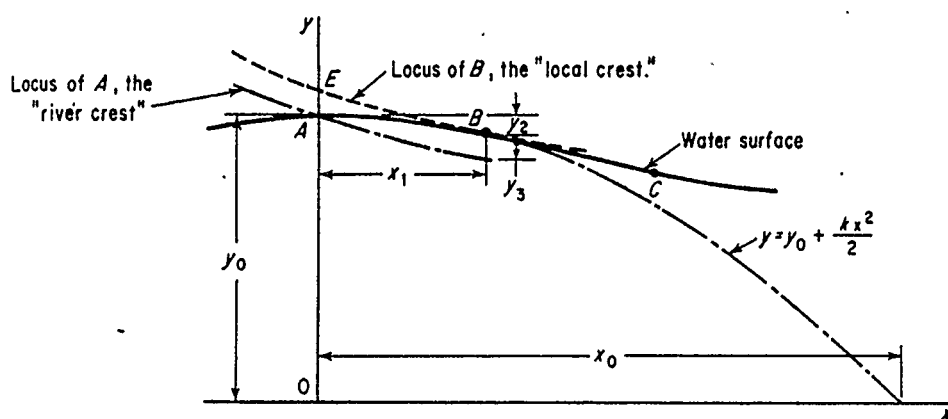


Figure 4.2: Crest profile of a flood wave (Henderson, 1966).

Physically, equation 4.5 means that the depth at B is the greatest that will occur at that section over the duration of the flood. The total derivative of y with respect to x at B is

$$\frac{dy_B}{dx} = \frac{\delta y_B}{\delta x} + \frac{dt}{dx} \frac{\delta y_B}{\delta t} \quad (4.6)$$

Because $\frac{\delta y_B}{\delta t} = 0$, therefore

$$\frac{dy_B}{dx} = \frac{\delta y_B}{\delta x} \quad (4.7)$$

Equation 4.7 states that $\frac{dy_B}{dx}$, the space rate of subsidence of y , is equal to $\frac{\delta y_B}{\delta x}$, the instantaneous slope of the wave profile at B . Henderson assumes that the shape of the wave profile between A and B can be approximated by a parabola with the vertex at A and one axis vertically through A . The equation of the parabola and its first and second derivatives are

$$y = y_A + k \frac{x^2}{2} \quad (4.8)$$

$$\frac{\delta y}{\delta x} = kx \quad (4.9)$$

$$\frac{\delta^2 y}{\delta x^2} = k \quad (4.10)$$

where k is a constant at a particular time and varies as the flood crest moves along the stream. x is the horizontal distance from A .

Using only the first two terms in the equation for the friction slope S_f :

$$S_f = S_o - \frac{\delta y}{\delta x} - \frac{v}{g} \frac{\delta v}{\delta x} - \frac{1}{g} \frac{\delta v}{\delta t} \quad (4.11)$$

where S_o is the slope of the stream and v is the velocity of flow, the discharge Q at B is given by

$$Q = \frac{b}{n} y_B^{5/3} \sqrt{S_o - \frac{\delta y_B}{\delta x}} \quad (4.12)$$

b is the width of the stream and n is the Manning's coefficient of roughness of the stream bottom. From equations 4.12, 4.3, 4.8, and 4.10 and after some algebraic manipulations and approximations, Henderson obtains an expression for the distance X_1 between A and B :

$$X_1 = \frac{y_A}{3S_o} \quad (4.13)$$

The space rate of subsidence, $\frac{dy_B}{dx}$, is then given by

$$\frac{dy_B}{dx} = \frac{\delta y_B}{\delta x} = kX_1 = \frac{ky_A}{3S_o} \quad (4.14)$$

From a consideration of the wave velocities C_A and C_B at A and B respectively, Henderson derives the following two equations involving k :

$$k = \frac{1}{C_A^2} \frac{\delta^2 y}{\delta t^2} \quad (4.15)$$

where $\frac{\delta^2 y}{\delta t^2}$ is the second derivative over the crest region of the $y - t$ curve (river stage record) at B .

$$\frac{dk}{dx} = \frac{5}{4} \frac{k^2}{S_o} \quad (4.16)$$

Using equations 4.15 and 4.16, equation 4.14 can now be integrated to give the depth y at any distance X from the station where the records are available :

$$y = y_A \left(1 - \frac{5}{4} \frac{\delta^2 y}{\delta t^2} \frac{X}{S_o}\right)^{-4/15} \quad (4.17)$$

If the $y - t$ curve is approximated by the gamma-type curve given by equation 4.1, then at the crest

$$\frac{\delta^2 y}{\delta t^2} = \frac{y_p(1 - \xi)}{t_p^2} \quad (4.18)$$

C_A can be written in terms of y_A by the following equation (Raudkivi, 1979) :

$$C_A = \frac{5}{3} \frac{\sqrt{S_o}}{n} y_A^{2/3} \quad (4.19)$$

Equation 4.17 can now be re-expressed as

$$y = y_A \left(1 - \frac{9}{20} \frac{y_p(1-\xi)}{t_p^2} \frac{n^2}{S_o^2} \frac{X}{y_A^{4/3}} \right)^{-4/15} \quad (4.20)$$

y_p is equal to y_A minus the uniform depth existing before the flood wave arrives.

Equation 4.20 gives an approximate but explicit expression for the maximum depth of flow along the stream as a function of the stream and flood characteristics.

4.2.3 Rate of Flood Peak Subsidence with Distance

Using the Manning's form of the resistance equation of flow, the flow rate can be expressed as

$$Q = \frac{b}{n} y R^{2/3} \sqrt{S_o - \frac{\delta y}{\delta x} - \frac{v}{g} \frac{\delta v}{\delta x} - \frac{1}{g} \frac{\delta v}{\delta t}} \quad (4.21)$$

where R is the hydraulic radius of the channel. When the last two terms under the square root sign are neglected and R is approximated to y for a wide rectangular channel, the flow rate can be re-expressed as

$$Q = \frac{b}{n} y^{5/3} \sqrt{S_o - \frac{\delta y}{\delta x}} \quad (4.22)$$

Equation 4.22 states that the flow rate is not a unique function of depth. On the rising stage of a flood, $\frac{\delta y}{\delta x}$ is negative and therefore Q will be greater than Q_o , the uniform flow discharge for the same depth y , given by

$$Q_o = \frac{b}{n} y^{5/3} \sqrt{S_o} \quad (4.23)$$

Conversely, on the falling stage of a flood, $\frac{\delta y}{\delta x}$ is positive and Q is less than the corresponding Q_0 . So, when the depth is plotted against the discharge at a particular section of the stream during the passage of a flood a closed loop is obtained. $\frac{\delta y}{\delta x}$ is a very difficult parameter to obtain directly. However, it can be expressed as a function of the stage-time relationship, the usual form of flow recording at a section.

$$\frac{\delta y}{\delta x} \approx -\frac{1}{C} \frac{\delta y}{\delta t} \quad (4.24)$$

Using equation 4.24, equation 4.22 can be recast as

$$Q = \frac{b}{n} y^{5/3} \sqrt{S_0 + \frac{1}{C} \frac{\delta y}{\delta t}} \quad (4.25)$$

Equation 4.25 is the "Jones formula". Henderson (1966) points out that there is a logical error in this equation. Equation 4.25 describes the effect of subsidence on the flow rate, yet it is based on equation 4.24 which assumes that $\frac{dy}{dt} = 0$, i.e., the flood wave is kinematic and therefore cannot subside. A more refined analysis, however, showed that the error is negligible.

For the flood inflow hydrograph characterized by equation 4.1, $\frac{\delta y}{\delta t}$ at time t is given by

$$\frac{\delta y}{\delta t} = y'_t \left(\frac{\xi - 1}{t} + \frac{1 - \xi}{t_p} \right) \quad (4.26)$$

where y'_t is the rise/fall after time t and is equal to $y_t - y_0$. C is given by

$$C = \frac{5}{3} y_t^{2/3} \sqrt{S_0} \quad (4.27)$$

Using equations 4.1, 4.25, 4.26, and 4.27 looping curves for two of the inflow hydrographs plotted in Figure 4.1 are illustrated in Figure 4.3. Curve number 2 clearly

shows that at a particular section, the depth keeps rising after the maximum discharge has occurred and on the falling stage the flow is momentarily uniform. Points A and B on curve number 2 in Figure 4.3 correspond to points A and B on Figure 4.2. Figure 4.3 also shows that the difference between the maximum discharge and maximum uniform discharge increases with maximum depth reached and ξ . As the flood wave moves downstream, these two factors (y_p and ξ) decrease and consequently Q tends towards Q_0 at maximum flow rate. It is this fact that is used to obtain the maximum flow rate along the length of the stream.

For the upstream section, the maximum flow rate is obtained by simulating the inflow hydrograph, calculating the corresponding stage-discharge curve, and determining the peak flow rate. The difference between the uniform and actual unsteady peak flow is expected to be greatest at the upstream section. At a distance X downstream, the maximum flood level reached is calculated by means of equation 4.20. This maximum depth is substituted into the equation for uniform flow :

$$Q_X = \frac{b}{n} y_X^{5/3} \sqrt{S_0} \quad (4.28)$$

to obtain the maximum discharge at a section X metres downstream.

4.2.4 Effects of Flood and Stream Parameters on the Statistical Characteristics of Random Peak Depths

The characteristics of the stream are as follows : slope = 0.0015, Manning's coefficient of roughness = 0.03, and its width is 50 m. The stream has a rectangular cross-section. The uniform base flow depth is assumed to be constant at 0.2 m. The peak depth at the upstream section of the stream is assumed to have a Nor-

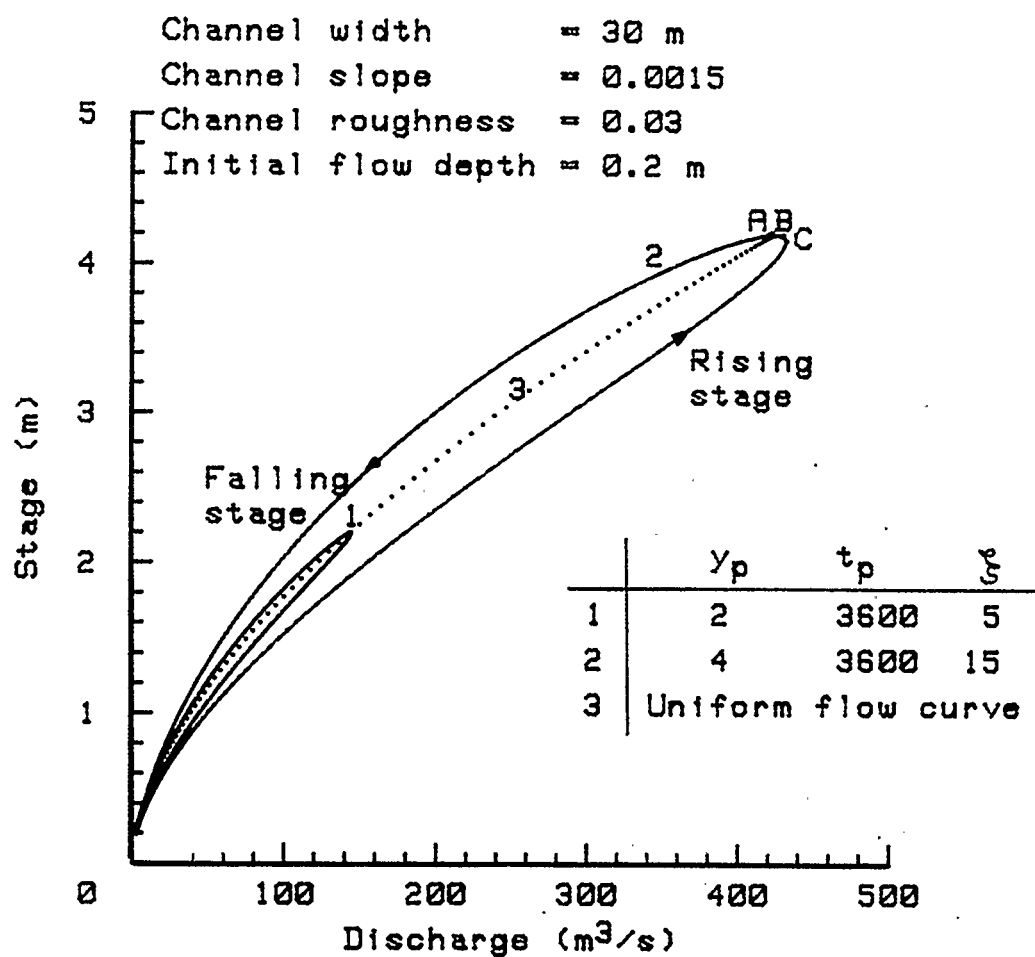


Figure 4.3: Stage-discharge curves for two shapes of flood hydrographs.

mal probability distribution function with mean y_{m1} and coefficient of variation Cv_{y1} . For y_{m1} and Cv_{y1} equal to 3 m and 0.25 respectively, 6000 random values of peak depths are generated using the Monte Carlo simulation technique. The corresponding subsided depths at distances along the stream starting at 20000 m from the upstream section and increasing in steps of 10000 m are determined using equation 4.20. Three cases of inflow hydrographs are considered, namely, the time to peak depth is constant, increases, and decreases with increasing peak depth of flow. For the first case, t_p is set to 3600 seconds. For the second case t_p is assumed to vary according to

$$t_p = 1800y_p^{0.4} \quad (4.29)$$

where t_p is the time to peak depth and y_p is the peak depth at the upstream section. For the third case

$$t_p = 7200y_p^{-0.6} \quad (4.30)$$

ξ , characterising the peakedness of the inflow hydrograph, is assigned a constant value of 15. The forms of and the numerical values in equations 4.29 and 4.30 are arbitrary and designed only to quantify the three cases to be studied. For each case, coefficients of variation and skewness of the generated subsided depths at each section are computed using standard formulae and plotted. The resulting $Cs_{y2} - Cv_{y2}$ curves are shown in Figure 4.4.

It can be observed from Figure 4.4 that the behaviour depends very much on the relationship between the time to peak depth and the peak depth itself. When the time to peak depth is increasing with peak depth, both the coefficient of variation and the coefficient of skewness increase along the downstream length. Conversely,

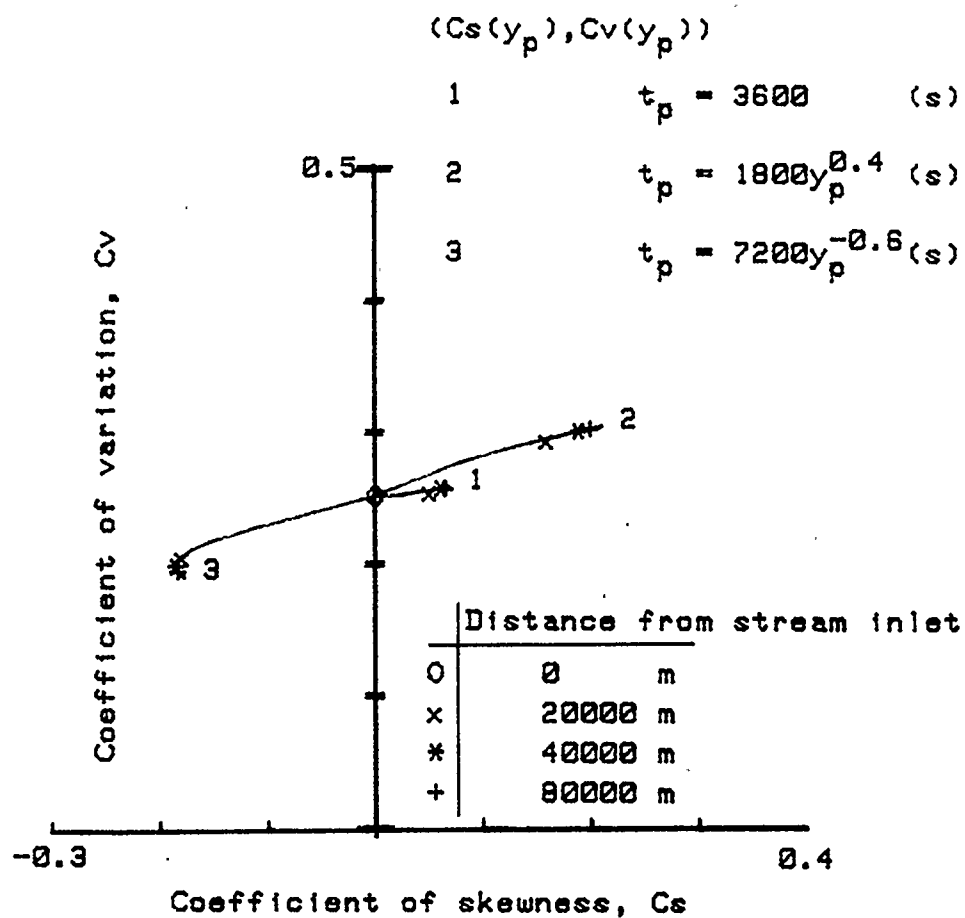


Figure 4.4: $Cs-Cv$ relationships of peak depth along the length of a stream for three types of time-to-peak-depth to peak-depth relationships.

for the case where the time to peak depth is decreasing with peak depth, the coefficient of variation decreases along the length of the stream. The coefficient of skewness initially decreases from its original value, i.e., it becomes negative. As the distance increases it reaches a minimum value and then starts to increase again, but it still remains negative for a considerable distance. Although equations 4.29 and 4.30 are arbitrary relationships between time to peak depth and peak depth, they do represent real physical possibilities. The conditions causing decreasing time to peak with peak depth could be a combination of high intensity short duration rainfalls, steep overland areas, and low infiltration rates in the upland regions of the basin. When the watershed is elongate and the rainfall events are of the low intensity-long duration type, then it is reasonable to expect greater depths of flow to occur further down along the time horizon.

Figure 4.4 also shows that as the distance from the upstream section is increasing, the rate of increase/decrease of the coefficients of variation and skewness decreases. The behaviour of Cv_{y2} and Cs_{y2} can be explained by an examination of the deterministic relationship between upstream and downstream depths as given by equation 4.20. At a given distance X , Figure 4.5 clearly demonstrates the difference between the two equations 4.29 and 4.30 relating time to peak depth to peak depth. When the time to peak increases with peak depth the curve (1 or 2) is increasingly steeper, i.e., $\frac{d^2y_{dn}}{dy_{up}^2}$ is greater than zero. For the other case, the curve (3 or 4) gets less and less steep as the upstream depth decreases, i.e., $\frac{d^2y_{dn}}{dy_{up}^2}$ is less than zero. As demonstrated in Figure 3.13, when the input distribution is Normal, $a \pm \frac{d^2y}{dx^2}$ indicates a \pm coefficient of skewness. The behaviour of $Cv_{y2} - Cs_{y2}$ in

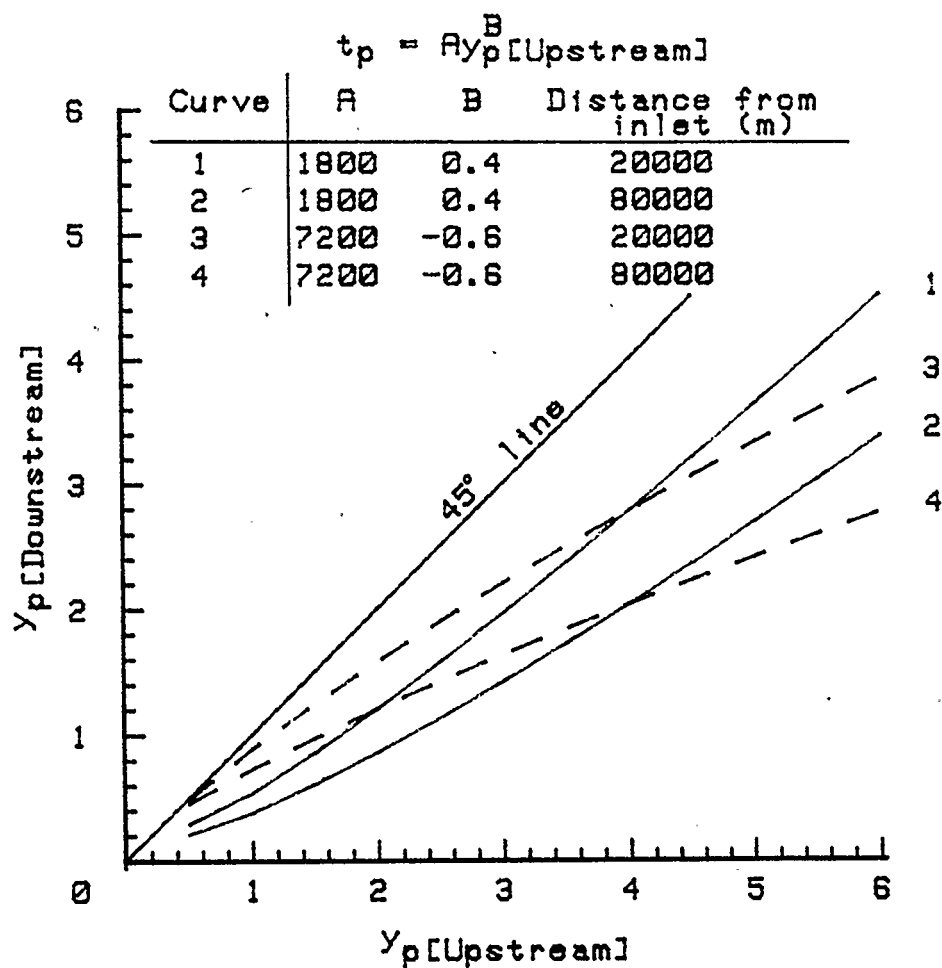


Figure 4.5: Relationships between upstream and downstream peak flow depths along a stream for two types of time to peak depth-peak depth relationships.

Figure 4.4 then becomes evident.

The physical reasons behind the curvatures of the relationships shown in Figure 4.5 can themselves be qualitatively explained as follows. When the time to peak depth is increasing more rapidly than the rate at which the peak depth is increasing, then the crest part of the stage record ($y - t$) becomes less sharp, i.e., $\frac{\delta^2 y}{\delta t^2}$ becomes closer to zero (or increases since $\frac{\delta^2 y}{\delta t^2}$ is always negative). According to equation 4.20 then, the rate of subsidence for increasing depths decreases. Hence the $y_{up} - y_{up}$ plot curves towards the 45° line representing no subsidence. Conversely, when the time to peak is decreasing while the peak depth is increasing, the absolute value of $\frac{\delta^2 y}{\delta t^2}$ increases because of the sharper crests. So, when the depth increases, the subsidence rate increases, and the $y_{up} - y_{dn}$ plot curves away from the 45° line. For both types of $y_{up} - y_{dn}$ relationships, the crest of the $y - t$ record at sections downstream is getting flatter. This means that for increasing distance downstream, the rate of change in the statistical parameters decreases until there is no significant increase/decrease in the statistical parameters. Curve number 3 on Figure 4.4 shows that the skewness actually starts to increase again after reaching a certain minimum value. This is explained as a consequence of curve number 4 in Figure 4.5 being flatter than curve number 3. The above discussion assumes that equation 4.20 is correct. As mentioned in section 4.2.2, this equation is only approximate and the errors in it may accumulate with distance.

The effects of the other stream and flood characteristics on the coefficients of variation and skewness can be discussed through an analysis of equation 4.20. First and foremost, it must be stressed that the direction the change in skewness takes

place is governed by the relationship between time to peak depth and peak depth. Equation 4.20 is an explicit relationship between the upstream and downstream depths. The factor $[(1 - \xi) \frac{n^2}{S_o^2} X]$ in equation 4.20 can be specified independently of the others (y and t_p). A change in this factor will affect the rate of change of the statistical parameters in the direction they have already taken (determined by y and t_p). Increasing ξ (sharpness of the crest of the stage record) and/or n (Manning's roughness coefficient) and/or S_o (slope of stream bed) will decrease the distance X needed to obtain a given (Cs_{y2}, Cv_{y2}) coordinate. This means that the space rate of change of Cv_{y2} and Cs_{y2} increases with increasing ξ , n , and decreasing S_o . This conclusion holds as long as the assumptions in the derivation of equation 4.20 are not violated.

4.2.5 Statistical Characteristics of Random Peak Flows

The method outlined in section 4.2.3 is used to determine the peak flow rates corresponding to the peak depths of flow generated by the Monte Carlo simulation in section 4.2.4. The coefficients of variation and skewness of the peak flow series are computed for the same conditions outlined in section 4.2.4. The equivalent curves corresponding to those in Figure 4.4, but for peak flows, are shown in Figure 4.6.

The (Cs, Cv) coordinate of the peak flow depth pdf at the upstream section is $(0.25, 0.0)$. The corresponding (Cs, Cv) coordinate for the peak flow rate pdf is $(0.40, 0.49)$. Since Q is a power function of y and the exponent is approximately $\frac{5}{3}$, the pdf of Q will have a positive skewness as discussed in section 3.3.1. The $Cs-Cv$ curves for the peak flow series follow the same pattern as those for peak depths. The absolute changes in the coefficients of variation and skewness are however

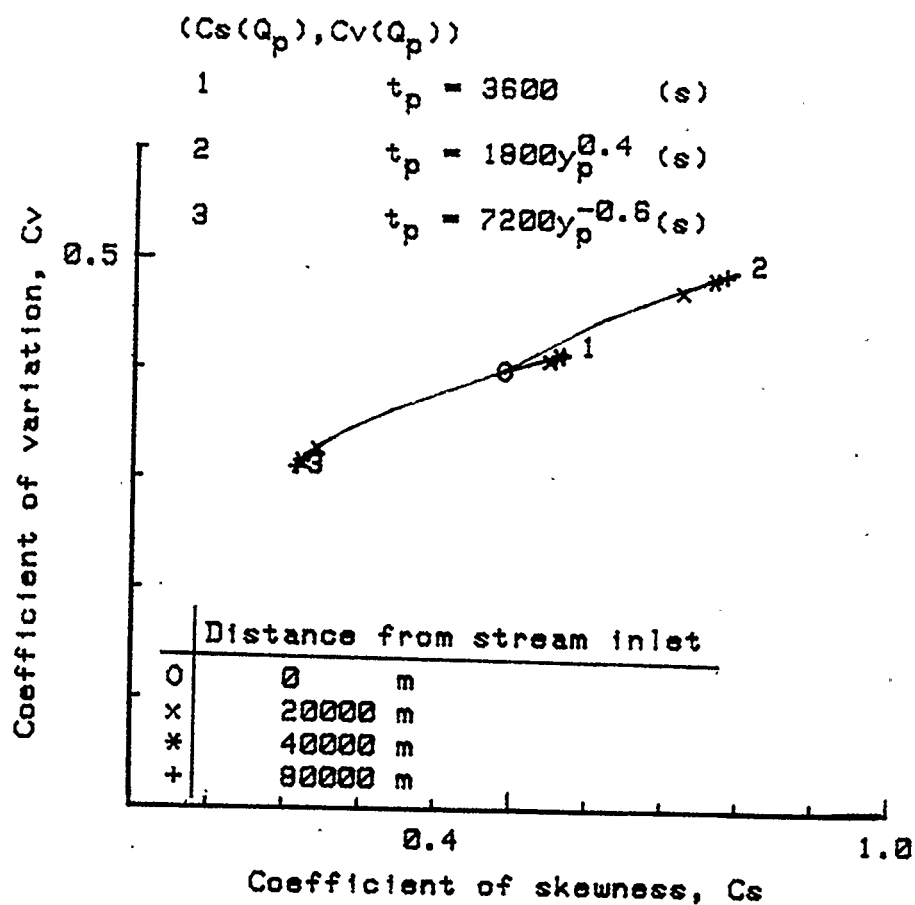


Figure 4.6: $C_s - C_v$ curves of peak flows along a stream for two types of time to peak-peak depth relationships.

greater for the peak flow than for peak depth. The same general conclusions as outlined in section 4.2.4 for peak depths apply to the case of peak flow rates.

4.3 Random Flood Events along a Stream with Lateral Inflow

The previous section dealt with point inflows as one mode of flood generation along a stream. Among the upper reaches of a watershed, and particularly in first-order streams, floods are characteristically generated by lateral inflows. In general, lateral inflow is the sum of groundwater, subsurface, and overland flows. In this section it is assumed that overland flow is the only mode of flood generation along a stream. First-order streams are usually steep and are of relatively short lengths. The catchment area contributing lateral inflow into the stream also has a relatively steep bed slope. Betson (1964) observed that the area actually producing lateral inflow is usually a fraction of the total basin drainage area. The percentage was found to be as low as 5% in some cases. The contributing area was situated alongside the streams where the initial soil moisture content is the highest. The physical first-order watershed can be conceptualized as a single stream with two side planes. A schematic of such a system is illustrated in Figure 4.7.

The nature of the statistical characteristics of random peak flow series at the edge of a sloping plane has been treated in Chapter 3. A similar study is done in this section on the stream-plane combination. The objective is to determine (1) the effect of the stream and plane parameters and (2) the effect of rainfall and infiltration parameters on the statistical characteristics of the peak flow series.

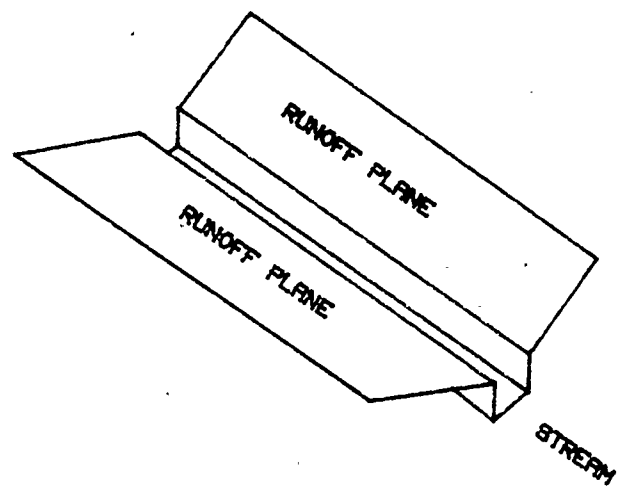


Figure 4.7: Schematic of a stream-plane configuration.

4.3.1 Numerical Simulation of Flow in a Stream-Plane Configuration

The equations of continuity and momentum are used to solve for the flow on the planes and in the stream. The numerical simulation of flow on the plane is exactly the same as described in section 3.2.2. When simulating flow in the stream, it is assumed that the momentum of the lateral inflow is negligible. Then, the same procedure as for the plane can be used to numerically solve for flow in the stream using similar continuity and momentum equations. Two modifications in the procedure are (1) i in equation 3.3 is replaced by the lateral inflow per unit width, and (2) equation 3.14 is replaced by

$$q_j = \frac{\sqrt{S_{f,j}}}{n} y_j \left(\frac{b y_j}{b + 2y_j} \right)^{2/3} \quad (4.31)$$

where b is the width of the stream. The latter is assumed to have a rectangular cross-section and to be prismatic. For given rainfall, plane, and stream characteristics the peak flow can then be obtained.

4.3.2 Method for obtaining Statistical Parameters of Random Peak Flows

The deterministic system of continuity and momentum equations is made probabilistic by assuming that each rainfall intensity (and infiltration rate if the latter is being considered) is one member of a random series with known pdf and statistical parameters. Monte Carlo simulation is used to generate 6000 random rainfall intensities. For a given set of stream-plane parameters and rainfall duration, peak flows were determined by numerically simulating rainfall intensities starting from 2 mm/hr and increasing in steps of 2 mm/hr up to a maximum, typically 150 mm/hr.

The peak flows corresponding to the 6000 random intensities are then obtained by linear interpolation if the random rainfall intensity falls between two consecutive intensities for which the peak flows are known. The peak flows are normalized by dividing by the total runoff contributing area upstream of the section of interest. Standard techniques are then used to determine the statistical parameters of the random peak flows for the given set of stream-plane parameters and rainfall duration. The procedure is repeated for other sets of physiographic and rainfall characteristics.

4.3.3 Uniform Rainfall Intensity on an Impervious Plane

$Cs(q_p) - Cv(q_p)$ relationship along the length of the stream

The simplest configuration of the stream-plane system is areally and temporally uniform rainfall intensity on a rectangular impervious plane on each side of a prismatic stream with a rectangular cross-section. Some of the system parameters are as follows : length of each runoff plane is 200 m, slope and roughness of each plane are respectively 0.02 and 0.04. The length of the stream is 20000 m, its width is 10 m, and the peak discharge is extracted at 4 km intervals for each simulation. Although a first-order stream of length 20 km is not very common, this length was chosen so that the asymptotic effects of stream length could be studied. For rainfall intensities starting from 2 mm/hr and increasing in steps of 2 mm/hr up to 150 mm/hr, the corresponding peak discharges are obtained for 3 cases : (1) rainfall duration = 3600 s, slope of stream = 0.01, (2) rainfall duration = 3600 s, slope of stream = 0.005, and (3) rainfall duration = 1800 s, slope of stream = 0.01. The roughness of the stream bed is kept constant at 0.04. For the statistical

analysis it was assumed that the pdf of i ($f(i)$) was (1) Gamma with a mean of 50 mm/hr and a standard deviation of 15 mm/hr ($Cv(i)$ is then 0.3 and $Cs(i)$ is 0.6) and (2) Normal with a mean of 50 mm/hr and a standard deviation of 10 mm/hr ($Cv(i) = 0.2$ and $Cs(i) = 0.0$). For both these cases, all the rainfall intensities (6000 of them) generated by Monte Carlo technique were between the lower and upper limits of the rainfall intensities simulated. The $Cv(q_p) - Cs(q_p)$ curves for the random peak flow series along the length of the stream are shown in Figures 4.8 and 4.9 for a Normal and Gamma pdf of i respectively. In each figure, the corresponding $Cv(q_p) - Cs(q_p)$ curves for random peak flows at the edge of a plane due to uniform rainfall intensity have been included. The latter curves are reproduced from Figures 3.11 and 3.14.

Some observations on Figures 4.8 and 4.9 are given below. As the distance from the most upstream cross-section increases, Cs and Cv for the random peak flow series increase. They start from (Cs, Cv) of the rainfall intensity pdf and seem to tend towards a maximum (Cs, Cv) identical to the limiting maximum (Cs, Cv) for the plane alone. The starting coordinate of the $(Cs(q_p), Cv(q_p))$ is explained as follows. For the given parameters of the planes, the k_m value as defined by equation 3.41 and reproduced below is greater than 1.8 for all 3 cases.

$$k_m = i_m^{0.4} t_{0.4} \left(\frac{\sqrt{S_o}}{nL} \right)^{0.6} \quad (4.32)$$

The discussion in section 3.3.1 and the results on Figures 3.11 and 3.14 indicate that for k_m greater than 1.8, the (Cs, Cv) of the peak flow series at the edge of the planes is equal to that of the rainfall pdf. Physically, it means that for most of the rainfall intensities generated, the flow on the planes has reached steady state in a

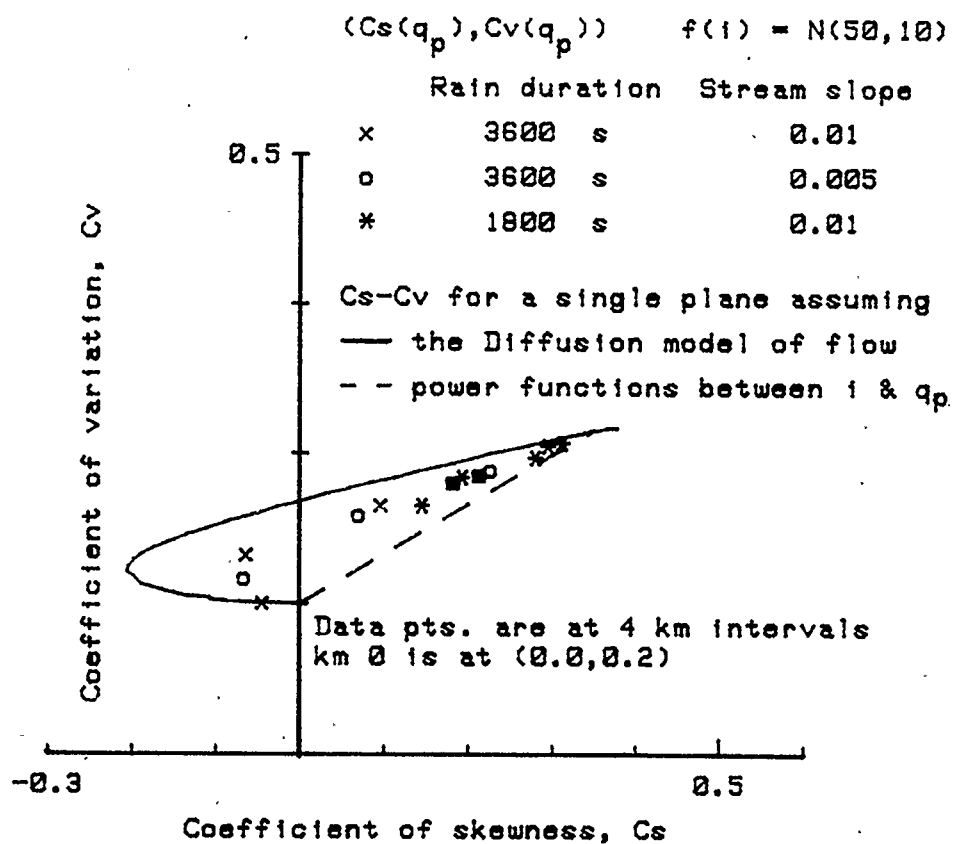


Figure 4.8: Change in Cs and Cv of peak flow pdf along the length of a stream for $f(i)$: Normal.

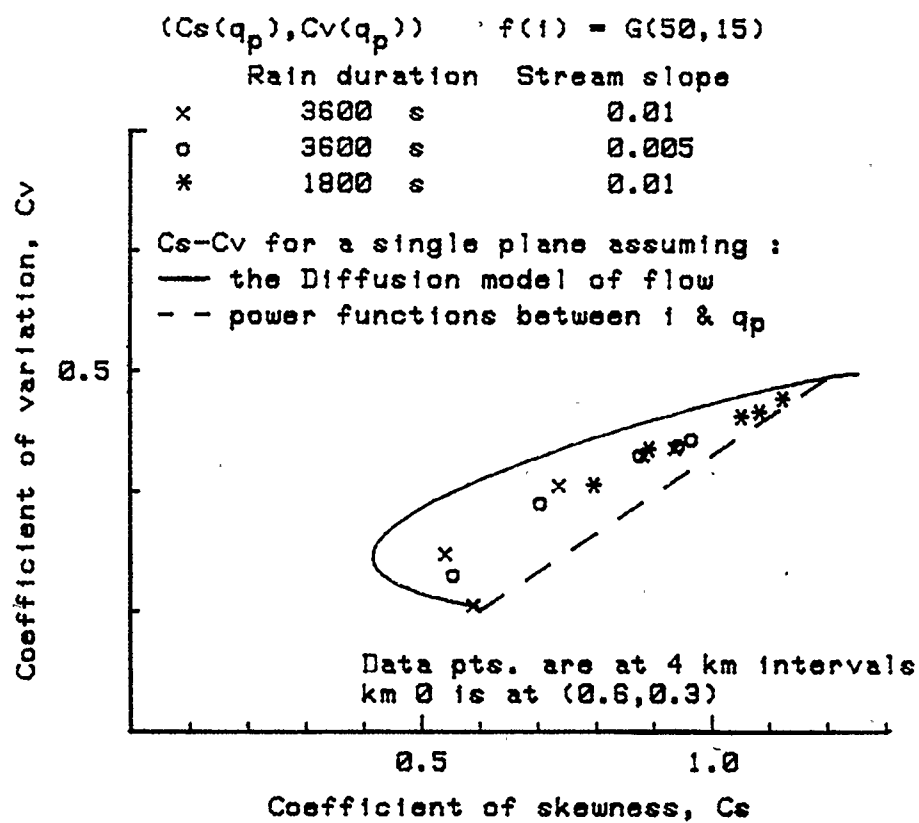


Figure 4.9: Change in Cs and Cv of peak flow pdf along the length of a stream for $f(i)$: Gamma.

time shorter than the duration of the rainfall. This condition is not uncommon in natural first-order basins (Eagleson, 1971,1972). So, for the most upstream section of the stream, $(Cs(q_p), Cv(q_p))$ is equal to (0.0,0.2) and (0.3,0.6) for the Normal and Gamma rainfall inputs respectively. As the distance from the upstream section increases, only some of the incoming stream flow will remain at steady state. The flow on the planes will still be at steady state, but the different characteristics of the stream will attenuate the steady lateral inflow. The results from Figures 3.12 and 3.13 demonstrate that when part of the random series contains steady state values and part non-steady values, then the coefficient of skewness has a tendency to decrease relative to the starting coordinate. At greater distances downstream, the peak flows (all peak flows have been normalized by dividing by the runoff contributing area above the section of interest) are all less than the rainfall intensities and hence the coefficients of variation and skewness of the peak flow series increase. The last two statements explain the general curvature and direction of the $(Cs(q_p), Cv(q_p))$ curves for the stream-plane configuration. It is noticed that the $Cs - Cv$ curve of the plane is similar in shape to the $(Cs(q_p), Cv(q_p))$ curves. In fact, if all parameters in equation 4.32 are kept constant and only L (the length of the plane) is allowed to increase, then both sets of curves exhibit the same characteristics with respect to L . The tendency of the $(Cs(q_p), Cv(q_p))$ curves for the stream-plane to converge towards a limiting maximum value can be qualitatively explained by the following arguments. For relatively long streams, the runoff contribution from the area of the planes in the lower reaches of the stream is negligible compared to the peak flow at those sections. By the time the major portion of the flow reaches the downstream section, the flow rate from the planes at that section

may be zero or in recession. Hence the flow along the stream may be approximated as a long-wave flood input hydrograph as far as the downstream section is concerned. And it has been shown in section 4.2.4 that $Cs(q_p)$ and $Cv(q_p)$ increase at a rapidly decreasing rate as the length of the stream increases. This explains the tendency of the $Cs(q_p) - Cv(q_p)$ curves to converge towards a limiting value. The flow on the planes and in the streams are governed by the same equations of continuity and momentum. It was shown in section 3.3.1 that for the plane, at low k_m values (that is, planes with long runoff lengths, mild slopes, and rough surfaces under low rainfall intensities) the relationship between peak flow and rainfall intensity degenerates into a power function relationship not too dissimilar from that derived from the kinematic wave equations. The power function had a constant exponent and it is proven in Appendix A that for a constant exponent, Cs and Cv become independent of all physiographic parameters and depend only on the particular value of the exponent and the coefficient of variation of the rainfall pdf. It is hypothesized that at long distances from the uppermost section of the stream where $Cs(q_p), Cv(q_p)$ tends towards a limiting value a similar power function exists.

Figures 4.8 and 4.9 show that although the $Cs(q_p) - Cv(q_p)$ curves for the sets of stream parameters and rainfall duration are similar in shape, they exhibit a tendency to move away from the corresponding curve for the plane alone for decreasing rainfall duration and stream slopes. This is a result of the fact that for decreasing rainfall durations, k_m for the planes decreases. The proportion of peak flows values that stays at steady state for a certain section in the stream decreases very rapidly and this causes the coefficient of skewness to increase almost

immediately after the most upstream section is past.

$Cs(q_p) - Cv(q_p)$ relationship for different mean rainfall intensities at a particular section

The analysis described in the previous section is repeated at three sections : 4, 12, and 20 km from upstream, for mean rainfall intensities ranging from 10 mm/hr to 50 mm/hr. The rainfall intensity pdf was the Gamma distribution with $Cv = 0.3$ and $Cs = 0.6$. The lower limit of the mean rainfall intensity was chosen such that k_m for the plane is at least 1.6, hence, about half of the lateral inflows would be at steady state. (When $k_m = 1.6$, the mean rainfall intensity i_m and all intensities greater than it would have reached steady state.) This situation may not be too dissimilar from what happens on natural first-order basins. The upper limit of the mean rainfall intensity was governed by the upper limit of the rainfall intensity for which a peak flow is available (150 mm/hr in the present case). The $Cs(q_p) - Cv(q_p)$ curves for the 3 sections along the stream are shown in Figure 4.10 together with the $Cs - Cv$ curve for the plane only. The rainfall duration was 3600 s and the slope and roughness of the stream were 0.01 and 0.04 respectively.

The shapes of the $Cs(q_p) - Cv(q_p)$ exhibit similar behaviour as those in Figures 4.8 and 4.9. The major parts of these curves lie inside the $Cs - Cv$ curve for the plane alone. For very small mean rainfall intensities ($Cs(q_p), Cv(q_p)$) curves exhibit some deviations. At low i_m the rainfall intensities generated are small and comparable to the step by which the simulated intensities are increasing (2 mm/hr). Hence, interpolation is not very accurate and this explains the deviations at low i_m . The rest of the curves are explained as follows. For large mean rainfall

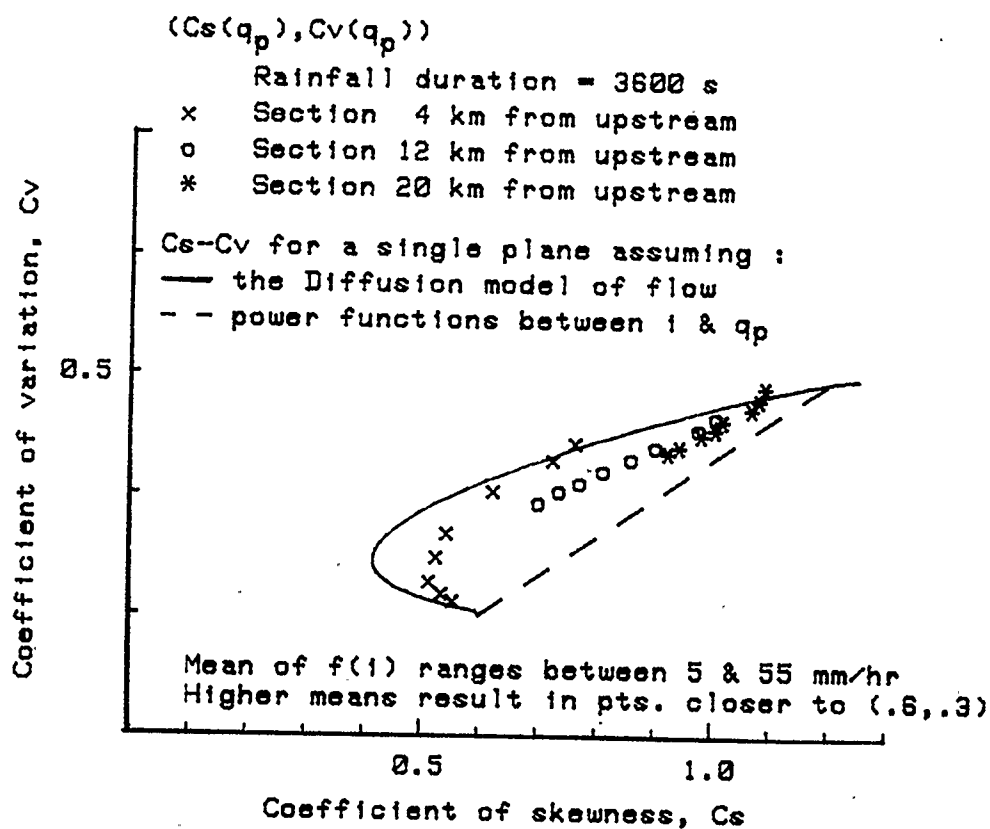


Figure 4.10: $Cs - Cv$ curves of peak flows at three sections along a stream for a range of mean spatially uniform rainfall intensities with $f(i)$: Gamma.

intensities the curves converge towards (Cs, Cv) of the rainfall pdf. For decreasing mean rainfall intensities, the effect is similar to increasing stream length, i.e, greater attenuation and increasing coefficient of skewness. Part of the explanation for the shift of the $Cs(q_p) - Cv(q_p)$ curves away from the $Cs - Cv$ curve for the plane alone can be ascribed to the temporal distribution of the lateral inflow into the stream. In section 3.4.1 the effect of a triangular distribution of rainfall intensity over time on the $Cs(q_p) - Cv(q_p)$ was discussed. It was shown in Figures 3.26 and 3.27 that a triangular distribution of rainfall intensity shifts the $Cs(q_p) - Cv(q_p)$ curves inwardly. A similar situation exists in the stream-plane configuration. The lateral inflow into the stream is uniform over space but is trapezoidally distributed over time. In section 3.4.1 the reasons why a temporally non-uniform distribution of rainfall intensity shifts the $Cs(q_p) - Cv(q_p)$ curves inwardly are given and the same reasons apply here.

Region within which $(Cs(q_p), Cv(q_p))$ is most likely to be found

Figures 4.8, 4.9, and 4.10 indicate that the limits of the $Cs(q_p) - Cv(q_p)$ curves for a stream are the $Cs - Cv$ curve for a plane and a line, almost straight, joining the (Cs, Cv) for the rainfall intensity pdf to the maximum (Cs, Cv) of the peak flow series for a plane only. It is hypothesized that the equation of this line is defined by assuming a power function between q_p and i of the form

$$q_p = ai^b \quad (4.33)$$

where b varies between 1 and 2. Under this assumption, for a Gamma pdf of rainfall intensity, the equation of the line is given by (see Appendix A)

$$Cs(qp)Cv^3(qp) = \frac{\Gamma^2(\eta)\Gamma(3b + \eta) - 3\Gamma(\eta)\Gamma(2b + \eta)\Gamma(b + \eta) + 2\Gamma^3(b + \eta)}{\Gamma^3(b + \eta)} \quad (4.34)$$

where η is equal to $\frac{1}{Cv(i)^2}$. Figure 4.11 shows the region within which $(Cs(qp), Cv(qp))$ is most likely to be found $f(i)$: Gamma and $Cv(i) = 0.3$. The effects of varying plane width and slope, non-uniform rainfall intensity, and infiltration on this hypothesis are examined in the following sections.

4.3.4 Uniform Rainfall Intensities on Planes with Non-uniform Characteristics

In a natural watershed, the slopes, widths, and roughnesses of the overland runoff areas are not constant along the length of the stream. The variations in these characteristics appear to be random. In general, though, the slopes of the runoff areas become smaller along the length of the stream and the widths of the runoff contributing areas decrease too. To simulate and examine the effects of such variations, the analysis of the previous section is repeated with the runoff length, slope, and roughness of the side planes taking different values for every 4 km along the length of the stream. The values are given in Table 4.1. The $Cs(qp) - Cv(qp)$ curves for two rainfall durations : 3600 and 1800 seconds are shown in Figure 4.12. The rainfall intensity is uniformly distributed has a Gamma pdf with mean ranging from 10 to 55 mm/hr. The hypothetical limits of $(Cs(qp), Cv(qp))$ have been superimposed for comparison purposes. The deviations at short rainfall durations and low mean rainfall intensities are the result of inaccurate interpolation for

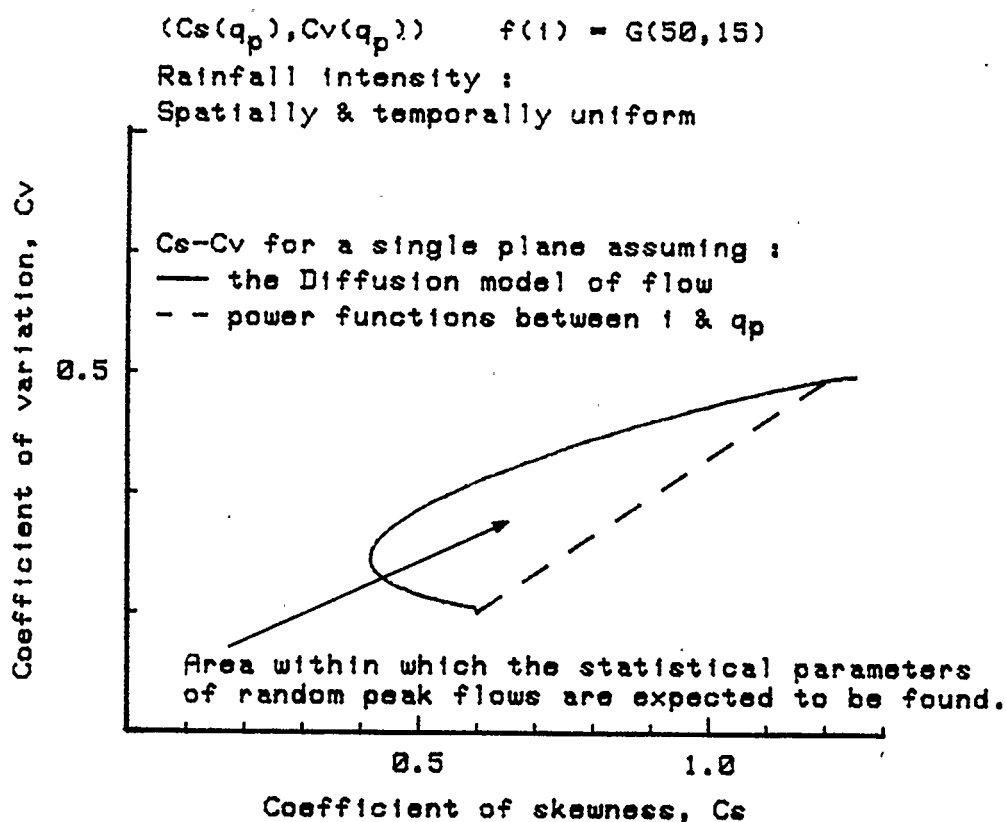


Figure 4.11: Limiting region within which the coefficients of skewness and variation of the peak flow pdf can be expected to be found when $f(i)$ is Gamma with $Cv(i) = 0.3$.

Table 4.1: Characteristics of stream-plane configuration

STREAM LENGTH (km)	PLANE		
	RUNOFF WIDTH (m)	SLOPE	ROUGHNESS
0 - 4	200	0.020	0.040
4 - 8	175	0.018	0.035
8 - 12	125	0.015	0.020
12 - 16	100	0.012	0.025
16 - 20	75	0.010	0.020

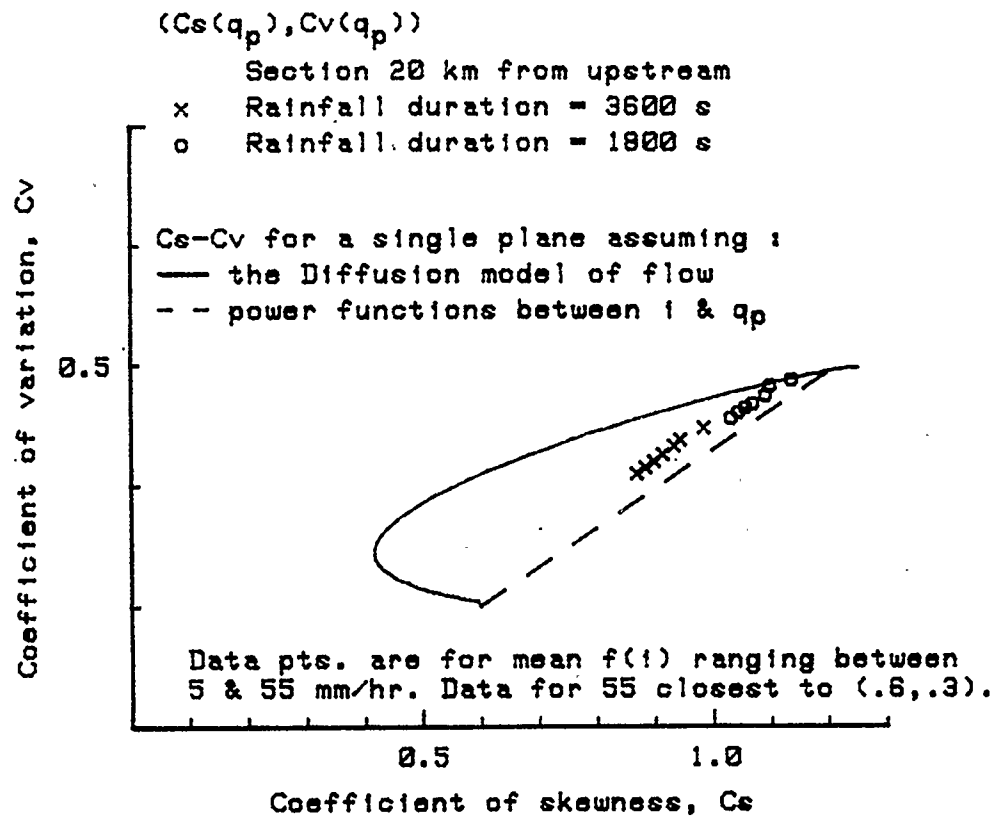


Figure 4.12: $Cs-Cv$ curves of peak flow pdfs from planes with non-uniform widths, slopes, and roughnesses when $f(i) : \text{Gamma}$.

small rainfall intensities. For "short" first-order streams with "high" bed slopes and "long" rainfall durations, however, the $(Cs(q_p), Cv(q_p))$ generated seem to lie within the hypothetical limits even if the physical characteristics of the runoff planes are not uniform along the length of the stream.

4.3.5 Spatially Non-uniform Rainfall Intensity

Natural storms usually have decreasing rainfall intensities from their centres to their peripheries. This possibility is simulated by assuming that different fractions of the rainfall intensity occur over five sections, each 4 km long, of the 20 km long stream. Three cases are considered. In the first case the maximum intensity occurs at the centre of the stream-plane combination with the intensity decreasing at the same rate both upstream and downstream. The chosen fractions are 0.625, 1.094, 1.562, 1.094, and 0.625. In the other cases the maximum intensity occurs at one end of the stream (upstream, downstream) and decreases towards the other end. The total rainfall was kept the same as the centred storm. The fractions for these cases are 0.625, 0.859, 0.938, 1.172, and 1.406. For the three cases, the areally average rainfall intensity is equal to the uniform rainfall intensity of section 4.3.3. The rainfall duration is 3600 seconds.

Analyses similar to those of the previous two sections are carried out. The objective is to determine whether $(Cs(q_p), Cv(q_p))$ is still within the hypothetical limits. Figure 4.13 shows that the $Cs(q_p) - Cv(q_p)$ curves for the differently positioned storms are within the limits. The $Cs(q_p) - Cv(q_p)$ curve for the storm with the highest intensity on the lower reaches of the stream is slightly different from the other two and the curves in Figure 4.12. With increasing mean rainfall

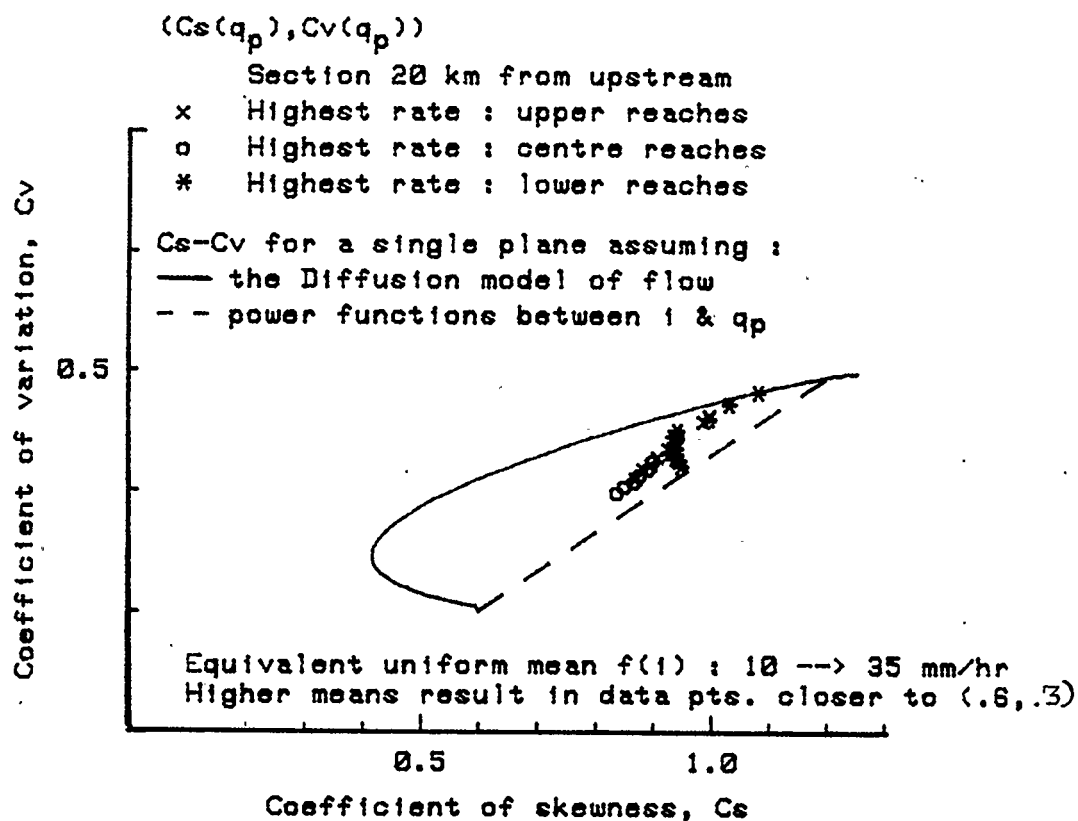


Figure 4.13: $Cs - Cv$ curves of peak flow pdfs for spatially non-uniform rainfall intensity when $f(i)$: Gamma and $Cv(i) = 0.3$.

intensity, instead of converging towards (Cs, Cv) of the rainfall intensity pdf, it makes a "u-turn" and moves towards the limiting line defined by a power function relationship between input and output. When the rainfall intensity is highest on the lower reaches, the peak flow at the outlet depends on the relative magnitude and time of arrival of the runoff from the lower and upper reaches. When the rainfall intensity is low, it is reasonable to assume that the peak flow at the outlet will depend mostly on the flow coming in from the upper reaches. In this case then, the situation is not very different from storms having their maximum intensity on the centre or upper reaches of the stream. At high rainfall intensities, however, the runoff from the lower reaches may dominate and be close to steady state. A random series of peak flows would then contain a mixture of steady state and non-steady state flows. For such mixtures, the direction that the coefficient of skewness takes depends on the proportion of either type of flow. The curvature of the curve for the bottom-centered storms may be due to the foregoing statement.

4.3.6 Temporally Non-uniform Rainfall Intensity

Temporally non-uniform rainfall intensity is simulated by a triangular hyetograph. Figure 3.25 shows a schematic of the non-uniform rainfall hyetographs. The $Cs(qp) - Cv(qp)$ curves for p (ratio of time to peak intensity to rainfall duration) equal to $\frac{1}{4}$, $\frac{1}{2}$, and $\frac{3}{4}$ are illustrated in Figure 4.14. They all lie within the hypothetical limits. The curves for $p = \frac{1}{2}$ and $\frac{3}{4}$ are almost indistinguishable from each other. When Figures 4.10 and 4.14 are compared with respect to the $Cs(qp) - Cv(qp)$ curve for $t_o = 3600$ seconds at a section 20 km from upstream, it is noticed that the effect of the triangular distribution of the rainfall intensity is not very significant as far as

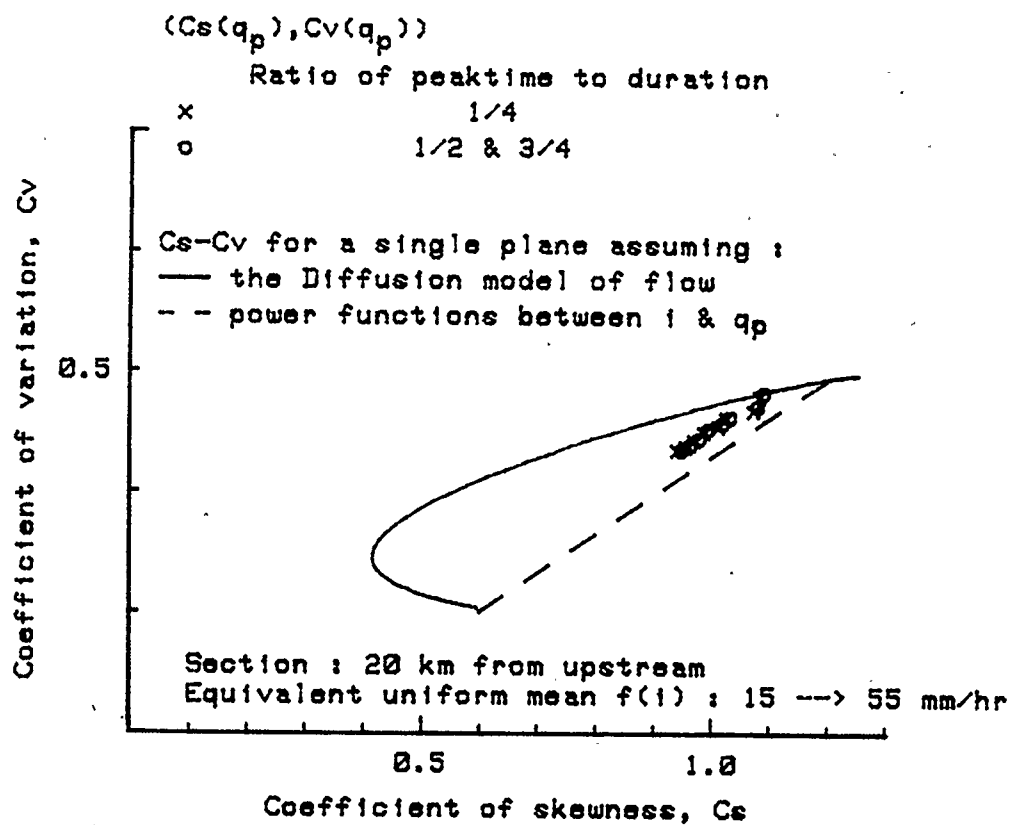


Figure 4.14: $Cs - Cv$ curves of peak flow pdfs for temporally non-uniform rainfall intensity when $f(i)$: Gamma.

C_s and C_v are concerned. The effects become significant only for sections closer to the upstream section.

4.3.7 Non-uniform Rainfall Intensities, Non-uniform Plane Characteristics, and Constant Infiltration Rate

In this section, the parameters of the stream-plane system are as follows :

1. The rainfall intensity has a triangular distribution over time with the peak intensity occurring at three-tenths of the total rainfall duration of 3600 seconds. This temporal distribution is the same over the entire watershed.
2. The spatial distribution of the rainfall intensity is expressed as a fraction of the uniform rainfall intensity generated. The total rainfall depth for the system is equal to that obtained assuming the equivalent uniform intensity. The fractions are as follows : 0.857 for 0-4 km section, 0.714 for 4-8 km section, 1.286 for 8-12 km section, 1.0 for 12-16 km section, and 1.143 for 16-20 km section.
3. There is a constant infiltration rate of 25 mm/hr over the entire watershed. The effect of the infiltration rate is to reduce the effective rainfall intensity and to vary its duration.
4. The watershed characteristics are as given in Table 4.2.

The stream has a rectangular cross-section with a width of 10 m. Its slope and roughness are 0.01 and 0.04 respectively.

Table 4.2: Non-uniform rainfall and plane characteristics along length of stream

STREAM LENGTH (km)	PLANE			FRACTION OF UNIFORM RAINFALL INTENSITY
	WIDTH (m)	SLOPE	ROUGHNESS	
0 - 4	200	0.025	0.040	0.957
4 - 8	150	0.020	0.030	0.714
8 - 12	100	0.015	0.035	1.298
12 - 16	100	0.025	0.025	1.000
16 - 20	75	0.010	0.020	1.143

Figure 4.15 shows the variation of $Cv(qp)$ and $Cs(qp)$ along a stream 20 km long. The pdf of the total rainfall intensity is Normal. Two cases of its coefficient of variation, 0.1 and 0.15, are considered. The mean equivalent (over whole basin) uniform rainfall intensity varies between 50 and 85 mm/hr. The interpretation of the curves in Figure 4.15 is made difficult by the fact that the coefficient of variation of the effective rainfall intensity pdf changes with the mean total rainfall intensity. This is so because $Cv(i_e)$, the coefficient of variation of the mean rainfall intensity pdf, is given by

$$Cv(i_e) = Cv(i) \frac{i_m}{i_m - f} \quad (4.35)$$

where f is the infiltration rate set to a constant value of 25 mm/hr, i_e is the effective rainfall intensity, and i is the total rainfall intensity. Also, along the length of the stream, different fractions of the mean uniform rainfall intensity occur and therefore $Cv(i_e)$ will change along the length of the stream too. However, all the transformations of the total rainfall intensity into effective rainfall intensity will be of the form

$$i_e = frac(i) - f \quad (4.36)$$

where $frac$ is the fraction given in Table 4.2 for each segment of the stream. This linear transformation means that the pdf of i_e will also be Normal. (This is the reason why $f(i)$ was chosen to be Normal. A linear transformation of a Gamma variable of the form given by equation 4.36 is not necessarily Gamma too.) If $f(i)$ is Normal, it was shown in section 3.3.1 (equation 3.47) that the extreme coefficients of variation and skewness of the random peak flows from a plane are related as

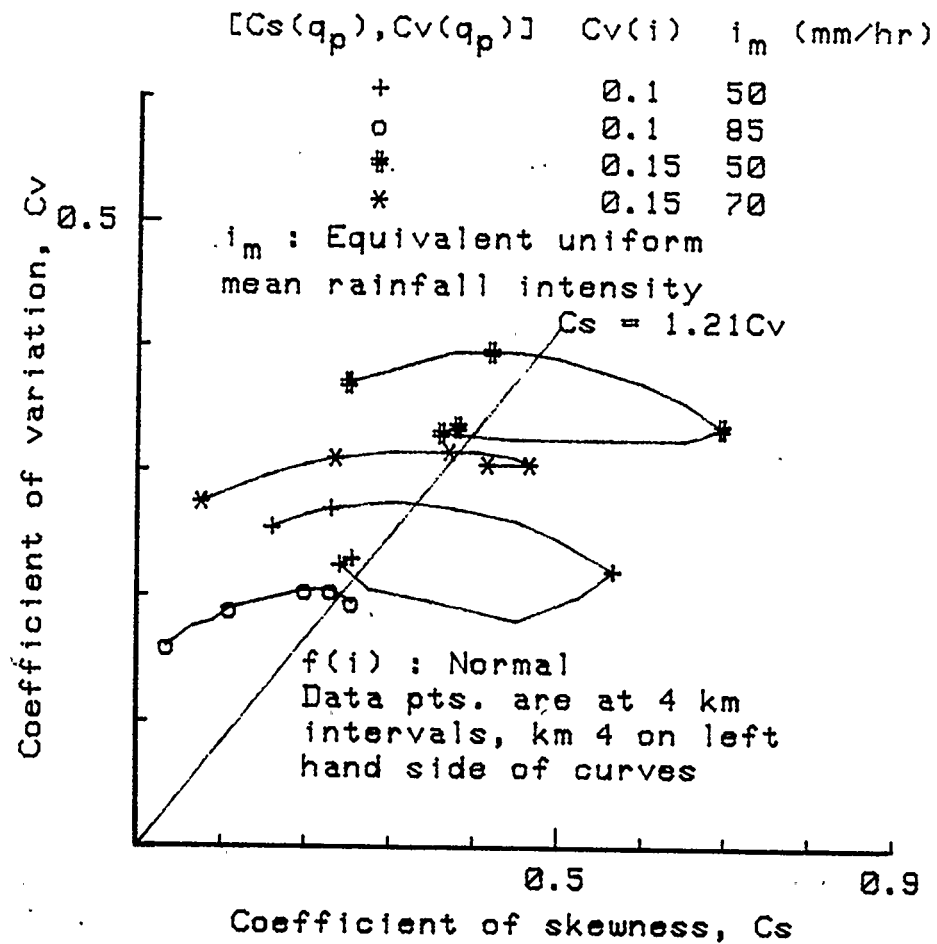


Figure 4.15: $Cs - Cv$ curves of peak flow pdfs along a stream for non-uniform rainfall and plane characteristics.

follows :

$$Cs(qp) \approx 1.21Cv(qp) \quad (4.37)$$

When the line defined by equation 4.37 is plotted on Figure 4.15, it is noticed that it fits the $(Cs(qp), Cv(qp))$ coordinates at sections greater than 12 km from the upstream for most of the input conditions. The $(Cs(qp), Cv(qp))$ coordinates for sections closer to the upstream end tend towards the line $Cs = 0$, which characterises the Normal distribution. This is an expected result because the pdf of i_e is Normal and for sections close to the upstream most of the peak flows may be at steady state and hence the coefficient of skewness of the latter must tend towards that of the Normal distribution (i.e. 0). Some $(Cs(qp), Cv(qp))$, especially those midway along the stream, exhibit large divergences from the limiting curves. The middle segment of the stream, according to Table 4.2, received the highest fraction of rainfall intensity. The $Cs(qp)$ and $Cv(qp)$ at this section is probably being very much influenced by the local conditions. This indicates that whereas non-uniform conditions (rainfall and plane characteristics) on their own do not affect the $Cs(qp) - Cv(qp)$ relationships significantly relative to uniform conditions as described in the previous sections, when mixed together, these non-uniform conditions can cause large localized deviations. However, it should be borne in mind that these deviations are conditional upon all rainfall and plane characteristics being exactly the same for all simulated rainfall intensities. In all the previous analyses it has been assumed that parameters such as duration of rainfall, width of runoff plane, roughness of stream, etc. remain the same for all generated rainfall intensities. In reality, all these parameters would be stochastic. It is conceivable then that these variations in the parameters may dampen the large deviations

in $Cs(q_p)$ and $Cv(q_p)$. The general conclusion from the above discussion seems to be that the $Cs - Cv$ limits as defined by that of a plane and a power function relationship between i and q_p are average loci for $Cs(q_p)$ and $Cv(q_p)$ from a stream-plane combination. And unless a section close to the upstream end is being considered, $(Cs(q_p), Cv(q_p))$ coordinates seem to lie mostly in the region close to the corresponding extreme coordinates for a plane.

4.4 Summary

This chapter dealt with the statistical characteristics of flood events from a stream-plane configuration. The effects of two modes of flood generation were examined. In the first mode, it was assumed that the flood wave was of the point input type. It is approximated by a hydrograph of a Gamma shape at the upstream end of the channel. No lateral inflow or outflow occurs along the stream. A composite physical-probabilistic approach based on a Monte Carlo simulation of the flood peaks/levels at the upstream section and a deterministic routing of the flood wave along the length of the stream indicates that the coefficients of skewness and variation of the random peaks/levels increase or decrease depending on the relative importance of the rate of rise of the inflow rate and the time to peak flow/depth. When the rate of rise of the inflow rate increases at a significantly higher rate than the time to peak for increasingly higher rate of flow/depth, the coefficients of variation and skewness decrease along the length of the stream. Conversely, when the characteristics of the flood wave are governed primarily by the time to peak flow rate/depth, the coefficients of variation and skewness increase along the

length of the stream. The rate of change in these statistical parameters decreases at an increasingly higher rate along the length of the stream, i.e., the coefficients become insensitive to further attenuation after a certain degree of attenuation has been reached.

The second mode of flood generation assumes that all the flow is generated from rainfall on the planes on the sides of the stream. There is no point input flow at the upstream end of the channel. The most significant result is that under various rainfall and stream-plane characteristics the $(Cs(qp), Cv(qp))$ coordinates of the random peak flow series lie within limits defined by the curve obtained for a single plane and a straight line joining the (Cs, Cv) of the rainfall intensity pdf to the maximum $(Cs(qp), Cv(qp))$ of the peak flow pdf for a plane only. At the most upstream section of the channel $(Cs(qp), Cv(qp))$ is identical with (Cs, Cv) of the rainfall pdf. This assumes that the width of the runoff planes is small enough for steady state to be reached earlier than the duration of the rainfall. This is not an inconceivable situation in first-order natural watersheds: As the distance from the most upstream section increases, $Cs(qp)$ and $Cv(qp)$ increase towards the limiting maximum obtained for a plane. The $Cs(qp) - Cv(qp)$ curves from a stream-plane combination are shifted inwardly from that obtained for uniformly distributed rainfall on a plane. The situation is analogous to the curves obtained from temporally non-uniform rainfall intensity on a plane, the inflow from the planes into the stream is trapezoidally distributed over time. The effect of spatially and temporally non-uniform rainfall intensity is to make the coefficients of variation and skewness of the peak flows from a stream to coalesce within a small region close to the theoretical maximum. When infiltration is superimposed on the rainfall hyetograph

the same conclusions are reached as long as $Cv(i)$ is changed to $Cv(i_e)$, the coefficient of variation of the effective rainfall intensity. The main conclusion is that for relatively low mean rainfall intensities, shallow stream and plane slopes, and a long distance downstream, the co-ordinates (coefficient of skewness, coefficient of variation) of the random peak flow series from a stream-plane combination are very close to one another and to the maximum obtained for a plane.

Chapter 5

STATISTICAL CHARACTERISTICS OF RANDOM PEAK FLOWS FROM A NETWORK OF STREAMS

5.1 Introduction

Over the years there have been many attempts to relate peak flows of various return periods to physiographic characteristics of watersheds. In a few cases climatic parameters have been included. Most of these relationships are of an empirical nature. Lacking a physical basis, they may not be suitable for use in areas other than those for which they have been developed. The effects of physical characteristics and spatial structure of a river system on the statistical characteristics of a random series of peak flow series in conjunction with the prevailing climatic regime is an ongoing field of research. It was demonstrated in the previous two chapters that at an elemental level of a watershed, that is, a single plane or a single stream with two side planes, the coefficients of variation and skewness of the random peak flow series lie within a mathematically definable region of the $C_s - C_v$ plane for given input parameters. For conditions which produce a slow response from a watershed, most of the coefficients of the variations and skewnesses from a stream-plane configuration were found to be concentrated within a small area of the hypothetical limits of $(C_s(q_p), C_v(q_p))$. In a network of streams, the peak flow at the outlet is

a mixture of flows from all the streams above the outlet. Because of the different flow velocities in each stream, the peak flow at the outlet is not a simple function of the local peak flows of the contributing streams. The randomness of the peak flows at the outlet is then not only a function of the randomness in the rainfall parameters but also of the spatial structure of the watershed. The objective of this chapter is to determine the effects of a network of streams on the statistical characteristics of random peak flow series.

The drainage network of a natural watershed is conceptualized as a combination of runoff planes and streams. Horton's laws of drainage network and Strahler's ordering procedures are used to generate stream networks and runoff contributing areas. For given rainfall and stream network characteristics peak flows corresponding to a range of rainfall intensities are determined by a numerical simulation of the equations of continuity and momentum. Monte Carlo simulation technique is used to generate random rainfall intensities within that range. The statistical characteristics of the corresponding random peak flow series are obtained using standard statistical techniques. The following sections examine the effects of node density, stream length ratio, runoff contributing area, and rainfall and infiltration characteristics.

5.2 Numerical Simulation of Peak Flows from Stream Networks

5.2.1 Numerical Simulation

The equations governing the flow through a stream network are the continuity equation,

$$\frac{\delta y}{\delta t} + \frac{\delta q}{\delta x} = i \quad (5.1)$$

and the approximate form of the momentum equation,

$$S_f = S_o - \frac{\delta y}{\delta x} \quad (5.2)$$

where y is the depth of flow, q is the flow rate per unit width, S_f is the energy slope, S_o is the slope of the runoff plane or a wide and rectangular stream, and i is the rainfall rate for a plane and the overland runoff rate for a stream. The numerical procedure for the solution of equations 5.1 and 5.2 is essentially the same as that described for the stream-plane configuration in section 4.3.2. The only major addition to the procedure is the specification of the boundary conditions at the junctions of streams. The simplest configuration of a stream network is one which contains only one junction as depicted in Figure 5.1. The conservation of mass and momentum equations are used to specify the boundary conditions at the confluence. The confluence is assumed to be of a point-junction type with no storage capacity. The conservation of mass equation is

$$Q_o = Q_1 + Q_2 \quad (5.3)$$

Q_i from the i^{th} upstream channel at the k^{th} time level is calculated from the depth of water in the first segment of the downstream channel at the $(k-1)^{th}$ time level.

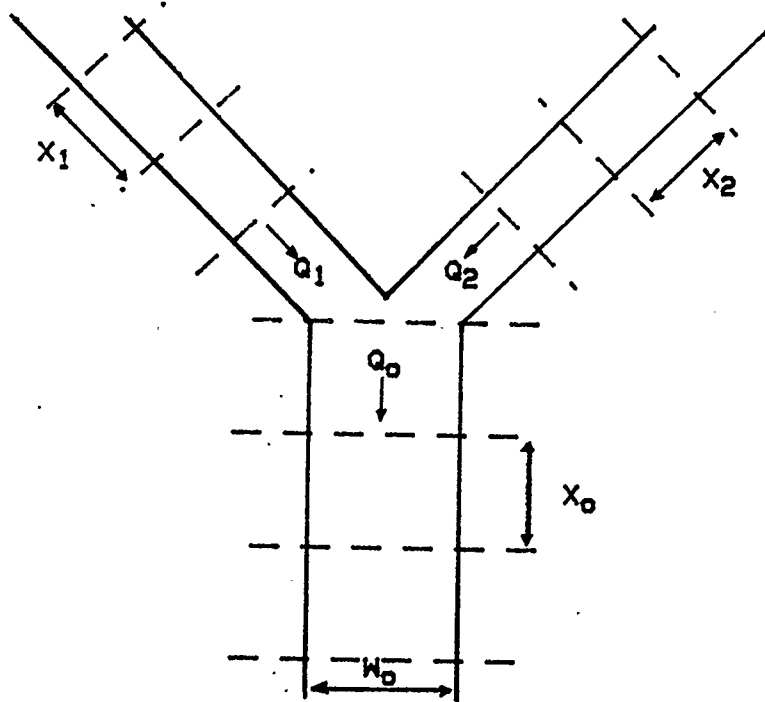


Figure 5.1: Schematic of flow at a confluence of streams.

The slope of the energy line, $S_{f,i}$, for the last segment of the i^{th} upstream channel at the k^{th} time level is obtained from the depths of flow in the penultimate segment of the i^{th} upstream channel and the first segment of the downstream channel at the k^{th} time level, that is,

$$S_{f,i,n} = S_{o,i} + \frac{y_{n-1,i} - y_{1,o}}{\Delta X_i + \Delta X_o} \quad (5.4)$$

where n is the number of segments in the i^{th} channel. In this way the effects of the water level downstream of the confluence are accounted for. The kinetic energy of the inflow is assumed to be lost in the junction and the sum $(Q_1 + Q_2)$ is uniformly distributed over $W_o \Delta X_o$.

5.2.2 Evaluation of the Numerical Procedure

The numerical procedure used to solve for q in equations 5.1 and 5.2 is an explicit finite difference scheme. In such a scheme, the unknown flow parameters (depth and flow rate) at the end of a time period and at a specified location are expressed as functions of the known parameters at the beginning of the same time period. Explicit schemes are the simplest of all numerical schemes, yet because of stability considerations require very small computational time steps. The latter are governed by the Courant conditions (equation 3.16). Analytical solutions of equations 5.1 and 5.2 are not available. The explicit finite difference solution for given network and rainfall input parameters was compared to the solution from a more sophisticated model which has been found to give very good results on actual watersheds.

The model is the one-dimensional hydrodynamic model developed by Environ-

ment Canada. Complete details on the model are given in Environment Canada One-Dimensional Hydrodynamic Model Computer Manual (1982). Only a brief description is presented here. The 1-D model is a numerical method to simulate transient water quality and flow conditions in river networks and tidal estuaries. The model is called one-dimensional because the velocity of flow across a channel cross-section is assumed to be uniform and called hydrodynamic because it uses the full St. Venant equations to simulate gradually varied unsteady flows. An implicit finite difference scheme is used to solve a simplified and linearized version of the St. Venant equations. A weighted residual method of optimization is applied to the linearized equations to minimize the difference between the continuous equations and the discrete approximations. Appropriate local and temporal adjustments are made to account for the non-linear characteristics of the governing equations. The implicit scheme is unconditionally stable and the Courant criterion governs the convergence of the scheme.

The 1-D model has been used on numerous projects. In the St. Lawrence study it was used to determine flood levels for the design of dykes in an area where the highly regulated flows of the St. Lawrence River meets the partially regulated flows of the Ottawa River. In the Peace-Athabasca study it was used to determine the effects of existing and proposed control structures on the channels within the delta. A 22-year period was simulated as opposed to the normally short simulation periods not exceeding several days required for flood studies. The model has been found capable of reproducing instantaneous discharges to within 4% to 7% of that actually measured (using conventional measuring techniques). Water balance checks showed discrepancies between $\pm 0.8\%$ and $\pm 1.5\%$ for the 22-year

simulation of the Peace-Athabasca Delta system.

The present numerical scheme and the 1-D model were used to simulate the flow from a synthetic network with only one confluence. The input conditions and stream characteristics were such that the discrepancy between the two schemes would be expected to be very large. The characteristics of the network are shown in Figure 5.2. Very shallow or very steep slopes of the streams make the approximate form of equation 5.2 very inaccurate compared to the full St. Venant equations. However, the discharge hydrograph shown in Figure 5.3 indicates that the difference in peak flow between the two numerical procedures is only of the order of 10%. The difference decreases for similar networks with steeper slopes. The slopes of the streams used for the simulation of random rainfall events are about fifty to a hundred times higher than that used in the comparison test. The inaccuracy in the peak flows for such networks may therefore be less than 10%, however, the errors would not necessarily be a monotonic function of slope. The influence of the rainfall intensity, as far as it determines the discharge in the network, may also be significant. Since this study is mainly concerned with the dimensionless statistical parameters of the random peak flows and not the actual peak flows, therefore, the absolute errors in the peak flows are not important as long as they are not so large as to distort the relationship between the rainfall parameters and the peak flow.

The 1-D model took about 45 seconds to produce the hydrograph shown in Figure 5.3 while the explicit scheme took only 2 seconds. The savings in computational time are quite substantial, especially, when considering the number of runs required to obtain the statistical characteristics of the peak flows (at least 200 runs are required for each $(Cs(qp), Cv(qp))$ co-ordinate). Furthermore, a more

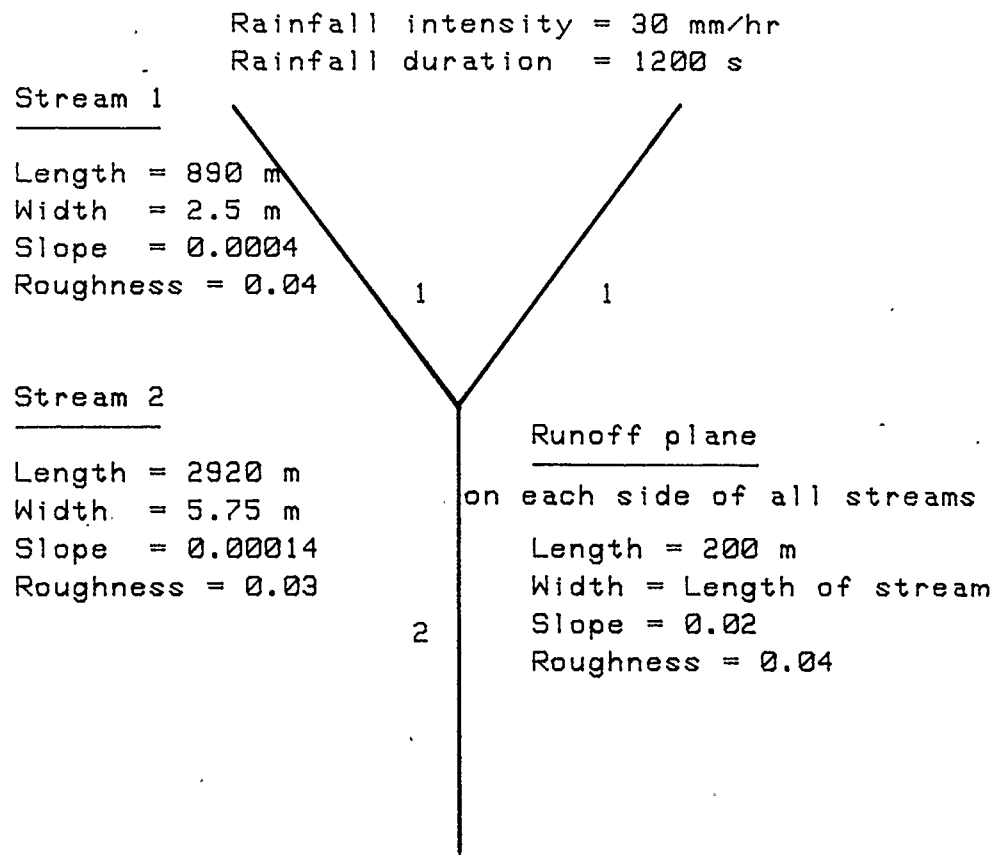


Figure 5.2: Schematic of river system used in testing the explicit numerical scheme against the 1-D hydrodynamic model.

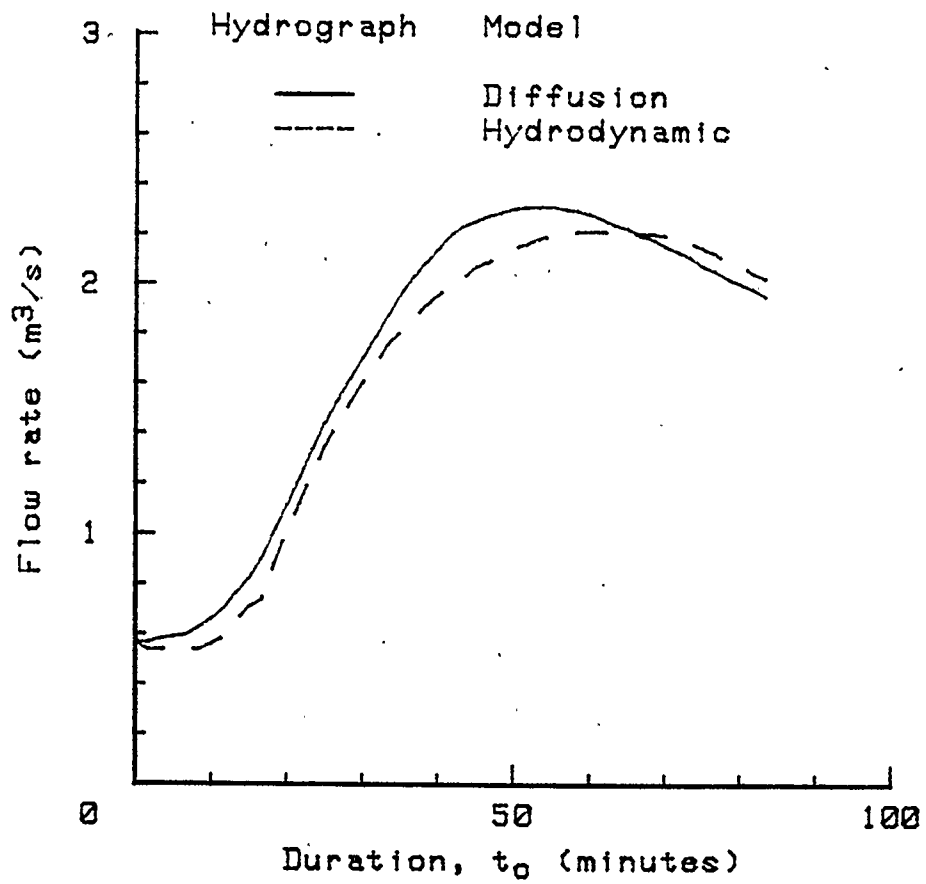


Figure 5.3: Comparison of hydrograph from the explicit numerical scheme with that from the 1-D hydrodynamic model.

sophisticated model such as the 1-D model requires more intricate programming to incorporate non-uniform rainfall inputs and to simulate more complex network patterns. So, while giving less accurate flow rates, as compared to the 1-D model, the explicit numerical scheme is the one better suited for the purposes of this study.

5.3 Statistical Characteristics of Random Peak Flows from Constant Duration Rainfalls

The distinguishing characteristics of a river network is the joining together of streams to form single streams which themselves may link with other streams further down the network. The presence of these confluences distorts the discharge hydrograph at the outlet of the network. The amount of distortion depends on the number and spatial distribution of the confluences, the individual characteristics of the streams and the associated runoff planes, and the rainfall parameters. When the rainfall input is random, the randomness in the peak flows at the outlet is expected to be a function of the randomness of the input as well as the structure of the network. It would be interesting to determine whether the presence of the confluences affects the relationship between the statistical characteristics of rainfall and peak flow in ways different from those of single planes and streams.

The statistical parameters of the random peak flow series are determined as follows. Numerical simulation using the procedure outlined in section 5.2 is used to generate peak flows corresponding to rainfall intensities increasing from 1 mm/hr to 150 mm/hr in steps of 1 mm/hr. Then for given rainfall pdf (Normal, Gamma, and/or Gumbel) with known parameters, Monte Carlo simulation technique is

used to generate 6000 random rainfall intensities. The corresponding 6000 random peak flows are obtained by interpolating between peak flows for known rainfall intensities. Standard statistical methods are then used to determine the mean, coefficient of variation, and coefficient of skewness of the random peakflow series.

5.3.1 Topological Description of a Network of Streams

Horton (1932), Langbein (1947), and Strahler (1957) are just a few of the scientists who have given the description of watershed and channel networks a quantitative basis. Numerous parameters exist to describe the physiographic and topological characteristics of a watershed. However, only a few of these are truly independent variables. Those which are relevant to this study are described below.

1. Basin order, u

The basin order, u , is the highest stream order in the basin. In natural basins u can range between 1 and 5 (Chow, 1964). The ordering scheme is that of Strahler (1957). Figure 2.2 shows a synthetic basin of order 3, ordered according to Strahler's rules which are :

- (a) Streams that originate at a source are first-order streams.
- (b) When two streams of the same order Φ join, the emerging stream is of order $\Phi + 1$.
- (c) When two streams of different order join, the emerging stream has the higher order of the two combining streams.

2. Bifurcation Ratio, R_B

This term represents the base of an inverse geometric series relating the number, N_Φ , of streams of order Φ to the basin order u .

$$N_\Phi = R_B^{u - \Phi} \quad (5.5)$$

or,

$$R_B = \frac{N_\Phi}{N_\Phi + 1} \quad (5.6)$$

In a natural basin R_B can range between 2 and 5.

3. Stream Length Ratio, R_L

R_L is the base of a direct geometric series relating the mean length L_Φ of streams of order Φ to the mean length L_1 of streams of order 1.

$$L_\Phi = L_1 R_L^{\Phi - 1} \quad (5.7)$$

or,

$$R_L = \frac{L_\Phi}{L_1} \quad (5.8)$$

In a natural basin R_L is between 1.5 and 3.5.

Synthetic networks for the purposes of this study are created by keeping u , R_B , and R_L within their respective range found in natural basins.

5.3.2 Effect of Basin Order

When the order of a drainage network with constant bifurcation ratio and runoff contributing area increases there is an increase in the number of streams and confluences in the network. This implies that the average length between reaches is shorter and hence the degree of attenuation of flow through the network is lesser.

The result is a basin with a faster response. The effect of the basin order on the statistical characteristics of the random peak runoff series is investigated through three synthetic networks illustrated in Figure 5.4. Networks (a) to (c) have order 2, 3, and 4 respectively. The characteristics of the 3 networks are given in Table 5.1. The number of confluences in each network is 1, 3, and 7. Network (c) therefore has the fastest response. Each network has a stream length ratio (R_L) of approximately 1.5 and a bifurcation ratio (R_B) of 2. The width of the overland runoff plane on each side of each stream is 200 m. The total length of all the streams is 42000 m, and the total runoff contributing area is 16800000 sq. metres for each network.

The statistical characteristics of the random peak runoff series from each network are determined as outlined in section 5.3. The pdf of the rainfall intensity is Normal with i_m ranging from 50 to 80 mm/hr and $Cv(i)$ equal to 0.2. The rainfall intensity is spatially and temporally uniform. The duration of the rainfall events is 1800 s for one set of simulations on the 3 networks. Rainfall durations of 3600 seconds are further simulated on network (c). Figure 5.5 shows the outcome of the statistical analysis. On the same figure, the limits of $(Cs(qp), Cv(qp))$ as hypothesised in the previous chapter have been superimposed. The first observation pertinent to all three networks under the various input conditions is that the coefficients of variation and skewness are within the hypothetical limits despite the distortion that the confluences in the networks may cause to the runoff hydrographs. It is further observed that the shorter duration and lower mean rainfall intensity conditions bring $(Cs(qp), Cv(qp))$ closer to the limiting maximum defined by the hypothetical region. These two observations are exactly the same as ob-

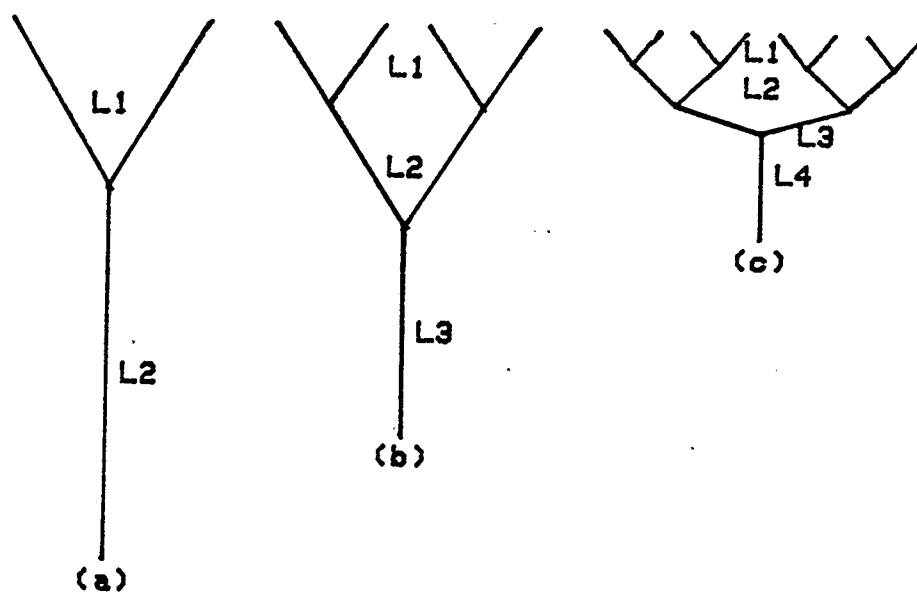


Figure 5.4: Synthetic networks of order 2, 3, and 4 with each having a stream length ratio ≈ 1.5 .

Table 5.1: Characteristics of networks illustrated in Figure 5.4.

Parameter	STREAM NETWORK		
	(a)	(b)	(c)
R_B	2	2	2
U	2	3	4
ΣL (m)	42000	42000	42000
R_L (app.)	1.5	1.5	1.5
L1 (m)	12000	4600	2000
L2 (m)	18000	6800	2800
L3 (m)	—	10000	4200
L4 (m)	—	—	6400
L1 (m)	30000	21400	15400
W1 (m)	15	15	15
W2 (m)	25	20	20
W3 (m)	—	25	25
W4 (m)	—	—	30
S1	0.015	0.015	0.015
S2	0.01	0.013	0.013
S3	—	0.01	0.01
S4	—	—	0.008
n1	0.035	0.035	0.035
n2	0.03	0.031	0.031
n3	—	0.029	0.029
n4	—	—	0.027

Width, slope, and roughness of side-planes are 200 m, 0.025, & 0.04 respectively.

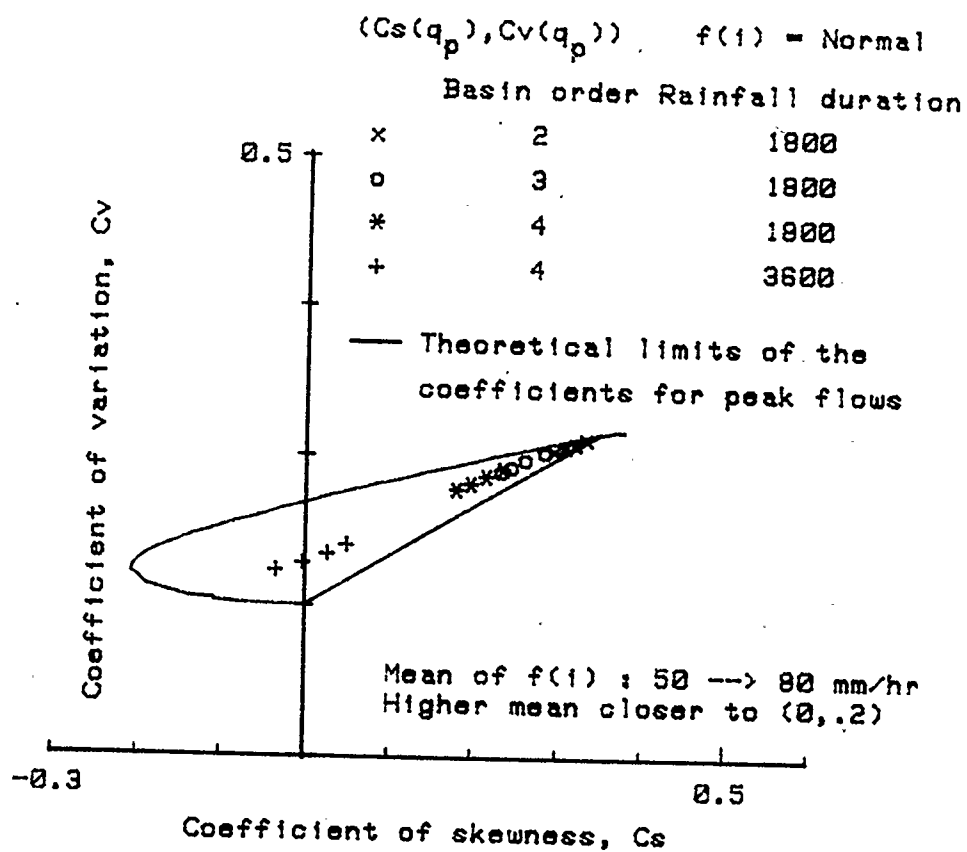


Figure 5.5: $Cs - Cv$ relationships of peak runoff from synthetic networks of order 2, 3, and 4.

tained for the single-stream system and are similar to the behaviour exhibited by the statistical parameters of peak runoff from a single plane. It can therefore be assumed that under the conditions specified above, a network of streams responds in the same way as a single plane/single stream-plane as far as the behaviour of the statistical parameters of the peak runoff series are concerned. This suggests that a characteristic common to the three systems (plane, single stream-plane, and stream network) is predominant in determining the coefficients of variation and skewness of the peak runoff series. A closer examination of the $(Cs(qp), Cv(qp))$ coordinates from three networks for constant input conditions reveals that an increase in the basin order u decreases both $Cs(qp)$ $Cv(qp)$. An increase in basin order decreases the length of the longest path of flow Ll from the furthest point in the network to its outlet. The longest flow path for the three networks (a), (b), and (c) are 31000 m, 21400 m, and 15400 m respectively. For i_m equal to 50 mm/hr and rainfall duration of 1800 s $(Cs(qp), Cv(qp))$ coordinates for the three networks are (0.312,0.335), (0.300,0.275), and (0.287,0.227) respectively. For i_m equal to 80 mm/hr and rainfall duration of 1800 s, and corresponding coordinates are (0.306,0.300), (0.291,0.238), and (0.278,0.184) respectively. $Cs(qp)$ is the parameter which is the more sensitive to the basin order. For the particular case being considered, a change in u from 2 to 4 decreases the longest path length by about 50% and the coefficient of skewness decreases by about 40% when $i_m = 80$ mm/hr. The coefficient of variation decreases by about 5% for the same case. The shallow gradient of the $Cs - Cv$ curve for the plane illustrates the sensitivity of the coefficient of skewness of the peak flows to runoff length. Under the conditions being considered in this section (constant duration of rainfall, uniform distribution

of rainfall intensity, etc.,) transferring coefficients of skewness from one watershed to another is permissible only if the longest runoff path of each watershed is not very different from each other.

5.3.3 Influence of Stream Length Ratio on Statistical Characteristics of Peak Flows

In the previous section the stream length ratio R_L was kept at a constant value of approximately 1.5. Increasing R_L for a given total stream length decreases the length of the first-order streams and increases the length of the highest order stream. The net effect is that for a given basin order, increasing R_L increases the length of the longest runoff path L_l . The three networks illustrated in Figure 5.5 were used as a base to create 2 new sets of three networks with R_L approximately equal to 2 and 2.5 for each set. The characteristics of the extra six synthetic networks (each still having $R_B = 2$) are given in Table 5.2. The total lengths of the streams were kept at 42000 m for each network.

The $Cs(q_p) - Cv(q_p)$ curves for peak flows from 3 networks of different stream-length ratios ($\approx 1.5, 2.0$, and 2.5) but same basin order ($u = 4$) are shown in Figure 5.6. The rainfall input parameters are the same as given in section 5.3.2. The patterns exhibited by the statistical parameters of the peak flows have not changed from those of Figure 5.5. Shorter duration rainfalls are more likely to produce $(Cs(q_p), Cv(q_p))$ closer to the extremity of the hypothetical region. Increasing the duration of the rainfall brings the coordinates towards the (Cs, Cv) of the rainfall intensity. As far as the network characteristics are concerned, their effects seem less direct. The $(Cs(q_p), Cv(q_p))$ coordinates for the nine networks with i_m equal

Table 5.2: Characteristics of 6 synthetic networks with different stream length ratios.

Parameter	STREAM NETWORK					
	(d)	(e)	(f)	(g)	(h)	(i)
R_B	2	2	2	2	2	2
U	2	3	4	2	3	4
ΣL (m)	42000	42000	42000	42000	42000	42000
R_L (app.)	2.0	2.0	2.0	2.5	2.5	2.5
L1 (m)	10600	3600	1400	9400	2800	800
L2 (m)	20800	7200	2600	23200	7000	2200
L3 (m)	—	13200	5000	—	16800	5800
L4 (m)	—	—	10400	—	—	15200
L1 (m)	31400	24000	19400	32600	26600	24000
W1 (m)	15	15	15	15	15	15
W2 (m)	25	20	20	25	20	20
W3 (m)	—	25	25	—	25	25
W4 (m)	—	—	30	—	—	30
S1	0.015	0.015	0.015	0.015	0.015	0.015
S2	0.01	0.013	0.013	0.01	0.013	0.013
S3	—	0.01	0.01	—	0.01	0.01
S4	—	—	0.008	—	—	0.008
n1	0.035	0.035	0.035	0.035	0.035	0.035
n2	0.03	0.031	0.031	0.03	0.031	0.031
n3	—	0.029	0.029	—	0.029	0.029
n4	—	—	0.027	—	—	0.027

Width, slope, and roughness of side-planes are 200 m, 0.025, & 0.04 respectively.

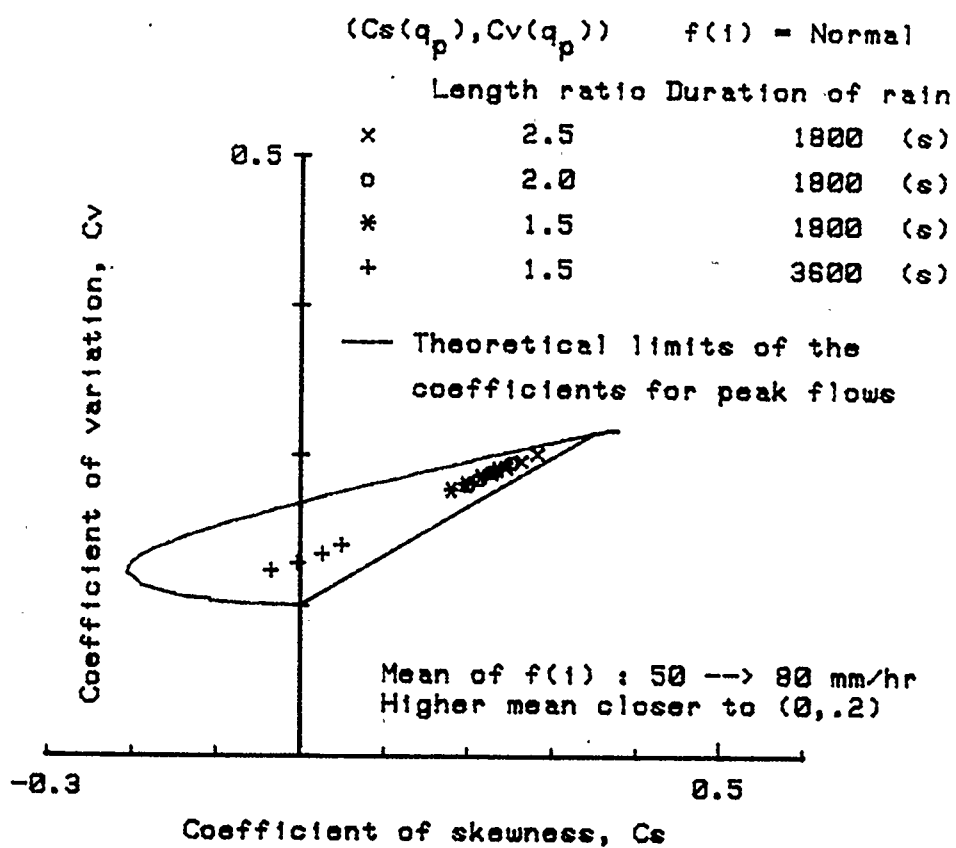


Figure 5.6: $Cs - Cv$ relationships of peak flows from networks of different stream-length ratios.

to 50 and 80 mm/hr are listed in Table 5.3. The statistical parameters from the network of order 2 are not sensitive to R_L while the same parameters increase with R_L for the higher order basins. The effect of the increased longest runoff path for higher order basins is therefore apparent. For two networks with the same length of the longest runoff path (24000 m) but with (u, R_L) equal to (3,2.0) and (4,2.5) respectively, the coefficient of variation is almost the same for both while the coefficient of skewness has increased for the one with the lower (u, R_L) . The conclusion from the results of this and the previous section seems to be that unless small watersheds are being considered, the effect of the network characteristics on the statistical parameters of the peak runoff is not very significant compared to the effects of the rainfall characteristics.

5.3.4 Spatially Non-uniform Runoff Contributing Areas

The previous section considered streams with runoff planes of constant width. In natural watersheds upland overland runoff areas usually have greater widths and steeper slopes than those in the lower reaches of the watershed. The number of synthetic networks that can be created to simulate non-uniform width and slope of runoff contributing areas is virtually infinite. The objective of this section will be restricted to determining whether under such conditions the statistical parameters of the peak runoff series are still within the limiting hypothetical region. Two synthetic networks were created. For both networks, $R_L = 1.5$ and $u = 4$. The widths of the runoff planes for the 1st, 2nd, 3rd, and 4th order streams were 200, 150, 100, and 50 m respectively for one network and 100, 75, 50, and 25 m respectively for the second network. The length of the longest runoff path is the

same for both cases.

The results of the statistical analysis of the random peak flows from each network are shown in Figure 5.7. Some individual results are as follows : for the first network (with the wider runoff planes for each stream) the $(Cs(qp), Cv(qp))$ coordinates for i_m equal to 50 and 80 mm/hr respectively are (0.288,0.217) and (0.276,0.162); for the second network the corresponding coordinates are (0.302,0.288) and (0.293,0.240) respectively. The duration of the rainfall events was set to 1800 seconds. Compared to the network with a uniform width of 200 m for all runoff planes, the coefficients of variation and skewness of the first network have decreased and increased for the second network. The change in the coefficient of variation for the first network is negligible. Explanation of the individual results are difficult because of the interaction of various parameters, not all of them changing the statistical parameters in one direction. One would expect that for the smaller plane widths of the second network the overland flow reaches steady state faster and stays there longer and according to previous results (plane or stream-plane combination) this should lead to a decrease in the coefficients of variation and skewness. The decrease does occur for the first network. For the second network it can only be speculated that smaller runoff widths produce smaller flows which are attenuated to a greater extent over the length of the streams. This is analogous to large rainfall intensities over long runoff planes, $(Cs(qp), Cv(qp))$ may be close to those of the rainfall close to the upstream end of the plane but both parameters increase for sections downstream. The main result seems to be that while non-uniform distribution of runoff contributing areas affect the coefficients of variation and skewness of the random peak flows, the influence is only significant

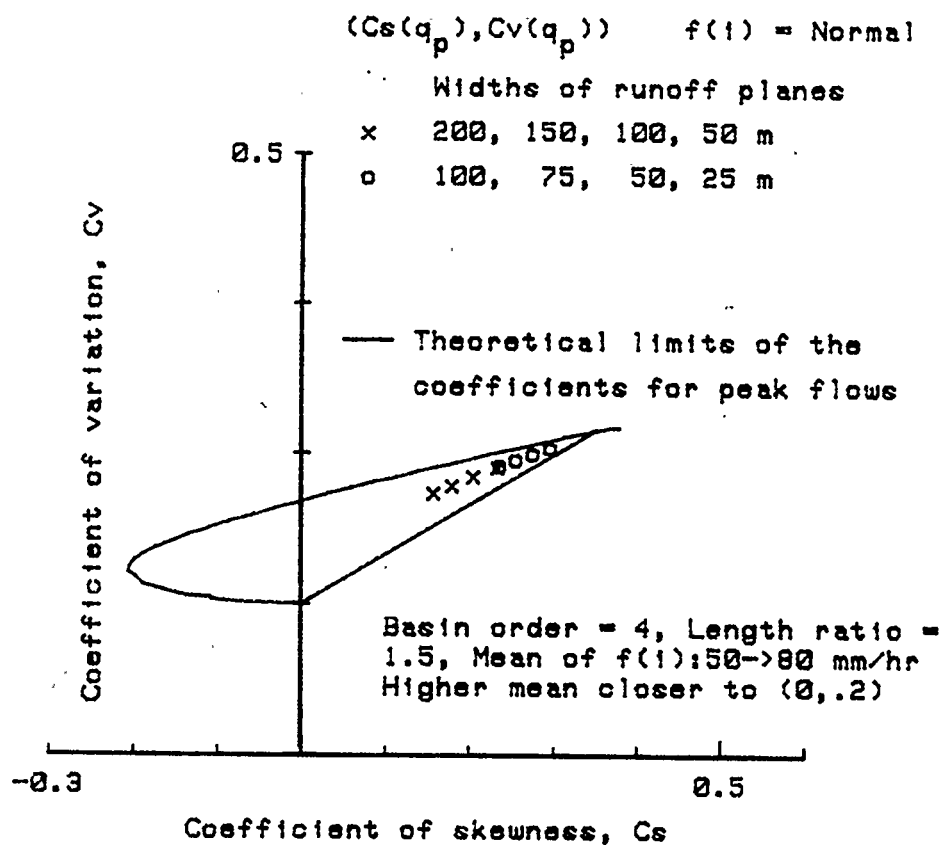


Figure 5.7: $Cs - Cv$ relationships of peak flows from two networks with non-uniform runoff contributing areas.

under extreme conditions. For conditions expected to prevail over natural basins, the statistical parameters of the peak flows are concentrated within a small area of their hypothetical limits.

5.3.5 Triangular Temporal Distribution of Rainfall Intensity

The effect of non-uniform temporal distribution of rainfall intensity is simulated by assuming that the rate of rainfall increases from 0 mm/hr at time $t = 0$, increases to a peak value of i_p at time $t = t_p$, and decreases back to 0 at time $t = t_o$. Two ratios p , defined as $\frac{t_p}{t_o}$ in section 3.4, are selected for study. They are $\frac{3}{10}$ and $\frac{7}{10}$. The peak rainfall intensity is twice the equivalent uniform rainfall intensity. Random rainfall intensities having the above characteristics are simulated over two networks. u and R_L are 3, 2.5 and 4, 1.5 for the two networks respectively. Both networks have a uniform width of 200 m for all the runoff planes. The pdf of the rainfall intensity is Normal with $Cv(i)$ equal to 0.2 and i_m ranging from 50 to 80 mm/hr. The duration of the rainfall events are 1800 s for one set of simulations and 3600 s for another. The results of the statistical simulation are shown in Figure 5.8.

The main observation from Figure 5.8 is that the effect of a triangular distribution of rainfall does not change the basic conclusion obtained from the other sections, namely, that $(Cs(q_p), Cv(q_p))$ of the peak runoff series lie within a region close to the extremity of their hypothetical limits. The statistical coefficients of the peak flows are relatively insensitive to the network characteristics. The duration of the rainfall events still has the predominant influence.

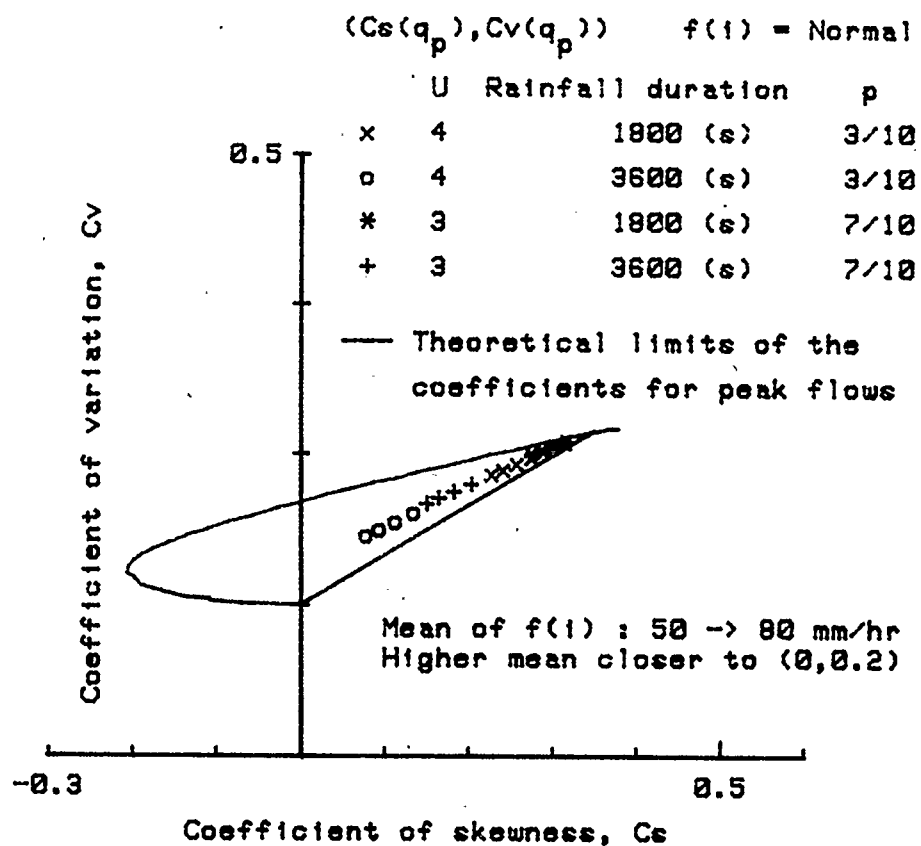


Figure 5.8: $Cs - Cv$ relationships of peak flows from networks under temporally non-uniform rainfall intensity.

5.3.6 Spatially Non-uniform Distribution of Rainfall Intensity

Analyses similar to the previous section are done with spatially non-uniform rainfall. The rainfall intensity is uniform over time. The spatial distribution of the rainfall intensity, specified as fractions of the equivalent uniform intensity giving the same depth of flow, is as follows : on the 1st, 2nd, 3rd, and 4th order streams for the network with u equal to 4, the fractions are 0.90, 1.50, 0.80, and 0.64 respectively; the network with u equal to 3 has fractions 0.90, 1.50, and 0.65 respectively on the 1st, 2nd, and 3rd order streams.

The results of the statistical analyses are shown in Figure 5.9. The effect of non-uniform spatial distribution of rainfall intensity is minimal as far as the area within which $(Cs(qp), Cv(qp))$ are located is concerned.

5.3.7 Spatially and Temporally Non-uniform Rainfall Intensity on Spatially Non-uniform Runoff Contributing Areas

This final section dealing with constant duration rainfall combines the non-uniformity of runoff contributing areas (section 5.3.4), temporally non-uniform rainfall (section 5.3.5), and spatially non-uniform rainfall (section 5.3.6) together. For the fourth order basin, the 1st, 2nd, 3rd, and 4th order streams have plane widths equal to 200, 150, 100, and 50 m respectively. The respective fractions of uniform rainfall intensity are 0.90, 1.40, 0.70, and 0.69. The equivalent uniform rainfall intensity over the whole basin gives the same depth of water as the non-uniform spatial distribution of rainfall intensity. For the third order network, the 1st, 2nd, and 3rd order streams have plane widths respectively equal to 200, 163.4, and 90 m. The respective fractions of uniform rainfall intensity are 0.80, 1.50, and 0.54.

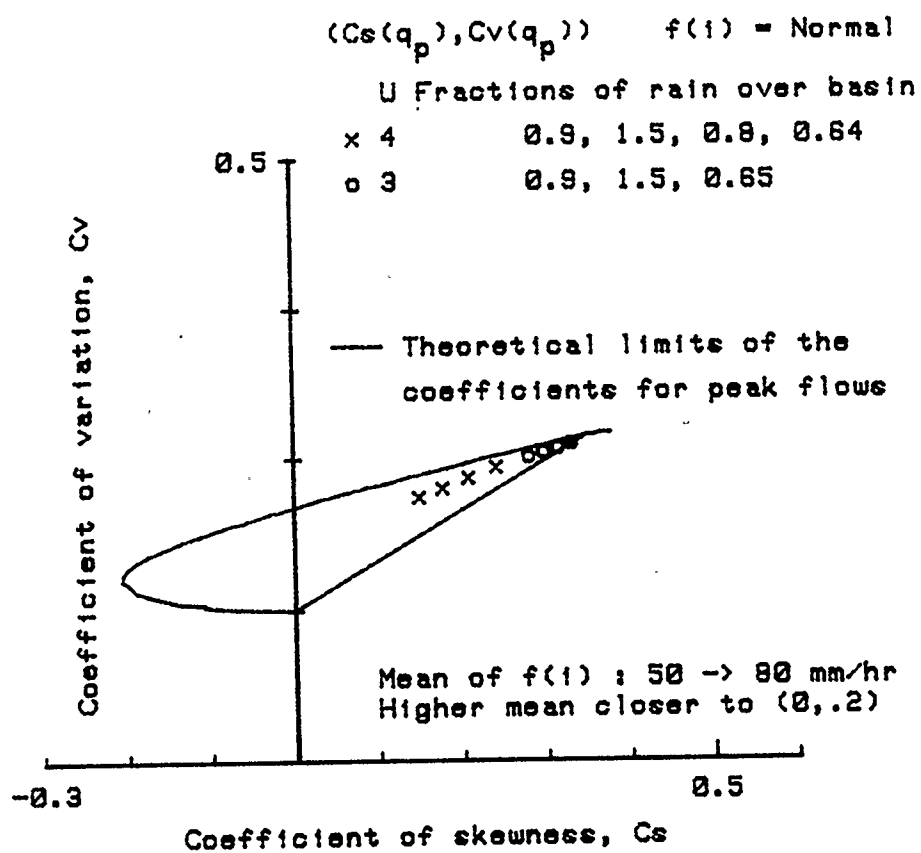


Figure 5.9: $Cs - Cv$ relationships of peak flows from two networks under spatially non-uniform rainfall intensity.

Both networks have the same runoff contributing areas. The results of the statistical analysis are shown in Figure 5.10. The results seem to indicate that as the basin and rainfall characteristics become more non-uniform, while still simulating "normal" conditions, the coefficients of variation and skewness of the peak runoff series coalesce in the region close to the extremity of their hypothetical limits.

Summary for Constant Duration Rainfall

The main result stemming from the simulation of random rainfall events of constant duration on stream networks is that the coefficients of variation and skewness of the random peak flows are concentrated within a small region at the extremity of the their hypothetical limits. While the characteristics of the networks do affect the coefficients, their influence is not very significant when compared to that exerted by the rainfall parameters. This has been shown to be the case even under non-uniform watershed and rainfall parameters.

5.4 Statistical Characteristics of Peak Flows from Correlated Rainfall Inputs

It is common knowledge that in natural rainfall events intensities and durations are correlated, high intensity events tend to be of "short" duration while low intensity events generally have relatively longer durations. Present day knowledge of rainfall physics is not sufficient to physically determine this correlation. An empirical-statistical analysis of rainfall records provides a set of synthetic curves relating rainfall intensity, rainfall duration, and frequency of occurrence. Figure 3.18 shows typical intensity-duration-frequency (IDF) curves. The effect of correlated rainfall

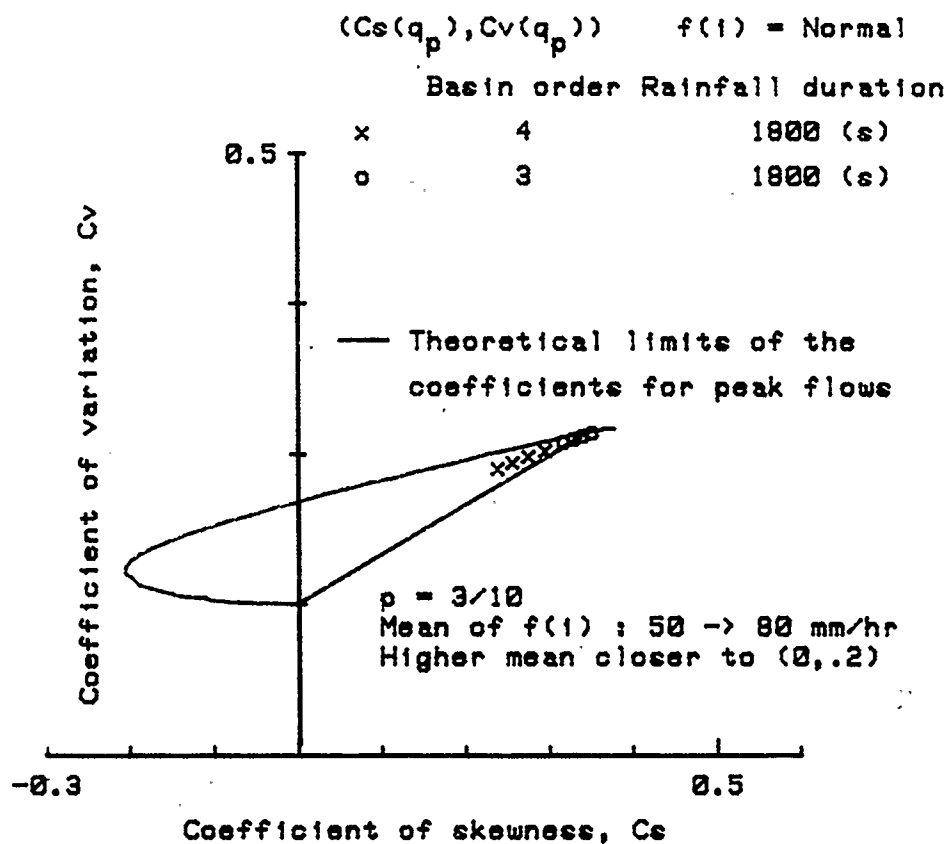


Figure 5.10: $Cs - Cv$ relationships of peak flows from networks with non-uniform distribution of runoff-contributing areas and non-uniform distribution of rainfall intensities.

inputs on the statistical parameters of peak flows from a network of streams is discussed in this section. As explained in section 3.3.2 for correlated rainfall inputs, only the extreme peak flows are considered. The analyses are performed on two networks with the first one having (u, R_L) equal to (3,2.5) and the second having (u, R_L) equal to (4,1.5). Both these networks have their characteristics listed in Tables 5.1 and 5.2 respectively. The pdf of i , $f(i)$, is the Gumbel Extreme-value distribution with a constant coefficient of skewness of 1.14. i_m varies with its duration t according to

$$i_m = \frac{a}{t^b} \quad (5.9)$$

where a and b , regionally determined constants, are equal to 338.7 and 0.7 respectively. t is in minutes and i in mm/hr. For a selected return period T of rainfall intensity and duration t , $i_{T,t}$ is calculated from

$$i_{T,t} = i_{m,t}(1 + Cv(i)K_T) \quad (5.10)$$

$Cv(i)$ is assumed to be 0.3 and K_T is the frequency factor of the Gumbel distribution for return period T . The rainfall events, $i_{T,t}$, are routed through the networks and the maximum peak flow determined for T ranging between 2 and 200. The rainfall intensity of return period T and duration t giving the maximum peak flow by I_T and the maximum peak flow is denoted by $q_{M,T}$. Both variables are plotted against t on the IDF figures.

5.4.1 Spatially and Temporally Uniform Rainfall Intensity

The rainfall intensity is spatially and temporally uniform. All streams have planes with runoff planes 200 m wide. Figure 5.11 shows the rainfall IDF curves together

with the plots of I_L and $q_{M,T}$ from the two networks described in section 5.4. They indicate that the low-frequency maximum peak flows occur for rainfall durations shorter than those for high-frequency maximum peak flows. The plots of both I_T and $q_{M,T}$ have similar shapes. The ratio C of $q_{M,T}$ to I_T , $\frac{q_{M,T}}{I_T}$, both networks is a constant for T 's between 2 and 200. C is equal to 0.70 and 0.64 for the first and second network respectively. A constant value for C is also a result obtained for single planes under correlated rainfall inputs. It was proven in section 3.3 that C is a constant for all T 's. It is reasonable to assume the same for the networks. The similarity of the results from the networks to those from single planes goes even further. The parameter $I_T^{0.4}t$, where t is the duration for which maximum peak flow occurs, is a constant for both networks. The same parameter is also a constant on single planes.

The constant of proportionality C on a single plane ranged between 0.95 and 0.89 with b in equation 3.70 between 0.52 and 0.72. It was shown in section 3.3.2 that C was dependent on b only and independent of the planes' characteristics (S_o , n , and L). When b is equal to 0.7, the constant C from the first and second networks are 0.70 and 0.64 respectively. C for the case of networks depends on b as well as the network characteristics. The lower values for C on stream networks are probably due to the combined effects of the stream characteristics and the confluences. The actual values of C for stream networks depend on accurate numerical methods of simulating flows. For the purposes of this study, an accurate value of C is not necessary. Whether it is constant or not with return periods T is more important. For the rest of this chapter, the values of C obtained will be presented, but their significance relative to network and climatic characteristics will not be discussed

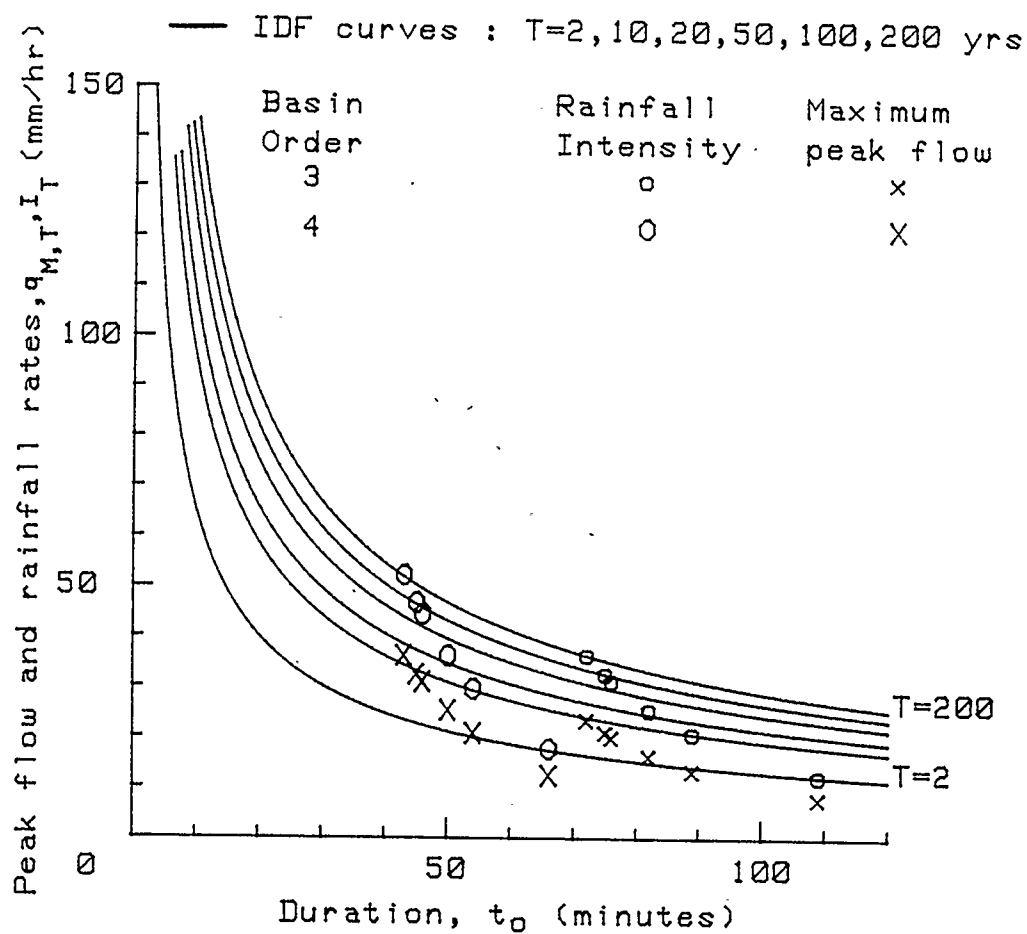


Figure 5.11: Return periods of maximum peak flows and corresponding rainfall intensities from two networks under uniform and correlated rainfall intensities.

in detail.

A constant ratio between $q_{M,T}$ and I_T combined with a constant value of $I_T^{0.4}t$ imply, by analogy with the case of single planes, that (1) the pdf of q_M and I are of the same functional form with exactly the same coefficients of variation and skewness, only the dimensional statistical parameters such as the mean, standard deviation, etc., differ, and (2) the coefficients of variation and skewness of q_M or I are functions of b , a regional climatic parameter describing the IDF curves, and $Cv(i)$ only. Note that $Cv(i)$ is the coefficient of variation of $f(i)$, the pdf of i of a constant duration. $f(i)$ is the Gumbel distribution in this case. If $f(i)$ were the Gamma distribution analytical solutions for $f(I)$, $Cv(I)$, and $Cs(I)$ are as presented in section 3.3.2. When $f(i)$ is the Gumbel distribution with $Cv(i)$ equal to 0.3 and b equal to 0.7, $Cv(I)$ and $Cs(I)$ are 0.426 and 1.626 respectively. These coordinates lie very close to the line joining the (Cs, Cv) coordinate of the rainfall intensity distribution to the upper limit of the $(Cs(q_p), Cv(q_p))$ coordinate of random peak flows from constant duration rainfall events. These and similar values for other $Cv(i)$ and b are obtained as follows. 6000 random values of i from $f(i)$ are generated. i are transformed into I using equation 3.86 reproduced below

$$I = (a \text{ constant}) \cdot i^{1/(1 - 0.4b)} \quad (5.11)$$

Statistical analyses are then performed on the corresponding random series of I . Since I and q_M are linearly related, therefore $Cv(q_M) = Cv(I)$ and $Cs(q_M) = Cs(I)$.

The results in this section indicate that as far as coefficients of variation and skewness of the maximum peak flows are concerned, they are (1) constants for a

given climatic regime, and (2) independent of the topological characteristics of the stream networks. The effects of non-uniform rainfall and network characteristics are investigated next.

5.4.2 Non-uniform Runoff Contributing Areas

Non-uniform runoff contributing areas are simulated by assigning runoff planes of different widths to each stream order. For the first network, the 1st, 2nd, 3rd, and 4th order streams have planes of widths 200, 150, 100, and 50 m respectively. For the second network, the widths of the runoff planes along the 1st, 2nd, and 3rd order streams are 200, 163.4, and 90 m respectively. Both networks have the same total area of runoff contributing areas. In the first network all other plane and stream characteristics have been kept the same as the first network with constant width runoff planes. In the second network, the widths, slopes, and roughnesses of the streams are different from those of the second network with constant width runoff planes. The same procedure as outlined in the previous section is used to determine the maximum peak runoff for return periods ranging from 2 to 200 years. The results are shown in Figure 5.12 for the first and second networks. The shapes of the $q_{M,T}$ and I_T curves are not different from those from the networks with uniformly distributed runoff contributing areas.

The ratio C is equal to 0.70 for the first network and 0.66 for the second network. The constant of proportionality for uniformly and non-uniformly distributed runoff areas in the first network is the same. C for the second network with the non-uniformly distributed areas is different from that with the uniformly distributed areas. In the second network the characteristics of the streams have been changed

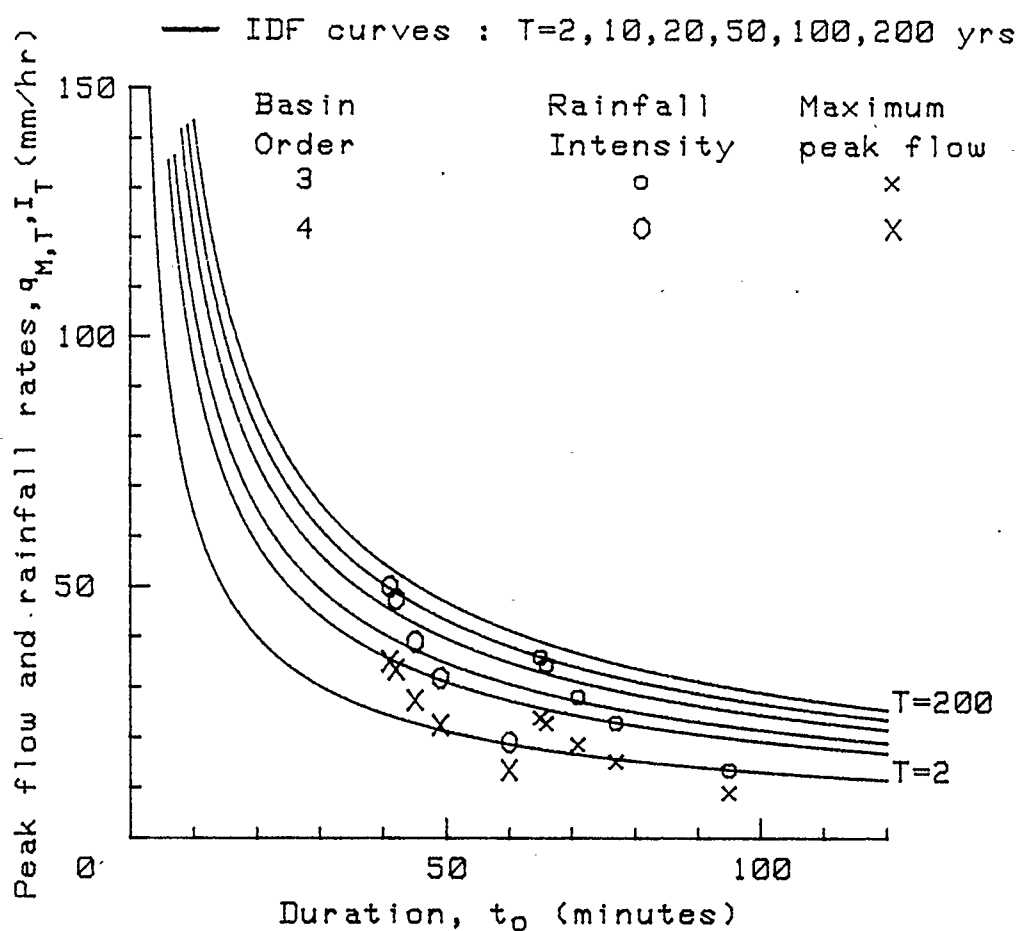


Figure 5.12: Return periods of maximum peak flows and corresponding rainfall intensities from two networks with non-uniform distribution of runoff areas and under uniform correlated rainfall intensities.

and this probably explains the difference in the C value.

For both networks, given that the ratio of maximum peak flow to rainfall intensity is a constant, it therefore implies that the coefficients of variation and skewness of the maximum peak flow pdf are constants for given b and $Cv(i)$ and independent of the network characteristics. For the given rainfall characteristics, $Cv(q_M) = 0.426$ and $Cs(q_m) = 1.626$.

5.4.3 Temporally Non-uniform Rainfall Intensity

Temporally non-uniform rainfall intensity is simulated by assuming a triangular variation of the rainfall rate with time. Two cases of temporally non-uniform rainfall intensity are considered for each of the two networks described in section 5.4.1 ; in the first case the ratio of time to peak intensity to duration of rainfall, $p = \frac{t_p}{t_o}$, is equal to $\frac{3}{10}$ and in the second case p is equal to $\frac{7}{10}$. The widths of the runoff planes for all streams are set to a constant value of 200 m. The equivalent uniform intensity is assumed to have a Gumbel pdf with $Cv(i) = 0.30$ as before.

The results are shown in Figures 5.13 and 5.14. The ratios $\frac{q_{M,T}}{I_T}$ for the two networks are as follows : for $p = \frac{3}{10}$ and $p = \frac{7}{10}$ the ratios are 1.07 and 1.08 respectively for the first network and 1.12 and 0.98 respectively for the second network. Since the C values are constant even for temporally non-uniform rainfall, therefore the coefficients of variation and skewness of the maximum peak flows are independent of the networks' characteristics and are equal to 0.426, 1.626 for the particular $f(i)$ and b -value under consideration.

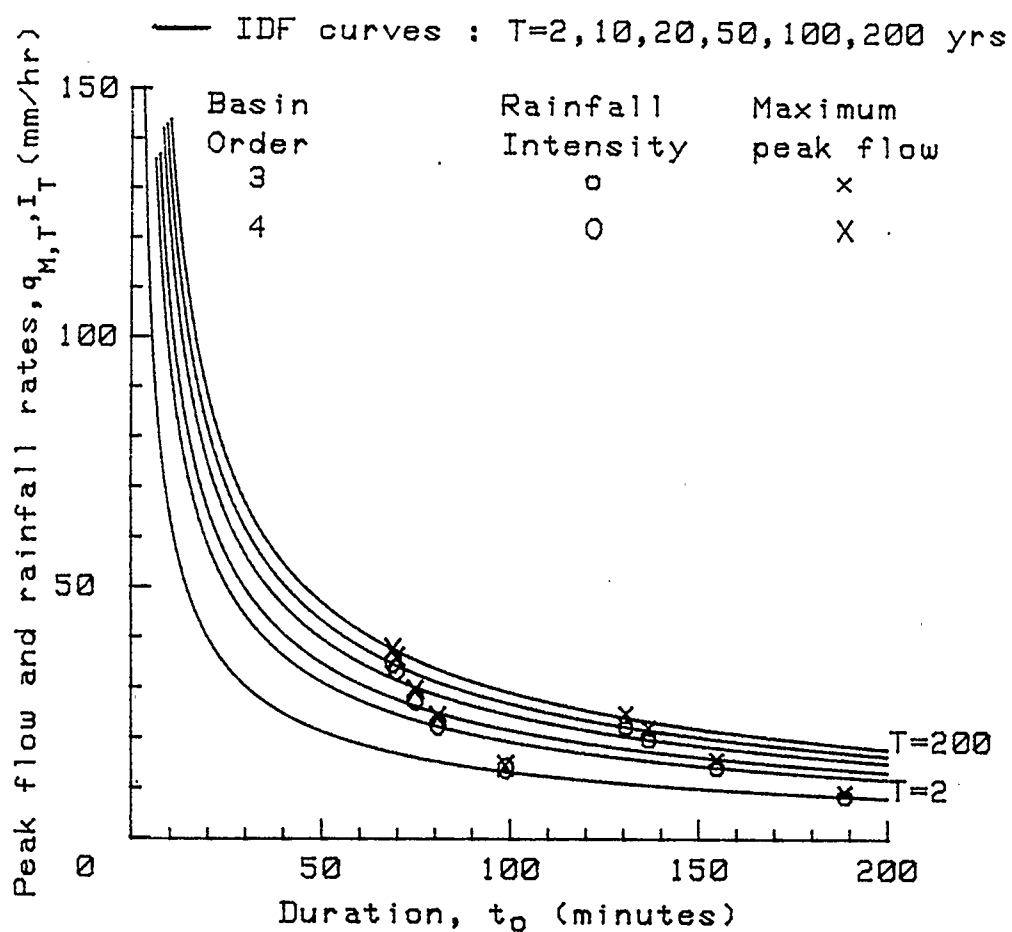


Figure 5.13: Return periods of maximum peak flows and corresponding rainfall intensities from two networks under temporally non-uniform and correlated rainfall intensities with $p = 3/10$.

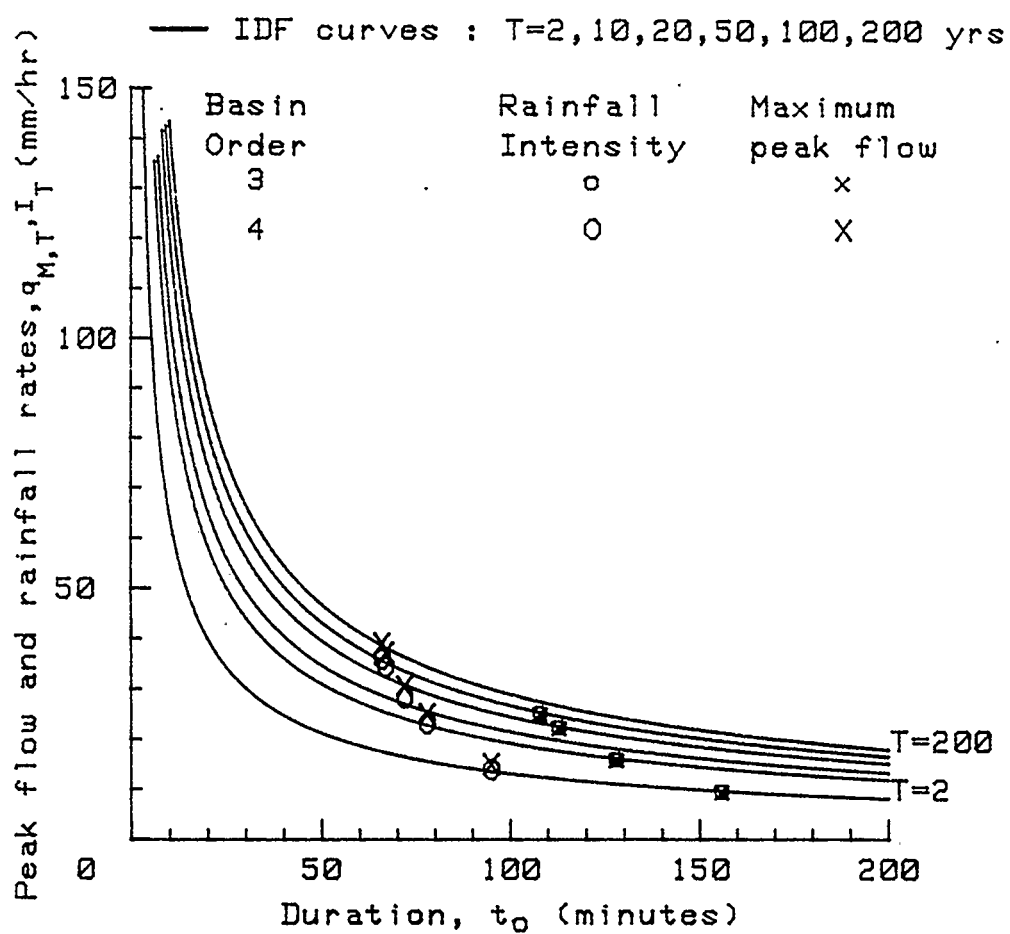


Figure 5.14: Return periods of maximum peak flows and corresponding rainfall intensities from two networks under temporally non-uniform and correlated rainfall intensities with $p = 7/10$.

5.4.4 Spatially Non-uniform Rainfall Intensity

All the streams have 200 m wide runoff planes. The rainfall intensity is uniformly distributed over its duration. Spatially non-uniform rainfall is simulated by assigning different fractions of equivalent spatially uniform rainfall intensities over the different stream orders such that the average depth of rain is equivalent to the spatially uniform depth of section 5.4.1. The first network had fractions 0.9, 1.5, 0.8, and 0.64 assigned to its 1st, 2nd, 3rd, and 4th order streams respectively. The second network had fractions 0.9, 1.5, and 0.65 over its 1st, 2nd, and 3rd order streams. The resulting plots of $q_{M,T}$ and I_T for the two networks are shown in Figure 5.15.

The C values are still constant for all return periods, 0.72 for the first network and 0.69 for the second network. This implies that for both networks $Cv(q_M) = 0.426$ and $Cs(q_M) = 1.626$, as before.

5.4.5 Combined Effect of Spatially and Temporally Non-uniform Rainfall Intensity

The distribution of the runoff planes' widths is as in section 5.4.2, the rainfall intensity is temporally distributed with $p = 0.3$, and is spatially distributed as in section 5.4.4. The resulting plots of $q_{M,T}$ and I_T for the two networks are shown in Figure 5.16. Even for these non-homogeneous conditions, the C values are constant for all return periods, 1.05 for the first network and 1.03 for the second network. This implies that for both networks, the coefficients of variation and skewness of the maximum peak flows have stayed the same as before. The emerging conclusion is that $Cv(q_M)$ and $Cs(q_M)$ are dependent only on b and

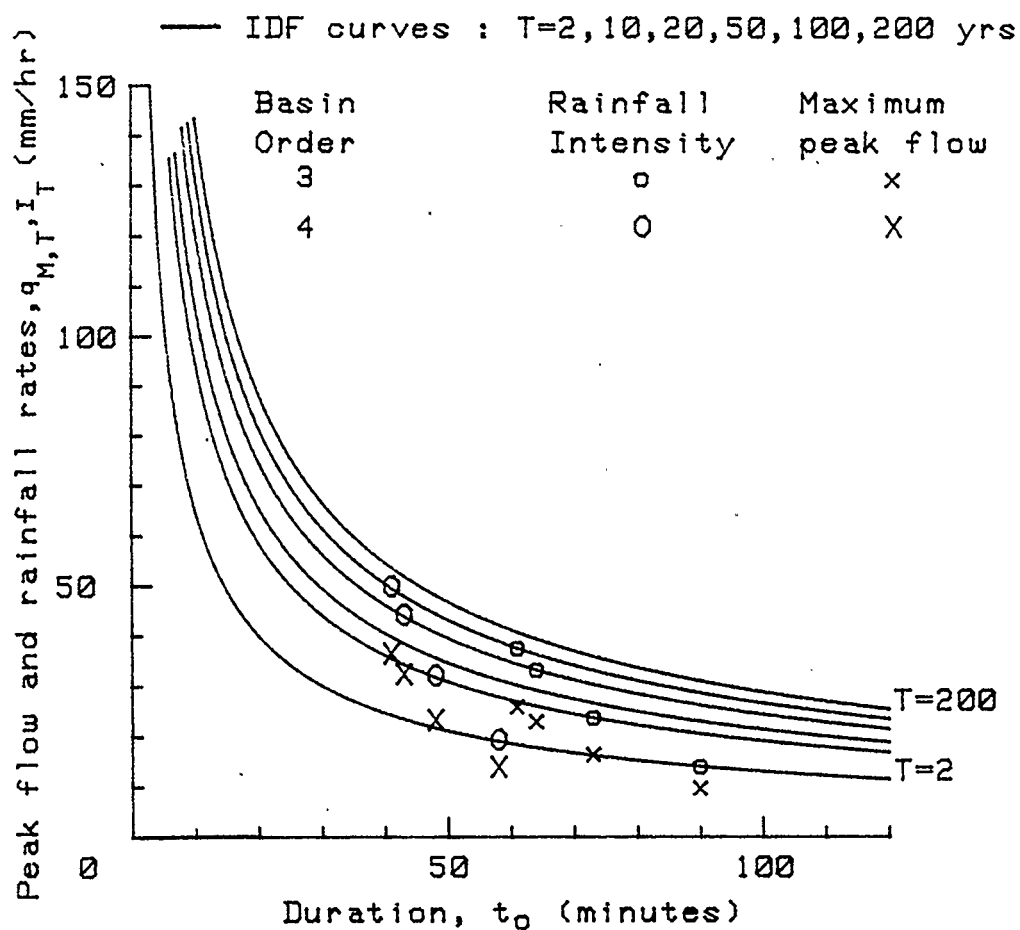


Figure 5.15: Return periods of maximum peak flows and corresponding rainfall intensities from two networks under spatially non-uniform and correlated rainfall intensities.

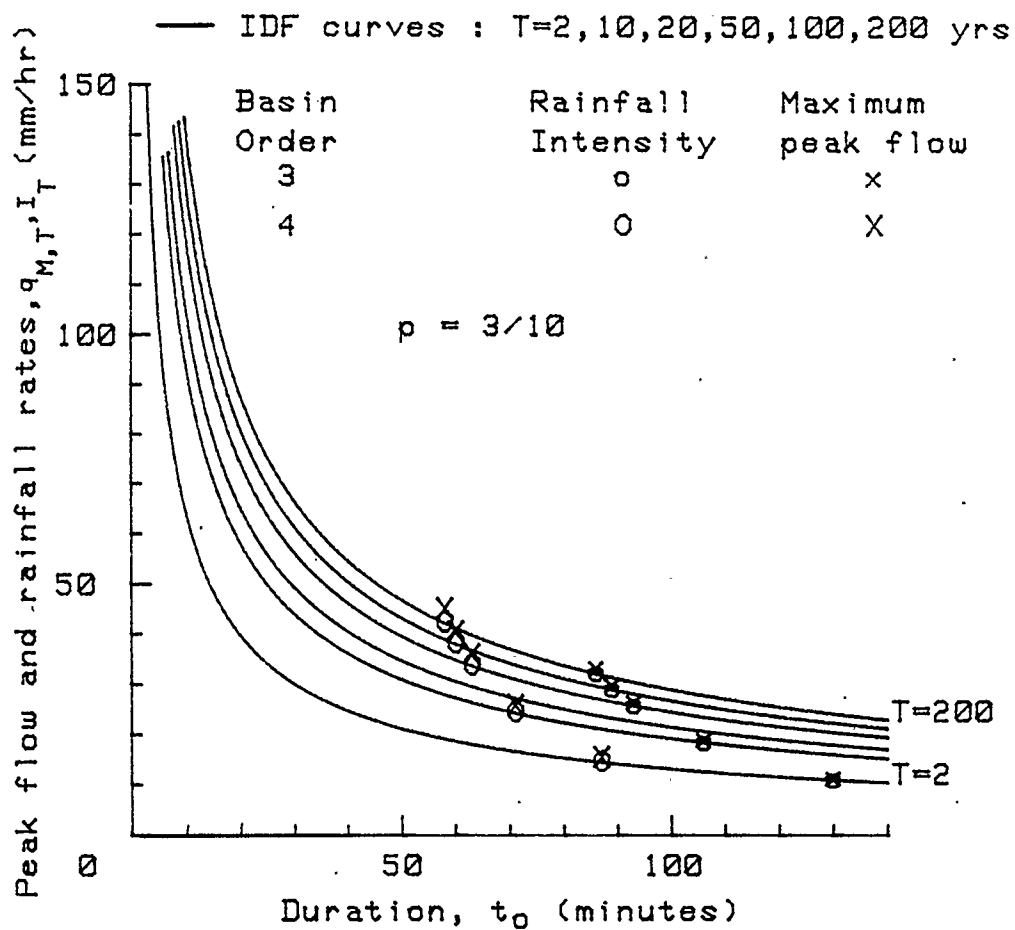


Figure 5.16: Return periods of maximum peak flows and corresponding rainfall intensities from two networks under spatially and temporally non-uniform and correlated rainfall intensities.

$Cv(i)$ for correlated rainfall events on stream networks with no infiltration.

5.4.6 Uniform Rainfall Intensity and Constant Infiltration Rate

The networks under study are still the same two as in the previous sections. The rainfall intensity is spatially and temporally uniform. All streams have runoff planes 200 m wide. A constant infiltration rate of f mm/hr is superimposed on the rainfall hyetograph. Three cases of f : 0, 5, and 20 mm/hr, are considered. The case $f = 0$ is the same as that of section 5.4.1. The plots of q_M and I_T are shown in Figures 5.17 and 5.18 for the two networks respectively. When $f = 0$, the curves for maximum peak flows and corresponding rainfall intensities have similar shapes and the low-frequency maximum peak flows are associated with shorter duration rainfall events than are the high-frequency flows. For $f > 0$, as expected $q_{M,T}$ have decreased and the corresponding I_T have increased. The durations of the rainfall events have consequently decreased. When $f = 5$ mm/hr, the durations of the rainfall events causing the high frequency maximum peak flows have decreased proportionately more than those for the low frequency flows. This is especially evident in the case of the second network. When $f = 20$ mm/hr, there is a complete reversal in the direction of the plots of $q_{M,T}$ and I_T compared to the $f = 0$ case. The low frequency maximum peak flows are now generated from rainfall events with longer durations than are the high frequency flows. The ratios C of $q_{M,T}$ to I_T are no longer constants for $f > 0$. In the case of the first network, C ranges between 0.34 for $T = 2$ and 0.56 for $T = 200$ when $f = 5$ mm/hr. When $f = 20$ mm/hr, C then ranges between 0.05 and 0.26. The ratios are still variable when effective rainfall intensity ($I_T - f$) is considered. All these results are similar

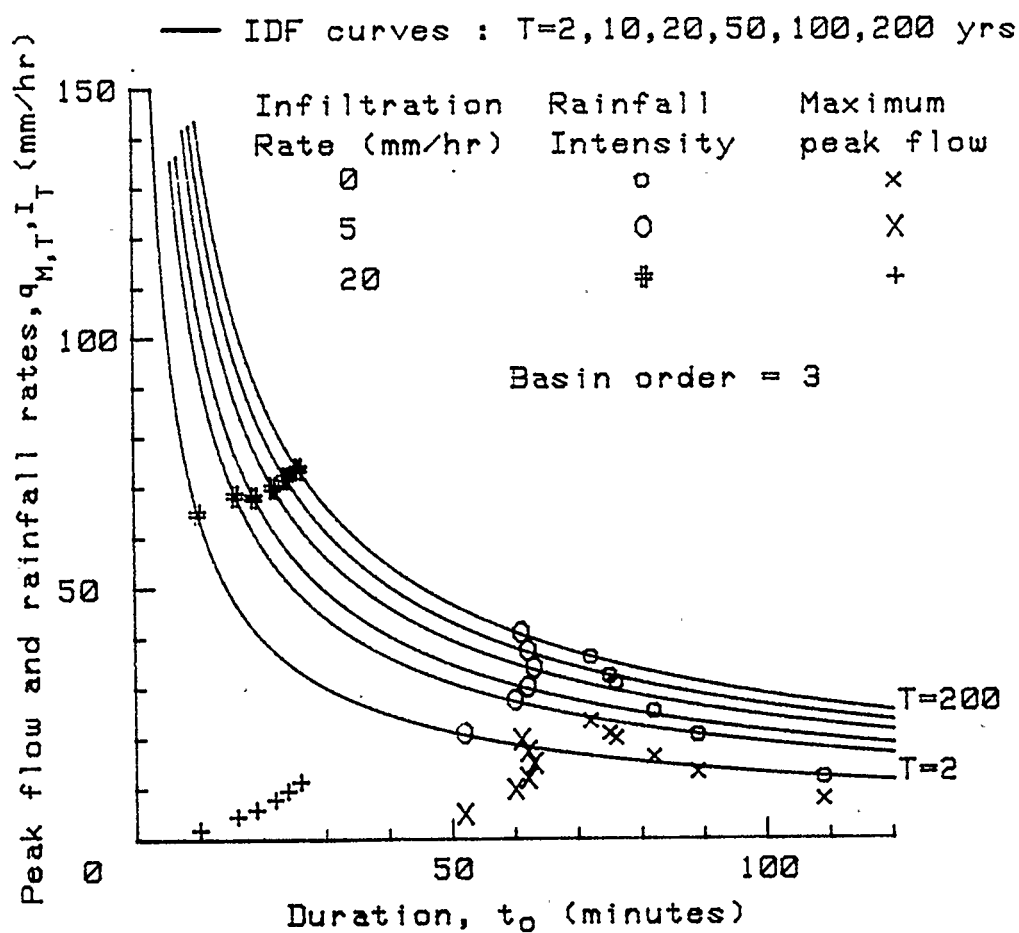


Figure 5.17: Return periods of maximum peak flows and corresponding rainfall intensities from network (1) under uniform and correlated rainfall intensities and constant infiltration rate.

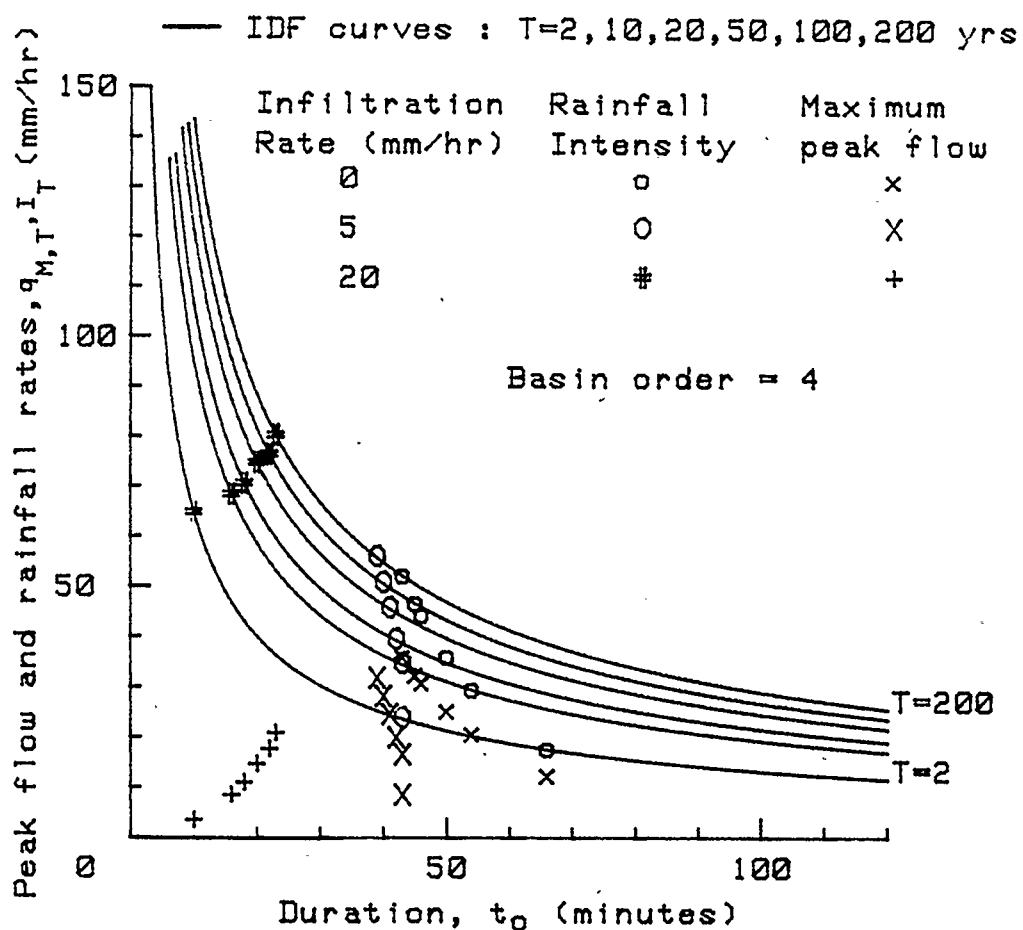


Figure 5.18: Return periods of maximum peak flows and corresponding rainfall intensities from network (2) under uniform and correlated rainfall intensities and constant infiltration rate.

to those obtained for pervious single planes under similar input conditions.

Infiltration rates are rarely uniformly distributed over time and space and also rarely constant for all rainfall events. As was discussed in section 3.3, the effect of constant/random, uniform/non-uniform infiltration is to increase $Cv(q_p)$ $Cs(q_p)$ and to decrease q_p for all return periods. Infiltration decreases the effective rainfall intensity and as a result Cv of the effective rainfall intensity increases and the effect on the statistical parameters of the peak flows follows. For design purposes, where only the extreme events are of importance, the no infiltration case is the most critical. If the runoff generating process is as assumed in this dissertation, i.e., the immediate runoff occurs only on a narrow strip of land close to the streams, then it is not inconceivable that these runoff contributing areas would be close to a state of permanent near-saturation. The widths of these saturated zones do not significantly affect the statistical parameters of the maximum peak flows, as discussed in section 5.4.4. So, although infiltration is an important variable in the rainfall-runoff process, it may have to be neglected for design purposes, in which case, the results of the sections for no infiltration are those to be used for estimating low frequency flows.

5.4.7 Non-uniform Rainfall and Runoff Area Parameters and Constant Infiltration Rate

In this section the analysis performed in section 5.4.4 is repeated for infiltration rates f of 0, 5, and 20 mm/hr. The rainfall intensity is spatially and temporally variable and the widths of the runoff contributing areas are different for each stream order. The results are shown in Figures 5.19 and 5.20 for the first and second

network respectively. The patterns of the $q_{M,T}$ and I_T plots are similar to those obtained for the two networks under uniform conditions. The ratios C are variable. For $f = 20$ mm/hr, the low frequency maximum peak flows are generated from rainfall events of longer durations than those for high frequency extreme flows. The behaviour is exactly the opposite observed for the no infiltration case.

5.5 Discussion of Results From Single Planes, Single Streams, and Networks of Streams

The objective of this study has been to determine the role that the mechanics of the hydrological process has in influencing the statistical parameters of the probability distribution of peak flows from conceptual watersheds. These watersheds ranged from single runoff planes and stream-planes combinations to networks of streams. The physiographic characteristics of the watersheds were assumed to be invariant over time, but, could be non-uniform spatially. The physical structure of the rainfall inputs ranged from spatially and temporally uniform distribution of rainfall intensities with constant duration to non-uniform rainfall intensities correlated with rainfall durations. The probability distributions of the rainfall inputs were assumed to be known. The Monte Carlo simulation technique was used to generate random rainfall intensity values. The flow was routed through the watersheds by using a finite difference scheme to solve for the equations of continuity and momentum. The resulting random series of peak flows were then analysed for their statistical characteristics.

The results indicate that the statistical characteristics of random peak flows

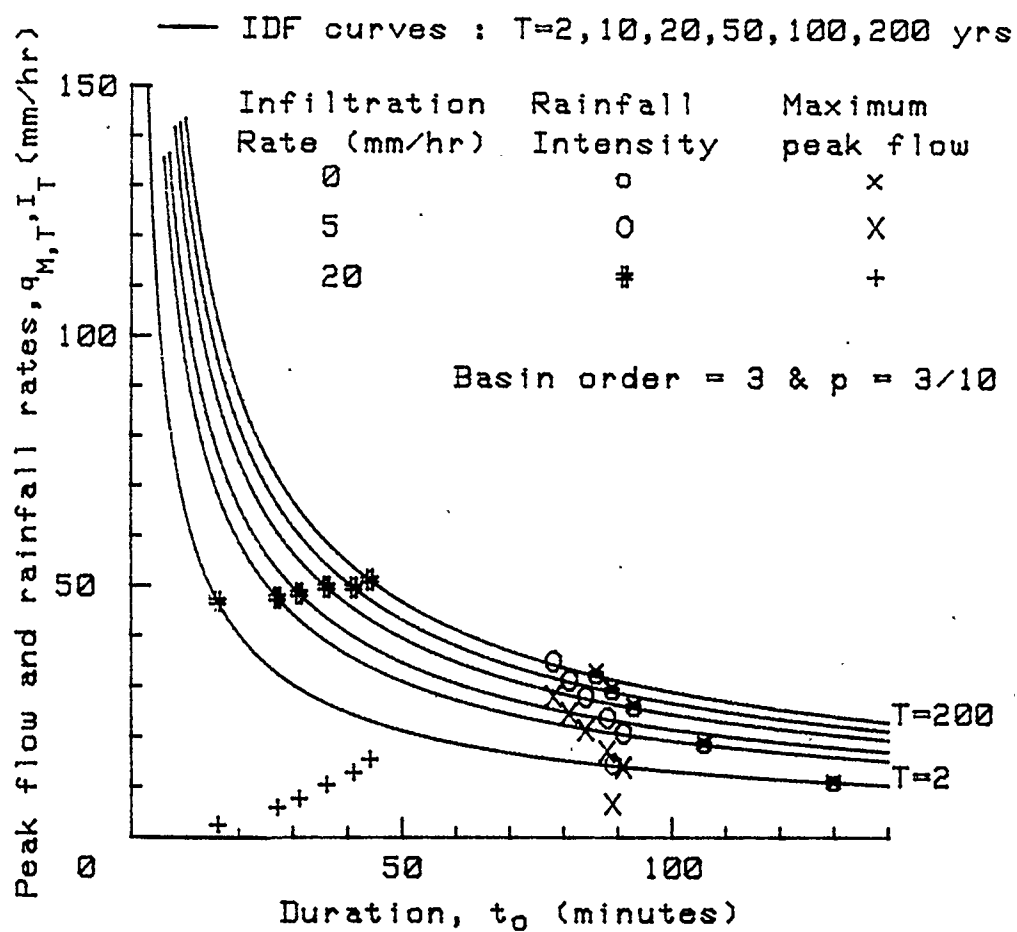


Figure 5.19: Return periods of maximum peak flows and corresponding rainfall intensities from network (1) under non-uniform distribution of runoff areas and non-uniform distribution of correlated rainfall intensities.

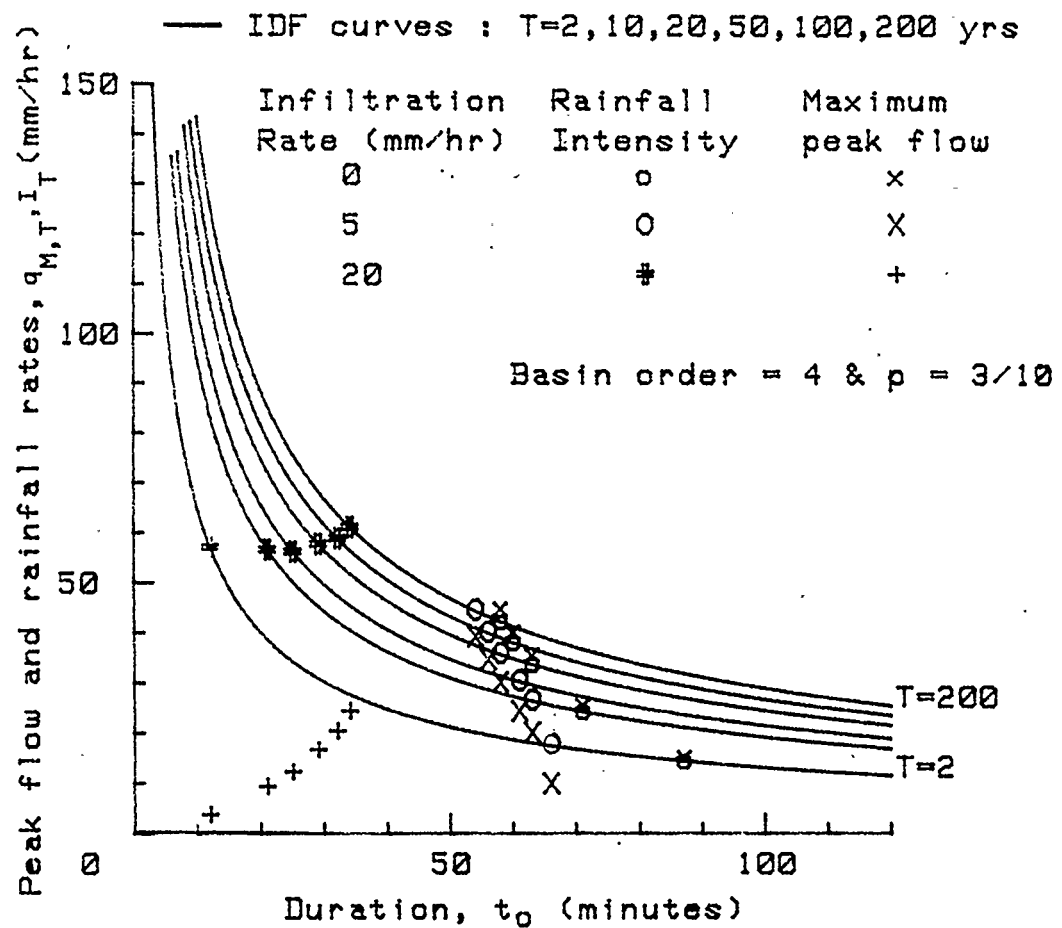


Figure 5.20: Return periods of maximum peak flows and corresponding rainfall intensities from network (2) under non-uniform distribution of runoff areas and non-uniform distribution of correlated rainfall intensities.

from the watersheds follow a consistent pattern determined by the equations of continuity and momentum. The response from the single planes are more sensitive to the specification of the rainfall and watershed characteristics than stream networks are if constant duration rainfall events are being considered. The statistical parameters of the peak flows from the planes only become insensitive to the rainfall and plane characteristics when certain conditions are met. These are planes of long runoff lengths, shallow slopes, and high Manning's roughness and rainfall of low mean intensities and short durations. In fact, for these combinations of factors, the coefficients of variation and skewness of the peak flows are at or close to their maximums for given pdf of rainfall intensity. And a given coefficient of variation of rainfall intensity yields a fixed (constant) maximum coordinate of coefficients of variation and skewness. The parameters are constants at their maximum values because under these conditions the relationship between peak flow and rainfall intensity is of a power function type and it has been proven that such equations produce constant coefficients of variation and skewness dependent only on the exponent of the power function and independent of the multiplying factor. The latter determines the mean of the peak flow pdf. The maximums occur for an exponent equal to $5/3$. The Kinematic Wave equations characterize this type of rainfall intensity-peak flow relationship and have been found by several investigators (Overton, 1970 and Wooding, 1966) to approximate actual watershed responses. In this thesis it has been proven that the Diffusion Wave equations degenerate into an equation very close to that obtained from a solution of the Kinematic Wave equations under conditions of low rainfall intensities with long durations over long runoff planes with shallow slopes and rough surfaces.

The insensitivity of the coefficients of variation and skewness to rainfall (except for the pdf type and its coefficient of variation) and watershed characteristics under conditions that generate slow responses carries through to stream-plane combinations and stream networks. In fact, for these configurations the insensitivity occurs for larger ranges of the input variables. This is so because the attenuating effects are more dominant than on a single plane. The coefficients of variation and skewness seem to coalesce close to the corresponding maximum value from a plane. The positions of the coordinates are not very sensitive to non-uniform rainfall and watershed characteristics.

The above results have been obtained only for conceptual watersheds. It is hypothesized that the same results can be extended to natural watersheds according to the following argument. Natural watersheds can be expected to attenuate flows to a greater extent than their corresponding conceptual representations. The latter can only be specified by average values for the stream and runoff plane characteristics. Since attenuation of flows directs the coefficients of variation and skewness towards their maximums, the natural watershed can only accelerate that pattern. And the maximum has been shown to correspond to that obtained from assuming that the flow is kinematic. Flows from natural watersheds have been found to be closely approximated by solutions of the Kinematic Wave equations. Both the pattern exhibited by the behaviour of the statistical parameters and the empirical evidence of the type of flow prevailing in natural watersheds lead one to expect the coefficients of variation and skewness of peak flow from natural watersheds to be close to the theoretical maximums.

If the rainfall inputs are correlated, then, the statistical characteristics (coef-

ficients of variation and skewness) of the random peak flows are independent of the physiographic characteristics of the watersheds and depend only on the pdf of the rainfall intensity for a particular duration and a parameter that relates the mean uniform rainfall intensities to their corresponding durations on the IDF curves. The foregoing statement is true only if effective rainfall intensity is being considered and it lends support to the practice of using regional skew coefficients for determining peak flows of various return periods. If the characteristics of the rainfall regime (intensity and duration) within a region can be specified by a set of IDF curves, then the coefficients of variation and skewness within that region are constants for all watersheds from single planes to stream networks. It is assumed that for any watershed being considered the rainfall pattern stays the same for each storm event. The effect of infiltration on this conclusion is very complex and needs further investigation. For relatively low infiltration rates the conclusion may still be approximately true if the analysis is performed with effective rainfall intensity. However, for relatively high infiltration rates, the effect of the latter on the coefficients of variation and skewness of the maximum peak flows has not been determined.

The study has dealt with two possible relationships between rainfall intensity and rainfall duration, either the duration is constant for all events or there is an inverse power function type of relationship between rainfall intensity and duration as given by equation 5.9. These two cases produce exactly the same coefficients of variation and skewness under only two situations. These are (1) for constant duration rainfall events, the peak flows are from watersheds with relatively high attenuating effects on the flow and the latter can be approximately characterised

by the Kinematic Wave equations; for correlated rainfall inputs, the exponent b in equation 5.9 is equal to 1, i.e., $i = \frac{a}{t}$ and (2) for constant duration rainfall events the peak flows are the steady state flows; for correlated rainfall inputs, the exponent b in equation 5.9 is equal to 0, i.e., rainfall intensity is independent of duration and the maximum peak flow is equal to the steady state flow. The discrepancy between the results from the two types of rainfall events increases as b decreases from 1, is greatest when $b \approx 0.4$, and is nil when b is equal to 1 or 0. The parameter b usually lies between 0.6 and 0.8 for natural rainfall events. Within this range the coordinates of coefficients of variation and skewness of the peak flows are close to those from constant duration events from slow response watersheds. This may suggest that for relatively large watersheds it may not be necessary to make a distinction between constant duration storms events and correlated rainfall inputs. The coefficients of variation and skewness for the random peak flows from such a watershed can be estimated from the rainfall data if there is not sufficient data on the annual peak flows.

Chapter 6

CONCLUSIONS AND RECOMMENDATIONS

6.1 Scope of Study

The objective of the study is to determine the intrinsic nature of the statistical characteristics of random peak flows generated from conceptual watersheds by using a composite deterministic-statistical approach. Assumptions are first made on the stochastic nature of the input variables, rainfall and infiltration. The Monte Carlo simulation technique is used to generate random series of each variable from its respective probability distribution function. The corresponding random series of peak flows from a watershed of given characteristics are then obtained by numerically solving the Diffusion Wave equations of continuity and momentum for each set of input random variables. The numerical scheme used is of the explicit finite difference type. The statistical characteristics of the random series of peak flows are obtained using standard techniques. The influence of rainfall, infiltration, and watershed characteristics is studied through their effects on the relationship between the coefficient of variation and coefficient of skewness of the random peak flow series.

The conceptual watersheds vary in complexity from a single impervious runoff plane under uniform rainfall intensities of constant durations to a network of streams and pervious planes under non-uniform rainfall intensities which are correlated with their durations. The runoff planes are rectangular and of constant

slope and roughness. Streams of a given order have rectangular cross-sections and are prismatic. The two runoff planes on each side of a stream can have variable characteristics along the length of the stream. The network of streams is characterised by the basin order, bifurcation ratio, stream length ratio, and longest continuous stream length. Rainfall intensities are either spatially and temporally uniform or have different mean values over different areas in a network and/or can be temporally non-uniform. In the latter case, the rainfall hyetograph is assumed to be triangular in shape with the peak intensity occurring at specified times along the duration axis. The rainfall durations can be constant for a given random series of rainfall intensities or are correlated with the rainfall intensities. In the latter case the correlation between rainfall intensity and duration is expressed through synthetic Intensity-Duration-Frequency curves. When rainfall intensity and duration are correlated the (maximum) peak flow is the maximum of all peak flows for a given return period of rainfall intensity. Infiltration rate is either uniform over time or decreases exponentially according to Horton's equation. In either case the rate is not necessarily the same over the entire watershed. The conclusions of this study pertain to the effects of these conditions on the relationship between the statistical parameters of the random peak flows.

6.2 Conclusions

The most important result of the study is that for a given probability distribution function of rainfall intensity with known coefficient of variation $Cv(i)$ and coefficient of skewness $Cs(i)$, the coefficients of variation $Cv(q_p)$ and skewness $Cs(q_p)$ of

the random peak flow series lie within a fixed and mathematically definable region on a plot of Cv against Cs . This conclusion holds for all the rainfall and conceptual watersheds' characteristics simulated, including the case when rainfall intensity and duration are correlated. In the latter case, the coefficients of variation and skewness of the maximum peak flows become independent of all watershed characteristics and depend only on a parameter characterising the Intensity-Duration-Frequency curves. When infiltration is included, then the pdf and coefficients of effective rainfall intensities must be used, instead of those of total rainfall intensity. The above result still holds for constant duration rainfalls, but not for correlated rainfall events.

The region within which the coordinates $(Cs(q_p), Cv(q_p))$ lie is enclosed by a curve and a line having $(Cs(i), Cv(i))$ and a maximum $(Cs(q_p), Cv(q_p))$ as common points. The maximum $(Cs(q_p), Cv(q_p))$ is determined by the coefficients of skewness and variation respectively of a transformed pdf of peak flow assuming a relationship of the form

$$q_p = ai^{5/3} \quad (6.1)$$

exists between peak flow q_p and rainfall intensity i . The factor a can take any constant value. The $(Cs(q_p), Cv(q_p))$ obtained from simulating random uniform rainfall intensities of constant durations on a single impervious plane define the path of the curve. A general analytical equation of the curve has not been found. The relationship between q_p and i defining this curve is given by

$$q_p = i(1 - \exp[-(\frac{k}{1.6 - k})^{1.3}]) \quad (6.2)$$

where k is

$$k = i^{0.4} t_o \left(\frac{\sqrt{S_o}}{nL} \right)^{0.6} \quad (6.3)$$

In equation 6.3, t_o is the duration of the rainfall, S_o is the slope of the runoff plane, and n and L are its roughness and length respectively. Equation 6.2 is a semi-empirical solution to the Diffusion Wave equations. The equation of the line joining the maximum coefficients of variation and skewness of the random peak flow series to the corresponding coordinate of the rainfall intensity is defined by assuming that a power function of the form given by equation 6.1, but with the exponent on i taking values between 1 and $5/3$, holds between q_p and i .

The effects of watershed and rainfall characteristics on the position of $(Cs(q_p), Cv(q_p))$ within that region are as follows. Runoff planes with high slopes, low roughnesses, and short runoff lengths under rainfall of relatively longer durations cause the coefficients of variation and skewness of random peak flows to move towards $(Cs(i), Cv(i))$. Conversely, conditions which promote slow runoff response (shallow slopes, long runoff lengths, etc.) generate $(Cs(q_p), Cv(q_p))$ closer to the maximum coordinate. Compared to temporally uniform rainfall intensity, triangular temporal distributions of rainfall intensities tend to shift the coordinates towards the maximum. For low mean rainfall intensities, the time at which the peak intensity occurs becomes insignificant. When rainfall intensity and duration are correlated and a relationship of the form

$$i_T = \frac{a}{t_o^b} \quad (6.4)$$

holds between rainfall intensities of a specified return period T and their respective durations, then the coefficients of variation and skewness of the maximum peak

flows lie on the line joining $(Cs(i), Cv(i))$ to the maximum $(Cs(q_p), Cv(q_p))$. This line is characteristic of power functions between i and q_p , and for the case of correlated rainfall events the exponent on i in equation 6.1 is $1/(1 - 0.4b)$. The coefficients of variation and skewness depend only on b and are independent of the characteristics of the plane.

The effects of the characteristics of a network of streams can be summarised by stating that conditions promoting greater attenuation of flow produce coefficients of variation and skewness closer to the maximum. These conditions are relatively smaller stream length ratio, smaller basin order, and longer distance between the most upstream point of the watershed and its outlet. For a network of streams, the characteristics of the watershed tend to be of relatively lower significance than the duration of the rainfall, especially when the coefficients of variation and skewness are already close to the maximum. Since rainfall durations are important parameters in the study of peak flows from a network of streams, it is therefore necessary to incorporate the correlation between rainfall duration and intensity in the analysis. When this is done, the result is identical to that obtained for a plane, i.e., the coefficients of variation and skewness of the maximum peak flows are constants for a given set of IDF curves and are independent of all watershed characteristics. This result is still valid for temporally and spatially non-uniform rainfall intensity.

The last two conclusions are significant as far as their application to "real" watersheds are concerned. The study has dealt solely with conceptual watersheds. Its results, however, indicate that the complexity of the individual components of the rainfall-runoff process may not carry through to the positions of the the coefficients of variation and skewness of the maximum peak flows on the $Cs - Cv$

plane for watersheds which have relatively high flow attenuating potential. "Real" watersheds may be expected to have features which promote attenuation of flow. Hence, even for constant duration rainfall events, where the characteristics of the watershed play some part in determining the coefficients of variation and skewness of the random peak flows, the latter may be so close to the maximum that they may be considered independent of the watershed characteristics.

As noted above, the effect of infiltration in the case of constant duration rainfall events can be taken account of by simply dealing with the pdf of effective rainfall intensity. When rainfall duration and intensity are correlated, however, the effect of infiltration on the statistical characteristics of maximum peak flows is not as quantifiable as is the case with impervious watersheds. The only significant result obtained is that while for impervious watersheds the peak flows with smaller probabilities of being exceeded are generated by rainfall events of shorter durations, for pervious watersheds, the peak flows with smaller probabilities of being exceeded are generated by rainfall events with the longer durations. In some cases, the intensities of rainfall generating all the maximum peak flows are close to a constant value, only the durations vary.

6.3 Recommendations

The following areas needing further research are suggested. They are based on the discussion of the results of this study.

A definition of the "size" of a watershed in terms of its physical characteristics and the prevailing rainfall characteristics is needed. One conclusion of this study is

that the coefficients of variation and skewness of random peak flows are expected to be at their maximums for watersheds which significantly attenuate the runoff. These watersheds include those with relatively large drainage areas and also the smaller ones under short duration, low intensity rainstorms. The definition may be similar to that derived for a plane. In the latter case, a parameter k_m less than 0.5 (equation 3.41), which includes the plane and rainfall characteristics, defines the conditions that will produce the theoretical maximum coefficients of variation and skewness for uniform rainfall intensities of constant durations. The investigation would follow the same lines as the present one but concentrate more on the mean value of the random peak flows than on the higher moments. This means that a relatively lesser number of random events may be simulated, thus considerably reducing the computational times. However, it also means that the numerical method for solving the equations of flow must be rigourously tested to provide accurate values of peak flows.

The effect of infiltration on the statistical parameters of random peak flows when rainfall intensities and durations are correlated needs further investigation.

Bibliography

- [1] Amorocho, J. and Wu, B., (1977), "Mathematical Models for the Simulation of Cyclonic Storms Sequences and Precipitation Fields", *Journal of Hydrology*, Vol. 32, pp. 329-345.
- [2] Betson, R. P., (1964), "What is Watershed Runoff?", *Journal of Geophysical Research*, April 1964, Vol. 69, No. 8, pp. 1541-1552.
- [3] Chow, V. T., (1964), *Handbook of Applied Hydrology*, McGraw-Hill, New York, U.S.A.
- [4] Cordova, J. R. and Bras, R. L., (1981), "Physically Based Probabilistic Models of Infiltration, Soil Moisture, and Actual Evapotranspiration", *Water Resources Research*, February 1981, Vol. 17, No. 1, pp. 93-106.
- [5] Cordova, J. R. and Rodriguez-Iturbe, I., (1983), "Geomorphoclimatic Estimation of Extreme Flow Probabilities", *Journal of Hydrology*, Vol. 65, pp. 159-173.
- [6] Diaz-Grandos, M. A., Valdes, J. B., and Bras, R. L., (1984), "A Physically Based Flood Frequency Distribution", *Water Resources Research*, July 1984, Vol. 20, No. 7, pp. 995-1002.
- [7] Eagleson, P. S., (1970), *Dynamic Hydrology*, McGraw-Hill, New York, U.S.A.
- [8] Eagleson, P. S., (1971), "The Stochastic Kinematic Wave", *Proceedings of the First Bilateral U.S.-Japan Seminar in Hydrology*, University of Hawaii, East-West Centre, Honolulu, Hawaii, U.S.A.
- [9] Eagleson, P. S., (1972), "Dynamics of Flood Frequency", *Water Resources Research*, Vol. 8, No. 4, pp. 878-897.
- [10] Eagleson, P. S., (1982), *Water Balance Dynamics - Climate, Soil, and Vegetation*, MIT Press, Cambridge, Massachusetts, U.S.A.
- [11] Environment Canada One-Dimensional Hydrodynamic Model Computer Manual, (1982), Water Planning and Management Branch, Inland Waters Directorate, Environment Canada, July 1982.
- [12] Frind, E. O., (1969), "Rainfall-Runoff Relationships Expressed by Distribution Parameters", *Journal of Hydrology*, Vol. 9, pp. 405-426.

- [13] Gupta, V. K. and Waymire, E., (1983), "On the Formulation of an Analytical Approach to Hydrologic Response and Similarity at the Basin Scale", *Journal of Hydrology*, Vol. 65, pp. 95-123.
- [14] Gupta, V. K., Waymire, E., and Wong, C. T., (1980), "A Representation of an Instantaneous Unit Hydrograph from Geomorphology", *Water Resources Research*, October 1980, Vol. 16, No. 5, pp. 855-862.
- [15] Henderson, F. M., (1963), "Flood Waves in Prismatic Channels", *Journal of the Hydraulics Division, Proceedings of the American Society of Civil Engineers*, July 1963, Vol. 69, No. HY4, pp. 39-67.
- [16] Henderson, F. M., (1966), *Open Channel Flow*, Macmillan Publishing Co., Inc., New York, U.S.A.
- [17] Horton, R. E., (1932), "Drainage Basin Characteristics", *American Geophysical Union Transaction* 13, 1932, pp. 350-361.
- [18] *Hydrological Atlas of Canada*, (1978), Supply and Services, Canada.
- [19] Kalinin, G. P., (1971), *Global Hydrology*, Israel Program for Scientific Translation, Jerusalem, Israel.
- [20] Kirshen, D. M. and Bras, R. L., (1983), "The Linear Channel and its Effect on the Geomorphologic IUH", *Journal of Hydrology*, Vol. 65, pp. 175-208.
- [21] Klemes, V., (1978), "Physically Based Stochastic Hydrologic Analysis", *Advances in Hydrosience*, Vol. 11, Academic Press, New York, U.S.A.
- [22] Langbein, W. B., (1947), "Topographic Characteristics of Drainage Basins", *U.S. Geol. Survey Water-Supply Paper* 968-C, pp. 99-114.
- [23] Lebedev, V. L., (1958), *Random Processes in Electrical and Mechanical Systems*, The State Publishing House of Physical and Mathematical Literature, Moscow, U.S.S.R.
- [24] Lighthill, M. J. and Whitlam, G. B., (1955), "On the Kinematic Waves : Flood Movement in Long Rivers", *Proceedings of the Royal Society, London*, Vol. 229, pp. 281-316.
- [25] Lloyd, E. H., O'Donnell, T., and Wilkinson, J. C., (1979), *The Mathematics of Hydrology and Water Resources*, Academic Press, London, England.
- [26] Muzik, I., (1974), "State Variable Model of Overland Flow", *Journal of Hydrology*, Vol. 22, pp. 347-364.

- [27] Muzik, I., (1976), "Determination of Design Hydrographs on Small Catchments by the State Variable Model", Canadian Journal of Civil Engineering, Vol. 3, No. 2, pp. 239-247.
- [28] Overton, D. E., (1970), "Route or Convolute ?", Water Resources Research, February 1970, Vol. 6, No. 1, pp. 43-52.
- [29] Pilgrim, D. H., (1977), "Isochrones of Travel Time and Distribution of Flood Storage from a Tracer Study on a Small Watershed", Water Resources Research, Vol. 13, No. 3, pp. 587-595.
- [30] Raudkivi, A. J., (1979), Hydrology, An Advanced Introduction to Hydrological Processes and Modelling, Pergamon Press, Oxford, England.
- [31] Rodriguez-Iturbe, I., Devoto, G., and Valdes, J. B., (1979), "Discharge Response Analysis and Hydrologic Similarity : The Interrelation Between the Geomorphologic IUH and the Storm Characteristics", Water Resources Research, December 1979, Vol. 15, No. 6, pp. 1435-1444.
- [32] Rodriguez-Iturbe, I., Gonzalez-Sanabria, M., and Bras, R. L., (1982), "A Geomorphoclimatic Theory of the Instantaneous Unit Hydrograph", Water Resources Research, August 1982, Vol. 18, No. 4, pp. 877-886.
- [33] Rodriguez-Iturbe, I., Sanabria, M. G., and Carmano, G., (1982), "On the Climatic Dependence of the IUH : A Rainfall-Runoff Analysis of the Nash Model and the Geomorphoclimatic Theory", Water Resources Research, August 1982, Vol. 18, No. 4, pp. 887-903.
- [34] Rodriguez-Iturbe, I. and Valdes, J. B., (1979), "The Geomorphologic Structure of Hydrologic Response", Water Resources Research, December 1979, Vol. 15, No. 6, pp. 1409-1420.
- [35] Steel, E. W., (1960), Water Supply and Sewerage, 4th ed., McGraw-Hill Book Co., New York, U.S.A.
- [36] Strahler, A. N., (1957), "Quantitative Analysis of Watershed Geomorphology", Amer. Geophys. Union Trans. 38, No. 6, 1957, pp. 913-920.
- [37] Sveshnikov, A. A., (1968), Problems in Probability Theory, Mathematical Statistics and Theory of Random Functions, Dover Publications, Inc., New York, U.S.A.
- [38] United States Bureau of Reclamation (U.S.B.R.), (1965), Design of Small Dams, U.S. Government Printing Office, Washington, D.C., U.S.A.

- [39] Valdes, J. B., Fiallo, Y., and Rodriduez-Iturbe, I., (1970), "A Rainfall-Runoff Analysis of the Geomorphologic IUH", Water Resources Research, December 1979, Vol. 15, No. 6, pp. 1421-1434.
- [40] Wang, C. T., Gupta, V. K., and Waymire, E., (1981), "A Geomorphologic Synthesis of Nonlinearity in Surface Runoff", Water Resources Research, June 1981, Vol. 17, No. 3, pp. 545-554.
- [41] Wood, E. F., (1976), "An Analysis of the Effects of Parameter Uncertainty in Deterministic Hydrologic Models", Water Resources Research, Vol. 12, No. 5, pp. 925-932.
- [42] Wooding, R. A., (1966), "A Hydraulic Model for the Catchment-Stream Problem III. Comparison with Runoff Observations", Journal of Hydrology, Vol. 4, pp. 21-37.
- [43] Yevjevich, V., (1972), Probability and Statistics in Hydrology, Water Resources Publications, Fort Collins, Colorado, U.S.A.

Appendix A

STATISTICAL CHARACTERISTICS OF POWER FUNCTIONS OF A GAMMA VARIABLE

Let the random variable Y be a power function of a random variable X . The power function is of the form

$$Y = aX^b, \quad a, b > 0 \quad (\text{A.1})$$

If the probability density $f(x)$ of X is known, then the k^{th} moment about the origin of Y is given by

$$m_k[Y] = \int_{-\infty}^{+\infty} f(x)[aX^b]^k dx \quad (\text{A.2})$$

Let $f(x)$ be the Gamma density function :

$$f(x) = \frac{\lambda^\eta x^{\eta-1} e^{-\lambda x}}{\Gamma(\eta)}, \quad x, \lambda, \eta > 0 \quad (\text{A.3})$$

The mean of X is

$$E(X) = \frac{\eta}{\lambda} \quad (\text{A.4})$$

The variance of X is

$$V(X) = \frac{\eta}{\lambda^2} \quad (\text{A.5})$$

The coefficient of variation of X is

$$Cv(X) = \frac{1}{\sqrt{\eta}} \quad (\text{A.6})$$

The coefficient of skewness of X is

$$C_s(X) = \frac{2}{\sqrt{\eta}} \quad (\text{A.7})$$

The k^{th} moment about the origin of Y is given by

$$m_k[Y] = \frac{\lambda\eta}{\Gamma(\eta)} \int_0^\infty x^{\eta-1} e^{-\lambda x} (ax^b)^k dx \quad (\text{A.8})$$

or,

$$m_k[Y] = \frac{a^k \lambda \eta}{\Gamma(\eta)} \int_0^\infty x^{kb + \eta - 1} e^{-\lambda x} dx \quad (\text{A.9})$$

Using the equality

$$\int_0^\infty x^{\eta-1} e^{-\lambda x} dx = \frac{\Gamma(\eta)}{\lambda^\eta} \quad (\text{A.10})$$

the 1^{st} moment about the origin of Y is

$$m_1[Y] = \frac{a\lambda\eta}{\Gamma(\eta)} \int_0^\infty x^{b+\eta-1} e^{-\lambda x} dx = \frac{a\lambda\eta}{\Gamma(\eta)} \frac{\Gamma(b+\eta)}{\lambda^{b+\eta}} \quad (\text{A.11})$$

the 2^{nd} moment about the origin of Y is

$$m_2[Y] = \frac{a^2 \lambda \eta}{\Gamma(\eta)} \int_0^\infty x^{2b+\eta-1} e^{-\lambda x} dx = \frac{a^2 \lambda \eta}{\Gamma(\eta)} \frac{\Gamma(2b+\eta)}{\lambda^{2b+\eta}} \quad (\text{A.12})$$

the 3^{rd} moment about the origin of Y is

$$m_3[Y] = \frac{a^3 \lambda \eta}{\Gamma(\eta)} \int_0^\infty x^{3b+\eta-1} e^{-\lambda x} dx = \frac{a^3 \lambda \eta}{\Gamma(\eta)} \frac{\Gamma(3b+\eta)}{\lambda^{3b+\eta}} \quad (\text{A.13})$$

The 2^{nd} and 3^{rd} central moments (about the mean) of Y are related to the moments about the origin as follows. Let $\mu_k[Y]$ denote the k^{th} central moment of Y .

$$\mu_2[Y] = m_2[Y] - m_1^2[Y] \quad (\text{A.14})$$

$$\mu_3[Y] = m_3[Y] - 3m_1[Y]m_2[Y] + 2m_1^3[Y] \quad (\text{A.15})$$

After some algebraic manipulations, the 2^{nd} and 3^{rd} central moments of Y respectively are

$$\mu_2[Y] = \left(\frac{a}{\lambda\eta}\right)^2 \frac{\Gamma(\eta)\Gamma(2b+\eta) - \Gamma^2(b+\eta)}{\Gamma^2(\eta)} \quad (\text{A.16})$$

$$\mu_3[Y] = \left(\frac{a}{\lambda\eta}\right)^3 \frac{\Gamma^2(\eta)\Gamma(3b+\eta) - 3\Gamma(\eta)\Gamma(2b+\eta)\Gamma(b+\eta) + 2\Gamma^3(b+\eta)}{\Gamma^3(\eta)} \quad (\text{A.17})$$

The statistical characteristics of the transformed random variable Y are as follows. The mean of Y is

$$E(Y) = m_1[Y] = \frac{a}{\lambda b} \frac{\Gamma(b+\eta)}{\Gamma(\eta)} \quad (\text{A.18})$$

The coefficient of variation of Y is

$$Cv(Y) = \frac{\sqrt{\mu_2[Y]}}{E(Y)} = \frac{(\Gamma(\eta)\Gamma(2b+\eta) - \Gamma^2(b+\eta))^{1/2}}{\Gamma(b+\eta)} \quad (\text{A.19})$$

The coefficient of skewness of Y is

$$Cs(Y) = \frac{\mu_3}{\mu_2^{3/2}} = \frac{\Gamma^2(\eta)\Gamma(3b+\eta) - 3\Gamma(\eta)\Gamma(2b+\eta)\Gamma(b+\eta) + 2\Gamma^3(b+\eta)}{(\Gamma(\eta)\Gamma(2b+\eta) - \Gamma^2(b+\eta))^{3/2}} \quad (\text{A.20})$$

The coefficients $Cv(Y)$ and $Cs(Y)$ are related according to the following equation

$$Cs(Y)Cv^3(Y) = \frac{\Gamma^2(\eta)\Gamma(3b+\eta) - 3\Gamma(\eta)\Gamma(2b+\eta)\Gamma(b+\eta) + 2\Gamma^3(b+\eta)}{\Gamma^3(b+\eta)} \quad (\text{A.21})$$